Important Notice

UNIVERSITY OF CALGARY

Scattering of Seismic Waves from Arbitrary Viscoelastic-Isotropic and Anisotropic Structures with Applications to Data Modelling, FWI Sensitivities and Linearized AVO-AVAz Analysis

by

Shahpoor Moradi

A THESIS
SUBMITTED TO THE FACULTY OF GRADUATE STUDIES
IN PARTIAL FULFILLMENT OF THE REQUIREMENTS FOR THE
DEGREE OF DOCTOR OF PHILOSOPHY

GRADUATE PROGRAM IN GEOLOGY AND GEOPHYSICS

CALGARY, ALBERTA
JUNE, 2017

Abstract

It is acknowledged that Full Waveform Inversion (FWI) techniques are sensitive to the set of model parameters that we choose for the minimization procedure. This model parametrization and sensitivity analysis for FWI has been extensively studied for acoustic and isotropic-elastic media. In order to obtain an accurate image of subsurface earth, it is necessary to include both anisotropy and attenuation in inversion procedures as subsurface materials are far from being isotropic or elastic. In this thesis, we formulate the sensitivity analysis for FWI in viscoelastic-isotropic/anisotropic media. To develop such analysis, we construct a framework based on the first order perturbation theory called the Born approximation to find the sensitivity of the FWI to isotropic, anelastic and anisotropic parameters. Sensitivities are, essentially, radiation patterns induced by scattering of the seismic waves from inclusions in medium properties in an isotropic background. Most importantly, we investigate the effect of the inhomogeneity angle which is unique to viscoelastic waves, on these radiation patterns (scattering potentials) and also on amplitude-variation-with-offset or azimuth (AVO/AVAz) analysis. By decomposition of the scattering potentials into isotropic, viscoelastic and anisotropic components, we specify the effects of anelasticity, inhomogeneity of wave and anisotropy on radiation patterns and the linearized AVO/AVAz equations. Moreover, we show how the obtained scattering potentials reduce to the linearized AVO/AVAz equations without using the solution of Zoeppritz equations. This analysis is the starting point for any FWI strategy in a complex media exhibiting both attenuation and anisotropy, as the scattering potentials that we obtained can be effectively implemented to choose a suitable model parametrization.

Preface

The current PhD thesis is written in manuscript-style format based on the two published papers, three submitted papers and one technical report. I am the first author of these papers. The full citation for chapter 2 is: Shahpoor Moradi, Kristopher A. Innanen, Scattering of homogeneous and inhomogeneous seismic waves in low-loss viscoelastic media, Geophysical Journal International (2015) 202 (3): 1722-1732. This paper is republished in this thesis with the permission from Oxford University Press. The full citation for chapter 3 is: Shahpoor Moradi, Hassan Khaniani and Kristopher A. Innanen, Numerical analysis of scattering in a viscoelastic medium, CREWES Research Report, Volume 26 (2014). The full citation for chapter 4 is: Shahpoor Moradi, Kristopher A. Innanen, Viscoelastic amplitude variation with offset equations with account taken of jumps in attenuation angle, Geophysics 81 (3), N17-N29. This paper is republished in this thesis with the permission from Society of Exploration Geophysicists.

Acknowledgements

I would like to thank several people and express my sincere gratitude to all of them. First of all, special thanks goes to my enthusiastic supervisor Dr. Kristopher A. Innanen for his tremendous academic support. Completion of this thesis was possible only because of his consistent encouragement. I gratefully acknowledge funding sources that made my Ph.D. work possible, the sponsors of Consortium for Research in Elastic Wave Exploration Seismology (CREWES) for continued support and the Natural Science and Engineering Research Council of Canada (NSERC) through the grant CRDPJ 461179-13. I am grateful to the Canadian Society of Exploration Geophysicists (CSEG) for awarding me the 2017 CSEG scholarship sponsored by CGG and University of Calgary for providing me Eyes High International Doctoral Scholarship in 2014 and 2106.

There are two people that I would like to express my special appreciation, my sister Dr. Shahin Moradi and my friend Dr. Hassan Khaniani for the very helpful discussions and their technical support.

I would like especially thank to my family. My wife, Mina has been extremely supportive to me not only during my education but also through our entire married life. My daughter, Zhouan for being such a good girl always cheering me up.

Last but not least, I would like to thank my parents, Maman and Kavka, my brother and sisters and in-laws for their love and support from oversees.

Dedication

To Mina and Zhouan (Jouje).

Contents

Abstract . . . i
Preface . . . ii
Acknowledgements . . . iii
Dedication . . . iv
Contents . . . v
List of Tables . . . viii
List of Figures . . . ix
1 Introduction . . . 1
1.1 Amplitude Variation with Offset and Azimuth in attenuative media . . . 1
1.2 Model parametrization in Full Waveform Inversion . . . 3
1.3 Thesis overview . . . 5
2 Scattering of homogeneous and inhomogeneous seismic waves in low-loss viscoelastic media . . . 8
2.1 Abstract . . . 8
2.2 Introduction . . . 9
2.3 Mathematical formulation and review . . . 11
2.3.1 Homogeneous and inhomogeneous waves in viscoelastic wave theory . . . 11
2.3.2 Viscoelastic waves . . . 12
2.4 The viscoelastic scattering operator and potentials . . . 16
2.4.1 The scattering operator in displacement space . . . 18
2.4.2 The scattering operator in P, SI and SII space . . . 20
2.5 Elements of the P-SI-SII scattering matrix . . . 22
2.5.1 Viscoelastic P-P scattering . . . 23
2.5.2 Viscoelastic P-SI scattering . . . 26
2.5.3 Viscoelastic SI-to-SI scattering . . . 29
2.5.4 Viscoelastic scattering of SII-waves . . . 31
2.6 Summary and conclusion . . . 33
A Perturbation in complex domain . . . 35
3 Numerical analysis of scattering in a viscoelastic medium . . . 36
3.1 Abstract . . . 36
3.2 Introduction . . . 36
3.3 Review of common viscoelastic models . . . 38
3.3.1 Equation of Motion . . . 41
3.4 Viscoelastic scattering amplitude . . . 42
3.5 Numerical implementation . . . 43
3.6 Summary and future direction . . . 51
B Appendixe: 3-D viscoelastic medium . . . 53
4 Viscoelastic amplitude variation with offset equations with account taken of jumps in attenuation angle . . . 55
4.1 Abstract . . . 55
4.2 Introduction . . . 55
4.3 Viscoelastic ray parameters and slownesses . . . 58

4.4 Viscoelastic Snell's law in the low-contrast approximation 60
4.5 Exact reflection/transmission coefficients 65
4.6 Linearization of reflectivity 68
4.6.1 P-to-P reflection coefficient 69
4.7 Linearized P-to-SI reflection 73
4.8 SI-to-SI reflection 75
4.9 The relationship between the reflectivity and the viscoelastic scattering potential 77
4.9.1 P-to-P scattering potential 80
4.9.2 SI-to-SI scattering potential 81
4.9.3 P-to-SI scattering potential 82
4.10 Conclusion 82
4.11 Summary 84
5 Significance and behaviour of the homogeneous and inhomogeneous components of linearized viscoelastic reflection coefficients 86
5.1 Abstract 86
5.2 Introduction 87
5.3 Preliminaries 90
5.4 Homogeneous and inhomogeneous parts of the slownesses 93
5.5 Decomposition of solutions of the viscoelastic Zoeppritz equations 95
5.6 The viscoelastic Shuey approximation 98
5.7 Converted wave approximations 105
5.8 Conclusions 109
C Complex coefficients 111
D Trigonometric functions for small angles 114
E Linearization procedure in viscoelastic media 115
6 Born scattering and inversion sensitivities in viscoelastic transversely isotropic media 120
6.1 Abstract 120
6.2 Introduction 120
6.3 The stiffness tensor for VTI-viscoelastic media and complex Thomsen parameters 123
6.4 Perturbations in the stiffness tensor and the Born approximation 126
6.5 Scattering potentials 130
6.6 Anisotropic-viscoelastic scattering processes and inversion sensitivities 134
6.7 Conclusion and summary 143
F Propagation and attenuation vectors 145
7 Compressional wave scattering potentials and linearized reflection coefficients in elastic and low-loss viscoelastic orthorhombic media 147
7.1 Abstract 147
7.2 Introduction 148
7.3 Viscoelastic orthorhombic media 150
7.4 Scattering potential 153
7.5 Scattering of P-wave to P-wave 155
7.6 Conclusion and summary 165
8 Summary and Future Work 168

References 170
Copyright and Permissions 184

List of Tables

5.1 Density, P and S-wave velocity used in the numerical tests for shale, salt, limestone and limestone(gas). For all models we assumed the P- and S-wave quality factors as $Q_{S1} = 5$, $Q_{S2} = 7$, $Q_{P1} = 9$ and $Q_{P2} = 11$. 96

F.1 Notation 146

7.1 Phase velocity for P-, SV and SH waves in terms of diagonal componenets of stiffness tensor. 152

7.2 Generalized Thomsen parameters for orthorhombic media in terms of VTI parameters in xz, xy and zy planes. 152

7.3 A table illustrating the perturbation terms used in volume scattering and low-contrast reflectivity. Medium properties are classified into isotropic-elastic, isotropic-viscoelastic, anisotropic-elastic and anisotropic-viscoelastic. In volume scattering scheme, the actual medium which is anisotropic-viscoelastic splits into the isotropic reference medium filled by the perturbations in medium properties. Since the reference medium is isotropic, anisotropic parameters in actual medium act as perturbations. 159

List of Figures

2.1 Magnitude of the minor axes of the elliptical motion for an inhomogeneous wave in a low-loss viscoelastic media versus attenuation angle δ for three values of reciprocal quality factor. 16

2.2 a) Homogeneous wave with propagation and attenuation vectors in the same direction ($\delta = 0$). b) Inhomogeneous wave with none zero attenuation angle between the propagation and attenuation vectors ($\delta \neq 0.$) 17

2.3 Schematic breakdown of actual medium into reference medium and perturbations. 19

2.4 Elastic and anelastic density(left) and S-wave velocity(right) components of the viscoelastic potential for scattering of incident inhomogeneous P-wave to inhomogeneous reflected P-wave versus of reflected wave angle σ, for $\delta_{\mathrm{P}} = 60°$. Quality factor of P-wave for reference medium is to be 10 and for S-wave is 7. Also the S-to P-wave velocity ratio for reference medium is chosen to be 1/2. Dash line is for anelastic part and solid line for elastic part. 25

2.5 Elastic and anelastic density(left) and S-wave velocity(right) components of the viscoelastic potential for scattering of incident inhomogeneous P-wave to inhomogeneous reflected SI-wave versus of reflected wave angle σ, for $\delta_{\mathrm{S}} = \delta_{\mathrm{P}} = 60°$. Quality factor of P-wave for reference medium is to be 10 and for S-wave is 7. Also the S- to P-wave velocity ratio for reference medium is chosen to be 1/2. Dash line is for anelastic part and solid line for elastic part. 27

2.6 Elastic and anelastic density(left) and S-wave velocity(right) components of the viscoelastic potential for scattering of incident inhomogeneous SI-wave to inhomogeneous reflected SI-wave versus of reflected wave angle σ, for $\delta_{\mathrm{S}} = 60°$. Quality factor for S-wave is 7. Also the S- to P-wave velocity ratio for reference medium is chosen to be 1/2. Dash line is for anelastic part and solid line for elastic part. 30

2.7 Elastic and anelastic density(left) and S-velocity(right) components of the viscoelastic potential for scattering of incident inhomogeneous SII-wave to inhomogeneous reflected SII-wave versus of reflected wave angle σ, for $\delta_{\mathrm{S}} = 60°$. Quality factor for S-wave is 7. Also the S-to P-velocity ratio for reference medium is chosen to be 1/2. Dash line is for anelastic part and solid line for elastic part. 32

3.1 Quality factor Q for different numbers of relaxation mechanisms in the frequency band from 0 to 120 Hz. The frequency band from 30 to 100 Hz, for which Q is constructed to be approximately constant, is separated by vertical lines. Dot line is for Q_p and dash line for Q_s 39

3.2 Model description of two layer viscoelastic medium. 45

3.3 Simulated seismic data corresponding to the contrast in P-wave velocity α. The left figure is the x-component of displacement and right is the y-component of displacement. 45

3.4 Simulated seismic data corresponding to the contrast in S-wave velocity β. The left figure is the x-component of displacement and right is the y-component of displacement. 46
3.5 Simulated seismic data corresponding to the contrast in density ρ.The left figure is the x-component of displacement and right is the y-component of displacement. 47
3.6 Simulated seismic data corresponding to the contrast in quality factor for P-wave velocity Q_p. The left figure is the x-component of displacement and right is the y-component of displacement. 48
3.7 Simulated seismic data corresponding to the contrast in quality factor for S-wave velocity Q_s. The left figure is the x-component of displacement and right is the y-component of displacement. 49
3.8 Comparison of theoretical results for PP scattering potential with numerical simulation of wave scattering from density scatter point in a) elastic background and b) viscoelastic background medium. σ is the opening angle between the incident and reflected (scattered) wave. 49
3.9 The same explanation as figure 3.8 for P-wave scatter point. 50
3.10 The same explanation as figure 3.8 for S-wave scatter point. 50
3.11 The same explanation as figure 3.8 for P- and S-wave quality factor scatter points. 51

4.1 Diagram illustrating the complex ray parameter for various values of reciprocal quality factor Q and attenuation angle δ. 59
4.2 Diagram illustrating the transmitted attenuation angle δ_{P2} versus incident angle θ_{P1} and incident attenuation angle δ_{P1}(a) contract in both velocity and quality factor (b) contrast in quality factor with constant velocity (c) contrast in velocity with constant quality factor. 62
4.3 Schematic diagram showing definitions of the phase and attenuation angles of the incident, reflected, and transmitted rays of an incident P-wave with non-normal incidence. Medium 1 is defined by its P-wave velocity V_{P1}, S-wave velocity V_{S1}, P-wave quality factor Q_{P1}, S-wave quality factor Q_{S1} and its density ρ_1; and for medium 2, by $V_{\mathrm{P2}}, V_{\mathrm{S2}}, Q_{\mathrm{P2}}, Q_{\mathrm{S2}}$ and ρ_2. Angles are defined as, θ_{P1} for the incident and reflected P-wave in medium 1, θ_{S1} for the reflected SI-wave, and θ_{P2} and θ_{S2} respectively for transmitted P- and SI-waves. Attenuation angle for incident and reflected P-wave is given by δ_{P1}, also attenuation angles for reflected SI-wave, transmitted P- and SI-waves respectively are given by δ_{S1}, δ_{S2} and δ_{P2}. ξ_{Pi}, ξ_{Pr} and ξ_{Pt} respectively denotes the complex polarization vectors for incident, reflected and transmitted P-waves and ζ_{Sr} and ζ_{St} are the polarizations for the reflected and transmitted SI-waves respectively. 66
4.4 Schematic diagram illustrating the terms in linearized P-to-P reflectivity. Incident, reflected and transmitted phase and attenuation angles can be expressed in terms of averages and differences in angles. Same interpretation is valid for SI-wave. 70

4.5 Elastic and anelastic parts of linearized reflectivities versus incident angle for $\rho_2/\rho_1 = V_{\mathrm{SE2}}/V_{\mathrm{SE1}} = V_{\mathrm{PE2}}/V_{\mathrm{PE1}} = Q_{\mathrm{P2}}/Q_{\mathrm{P1}} = Q_{\mathrm{S2}}/Q_{\mathrm{S1}} = 1.35$ and average attenuation angles $\delta_{\mathrm{S}} = \delta_{\mathrm{P}} = 60°$. Dash line is for anelastic part and solid line for elastic part. 76
4.6 The maps of imaginary part of density component of the linearized reflectivities. The vertical axis indicates the attenuation angle and horizontal axis incident angle. Physical proprieties of layers are the same as figure 4.5. We assumed that attenuation angles for P- and S-waves are the same. 77
4.7 The reflectivity model vs volume scattering model. (a) The boundary is assumed to involved welded contact between two media whose properties differ only slightly. Incident, reflected and transsmited rays are related by Snell's law;interface normal helps define ray angles. (b) Reference medium is perturbed by one or more volume scattering inclusions; ray angles are defined in terms of the opening angle between incident and scattered rays. $\sigma_{\mathrm{PP}} = 2\theta_{\mathrm{P}}$, is the opening angle between the incident and scattered P-waves, where θ_{P} is the average of incident and transmitted angles. $\sigma_{\mathrm{PS}} = \theta_{\mathrm{P}} + \theta_{\mathrm{S}}$, is the opening angle between the incident P-wave and scattered SI-wave, where θ_{S} is the average of incident and transmitted SI-waves. 79

5.1 Incident inhomogeneous wave ($\delta \neq 0$). $\mathbf{P}$ is the propagation vector, $\mathbf{A}$ is the attenuation vector, θ is the incident phase angle and δ is the incident attenuation angle. 92
5.2 Plots of the viscoelastic ray parameter p in the complex plane for $Q = 10$ over a range of attenuation angles, from 0° to 70°. 93
5.3 Comparing the real part of the exact viscoelastic PP and PS-reflectivity for $\delta_P = 0°, 45°, 70°$ for four selected models from table 5.1. 96
5.4 Comparing the two and three term AVO responses for the decomposed PP reflectivity. 100
5.5 The maps of the inhomogeneous part of the PP-reflectivity for three models in table 1. The vertical axis indicates the attenuation angle and horizontal axis incident angle. 100
5.6 Components of the PP-reflection coefficients versus incident angle θ_{P} for three two layer mineral models introduced in table 5.1. Solid line represent the exact reflectivity calculated from the Zoeppritz equation (Eq. 5.20), star and circle-dot lines respectively are related to the two and three terms (Figures 5.6b and 5.6c). Reflectivity components corresponding to the interface models of Shale/salt, Shale/Limestone(gas) and Limestone/Salt. 101
5.7 Components of the PP-reflection coefficients versus $\sin^2\theta_{\mathrm{P}}$ for three two layer mineral models introduced in table 5.1. Solid line represent the exact reflectivity calculated from the Zoeppritz equation (Eq. 5.20)and circle-dot lines corresponds to the two term approximation. Reflectivity components corresponding to the interface models of Shale/salt, Shale/Limestone(gas) and Limestone/Salt. Figure(5.6d) corresponds to the inhomogeneous components normalized by dividing to $\tan\theta_{\mathrm{P}}$ 102

5.8 Numerical modeling of elastic, homogeneous and inhomogeneous terms in linearized P-to-P reflection coefficient for contrast in density. 104
5.9 Components of the PS-reflection coefficients versus incident angle and $\sin^2\theta_{\rm P}$ for three two layer mineral models introduced in table 5.1. Solid line represent the exact reflectivity calculated from the Zoeppritz equation (Eq. 5.21)and circle-dot lines corresponds to the two term approximation. Reflectivity components corresponding to the interface models of Shale/salt, Shale/Limestone(gas) and Limestone/Salt. Figures (5.9d,f) to corresponds to the components normalized by dividing to $\sin\theta_{\rm P}$ 108
5.10 Numerical modeling of elastic, homogeneous and inhomogeneous terms in linearized P-to-S reflection coefficient for contrast in density. 108

6.1 Schematic description of Born approximation based on the perturbation theory. The reference medium is characterized by its three elastic parameters P-wave velocity $V_{\rm P0}$, S-wave velocity $V_{\rm S0}$ and density ρ_0; two viscoelastic parameters P-wave quality factor $Q_{\rm P0}$ and S-wave quality factor $Q_{\rm S0}$; three anisotropic Thomsen parameters $(\varepsilon_0, \delta_0, \gamma_0)$ and corresponding Q-dependent Thomsen parameters $(\varepsilon_{Q0}, \delta_{Q0}, \gamma_{Q0})$. Perturbations are characterized by 11 components represented by $(\Delta\rho, \Delta V_{\rm P}, \Delta V_{\rm S}, \Delta\varepsilon, \Delta\delta, \Delta\gamma, \Delta Q_{\rm P}, \Delta Q_{\rm S}, \Delta\varepsilon_Q, \Delta\delta_Q, \Delta\gamma_Q)$. Other quantities are defined in table F.1. 127
6.2 Sensitivity of the elastic part of the P-to-P scattering potential to the changes in properties versus incident P-wave angle $\theta_{\rm P}$. The S- to P-wave velocity ratio for reference medium is chosen to be $1/2$. 137
6.3 Sensitivity of the viscoelastic part of the P-to-P scattering potential to the changes in properties versus incident P-wave angle $\theta_{\rm P}$. Top plots are the sensitivity of the isotropic viscoelastic components and lower plots are the sensitivity of the anisotropic viscoelastic components. Quality factor of P-wave for reference medium is to be 10 and for S-wave is 7. Also the S- to P-wave velocity ratio for reference medium is chosen to be $1/2$. P-wave attenuation angle is chosen to be $\delta_{\rm P} = \pi/6$. 137
6.4 Sensitivity of the isotropic elastic and isotropic viscoelastic parts of the P-to-SI scattering potential to the changes in properties versus the average of incident P-wave angle $\theta_{\rm P}$ and scattered S-wave angle $\theta_{\rm S}$. S-to-P velocity ratio, quality factor and attention angle same as figure 6.3. 138
6.5 Sensitivity of the elastic part of the SI-to-SI scattering potential to the changes in properties versus incident S-wave angle $\theta_{\rm S}$. 139
6.6 Sensitivity of the viscoelastic part of the SI-to-SI scattering potential to the changes in properties versus incident S-wave angle $\theta_{\rm S}$. Top plots are the sensitivity of the isotropic viscoelastic components and lower plots are the sensitivity of the anisotropic viscoelastic components. S-to-P velocity ratio, quality factor and attention angle same as figure 6.3. 140
6.7 Sensitivity of the elastic part of the SII-to-SII scattering potential to the changes in properties. 142

6.8 Sensitivity of the viscoelastic part of the SII-to-SII scattering potential to the changes in properties versus incident S-wave angle $\theta_{\rm S}$. S-to-P velocity ratio, quality factor and attention angle same as figure 6.3. 143

7.1 Schematic representation of orthorhombic media. 151
7.2 The low contrast model vs volume scattering model. (a) The boundary is assumed to involved welded contact between two media whose properties differ only slightly. Upper layer is isotropic elastic media defined by its P-wave velocity $V_{\rm P1}$, S-wave velocity $V_{\rm S1}$, and its density ρ_1. Lower layer is elastic orthorhombic media, by $V_{\rm P2}, V_{\rm S2}, \rho_2$ and seven Thompson parameters $\varepsilon_2^{(1)}, \varepsilon_2^{(2)}, \delta_2^{(1)}, \delta_2^{(2)}, \delta_2^{(3)}, \gamma_2^{(1)}, \gamma_2^{(2)}$. Incident and reflected propagation vectors are denoted by $\mathbf{P}_{\rm i}$ and $\mathbf{P}_{\rm r}$ respectively and $\theta_{\rm P}$ is the incident phase angle. (b) Reference medium is perturbed by volume scattering perturbations; Back ground medium is isotropic elastic characterized by $V_{\rm P0}, V_{\rm S0}, \rho_0$ and perturbations are $\Delta V_{\rm P}, \Delta V_{\rm S}, \Delta\rho$ and in anisotropic parameters $\varepsilon^{(1)}$,$\varepsilon^{(2)}$, $\delta^{(1)}$,$\delta^{(2)}$,$\delta^{(3)}$,$\gamma^{(1)}$,$\gamma^{(2)}$ . . 157
7.3 The maps of sensitivity of PP-scatter wave to the Thomsen parameters. Vertical axis is azimuth angle and horizontal axis is incident phase angle. 158
7.4 Sensitivity of the PP-scatter wave to the Thomsen parameters for azimuth angles 0°, 45°, 60°, 90°. Horizontal axis is opening angle $2\theta_P$. 160
7.5 The low contrast model vs volume scattering model. (a) The boundary is assumed to involved welded contact between two media whose properties differ only slightly. Upper layer is isotropic viscoelastic media defined by its P-wave velocity $V_{\rm P1}$, S-wave velocity $V_{\rm S1}$, P-wave quality factor $Q_{\rm P1}$, S-wave quality factor $Q_{\rm S1}$ and its density ρ_1; Lower layer is viscoelastic orthorhombic media, by by $V_{\rm P2}, V_{\rm S2}, Q_{\rm P2}, Q_{\rm S2}$ and ρ_2, seven anisotropic Thompson parameters $\varepsilon_2^{(1)}, \varepsilon_2^{(2)}, \delta_2^{(1)}, \delta_2^{(2)}, \delta_2^{(3)}, \gamma^{(1)}, \gamma^{(2)}$ and seven anisotropic-viscoelastic Thompson parameters $\varepsilon_{\rm Q2}^{(1)}, \varepsilon_{\rm Q2}^{(2)}, \delta_{\rm Q2}^{(1)}, \delta_{\rm Q2}^{(2)}, \delta_{\rm Q2}^{(3)}, \gamma_{\rm Q2}^{(1)}, \gamma_{\rm Q2}^{(2)}$. Incident and reflected attenuation angles are the equal by applying the Snell's law denoted by $\delta_{\rm i}$.(b) Reference medium is perturbed by volume scattering perturbations; Back ground medium is isotropic viscoelastic characterized by $V_{\rm P0}, V_{\rm S0}, Q_{\rm P0}, Q_{\rm S0}, \rho_0$ and perturbations are $\Delta V_{\rm P}$,$\Delta V_{\rm S}$,$\Delta\rho$ and in anisotropic parameters $\varepsilon^{(1)}$,$\varepsilon^{(2)}$,$\delta^{(1)}$,$\delta^{(2)}$,$\delta^{(3)}$, $\gamma^{(1)}$,$\gamma^{(2)}$ and anisotropic viscoelastic parameters $\varepsilon_{\rm Q}^{(1)}$,$\varepsilon_{\rm Q}^{(2)}$,$\delta_{\rm Q}^{(1)}$,$\delta_{\rm Q}^{(2)}$,$\delta_{\rm Q}^{(3)}$,$\gamma_{\rm Q}^{(1)}$,$\gamma_{\rm Q}^{(2)}$. $\mathbf{P}_{\rm Pi}$ is the incident propagation vector; $\mathbf{P}_{\rm Pr}$ is the reflected(scattered) propagation vector; $\mathbf{A}_{\rm Pi}$ is the incident attenuation vector; $\mathbf{A}_{\rm Pr}$ is the reflected(scattered) attenuation vector and $\delta_{\rm P}$ is the attenuation angle which is the same for incident and reflected wave. 161
7.6 Sensitivity of the PP-scatter wave to the anisotropic-viscoelastic parameters for azimuth angles 0°, 45°, 60°, 90°. Horizontal axis is opening angle $2\theta_P$. . . 164

Chapter 1

Introduction

1.1 Amplitude Variation with Offset and Azimuth in attenuative media

Amplitude Variation with Offset (AVO) or Angle (AVA) is a technique in reflection seismology that is employed to extract information about the subsurface earth properties, such as P-wave velocity, S-wave velocity, density, attenuation and anisotropic parameters. In AVO, amplitude refers to the amplitude of the reflected wave from subsurface; offset refers to the distance between the man-made source and the receiver (geophone) and angle is defined between the direction of the incident wave from source and the normal to the surface plane. AVO analysis based on the reflections from gas-sand (sandstones with low-+permeability) reservoirs reveals that amplitude mostly vary with the normal-incidence reflection coefficient and Poissons ratio, which can be used to classify the seismic data in terms of these two parameters (Ostrander, 1984; Rutherford and Williams, 1989). An elastic-isotropic earth is characterized by density, compressional wave or P-wave (P stands for primary) velocity and shear wave (S-wave) velocity. However, accurate modeling of hydrocarbon reservoirs requires understanding the way rock properties affect other, second order features of the seismic amplitudes such as anisotropy and attenuation. Anisotropy refers to a rock property in which the seismic velocities are angle dependent. Taking into account the anisotropy, the ray parameter and slowness vectors becomes more complicated in these environments than in their isotropic counterparts. Another rock characteristic that has been observed in seismic data is attenuation, which appears as amplitude damping in reflected seismic wave. Seismic attenuation is defined by one or more quality factors, whose reciprocals measure the energy loss of the wave while propagating through the subsurface (Barton, 2007). Attenuation can be caused by amplitude reduction due to scattering and intrinsic micro-structures in rock. The first one is called the coda quality factor and the second one the intrinsic quality factor.

The heart of AVO analysis is to find how reflected wave from an interface between two layers varies with the changes in medium properties. From exact solutions of the wave

equation it is difficult to evaluate the variation of the reflected wave with offset and changes in medium properties across the boundary. However in the case that properties only vary a small amount across the reflecting boundary, a situation called "low contrast, we can expand the exact reflection coefficients in terms of changes in medium properties to obtain linearized AVO equations. The full description of this procedure for an isotropic-elastic medium can be found in many standard seismic books (Aki and Richards, 2002; Castagna and Backus, 1993; Ikelle and Amundsen, 2005). Seismic wave propagation in anisotropic media in general is a complicated problem because of the dependency of the velocities to angle and anisotropic parameters. However, the assumption of weak anisotropy with a specific type of symmetry greatly simplifies the problem (Thomsen, 1986). For example, the most common anisotropic symmetry demonstrated for sedimentary rock and shale is transversely isotropic. In a transversely isotropic medium with both a horizontal axis of symmetry (HTI-medium with a stack of vertical fractures embedded in an isotropic background) and vertical axis of symmetry (VTI-medium with a stack of horizontal fractures embedded in an isotropic background) AVO analysis has been studied by Rüger (1997, 1998, 2002). PP reflection coefficients for weak-contrast interfaces separating two weakly, but arbitrarily, anisotropic media were derived by Cervený and Psencík (1998). Jílek (2001, 2002) studied the linearized converted PS-wave reflectivity equations for general anisotropic media using first-order perturbation of the exact reflection coefficients and proposed an algorithm for joint inversion of PP- and PS-waves acquired for a wide range of azimuths. Multicomponent seismic data processing provides additional information about subsurface physical properties (Stewart et al., 2002, 2003). Seismic characterization of naturally-fractured reservoirs is investigated in various types of anisotropic media, including single vertical fracture system in an isotropic background rock (HTI medium) (Bakulin et al., 2000a), two orthogonal fracture sets in a isotropic host rock (orthorhombic medium) (Bakulin et al., 2000c) and a medium with two nonorthogonal sets of rotationally invariant fractures (monoclinic medium) (Bakulin et al., 2000b).

Fracture characterization plays a significant role in determining fluid flow during the production(Far, 2011; Far et al., 2013a). The effects of natural fractures on the azimuth, reflection PP-wave data is investigated extensively by many authors, for fractured gas sands

(Sayers and Rickett, 1997); reservoirs containing multiple fracture sets (Sayers and Dean, 2001) and non-orthogonal fracture sets (Sayers, 2009; Far et al., 2013b). It has been shown that reflection amplitude variations with offset and azimuth for converted PS-waves reveals more information concerning the reservoir characterization than the PP-wave reflection amplitudes (Far and Hardage, 2016).

For isotropic viscoelastic media, reflection/transmission coefficients were derived by many authors (Krebes, 1984, 1983; Ursin and Stovas, 2002; Stovas and Ursin, 2003; Borcherdt, 2009). For isotropic/anisotropic viscoelastic media linearized reflection coefficients based of the exact solutions of the Zoeppritz equation are adopted widely to analyse the amplitude variation with offset inversion/modeling. Moradi and Innanen (2016) derived the amplitude variation with offset equations taking into account the jumps in attenuation angle for inhomogeneous waves. It has been shown how attenuation in media impact the amplitude variation with offset equations induced by the perturbations in five viscoelastic parameters.

In the presence of anelasticity in anisotropic media, near and beyond the critical angle the P-wave reflection coefficient can vary remarkably strongly. Neither quality factors nor anisotropic parameters have an effect on the zero offset P-wave reflection coefficients, and anisotropy has more influence on small angle reflectivity than the attenuation (Carcione et al., 1998). The reflection-transmission problem in viscoelastic transversely isotropic media for incident homogeneous wave is studied by Carcione (1997) and Ursin and Stovas (2002) and for incident inhomogeneous wave by Zhu and Tsvankin (2006b); Behura and Tsvankin (2009b,a).

1.2 Model parametrization in Full Waveform Inversion

One of the most frequently-used methods for inversion of seismic data is wave-equation-based inversion (Sava and Biondi, 2004b,a). The mathematical framework of this method is based on two integral equations. The first one is the Lippmann-Schwinger integral equation whose expansion in terms of perturbations in medium properties results in the Born scattering series. The second integral equation is the representation theorem which leads to the Kirchhoff scattering series. The Born scattering series can be utilized for linearized inversion and Kirch-

hoff scattering series to demultiple and to deghost the seismic data (Beylkin and Burridge, 1990; Matson, 1997; Weglein et al., 1997, 2003; Ikelle et al., 2003). Basically, after removing ghosts and multiples we only deal with primaries to image the subsurface. The essential step in inversion is forward modeling of wave propagation. One critical approach to forward modeling of reflected seismic primary reflections is the Born approximation, which is based on the linearization of the Lippmann-Schwinger equation. In this approximation wave propagation take places in so-called background or reference medium. The background medium is altered by a system of inclusions in which medium properties deviate from the background, called perturbations. To consider only single scattering from these perturbations, the series can be truncated at first order, and this truncation is called the Born approximation. From the numerical point of view Born modeling is a low-cost technique as it does not contain any iterations, (in contrast to the Lippmann-Schwinger integral equation). In addition the relationship between the synthetic data and perturbations is linear which makes inversion and analysis simpler. However, if the background medium is not completely known the Born approximation can involve significant errors. Full consideration of seismic imaging and inversion principles incorporating the inverse scattering series for scalar, acoustic and elastic wave equation is presented by Stolt and Weglein (2012). Since the conventional Amplitude Variation with Offset and Azimuth based inversion is not applicable for laterally varying media, the Born-approximation-based inversion method can be implemented to invert the fracture parameters (Bansal and Sen, 2010).

Among up-and-coming techniques for seismic estimation of subsurface properties, full waveform inversion (FWI) ranks high, as a novel and powerful approach that can produce highly-resolved images of the subsurface properties from single and multicomponent seismic data (Fichtner, 2010; Virieux and Operto, 2009). The essence of FWI is based on the minimization of the misfit function between the measured (or observed) seismic data with the modelled (or synthetic) data. The advantage of FWI over other techniques is that all information content of the wavefield is utilized in minimization procedure; in other words, minimization of differences in amplitudes, converted waves, multiples, traveltimes, etc are taken into account between the seismic data and synthetic data. The disadvantage of FWI is that the seismic data may contain recordings unrelated to properties of the Earth.

Model parameterizations is a key issue in multi-parameter FWI updates. A successful FWI procedure depends on choosing the right model parameterizations; for example, one model parametrization might lead to damaging artifacts in density estimation whereas in another no artifacts arise (Tarantola, 1986). Sensitivity analysis is the tool by which we survey and determine suitable model parametrization; it can be set up in the framework of scattering theory based on the Born approximation. Numerical analysis of the scattering patterns versus opening angle between incident and scattered waves, gives insights into the influence of the different parametrization on the FWI.

In acoustic medium for long offset, P-wave velocity-density parametrization is more reliable to invert density than P-wave impedance-density parametrization (Prieux et al., 2013; Gholami et al., 2013). In the context of anisotropic-acoustic FWI, based on the analysis of the radiation patterns of different parameters, it has been shown that the influence of the anisotropic parameter compared to the horizontal and vertical wave velocities remains weak (Gholami et al., 2013). For large opening angles between the incident and reflected wavevectors, a parametrization including one velocity and two anisotropic parameters maximal trade-off, which results in the low resolution for inverted anisotropy (da Silva et al., 2016). Similarly efficient FWI models have been designed for acoustic vertical transversely isotropic (VTI) (Plessix and Cao, 2011; Alkhalifah and Plessix, 2014; Operto et al., 2015; He and Plessix, 2016) and acoustic orthorhombic media (Masmoudi and Alkhalifah, 2016). In FWI, three parameter isotropic inversion is a challenging matter and not yet fully understood; anisotropy and attenuation are not even yet themselves sufficiently well understood in cases when both are active, to be included as unknowns in practical FWI. Anisotropic-viscoelastic FWI therefore remains a "high value target for future technology development, as the math-physics and numerical representation of the processes of wave propagation in such media develop.

1.3 Thesis overview

The main objective of this thesis is to develop the theory of scattering of seismic waves from arbitrary viscoelastic and anisotropic structures with applications to linearized AVO/AVAz

analysis, model parametrization and sensitivity analysis in FWI. Necessary background material on the notion of viscoelastic waves, the Born approximation, and the scattering potential are presented for isotropic-viscoelastic media in chapter 2 and for viscoelastic-anisotropic media in chapters 6 and 7. A detailed discussion on the low-contrast linearization in viscoelastic-isotropic media introduced in chapter 4 and in viscoelastic-anisotropic media in chapters 7. The rest of the thesis is organized as follows.

Chapter 2 is devoted to the scattering of the inhomogeneous (and homogeneous) seismic waves in a low-loss isotropic-viscoelastic media. First three different types of wave, P-, SI and SII are introduced based on the notation of Borcherdt (2009). Afterwards the mathematical framework of the scattering potential based on the perturbation theory in the complex domain is presented in both Cartesian and displacement coordinate systems. Finally, the potentials for scattering of various types of viscoelastic waves are derived in terms of perturbations in both isotropic and viscoelastic parameters, opening angle (the angle between the directions of incident and scattered waves) and attenuation angle.

Chapter 3 presents a numerical implementation of the theoretical framework developed in chapter 2. The modelling of viscoelastic wavefields is performed with a finite-difference solver in time domain for a simple two layer medium. It is shown how contrasts in P- and S-wave quality factors create reflections which are quantitatively in agreement with those derived theoretically by Born approximation.

Chapter 4 deals with amplitude variation with offset in viscoelastic media when the changes in attenuation angles across the boundary is taken into account. First viscoelastic Snell's law is discussed based on the complex ray parameter. By linearization of Snell's law, changes in phase and attenuation angles between two layers are expressed in terms of changes in velocity and quality factors. Then, the exact reflection/transmission coefficients are derived followed by linearized AVO equations. Finally, it is shown that how the linearized AVO equations based on the perturbed Zoeppritz equation are equivalent to the scattering potentials derived using the volume scattering approach explained in chapter 2.

Chapter 5 is dedicated to the importance of the effects of attenuation angle on the both linear and nonlinear reflection coefficients. Taking into account Snell's law in complex domain, linearized AVO equations and exact reflection coefficients are decomposed into three

terms, elastic, homogeneous and inhomogeneous. It is shown that how this decomposition can be used to invert the quality factors in an appropriate inversion technique.

Chapter 6 contains a detailed analysis of how the scattering radiation patterns depend on fractional and absolute changes in anisotropic and attenuative properties of the medium. It is showed how P-to-P, P-to-SI, SI-to-SI and SII-to-SII scattering potentials can be decomposed into elastic, anisotropic, viscoelastic and anisotropic-viscoelastic components.

Chapter 7 is concerned with the scattering potentials and linearized reflection coefficients associated with weakly anisotropic, low-loss viscoelastic orthorhombic media. The equations are obtained by applying the Born approximation based on the first order perturbation theory. An elastic-orthorhombic stiffness tensor is described by nine real independent parameters, vertical P- and S-wave velocity and seven generalized Thompson parameters characterize the anisotropy in medium. If attenuation is taken into account, the stiffness tensor components become complex, with imaginary parts that are connected to the quality factors and Q-Thompson parameters. In deriving the results we assume that the background medium is viscoelastic, however the perturbations are both in anisotropic and viscoelastic properties. The obtained result is closely related to the linearized reflection coefficients derived from the linearization of the exact solutions of the Zoeppritz equation.

Chapter 8 contains a summary and set of conclusions of this thesis.

Chapter 2

Scattering of homogeneous and inhomogeneous seismic waves in low-loss viscoelastic media

2.1 Abstract

Motivated by the need to derive and characterize increasingly sophisticated seismic data analysis and inversion methods incorporating wave dissipation, we consider the problem of scattering of homogeneous and inhomogeneous waves from perturbations in five viscoelastic parameters (density, P- and S-wave velocities, and P- and S-wave quality factors), as formulated in the context of the Born approximation. Within this approximation the total wave field is the superposition of an incident plane wave and a scattered wave, the latter being a spherical wave weighted by a function of solid angle called the scattering potential. In elastic media the scattering potential is real, but if dissipation is included through a viscoelastic model, the potential becomes complex and thus impacts the amplitude and phase of the outgoing wave. The isotropic-elastic scattering framework of Stolt and Weglein (2012), extended to admit viscoelastic media, exposes these amplitude and phase phenomena to study, and in particular allows certain well-known layered-medium viscoelastic results due to Borcherdt to be re-considered in an arbitrary heterogeneous Earth. The main theoretical challenge in doing this involves the choice of coordinate system over which to evaluate and analyze the waves, which in the viscoelastic case must be based on complex vector analysis. We present a candidate system within which several of Borcherdt's key results carry over; for instance, we show that elliptically polarized P- and SI- waves cannot be scattered into linearly polarized SII-waves. Furthermore, the elastic formulation is straightforwardly recovered in the limit as P- and S-wave quality factors tend to infinity.

2.2 Introduction

Accurate and tractable mathematical models of wave propagation are a key to reliable seismic data analysis. Our current ability to analytically describe seismic waves interacting with arbitrary viscoelastic heterogeneities, in support of the derivation and characterization of attenuation analysis methods and seismic full waveform inversion, is quite limited. Motivated by this, we present a particular approach to the problem of scattering of homogeneous and inhomogeneous viscoelastic waves from perturbations in density, P- and S-wave velocities, and P- and S-wave quality factors, as formulated in the context of the Born approximation.

The scattering of seismic waves by purely elastic heterogeneities under the Born approximation has been investigated by many authors (Beylkin and Burridge, 1990; Sato et al., 2012; Stolt and Weglein, 2012; Wu and Aki, 1985). Stolt and Weglein (2012) introduced a formal theory for the description of the multidimensional scattering of seismic waves based on an isotropic-elastic model. We identify as a research priority the adaptation of this approach to incorporate other, more complete pictures of seismic wave propagation. Amongst these, the extension to include anelasticity and/or viscoelasticity (Flugge, 1967), which brings to the wave model the capacity to transform elastic energy into heat, ranks very high. Anelasticity is generally held to be a key contributor to seismic attenuation, or "seismic Q", which has received several decades worth of careful attention in the literature (Aki and Richards, 2002; Futterman, 1962). Development of methods for analysis (Tonn, 1990), processing (Bickel and Natarajan, 1985; Hargreaves and Calvert, 1991; Innanen and Lira, 2010; Schwaiger et al., 2007; Wang, 2006; Zhang and Ulrych, 2007), and inversion (Dahl et al., 1992; Causse et al., 1999; Innanen and Weglein, 2007; Hicks and Pratt, 2001; Ribodetti and Virieux, 1998) of wave data exhibiting the attenuation and dispersion associated with seismic Q remains a very active research area.

Wave propagation in linear viscoelastic media has been extensively studied, both numerically and analytically (Borcherdt, 1971, 1973a,b, 1977, 1982; Borcherdt and Wennerberg, 1985; Borcherdt et al., 1986; Borcherdt, 1988, 2009; Carcione et al., 1988b; Carcione, 1993; Carcione et al., 1988a). Results for viscoelastic anisotropic media have also been derived (Behura and Tsvankin, 2009b; Cervený and Psencík, 2005a,b, 2008; Ursin and Stovas, 2002;

Cervený and Psencík, 1998). Borcherdt (2009) has presented a complete theory for seismic waves propagating in layered linear viscoelastic media, describing reflection and refraction of plane homogenous and inhomogeneous P, SI, and SII waves at planar viscoelastic boundaries.

In an elastic-isotropic setting, beginning with a plane defined by the incoming wave vector and the outgoing wave vector, Stolt and Weglein (2012) develop scattering quantities which in an intuitive manner generalize the layered-medium notions of reflections and conversions of P, SV and SH-waves. The results are forms for the scattering operator whose diagonal elements describe the potential of a volume scattering element to scatter a P-wave to a P-wave, an SV to an SV-wave, and an SH to an SH-wave, and whose off-diagonal elements describe the potential to convert, from, say, a P-wave to an SV-wave, etc. Having made a "good" choice of coordinate systems, canonical results, such as the lack of P-SH and SV-SH mode conversions, are naturally reproduced in their formulation: the off-diagonal element corresponding to P-SH scattering is, for instance, seen to be identically zero.

Generalizing this approach to allow for viscoelastic waves of the type described by Borcherdt has several positive outcomes. First, and foremost, it provides an analytical framework for the examination of processes of scattering of viscoelastic waves from arbitrary three-dimensional heterogeneities, as opposed to layered media. Second, it provides a foundation for direct linear and nonlinear inversion methods for reflection seismic data, which go well beyond existing an-acoustic results (Innanen and Weglein, 2007; Innanen and Lira, 2010; Weglein et al., 2009; Weglein, 2013). And third, it provides a means to compute and analyze the gradient and Hessian quantities used in iterative seismic inversion (Virieux and Operto, 2009). The main challenge lies in the need to choose from a much wider range of possible systems of coordinates. Because viscoelastic wave vectors are complex, and the real and imaginary components of these wave vectors are not necessarily parallel, the use of incident and scattered wave vectors as the starting point for coordinate system selection is a richer but more complicated idea. Nevertheless, judicious choices are possible, and we arrive at a complex, or bivector coordinate system which appears to naturally extend the concepts of Borcherdt (2009) to arbitrary 3D scattering.

We organize the paper as follows. Section 2.3 describes the mathematical framework used to evaluate the wave propagation in a viscoelastic medium. Section 2.4 provides an

explanation of viscoelastic scattering potential in displacement space based on the perturbation theory. Section 2.5 develops the elements of scattering potential for various types of viscoelastic wave scattering. Finally, section 2.6 offers some concluding remarks.

2.3 Mathematical formulation and review

2.3.1 Homogeneous and inhomogeneous waves in viscoelastic wave theory

The mathematical theory for the propagation of P, SI and SII waves in general viscoleastic media is required to provide a rigorous basis for derivation of corresponding scattering potentials. A brief summary of the theory as developed by Borcherdt (2009) is presented here.

There are three types of waves in a viscoelastic medium: P, Type-I S, and Type-II S. For each wave type there is a corresponding seismic quality factor. The quality factors for homogenous waves can be expressed in terms of ratios of the real and imaginary parts of the complex moduli, while those for inhomogeneous waves may be expressed in terms of the quality factors and wave speeds for homogenous waves and the degree of inhomogeneity of the waves. For low-loss media the quality factors for inhomogeneous waves do not necessarily reduce to those for homogenous waves.

In this paper we will write quantities such as the viscoelastic wave vector and velocity for inhomogeneous waves in terms of the reciprocal quality factors for homogenous waves, i.e., Q_{P} and Q_{S}. Of the several mathematical possibilities this choice seems to be the most convenient, expressing our results in the language of standard exploration and monitoring seismology. As a consequence, the key result of this paper, the enumeration of the explicit elements of the multidimensional viscoelastic scattering operator, appears in terms of perturbations in Q_{P} and Q_{S}. These perturbations correspond to the relative-change quantities involved in anelastic amplitude-variation-with-angle (AVA) and amplitude-variation-with-frequency (AVF) expressions (Innanen, 2011).

In the case of inhomogeneous waves, the attenuation and propagation vectors are not in the same direction. This makes the displacement vectors different from those of the homogenous case. The particle motion for P-waves is elliptical in the plane constructed by

attenuation and propagation vectors. This elliptical motion reduces to a linear motion in the homogenous limit. Particle motion also distinguishes the two types of shear waves, SI and SII. The first, which is the generalization of the SV-wave, has an elliptical displacement vector in the propagation-attenuation plane. This is the SI-type wave. The second one, which is the generalization of the SH wave, has linear particle motion perpendicular to the propagation-attenuation plane. This is the SII-type wave.

2.3.2 Viscoelastic waves

Wave equations for the P- and S-wave potentials Φ and $\mathbf{\Psi}$, respectively,

$$\nabla^2\Phi - \alpha^{-2}\partial_t^2\Phi = 0, \tag{2.1}$$

$$\nabla^2\mathbf{\Psi} - \beta^{-2}\partial_t^2\mathbf{\Psi} = 0, \tag{2.2}$$

have plane wave solutions

$$\Phi = \alpha\Phi_0 \exp\left[-i(\mathbf{K}_\mathrm{P}\cdot\mathbf{r} - \omega t)\right], \tag{2.3}$$

$$\mathbf{\Psi} = \beta\mathbf{\Psi}_0 \exp\left[-i(\mathbf{K}_\mathrm{S}\cdot\mathbf{r} - \omega t)\right], \tag{2.4}$$

where

$$\sqrt{\mathbf{K}_\mathrm{P}\cdot\mathbf{K}_\mathrm{P}} = K_\mathrm{P} = \frac{\omega}{\alpha}, \tag{2.5}$$

and

$$\sqrt{\mathbf{K}_\mathrm{S}\cdot\mathbf{K}_\mathrm{S}} = K_\mathrm{S} = \frac{\omega}{\beta}, \tag{2.6}$$

additionally, Φ_0 and $\mathbf{\Psi}_0$ are complex scalar and vector constants (potentials respectively). Also α and β are the complex numbers that, reduce to the P- and S-wave velocities respectively in the case that attenuation in the medium goes to zero. For the low-loss viscoelastic medium approximation where $Q_\mathrm{P}^{-1}, Q_\mathrm{S}^{-1} \ll 1$, α and β reduce to

$$\alpha \approx \alpha_\mathrm{L} = \alpha_\mathrm{E}\left(1 + \frac{i}{2}Q_\mathrm{P}^{-1}\right), \tag{2.7}$$

$$\beta \approx \beta_\mathrm{L} = \beta_\mathrm{E}\left(1 + \frac{i}{2}Q_\mathrm{S}^{-1}\right), \tag{2.8}$$

where, α_{E} and β_{E}, respectively are P- and S-wave velocities and subscripts L indicates a low-loss medium. The displacement vectors for P- and S-waves are given by

$$\mathbf{U}_{\mathrm{P}} = \boldsymbol{\nabla}\Phi = -i\alpha\mathbf{K}_{\mathrm{P}}\Phi_0 \exp\left[-i(\mathbf{K}_{\mathrm{P}} \cdot \mathbf{r} - \omega t)\right], \tag{2.9}$$

$$\mathbf{U}_{\mathrm{S}} = \boldsymbol{\nabla} \times \boldsymbol{\Psi} = -i\beta(\mathbf{K}_{\mathrm{S}} \times \boldsymbol{\Psi}_0) \exp\left[-i(\mathbf{K}_{\mathrm{S}} \cdot \mathbf{r} - \omega t)\right]. \tag{2.10}$$

If $\boldsymbol{\Psi}_0 = \Psi_0\mathbf{n}$, where $\mathbf{n}$ is a unit vector orthogonal to the plane formed by $\mathbf{P}_{\mathrm{S}} - \mathbf{A}_{\mathrm{S}}$ (Eq. 2.11), the corresponding wave is considered to be of S type-I (SI) wave. Displacement vectors for P- and S-waves with complex polarization vectors describe elliptical particle motion. The wavevector of inhomogeneous waves is represented by

$$\mathbf{K} = \mathbf{P} - i\mathbf{A}. \tag{2.11}$$

Here $\mathbf{P}$ is the propagation vector, perpendicular to the constant phase plane $\mathbf{P}\cdot\mathbf{r} = \textit{constant}$, and $\mathbf{A}$ is the attenuation vector perpendicular to the amplitude constant plane $\mathbf{A} \cdot \mathbf{r} = \textit{constant}$, and $\mathbf{r}$ is the position vector. The attenuation vector $\mathbf{A}$ is in the direction of maximum amplitude decay. If the attenuation and propagation vectors are parallel, the wave is homogeneous (elastic behaviour is recovered in the limit as $\mathbf{A}$ vanishes) (figure 2.2). If we represent the angle between $\mathbf{P}$ and $\mathbf{A}$ by δ, for $\delta \neq 90°$ we have

$$|\mathbf{P}| = 2^{-\frac{1}{2}}\left[\Re(\mathbf{K}\cdot\mathbf{K}) + \sqrt{[\Re(\mathbf{K}\cdot\mathbf{K})]^2 + [(\Im\mathbf{K}\cdot\mathbf{K})]^2\sec^2\delta}\right]^{\frac{1}{2}}, \tag{2.12}$$

and

$$|\mathbf{A}| = 2^{-\frac{1}{2}}\left[-\Re(\mathbf{K}\cdot\mathbf{K}) + \sqrt{[\Re(\mathbf{K}\cdot\mathbf{K})]^2 + [(\Im\mathbf{K}\cdot\mathbf{K})]^2\sec^2\delta}\right]^{\frac{1}{2}}, \tag{2.13}$$

where

$$\mathbf{K}\cdot\mathbf{K} = |\mathbf{P}|^2 - |\mathbf{A}|^2 - 2i|\mathbf{P}||\mathbf{A}|\cos\delta, \tag{2.14}$$

and where $\Re(\mathbf{K}\cdot\mathbf{K})$ and $\Im(\mathbf{K}\cdot\mathbf{K})$ represent the real and imaginary parts of $\mathbf{K}\cdot\mathbf{K}$ respectively. According to equation (2.14)

$$\Im(\mathbf{K}\cdot\mathbf{K}) = -2|\mathbf{P}||\mathbf{A}|\cos\delta, \tag{2.15}$$

so, because in a viscoelastic medium $\Im(\mathbf{K}\cdot\mathbf{K}) \neq 0$, this implies that the maximum attenuation $|\mathbf{A}|$ is not zero, and also that the direction of maximum attenuation cannot be

perpendicular to the direction of phase propagation. As a result the attenuation angle varies between $0° \leq \delta < 90°$. The attenuation angle δ for an isotropic viscoelastic medium thus always varies between 0° and 90° (in anisotropic media it can exceed 90° (Behura and Tsvankin, 2009a)). From this general framework we may now follow Borcherdt (2009) in analyzing three types of independently propagating wave.

To understand the nature of the motion characterized by (2.9) and (2.10), consider a complex number $V = \Re V + i\Im V$, multiplication of V with the complex wavevector $\mathbf{K}$ leads to

$$V\mathbf{K} = (\Re V + i\Im V)(\mathbf{P} - i\mathbf{A}) = (\mathbf{P}\Re V + \mathbf{A}\Im V) + i(\mathbf{P}\Im V - \mathbf{A}\Re V). \tag{2.16}$$

If V is interpreted as a velocity, related to the wavevector via $KV = \omega$, its real and imaginary parts are

$$\Re V = \frac{\omega \Re K}{(\Re K)^2 + (\Im K)^2}, \tag{2.17}$$

$$\Im V = -\frac{\omega \Im K}{(\Re K)^2 + (\Im K)^2}. \tag{2.18}$$

Because the polarization vector can be defined with the complex vector $\boldsymbol{\xi}$ as

$$\boldsymbol{\xi} = \Re\boldsymbol{\xi} + i\Im\boldsymbol{\xi} = \frac{V}{\omega}\mathbf{K}, \tag{2.19}$$

its real and imaginary parts of the polarization vectors are therefore

$$\Re\boldsymbol{\xi} = \frac{\mathbf{P}\Re K - \mathbf{A}\Im K}{(\Re K)^2 + (\Im K)^2}, \tag{2.20}$$

$$\Im\boldsymbol{\xi} = -\frac{\mathbf{P}\Im K + \mathbf{A}\Re K}{(\Re K)^2 + (\Im K)^2}. \tag{2.21}$$

These two vectors are orthogonal, and $|\Re\boldsymbol{\xi}|^2 - |\Im\boldsymbol{\xi}|^2 = 1$. A simple analysis indicates that particle motion related to the displacement for P-wave in equation (2.9) is an ellipse with major axes $|\Re\boldsymbol{\xi}|$ and minor axes $|\Im\boldsymbol{\xi}|$. In a similar manner, we can show that the polarization vector for SI wave can be written as

$$\boldsymbol{\zeta}_{\mathrm{S}} = \Re\boldsymbol{\zeta}_{\mathrm{S}} + i\Im\boldsymbol{\zeta}_{\mathrm{S}} = (\Re\boldsymbol{\xi}_{\mathrm{S}} + i\Im\boldsymbol{\xi}_{\mathrm{S}}) \times \mathbf{n}. \tag{2.22}$$

As a result, for low-loss viscoelastic media the elliptical polarization takes the form

$$\boldsymbol{\xi}_{\mathrm{LP}} = \frac{\alpha_{\mathrm{E}}}{\omega}\left(\mathbf{K}_{\mathrm{LP}} + \frac{i}{2}Q_{\mathrm{P}}^{-1}\mathbf{P}_{\mathrm{LP}}\right), \tag{2.23}$$

$$\boldsymbol{\zeta}_{\mathrm{LS}} = \frac{\beta_{\mathrm{E}}}{\omega}\left(\mathbf{K}_{\mathrm{LS}} + \frac{i}{2}Q_{\mathrm{S}}^{-1}\mathbf{P}_{\mathrm{LS}}\right) \times \mathbf{n}. \tag{2.24}$$

Finally, we can redefine the displacement vectors for P- and S-waves as

$$\mathbf{U}_{\mathrm{LP}} = \boldsymbol{\xi}_{\mathrm{LP}}\Phi_0' \exp\left[-i(\mathbf{K}_{\mathrm{LP}} \cdot \mathbf{r} - \omega t)\right], \tag{2.25}$$

$$\mathbf{U}_{\mathrm{LS}} = \boldsymbol{\zeta}_{\mathrm{LS}}\Psi_0' \exp\left[-i(\mathbf{K}_{\mathrm{LS}} \cdot \mathbf{r} - \omega t)\right], \tag{2.26}$$

Where we have defined $\Phi_0' = -i\omega\Phi_0$ and $\Psi_0' = -i\omega\Psi_0$. Since we are interested in low-loss viscoelastic medium, in what follows we will ignore the subscript L for notational simplicity.

We can rewrite the parameters that describe the elliptical motion for P- and SI-waves in terms of attenuation angles and quality factors. For low-loss media, the major axis of ellipse for P-wave particle motion, takes the form

$$|\Re\boldsymbol{\xi}_{\mathrm{P}}|^2 \approx \frac{1}{2}\left(\sqrt{1 + Q_{\mathrm{P}}^{-2}\sec^2\delta_{\mathrm{P}}} + 1\right), \tag{2.27}$$

and the minor axes take the form

$$|\Im\boldsymbol{\xi}_{\mathrm{P}}|^2 \approx \frac{1}{2}\left(\sqrt{1 + Q_{\mathrm{P}}^{-2}\sec^2\delta_{\mathrm{P}}} - 1\right). \tag{2.28}$$

If wave is excited by a point source in a weakly attenuating medium, the attenuation angle is usually small (Zhu and Tsvankin, 2006b). If the attenuation vector forms an angle with the propagation vector of $0^\circ \leq \delta_{\mathrm{P}} \leq 70^\circ$ always $Q_{\mathrm{P}}^{-2}\sec^2\delta_{\mathrm{P}} \leq 0.1$, then the absolute values of the minor axes reduce to

$$|\Im\boldsymbol{\xi}_{\mathrm{P}}| = \frac{1}{2}Q_{\mathrm{P}}^{-1}\sec\delta_{\mathrm{P}}. \tag{2.29}$$

In Figure 2.1, we plot the magnitude of the minor axis of the ellipse of the P-wave particle motion for the inhomogeneous P-wave vs. the attenuation angle δ (which varies from 0°-70°). We repeat the plot for three values of reciprocal Q_{P}. The curves indicate that for fixed material parameter values, $|\Im\boldsymbol{\xi}_{\mathrm{P}}|$ increases with increasing degree of inhomogeneity, but this increase is very small at small values of δ. For degrees of inhomogeneity of greater than 70 degrees the magnitude of the minor axis is significant for high absorption ($Q_{\mathrm{P}}^{-1} > 0.1$). When $\delta_{\mathrm{P}} = 0$, the wave is homogeneous and the elliptical motion degenerates into linear motion in the direction of propagation of the homogeneous wave. For high degrees of inhomogeneity

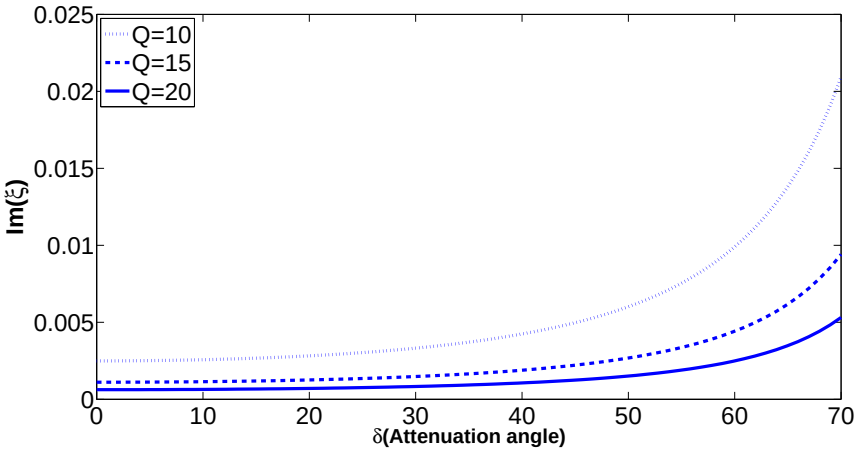

Figure 2.1: Magnitude of the minor axes of the elliptical motion for an inhomogeneous wave in a low-loss viscoelastic media versus attenuation angle δ for three values of reciprocal quality factor.

($\delta_{\mathrm{P}} \to 90°$) equation (2.29) is not satisfied. In this limit, $Q_{\mathrm{P}}^{-1} \sec \delta_{\mathrm{P}} \gg 1$, so the minor and major axes are equal:

$$|\Im \boldsymbol{\xi}_{\mathrm{P}}| \approx |\Re \boldsymbol{\xi}_{\mathrm{P}}| \approx \sqrt{\frac{1}{2} Q_{\mathrm{P}}^{-1} \sec \delta_{\mathrm{P}}}. \tag{2.30}$$

In this case polarization for inhomogeneous waves is circular.

Next, we assume that $\boldsymbol{\Psi}_0$ is not simply a complex number multiplied by a real unit vector but is a complex vector in the xz-plane. In this case, the corresponding wave is considered to be of SII-type (sometimes referred to as a linear S-wave). The particle motion for SII-wave is linear for both homogeneous and inhomogeneous waves and perpendicular to the wavevector $\mathbf{K}_{\mathrm{S}}$. In this case the displacement vector takes the form

$$\mathbf{U}_{\mathrm{SII}} = \mathbf{y} \left\{ \mathbf{K}_{\mathrm{S}} \cdot (\Psi_{0z} \mathbf{x} - \Psi_{0x} \mathbf{z}) \right\} e^{i(-\mathbf{K}_{\mathrm{S}} \cdot \mathbf{r} + \omega t)}. \tag{2.31}$$

Equation (2.31) indicates that the particle motion for SII-wave is linear perpendicular to the $(\mathbf{P}_{\mathrm{S}} - \mathbf{A}_{\mathrm{S}})$-plane.

2.4 The viscoelastic scattering operator and potentials

We next extend the elastic scattering theoretical framework of Stolt and Weglein (2012) to accommodate the preceding viscoelastic quantities. We build on the above framework,

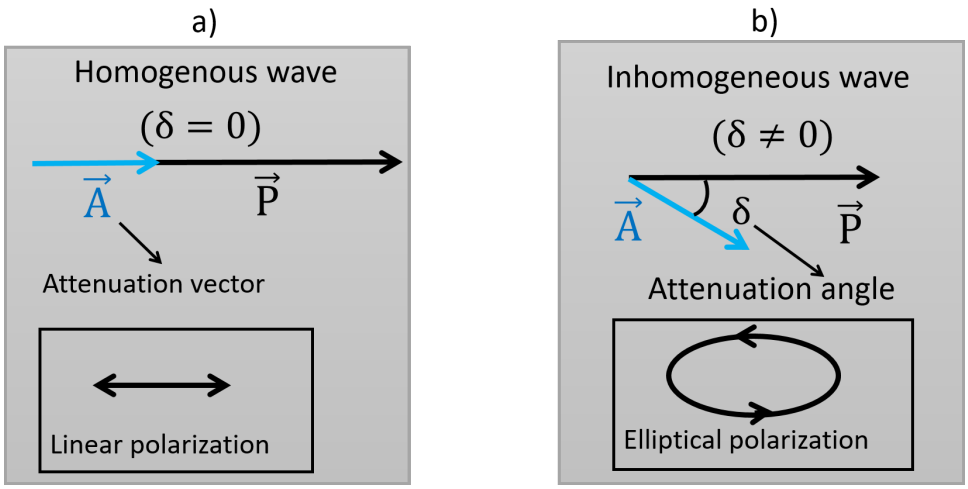

Figure 2.2: a) Homogeneous wave with propagation and attenuation vectors in the same direction ($\delta = 0$). b) Inhomogeneous wave with none zero attenuation angle between the propagation and attenuation vectors ($\delta \neq 0$.)

formulating a description of scattering of homogeneous and inhomogeneous seismic waves from arbitrary viscoelastic heterogeneities in the Earth. Scattering theory is a framework within which various kinds of interactions of waves and particles can be analyzed. In the context of seismic exploration, scattering theory relates perturbations in the properties of the medium to the seismic waves that propagate through those perturbations (Weglein et al., 2003). The perturbations are assembled, along with reference medium properties, in a core quantity called the scattering operator, the construction of which for viscoelastic waves will be the subject of this section.

The Born approximation is a solution accurate to first order in the scattering operator, and is used as the basis for many types of migration and linearized inversion in seismic applications (Bleistein, 1979; Clayton and Stolt, 1981; Beylkin, 1985). Mapping between the scattering operator and the Born approximate model of seismic data usually involves integrating the product of the scattering operator with Green's functions, whose role is to model wave propagation through the smooth parts of the Earth model. In this framework the scattering operator studied in isolation provides insight into the physics of the interactions of the wave with rapidly varying parts of the Earth. In this section we arrive at interpretable forms of the viscoelastic scattering operator, including explicit expressions for the elements

of the operator. Each element will represent the potential of a point in space to scatter a P to a P wave, a P to an SI wave, etc. Then we will be in a position to analyze the viscoelastic scattering problem for general insights.

2.4.1 The scattering operator in displacement space

In the scattering framework, the unperturbed medium is a reference medium and the perturbed medium is associated with the actual medium. The difference between the actual and reference medium wave operators is the perturbation operator or scattering operator (figure 2.3). In the elastic-isotropic case, this operator can be expressed in terms of a 3×3 matrix, each element of which corresponds to the scattering of one wave type to another. The diagonal elements refer to scattering which conserves wave type, and off-diagonal elements refer to the those which convert wave type. In viscoelastic case, the wave operator is complex, as a result we have the differences in complex quantities. However we do not define the perturbation in complex quantities explicitly, but we define the perturbation in real physical quantities (Appendix A). To begin the process of form a viscoelastic scattering operator, we express the viscoelastic wave equation as

$$L_{\mathrm{VE}}(\mathbf{r},\omega)\mathbf{U}(\mathbf{r},\omega) = 0. \tag{2.32}$$

Here the wave operator in Cartesian coordinates is

$$L_{\mathrm{VE}} = \begin{pmatrix} L_{xx} & L_{xy} & L_{xz} \\ L_{yx} & L_{yy} & L_{yz} \\ L_{zx} & L_{zy} & L_{zz} \end{pmatrix}, \tag{2.33}$$

with the elements

$$(L_{\mathrm{VE}})_{ij} = \rho\omega^2\delta_{ij} + \partial_i(\rho\alpha^2)\partial_j + \delta_{ij}\partial_k(\rho\beta^2)\partial_k - 2\partial_i(\rho\beta^2)\partial_j + \partial_j(\rho\beta^2)\partial_i, \tag{2.34}$$

for $i, j, k = x, y, z$. In the above equation we used the sum rule notation. The P- and S-wave velocities are defined as

$$\alpha = \sqrt{\rho^{-1}\left(\mathsf{K} + \frac{4\mathsf{M}}{3}\right)}, \tag{2.35}$$

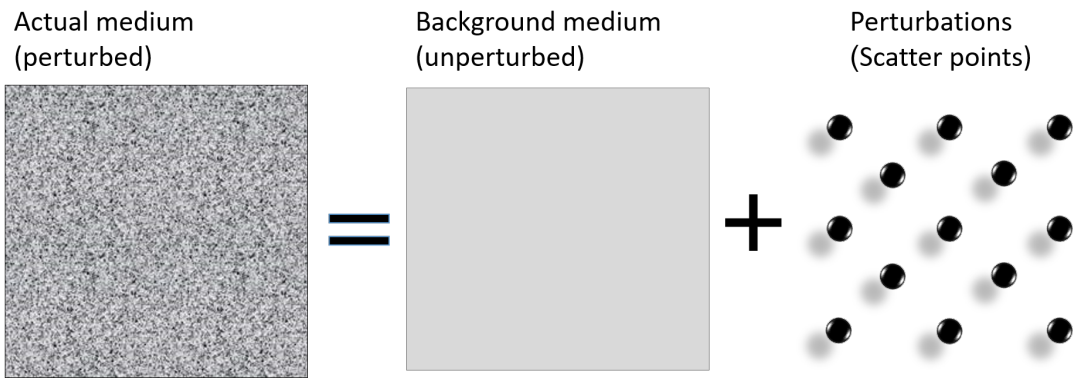

Figure 2.3: Schematic breakdown of actual medium into reference medium and perturbations.

and

$$\beta = \sqrt{\rho^{-1}\mathsf{M}}, \tag{2.36}$$

where ρ is the mass density, and M and K are viscoelastic moduli which are generally complex and frequency dependent. The scattering matrix is the difference between perturbed and unperturbed wave operators of the type in equation (2.33):

$$V_{\mathrm{VE}}(\mathbf{r},\omega) = L_{\mathrm{VE}}(\mathbf{r},\omega) - L_{\mathrm{VE0}}(\mathbf{r},\omega) = \begin{pmatrix} V_{xx} & V_{xy} & V_{xz} \\ V_{yx} & V_{yy} & V_{yz} \\ V_{zx} & V_{zy} & V_{zz} \end{pmatrix}, \tag{2.37}$$

where subscript "0" denotes the reference medium.

We restrict ourselves to scattering in locally isotropic viscoelastic medium. The fractional variation in density, velocities and quality factors for S and P-waves are

$$A_\tau = \frac{\tau - \tau_0}{\tau} \ll 1, \tag{2.38}$$

where $\tau = \rho, \alpha_{\mathrm{E}}, \beta_{\mathrm{E}}, Q_{\mathrm{P}}, Q_{\mathrm{S}}$. Furthermore using equations (2.7) and (2.8), we can write

$$\rho\alpha^2 - \rho_0\alpha_0^2 = \rho_0\alpha_0^2(A_\rho + 2A_{\alpha_{\mathrm{E}}} - iQ_{\mathrm{P0}}^{-1}A_{Q_{\mathrm{P}}}) \tag{2.39}$$

and

$$\rho\beta^2 - \rho_0\beta_0^2 = \rho_0\beta_0^2(A_\rho + 2A_{\beta_{\mathrm{E}}} - iQ_{\mathrm{S0}}^{-1}A_{Q_{\mathrm{S}}}). \tag{2.40}$$

The elements of the scattering potential, in terms of these perturbations, are

$$\rho_0^{-1}(V_{\mathrm{VE}}^{\rho})_{kl} = A_\rho\omega^2\delta_{kl} + \alpha_0^2\partial_k A_\rho\partial_l + \beta_0^2\left(\delta_{kl}\partial_m A_\rho\partial_m - 2\partial_k A_\rho\partial_l + \partial_l A_\rho\partial_k\right), \tag{2.41}$$

$$\rho_0^{-1}(V_{\mathrm{VE}}^{\alpha_{\mathrm{E}}})_{kl} = 2\alpha_0^2 \partial_k A_{\alpha_{\mathrm{E}}} \partial_l, \tag{2.42}$$

$$\rho_0^{-1}(V_{\mathrm{VE}}^{\beta_{\mathrm{E}}})_{kl} = 2\beta_0^2 \left(\delta_{kl}\partial_m A_{\beta_{\mathrm{E}}} \partial_m - 2\partial_k A_{\beta_{\mathrm{E}}} \partial_l + \partial_l A_{\beta_{\mathrm{E}}} \partial_k\right), \tag{2.43}$$

$$\rho_0^{-1}(V_{\mathrm{VE}}^{Q_{\mathrm{P}}})_{kl} = -i\alpha_0^2 Q_{\mathrm{P}0}^{-1} \partial_k A_{QP} \partial_l, \tag{2.44}$$

and

$$\rho_0^{-1}(V_{\mathrm{VE}}^{Q_{\mathrm{S}}})_{kl} = -i\beta_0^2 Q_{\mathrm{S}0}^{-1} \left(\delta_{kl}\partial_m A_{Q_{\mathrm{S}}} \partial_m - 2\partial_k A_{Q_{\mathrm{S}}} \partial_l + \partial_l A_{Q_{\mathrm{S}}} \partial_k\right), \tag{2.45}$$

where we have defined

$$V_{\mathrm{VE}} = V_{\mathrm{VE}}^{\rho} + V_{\mathrm{VE}}^{\alpha_{\mathrm{E}}} + V_{\mathrm{VE}}^{\beta_{\mathrm{E}}} + V_{\mathrm{VE}}^{Q_{\mathrm{P}}} + V_{\mathrm{VE}}^{Q_{\mathrm{S}}}. \tag{2.46}$$

2.4.2 The scattering operator in P, SI and SII space

The next task is to evaluate the scattering matrix in a coordinate system which naturally describes Borcherdt's viscoelastic modes $\mathrm{P}, \mathrm{SI}, \mathrm{SII}$, namely

$$\mathcal{V}_{\mathrm{VE}} = \begin{pmatrix} {}^{\mathrm{P}}_{\mathrm{P}}\mathcal{V}_{\mathrm{VE}} & {}^{\mathrm{P}}_{\mathrm{SII}}\mathcal{V}_{\mathrm{VE}} & {}^{\mathrm{P}}_{\mathrm{SI}}\mathcal{V}_{\mathrm{VE}} \\ {}^{\mathrm{SII}}_{\mathrm{P}}\mathcal{V}_{\mathrm{VE}} & {}^{\mathrm{SII}}_{\mathrm{SII}}\mathcal{V}_{\mathrm{VE}} & {}^{\mathrm{SII}}_{\mathrm{SI}}\mathcal{V}_{\mathrm{VE}} \\ {}^{\mathrm{SI}}_{\mathrm{P}}\mathcal{V}_{\mathrm{VE}} & {}^{\mathrm{SI}}_{\mathrm{SII}}\mathcal{V}_{\mathrm{VE}} & {}^{\mathrm{SI}}_{\mathrm{SI}}\mathcal{V}_{\mathrm{VE}} \end{pmatrix}. \tag{2.47}$$

Here, as in the original elastic-isotropic theory of Stolt and Weglein (2012), the diagonal elements represent scattering which preserves the wave types and off-diagonal elements refer to scattering which converts the type of waves. For example, ${}^{\mathrm{P}}_{\mathrm{SI}}\mathcal{V}_{\mathrm{VE}}$ represents the potential of a scattering point to convert a P-wave into an SI-type wave. Some elements are identically zero, for instance ${}^{\mathrm{P}}_{\mathrm{SII}}\mathcal{V}_{\mathrm{VE}} = 0$, as we shall show presently. This means that a P-wave with elliptical polarization cannot convert into an SII wave with linear polarization. Since the particle motion for SII-type wave is in the $\mathbf{n}$ direction we can define the normal polarization vector in this direction.

Now, the scattering potential in displacement space can be written (Beylkin and Burridge, 1990)

$${}^{\mathrm{I}}_{\mathrm{R}}\mathcal{V}_{\mathrm{VE}} = \boldsymbol{\xi}_{\mathrm{I}}^T V_{\mathrm{VE}} \boldsymbol{\xi}_{\mathrm{R}}. \tag{2.48}$$

Here $\boldsymbol{\xi}$ is the polarization vector, V_{VE} is the scattering operator and subscripts I and R respectively refer to the incident and reflected waves. Each type of displacement is determined by two angles, σ and δ, which indicate the directions of propagation and attenuation. The vectors $\mathbf{P}_i$ and $\mathbf{A}_i$ (propagation and attenuation vectors for the incident wave) point towards the scatterer while the vectors $\mathbf{P}_r$ and $\mathbf{A}_r$ for the reflected waves point away from the scatterer. Without loss of generality we assume that the incident propagation vector is in the z-direction, so the reflected and incident propagation and attenuation vectors can be written as

$$\mathbf{P}_r = \frac{\omega}{V_{\mathrm{E}}}(\mathbf{x}\sin\sigma - \mathbf{z}\cos\sigma), \tag{2.49}$$

$$\mathbf{P}_i = \frac{\omega}{V_{\mathrm{E}}}\mathbf{z}, \tag{2.50}$$

$$\mathbf{A}_r = \frac{\omega}{2V_{\mathrm{E}}}Q^{-1}(\mathbf{x}\sin\sigma - \mathbf{z}\cos\sigma - \tan\delta_r(\mathbf{x}\cos\sigma + \mathbf{z}\sin\sigma)), \tag{2.51}$$

$$\mathbf{A}_i = \frac{\omega}{2V_{\mathrm{E}}}Q^{-1}(\mathbf{z} - \mathbf{x}\tan\delta_i). \tag{2.52}$$

Here σ, with $0^\circ < \sigma < 180^\circ$, denotes the opening angle between the incident and reflected propagation vectors and δ_r and δ_i are the angles between the attenuation and propagation vectors for reflected and incident waves respectively, $\mathbf{x}$ is the unit vector in x-direction and $\mathbf{z}$ is the unit vector in z-direction. In addition V_{E} refers to elastic velocities α_{E} and β_{E}. The angle that the attenuation vector makes with the z-axis is $\sigma - \delta$. Regarding the displacements, for inhomogeneous P- and SI-waves, the polarization vectors display an elliptical motion in the x-z plane. In the homogeneous case P-wave particle motion is in the direction of the propagation vector $\mathbf{P}$ and for SI-waves is a unit vector in the direction of $\mathbf{P} \times \mathbf{y}$. For SII-waves for both inhomogeneous and homogeneous waves the polarization is linear in the y-direction. The polarizations vectors for incident and reflected P-waves using the propagation and attenuation vectors are given by

$$\boldsymbol{\xi}_{\mathrm{P}i} = \mathbf{z} + \mathbf{x}\frac{i}{2}Q_{\mathrm{P}}^{-1}\tan\delta_{\mathrm{P}i}, \tag{2.53}$$

$$\boldsymbol{\xi}_{\mathrm{P}r} = [\mathbf{x}\sin\sigma - \mathbf{z}\cos\sigma] + \frac{i}{2}Q_{\mathrm{P}}^{-1}\tan\delta_{\mathrm{P}r}\left[\mathbf{x}\cos\sigma + \mathbf{z}\sin\sigma\right]. \tag{2.54}$$

The slowness vectors for incident and reflected waves are

$$\mathbf{k}_{\mathrm{P}i} = \frac{\mathbf{K}_{\mathrm{P}i}}{\omega} = \frac{1}{\alpha_{\mathrm{E}}}\left(\mathbf{z} - \frac{i}{2}Q_{\mathrm{P}}^{-1}\left[\mathbf{z} - \mathbf{x}\tan\delta_{\mathrm{P}i}\right]\right), \tag{2.55}$$

$$\mathbf{k}_{\mathrm{P}r} = \frac{\mathbf{K}_{\mathrm{P}r}}{\omega} = \frac{1}{\alpha_{\mathrm{E}}}\left[\mathbf{x}\sin\sigma - \mathbf{z}\cos\sigma\right] -$$

$$\frac{i}{2\alpha_{\mathrm{E}}}Q_{\mathrm{P}}^{-1}\left[\mathbf{x}\sin\sigma - \mathbf{z}\cos\sigma - \tan\delta_{\mathrm{P}r}(\mathbf{x}\cos\sigma + \mathbf{z}\sin\sigma)\right]. \tag{2.56}$$

In this case the polarizations for incident and reflected SI waves are given by

$$\boldsymbol{\zeta}_{\mathrm{S}i} = -\mathbf{x} + \mathbf{z}\frac{i}{2}Q_{\mathrm{S}}^{-1}\tan\delta_{\mathrm{S}i}, \tag{2.57}$$

$$\boldsymbol{\zeta}_{\mathrm{S}r} = \left[\mathbf{z}\sin\sigma + \mathbf{x}\cos\sigma\right] + \frac{i}{2}Q_{\mathrm{S}}^{-1}\tan\delta_{\mathrm{S}r}\left[\mathbf{z}\cos\sigma - \mathbf{x}\sin\sigma\right]. \tag{2.58}$$

The slowness vectors for incident and reflected waves are

$$\mathbf{k}_{\mathrm{S}i} = \frac{\mathbf{K}_{\mathrm{S}i}}{\omega} = \frac{1}{\beta_{\mathrm{E}}}\left(\mathbf{z} - \frac{i}{2}Q_{\mathrm{S}}^{-1}\left[\mathbf{z} - \mathbf{x}\tan\delta_{\mathrm{S}i}\right]\right), \tag{2.59}$$

$$\mathbf{k}_{\mathrm{S}r} = \frac{\mathbf{K}_{\mathrm{S}r}}{\omega} = \frac{1}{\beta_{\mathrm{E}}}\left[\mathbf{x}\sin\sigma - \mathbf{z}\cos\sigma\right] -$$

$$\frac{i}{2\beta_{\mathrm{E}}}Q_{\mathrm{S}}^{-1}\left[\mathbf{x}\sin\sigma - \mathbf{z}\cos\sigma - \tan\delta_{\mathrm{S}r}(\mathbf{x}\cos\sigma + \mathbf{z}\sin\sigma)\right]. \tag{2.60}$$

2.5 Elements of the P-SI-SII scattering matrix

We next write the scattering matrix element in frequency-independent form (Stolt and Weglein, 2012). Since the differential operators are sandwiched between unperturbed Green's functions, we replace the left derivatives with i multiplied by the reflected wavevector $\mathbf{K}_r$ and right derivative with i multiplied by the incident wavevector $\mathbf{K}_i$. After replacing the left and right derivatives by the appropriate wavevectors, the frequency independent scattering potential is given by

$$\frac{V_{\mathrm{VE}}}{\rho_0\omega^2} = \mathbb{V}_{\mathrm{VE}} = \mathbb{V}_{\mathrm{VE}}^{\rho}A_{\rho} + \mathbb{V}_{\mathrm{VE}}^{\alpha_{\mathrm{E}}}A_{\alpha_{\mathrm{E}}} + \mathbb{V}_{\mathrm{VE}}^{\beta_{\mathrm{E}}}A_{\beta_{\mathrm{E}}} + \mathbb{V}_{\mathrm{VE}}^{Q_{\mathrm{P}}}A_{Q_{\mathrm{P}}} + \mathbb{V}_{\mathrm{VE}}^{Q_{\mathrm{S}}}A_{Q_{\mathrm{S}}}, \tag{2.61}$$

with the following components

$$(\mathbb{V}_{\mathrm{VE}}^{\rho})_{kl} = \delta_{kl} - \alpha_0^2 k_k^r k_l^i - \beta_0^2\left(\delta_{kl}k_m^r k_m^i - 2k_k^r k_l^i + k_l^r k_k^i\right), \tag{2.62}$$

$$(\mathbb{V}_{\mathrm{VE}}^{\alpha_{\mathrm{E}}})_{kl} = -2\alpha_0^2 k_k^r k_l^i, \tag{2.63}$$

$$(\mathbb{V}_{\mathrm{VE}}^{\beta_{\mathrm{E}}})_{kl} = -2\beta_0^2\left(\delta_{kl}k_m^r k_m^i - 2k_k^r k_l^i + k_l^r k_k^i\right), \tag{2.64}$$

$$(\mathbb{V}_{\mathrm{VE}}^{Q_{\mathrm{P}}})_{kl} = iQ_{\mathrm{P}0}^{-1}\alpha_0^2 k_k^r k_l^i, \tag{2.65}$$

and

$$(\mathbb{V}_{\mathrm{VE}}^{Q_{\mathrm{S}}})_{kl} = iQ_{\mathrm{S}0}^{-1}\beta_0^2 \left(\delta_{kl}k_m^r k_m^i - 2k_k^r k_l^i + k_l^r k_k^i\right). \tag{2.66}$$

Now to obtain the scattering matrix we sandwich the above expressions with the proper polarization vectors. We use the vectors $\mathbf{R}$ and $\mathbf{I}$ to indicate the reflected and incident polarization vectors, respectively. For perturbation terms we will write

$${}_{\mathrm{R}}^{\mathrm{I}}\mathbb{V}_{\mathrm{VE}}^{\rho} = {}_{\mathrm{R}}^{\mathrm{I}}\mathcal{F} - {}_{\mathrm{R}}^{\mathrm{I}}\mathcal{G}_{\alpha} - {}_{\mathrm{R}}^{\mathrm{I}}\mathcal{G}_{\beta}, \tag{2.67}$$

$${}_{\mathrm{R}}^{\mathrm{I}}\mathbb{V}_{\mathrm{VE}}^{Q_{\mathrm{P}}} = -\frac{i}{2}Q_{\mathrm{P}0}^{-1}\left\{{}_{\mathrm{R}}^{\mathrm{I}}\mathbb{V}_{\mathrm{VE}}^{\alpha_{\mathrm{E}}}\right\} = \left(iQ_{\mathrm{P}0}^{-1}\right){}_{\mathrm{R}}^{\mathrm{I}}\mathcal{G}_{\alpha}, \tag{2.68}$$

$${}_{\mathrm{R}}^{\mathrm{I}}\mathbb{V}_{\mathrm{VE}}^{Q_{\mathrm{S}}} = -\frac{i}{2}Q_{\mathrm{S}0}^{-1}\left\{{}_{\mathrm{R}}^{\mathrm{I}}\mathbb{V}_{\mathrm{VE}}^{\beta_{\mathrm{E}}}\right\} = \left(iQ_{\mathrm{S}0}^{-1}\right){}_{\mathrm{R}}^{\mathrm{I}}\mathcal{G}_{\beta}, \tag{2.69}$$

where we have defined

$${}_{\mathrm{R}}^{\mathrm{I}}\mathcal{F} = \mathbf{R}\cdot\mathbf{I}, \tag{2.70}$$

$${}_{\mathrm{R}}^{\mathrm{I}}\mathcal{G}_{\alpha} = \alpha_0^2(\mathbf{R}\cdot\mathbf{k}_r)(\mathbf{I}\cdot\mathbf{k}_i), \tag{2.71}$$

$${}_{\mathrm{R}}^{\mathrm{I}}\mathcal{G}_{\beta} = \beta_0^2\left\{(\mathbf{R}\cdot\mathbf{I})(\mathbf{k}_r\cdot\mathbf{k}_i) - 2(\mathbf{R}\cdot\mathbf{k}_r)(\mathbf{I}\cdot\mathbf{k}_i) + (\mathbf{I}\cdot\mathbf{k}_r)(\mathbf{R}\cdot\mathbf{k}_i)\right\}. \tag{2.72}$$

To determine the explicit forms for each component of the scattering potential, we need to calculate ${}_{\mathrm{R}}^{\mathrm{I}}\mathcal{F}$, ${}_{\mathrm{R}}^{\mathrm{I}}\mathcal{G}_{\alpha}$ and ${}_{\mathrm{R}}^{\mathrm{I}}\mathcal{G}_{\beta}$.

2.5.1 Viscoelastic P-P scattering

This element quantifies the potential for a point in a viscoelastic medium to scatter a P-wave into a P-wave. The incident and reflected P-waves can be either inhomogeneous with elliptical motion or homogeneous with linear motion in the direction of propagation, depending on the angle between the propagation and attenuation vectors. In this case incident and reflected waves are P-waves, $\mathbf{R} = \boldsymbol{\xi}_{\mathrm{P}r}$ and $\mathbf{I} = \boldsymbol{\xi}_{\mathrm{P}i}$, and so we have

$${}_{\mathrm{P}}^{\mathrm{P}}\mathcal{F} = \boldsymbol{\xi}_{\mathrm{P}r}\cdot\boldsymbol{\xi}_{\mathrm{P}i}, \tag{2.73}$$

$${}_{\mathrm{P}}^{\mathrm{P}}\mathcal{G}_{\alpha} = \alpha_0^2(\boldsymbol{\xi}_{\mathrm{P}r}\cdot\mathbf{k}_{\mathrm{P}r})(\boldsymbol{\xi}_{\mathrm{P}i}\cdot\mathbf{k}_{\mathrm{P}i}), \tag{2.74}$$

$${}_{\mathrm{P}}^{\mathrm{P}}\mathcal{G}_{\beta} = \beta_0^2\left\{(\boldsymbol{\xi}_{\mathrm{P}r}\cdot\boldsymbol{\xi}_{\mathrm{P}i})(\mathbf{k}_{\mathrm{P}r}\cdot\mathbf{k}_{\mathrm{P}i}) - 2(\boldsymbol{\xi}_{\mathrm{P}r}\cdot\mathbf{k}_{\mathrm{P}r})(\boldsymbol{\xi}_{\mathrm{P}i}\cdot\mathbf{k}_{\mathrm{P}i}) + (\boldsymbol{\xi}_{\mathrm{P}i}\cdot\mathbf{k}_{\mathrm{P}r})(\boldsymbol{\xi}_{\mathrm{P}r}\cdot\mathbf{k}_{\mathrm{P}i})\right\}. \tag{2.75}$$

Using the dot products of various types of polarizations and slowness vectors we have

$$\boldsymbol{\xi}_{\mathrm{P}r} \cdot \boldsymbol{\xi}_{\mathrm{P}i} = -\cos\sigma + \frac{i}{2} Q_{\mathrm{P}0}^{-1} \sin\sigma \left(\tan\delta_{\mathrm{P}r} + \tan\delta_{\mathrm{P}i}\right), \tag{2.76}$$

$$\boldsymbol{\xi}_{\mathrm{P}r} \cdot \mathbf{k}_{\mathrm{P}r} = \boldsymbol{\xi}_{\mathrm{P}i} \cdot \mathbf{k}_{\mathrm{P}i} = \frac{1}{\alpha_{\mathrm{E}0}} \left(1 - \frac{i}{2} Q_{\mathrm{P}0}^{-1}\right), \tag{2.77}$$

$$\boldsymbol{\xi}_{\mathrm{P}r} \cdot \mathbf{k}_{\mathrm{P}i} = \boldsymbol{\xi}_{\mathrm{P}i} \cdot \mathbf{k}_{\mathrm{P}r} = \frac{1}{\alpha_{\mathrm{E}0}} \left\{ -\cos\sigma \left(1 - \frac{i}{2} Q_{\mathrm{P}0}^{-1}\right) + \frac{i}{2} Q_{\mathrm{P}0}^{-1} \sin\sigma \left(\tan\delta_{\mathrm{P}r} + \tan\delta_{\mathrm{P}i}\right) \right\}, \tag{2.78}$$

$$\mathbf{k}_{\mathrm{P}r} \cdot \mathbf{k}_{\mathrm{P}i} = \frac{1}{\alpha_{\mathrm{E}0}^2} \left[-\cos\sigma \left(1 - i Q_{\mathrm{P}0}^{-1}\right) + \frac{i}{2} Q_{\mathrm{P}0}^{-1} \sin\sigma \left(\tan\delta_{\mathrm{P}r} + \tan\delta_{\mathrm{P}i}\right) \right]. \tag{2.79}$$

The scattering potential for PP mode is

$${}_{\mathrm{P}}^{\mathrm{P}}\mathbb{V}_{\mathrm{VE}} = {}_{\mathrm{P}}^{\mathrm{P}}\mathbb{V}_{\mathrm{E}} + i {}_{\mathrm{P}}^{\mathrm{P}}\mathbb{V}_{\mathrm{AE}}, \tag{2.80}$$

where elastic scattering potential ${}_{\mathrm{P}}^{\mathrm{P}}\mathbb{V}_{\mathrm{E}}$ is given by

$${}_{\mathrm{P}}^{\mathrm{P}}\mathbb{V}_{\mathrm{E}} = \left[-1 - \cos\sigma + 2 \left(\frac{\beta_{\mathrm{E}0}}{\alpha_{\mathrm{E}0}}\right)^2 \sin^2\sigma \right] A_\rho + 4 \left[\left(\frac{\beta_{\mathrm{E}0}}{\alpha_{\mathrm{E}0}}\right)^2 \sin^2\sigma \right] A_\beta - 2 A_\alpha \tag{2.81}$$

and anelastic part of the scattering

$${}_{\mathrm{P}}^{\mathrm{P}}\mathbb{V}_{\mathrm{AE}} = {}_{\mathrm{P}}^{\mathrm{P}}\mathbb{V}_{\mathrm{AE}}^{\rho} A_\rho + {}_{\mathrm{P}}^{\mathrm{P}}\mathbb{V}_{\mathrm{AE}}^{\beta} A_\beta + {}_{\mathrm{P}}^{\mathrm{P}}\mathbb{V}_{\mathrm{AE}}^{Q_{\mathrm{S}}} A_{Q_{\mathrm{S}}} + {}_{\mathrm{P}}^{\mathrm{P}}\mathbb{V}_{\mathrm{AE}}^{Q_{\mathrm{P}}} A_{Q_{\mathrm{P}}} \tag{2.82}$$

with

$${}_{\mathrm{P}}^{\mathrm{P}}\mathbb{V}_{\mathrm{AE}}^{\rho} = 2 \left(\frac{\beta_{\mathrm{E}0}}{\alpha_{\mathrm{E}0}}\right)^2 \left\{ \sin^2\sigma (Q_{\mathrm{S}0}^{-1} - Q_{\mathrm{P}0}^{-1}) + Q_{\mathrm{P}0}^{-1} \left[\sin 2\sigma + \frac{1}{2} \left(\frac{\alpha_{\mathrm{E}0}}{\beta_{\mathrm{E}0}}\right)^2 \sin\sigma \right] \tan\delta_{\mathrm{P}} \right\} \tag{2.83}$$

$${}_{\mathrm{P}}^{\mathrm{P}}\mathbb{V}_{\mathrm{AE}}^{\beta} = 4 \left(\frac{\beta_{\mathrm{E}0}}{\alpha_{\mathrm{E}0}}\right)^2 \left\{ \sin^2\sigma (Q_{\mathrm{S}0}^{-1} - Q_{\mathrm{P}0}^{-1}) + Q_{\mathrm{P}0}^{-1} \sin 2\sigma \tan\delta_{\mathrm{P}} \right\} \tag{2.84}$$

$${}_{\mathrm{P}}^{\mathrm{P}}\mathbb{V}_{\mathrm{AE}}^{Q_{\mathrm{S}}} = -2 Q_{\mathrm{S}0}^{-1} \left(\frac{\beta_{\mathrm{E}0}}{\alpha_{\mathrm{E}0}}\right)^2 \sin^2\sigma \tag{2.85}$$

$${}_{\mathrm{P}}^{\mathrm{P}}\mathbb{V}_{\mathrm{AE}}^{Q_{\mathrm{P}}} = Q_{\mathrm{P}0}^{-1} \tag{2.86}$$

In above equations we used the average attenuation angle $\delta_{\mathrm{P}} = (\delta_{\mathrm{P}r} + \delta_{\mathrm{P}i})/2$. From equation (2.80) it is evident that the viscoelastic scattering potential is complex. The real part is the elastic scattering potential and the imaginary part is the term induced by the anelasticity of the medium. Let us consider as a special case the situation that the incident and reflected waves are homogeneous. In this case (2.83) and (2.84) reduce to

$${}_{\mathrm{P}}^{\mathrm{P}}\mathbb{V}_{\mathrm{AE}}^{\beta} = 2 \left({}_{\mathrm{P}}^{\mathrm{P}}\mathbb{V}_{\mathrm{AE}}^{\rho}\right) = 4 \left(\frac{\beta_{\mathrm{E}0}}{\alpha_{\mathrm{E}0}}\right)^2 (Q_{\mathrm{S}0}^{-1} - Q_{\mathrm{P}0}^{-1}) \sin^2\sigma. \tag{2.87}$$

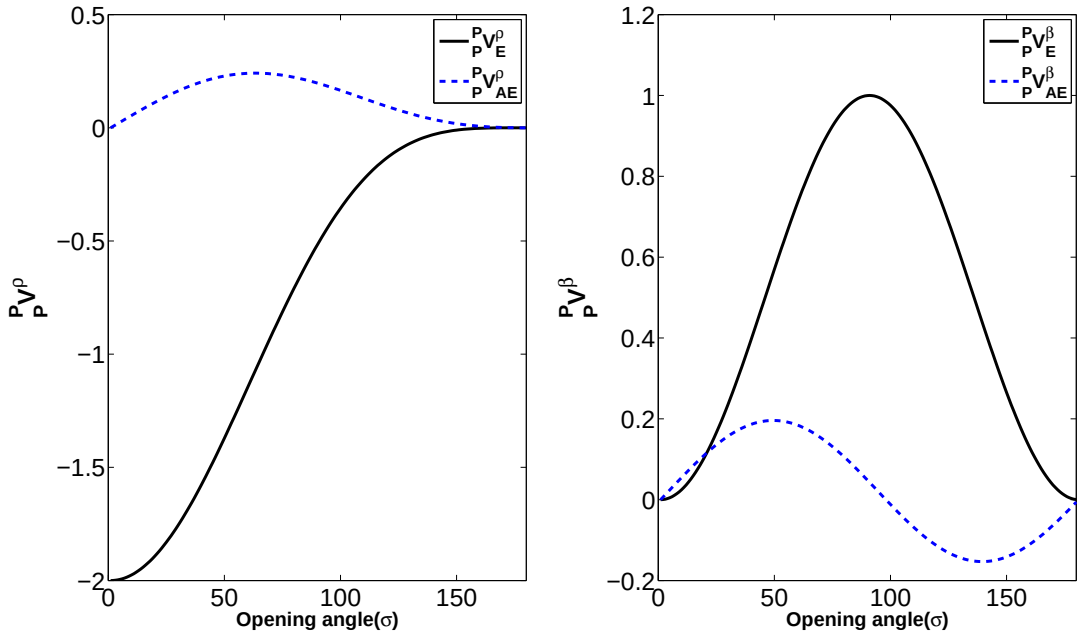

Figure 2.4: Elastic and anelastic density(left) and S-wave velocity(right) components of the viscoelastic potential for scattering of incident inhomogeneous P-wave to inhomogeneous reflected P-wave versus of reflected wave angle σ, for $\delta_{\mathrm{P}} = 60°$. Quality factor of P-wave for reference medium is to be 10 and for S-wave is 7. Also the S-to P-wave velocity ratio for reference medium is chosen to be 1/2. Dash line is for anelastic part and solid line for elastic part.

Here the angle dependences of density, S-wave velocity and S-wave quality factor are the same. As a result the scattering patterns for these three parts are the same. In Figure 2.4 we plot the elastic and anelastic parts of the density and S-wave velocity components of the potential for scattering of an inhomogeneous P-wave to an inhomogeneous P-wave. We observe that the anelastic density component is comparatively small and the major contribution comes from the elastic part. In the limit of normal incidence ($\sigma = 0$), where incident and reflected propagation vectors are in the opposite direction, the absolute value of the density part of the elastic scattering potential goes to its maximum value, and the anelastic part approaches zero. For S-wave velocity component of the scattering potential, similar to the density component, the major contribution to the reflectivity is from the elastic part. In this case both elastic and anelastic components approach zero for normal incidence as expected.

2.5.2 Viscoelastic P-SI scattering

In this case the reflected wave is of type SI, $\mathbf{R} = \boldsymbol{\zeta}_{\mathrm{S}r}$, and the incident wave is a P-wave, $\mathbf{I} = \boldsymbol{\xi}_{\mathrm{P}i}$. We have

$$\overset{\mathrm{P}}{_{\mathrm{SI}}}\mathcal{F} = \boldsymbol{\zeta}_{\mathrm{S}r} \cdot \boldsymbol{\xi}_{\mathrm{P}i} \tag{2.88}$$

$$\overset{\mathrm{P}}{_{\mathrm{SI}}}\mathcal{G}_{\alpha} = \alpha_0^2 (\boldsymbol{\zeta}_{\mathrm{S}r} \cdot \mathbf{k}_{\mathrm{S}r})(\boldsymbol{\xi}_{\mathrm{P}i} \cdot \mathbf{k}_{\mathrm{P}i}) \tag{2.89}$$

$$\overset{\mathrm{P}}{_{\mathrm{SI}}}\mathcal{G}_{\beta} = \beta_0^2 \left\{ (\boldsymbol{\zeta}_{\mathrm{S}r} \cdot \boldsymbol{\xi}_{\mathrm{P}i})(\mathbf{k}_{\mathrm{S}r} \cdot \mathbf{k}_{\mathrm{P}i}) - 2(\boldsymbol{\zeta}_{\mathrm{S}r} \cdot \mathbf{k}_{\mathrm{S}r})(\boldsymbol{\xi}_{\mathrm{P}i} \cdot \mathbf{k}_{\mathrm{P}i}) + (\boldsymbol{\xi}_{\mathrm{P}i} \cdot \mathbf{k}_{\mathrm{S}r})(\boldsymbol{\zeta}_{\mathrm{S}r} \cdot \mathbf{k}_{\mathrm{P}i}) \right\}. \tag{2.90}$$

The dot products of the polarization and slowness vectors can be expressed in terms of the angle of the reflected propagation vector and the angles between the propagation and attenuation vectors:

$$\boldsymbol{\zeta}_{\mathrm{S}r} \cdot \boldsymbol{\xi}_{\mathrm{P}i} = -\sin\sigma - \frac{i}{2}\cos\sigma (Q_{\mathrm{S}0}^{-1}\tan\delta_{\mathrm{S}r} + Q_{\mathrm{P}0}^{-1}\tan\delta_{\mathrm{P}i}) \tag{2.91}$$

$$\boldsymbol{\xi}_{\mathrm{P}i} \cdot \mathbf{k}_{\mathrm{S}r} = \frac{1}{\beta_{\mathrm{E}0}} \left\{ -\cos\sigma \left(1 - \frac{i}{2}Q_{\mathrm{S}0}^{-1}\right) + \frac{i}{2}\sin\sigma (Q_{\mathrm{S}0}^{-1}\tan\delta_{\mathrm{S}r} + Q_{\mathrm{P}0}^{-1}\tan\delta_{\mathrm{P}i}) \right\} \tag{2.92}$$

$$\boldsymbol{\zeta}_{\mathrm{S}r} \cdot \mathbf{k}_{\mathrm{P}i} = -\frac{1}{\alpha_{\mathrm{E}0}} \left\{ \sin\sigma \left(1 - \frac{i}{2}Q_{\mathrm{P}0}^{-1}\right) + \frac{i}{2}\cos\sigma (Q_{\mathrm{S}0}^{-1}\tan\delta_{\mathrm{S}r} + Q_{\mathrm{P}0}^{-1}\tan\delta_{\mathrm{P}i}) \right\} \tag{2.93}$$

$$\mathbf{k}_{\mathrm{S}r} \cdot \mathbf{k}_{\mathrm{P}i} = \frac{1}{\alpha_{\mathrm{E}0}\beta_{\mathrm{E}0}} \left\{ -\cos\sigma \left(1 - \frac{i}{2}(Q_{\mathrm{P}0}^{-1} + Q_{\mathrm{S}0}^{-1})\right) + \frac{i}{2}\sin\sigma (Q_{\mathrm{S}0}^{-1}\tan\delta_{\mathrm{S}r} + Q_{\mathrm{P}0}^{-1}\tan\delta_{\mathrm{P}i}) \right\}. \tag{2.94}$$

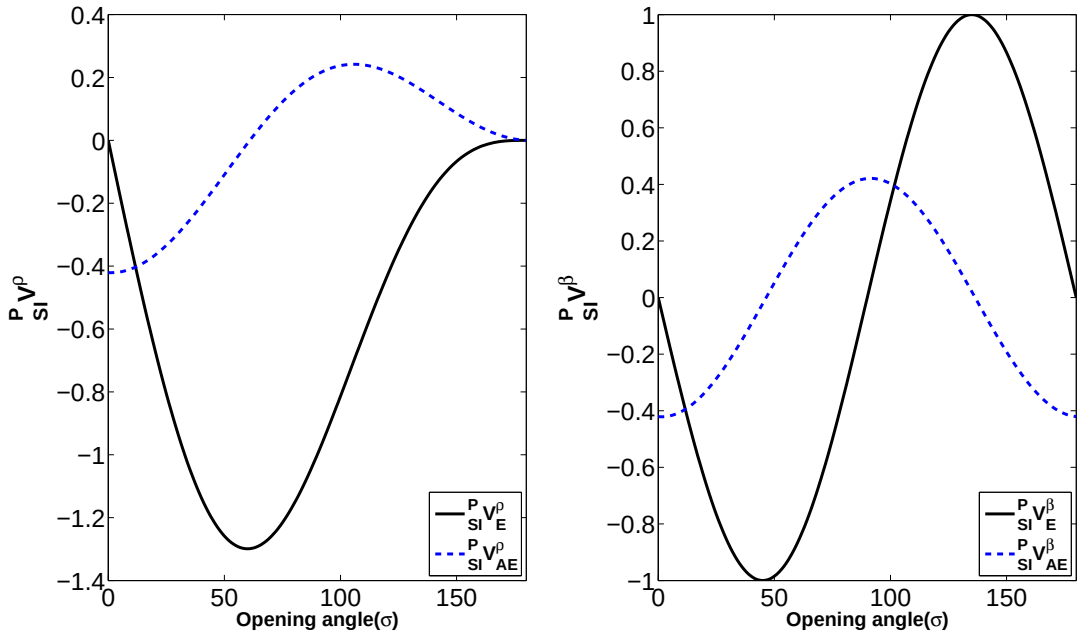

Figure 2.5: Elastic and anelastic density(left) and S-wave velocity(right) components of the viscoelastic potential for scattering of incident inhomogeneous P-wave to inhomogeneous reflected SI-wave versus of reflected wave angle σ, for $\delta_S = \delta_P = 60°$. Quality factor of P-wave for reference medium is to be 10 and for S-wave is 7. Also the S- to P-wave velocity ratio for reference medium is chosen to be 1/2. Dash line is for anelastic part and solid line for elastic part.

The scattering potential for P to SI is, consequently,

$$ {}^{\mathrm{P}}_{\mathrm{SI}}\mathbb{V}_{\mathrm{VE}} = {}^{\mathrm{P}}_{\mathrm{SI}}\mathbb{V}_{\mathrm{E}} + i{}^{\mathrm{P}}_{\mathrm{SI}}\mathbb{V}_{\mathrm{AE}} \tag{2.95} $$

where the elastic part of the scattering potential ${}^{\mathrm{P}}_{\mathrm{SI}}\mathbb{V}_{\mathrm{E}}$ is given by

$$ {}^{\mathrm{P}}_{\mathrm{SI}}\mathbb{V}_{\mathrm{E}} = -\left[\sin\sigma + \left(\frac{\beta_{\mathrm{E0}}}{\alpha_{\mathrm{E0}}}\right)\sin 2\sigma\right] A_\rho - 2\left[\left(\frac{\beta_{\mathrm{E0}}}{\alpha_{\mathrm{E0}}}\right)\sin 2\sigma\right] A_\beta \tag{2.96} $$

and anelastic part is given by

$$ {}^{\mathrm{P}}_{\mathrm{SI}}\mathbb{V}_{\mathrm{AE}} = {}^{\mathrm{P}}_{\mathrm{SI}}\mathbb{V}^{\rho}_{\mathrm{AE}} A_\rho + {}^{\mathrm{P}}_{\mathrm{SI}}\mathbb{V}^{\beta}_{\mathrm{AE}} A_\beta + {}^{\mathrm{P}}_{\mathrm{SI}}\mathbb{V}^{Q_{\mathrm{S}}}_{\mathrm{AE}} A_{Q_{\mathrm{S}}} \tag{2.97} $$

with

$$ \begin{aligned} {}^{\mathrm{P}}_{\mathrm{SI}}\mathbb{V}^{\rho}_{\mathrm{AE}} = &-\frac{1}{2}\left(\frac{\beta_{\mathrm{E0}}}{\alpha_{\mathrm{E0}}}\right)\times \\ &\left\{\sin 2\sigma(Q_{\mathrm{S0}}^{-1} - Q_{\mathrm{P0}}^{-1}) + \left[2\cos 2\sigma + \left(\frac{\alpha_{\mathrm{E0}}}{\beta_{\mathrm{E0}}}\right)\cos\sigma\right](Q_{\mathrm{S0}}^{-1}\tan\delta_{\mathrm{S}} + Q_{\mathrm{P0}}^{-1}\tan\delta_{\mathrm{P}})\right\} \end{aligned} \tag{2.98} $$

$$ {}^{\mathrm{P}}_{\mathrm{SI}}\mathbb{V}^{\beta}_{\mathrm{AE}} = -\left(\frac{\beta_{\mathrm{E0}}}{\alpha_{\mathrm{E0}}}\right)\left\{\sin 2\sigma(Q_{\mathrm{S0}}^{-1} - Q_{\mathrm{P0}}^{-1}) + 2\cos 2\sigma(Q_{\mathrm{S0}}^{-1}\tan\delta_{\mathrm{S}} + Q_{\mathrm{P0}}^{-1}\tan\delta_{\mathrm{P}})\right\} \tag{2.99} $$

$$ {}^{\mathrm{P}}_{\mathrm{SI}}\mathbb{V}^{Q_{\mathrm{S}}}_{\mathrm{AE}} = \left(\frac{\beta_{\mathrm{E0}}}{\alpha_{\mathrm{E0}}}\right) Q_{\mathrm{S0}}^{-1}\sin 2\sigma. \tag{2.100} $$

Similarly to the P-P case, the P-SI scattering potential is a complex function whose real part corresponds to the potential for elastic P-SV scattering, and whose imaginary part corresponds to the part of the reflectivity due to the anelasticity of the medium. The correspondence is qualitatively as expected given standard AVO results. For instance, in P-SI scattering there is no contribution from the change in P-wave velocity to reflection response.

In the special case that both reflected and incident waves are homogeneous the density and S-wave velocity parts reduce to

$$ {}^{\mathrm{P}}_{\mathrm{SI}}\mathbb{V}^{\beta}_{\mathrm{AE}} = 2{}^{\mathrm{P}}_{\mathrm{SI}}\mathbb{V}^{\rho}_{\mathrm{AE}} = -\left(\frac{\beta_{\mathrm{E0}}}{\alpha_{\mathrm{E0}}}\right)(Q_{\mathrm{S0}}^{-1} - Q_{\mathrm{P0}}^{-1})\sin 2\sigma, \tag{2.101} $$

from which we discern that the contributions from density, S-wave velocity and its quality factor have the same angle dependencies. In contrast with the P-P scattering potential, for a P-SI element at small angles, the relative change in S-wave quality factor does make a contribution to the anelastic part. At normal incidence, the elastic part of the scattering potential

is zero, however the anelastic part due to relative change in density and S-wave velocity is not zero. In Figure 2.5 we plot the elastic and anelastic parts of the potential of density and S-wave velocity perturbations to scatter an inhomogeneous P-wave into an inhomogeneous SI-wave. At normal incidence, the density component of the scattering potential is zero for any background attenuation angle, but the anelastic part goes to its maximum value. In contrast to the case of P-P scattering, here the contribution of density to the anelastic part of the scattering is considerable. For the S-wave velocity component, the elastic and anelastic parts of the scattering potential have the almost the same contribution to the change in reflectivity but the opposite phase. In other words, for normal incidence the anelastic part goes to its maximum value and the elastic part is zero. Comparing this to the case of P-P scattering, we conclude that the anelasticity of a scattering heterogeneity has a greater influence on the P-SI mode than on the P-P mode.

2.5.3 Viscoelastic SI-to-SI scattering

The third diagonal element of the scattering matrix refers to the scattering of an SI-wave to another SI-wave. In this case both incident and reflected waves are S-waves, respectively represented by wave number vectors $\boldsymbol{\zeta}_{\mathrm{S}r}$ and $\boldsymbol{\zeta}_{\mathrm{S}i}$. We have, to begin,

$$\underset{\mathrm{SI}}{\overset{\mathrm{SI}}{\mathcal{F}}} = \boldsymbol{\zeta}_{\mathrm{S}r} \cdot \boldsymbol{\zeta}_{\mathrm{S}i} \tag{2.102}$$

$$\underset{\mathrm{SI}}{\overset{\mathrm{SI}}{\mathcal{G}_\beta}} = \beta_0^2 \left\{ (\boldsymbol{\zeta}_{\mathrm{S}r} \cdot \boldsymbol{\zeta}_{\mathrm{S}i})(\mathbf{k}_{\mathrm{S}r} \cdot \mathbf{k}_{\mathrm{S}i}) + (\boldsymbol{\zeta}_{\mathrm{S}i} \cdot \mathbf{k}_{\mathrm{S}r})(\boldsymbol{\zeta}_{\mathrm{S}r} \cdot \mathbf{k}_{\mathrm{S}i}) \right\}. \tag{2.103}$$

Using the dot product

$$\boldsymbol{\zeta}_{\mathrm{S}r} \cdot \boldsymbol{\zeta}_{\mathrm{S}i} = -\cos\sigma + \frac{i}{2} Q_{\mathrm{S}0}^{-1} \sin\sigma \left(\tan\delta_{\mathrm{S}r} + \tan\delta_{\mathrm{S}i}\right) \tag{2.104}$$

$$\boldsymbol{\zeta}_{\mathrm{S}r} \cdot \mathbf{k}_{\mathrm{S}i} = -\boldsymbol{\zeta}_{\mathrm{S}i} \cdot \mathbf{k}_{\mathrm{S}r} = \frac{1}{\beta_{\mathrm{E}0}} \left\{ \sin\sigma \left(1 - \frac{i}{2} Q_{\mathrm{S}0}^{-1}\right) + \frac{i}{2} Q_{\mathrm{S}0}^{-1} \cos\sigma (\tan\delta_{\mathrm{S}}^r + \tan\delta_{\mathrm{S}}^i) \right\}, \tag{2.105}$$

the related scattering element is

$$\underset{\mathrm{SI}}{\overset{\mathrm{SI}}{\mathbb{V}_{\mathrm{VE}}}} = \underset{\mathrm{SI}}{\overset{\mathrm{SI}}{\mathbb{V}_{\mathrm{E}}}} + i \underset{\mathrm{SI}}{\overset{\mathrm{SI}}{\mathbb{V}_{\mathrm{AE}}}} \tag{2.106}$$

where the elastic part of the scattering potential $\underset{\mathrm{SI}}{\overset{\mathrm{SI}}{\mathbb{V}_{\mathrm{E}}}}$ is given by

$$\underset{\mathrm{SI}}{\overset{\mathrm{SI}}{\mathbb{V}_{\mathrm{E}}}} = -\left(\cos\sigma + \cos 2\sigma\right) A_\rho - \left(2\cos 2\sigma\right) A_\beta \tag{2.107}$$

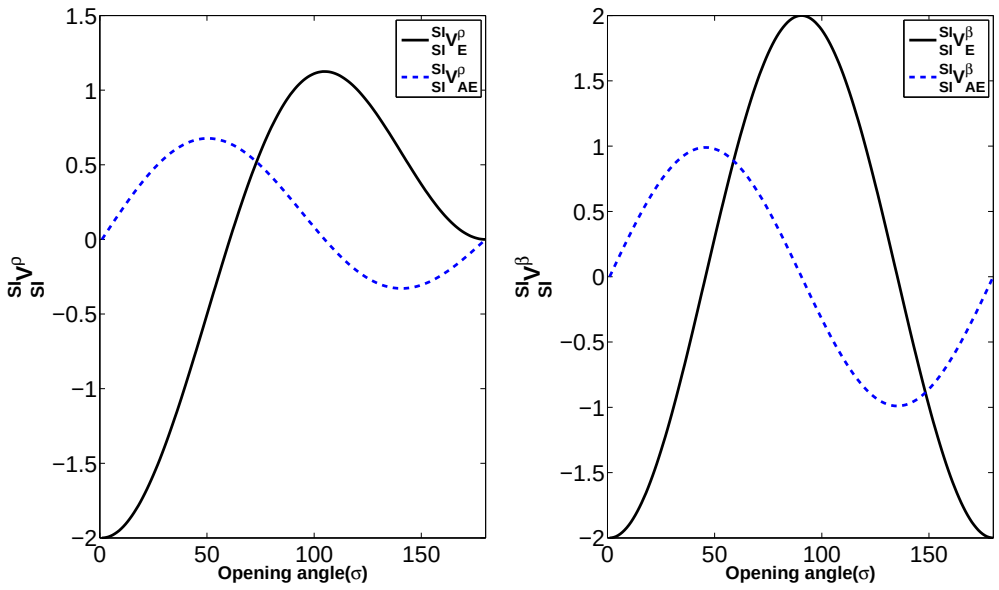

Figure 2.6: Elastic and anelastic density(left) and S-wave velocity(right) components of the viscoelastic potential for scattering of incident inhomogeneous SI-wave to inhomogeneous reflected SI-wave versus of reflected wave angle σ, for $\delta_{\rm S} = 60°$. Quality factor for S-wave is 7. Also the S- to P-wave velocity ratio for reference medium is chosen to be 1/2. Dash line is for anelastic part and solid line for elastic part.

and anelastic part by

$$ {}^{\rm SI}_{\rm SI}\mathbb{V}_{\rm AE} = {}^{\rm SI}_{\rm SI}\mathbb{V}^{\rho}_{\rm AE} A_{\rho} + {}^{\rm SI}_{\rm SI}\mathbb{V}^{\beta}_{\rm AE} A_{\beta} + {}^{\rm SI}_{\rm SI}\mathbb{V}^{Q_{\rm S}}_{\rm AE} A_{Q_{\rm S}}, \tag{2.108} $$

with

$$ {}^{\rm SI}_{\rm SI}\mathbb{V}^{\rho}_{\rm AE} = Q^{-1}_{\rm S0}(\sin\sigma + 2\sin 2\sigma)\tan\delta_{\rm S} \tag{2.109} $$

$$ {}^{\rm SI}_{\rm SI}\mathbb{V}^{\beta}_{\rm AE} = 4Q^{-1}_{\rm S0}\sin 2\sigma\tan\delta_{\rm S} \tag{2.110} $$

$$ {}^{\rm SI}_{\rm SI}\mathbb{V}^{Q_{\rm S}}_{\rm AE} = Q^{-1}_{\rm S0}\cos 2\sigma. \tag{2.111} $$

At normal incidence the scattering potential is zero. Also, in the case of zero background attenuation angle, only the $A_{Q_{\rm S}}$ influences the scattering potential, with the contribution from density and the S-wave velocity vanishing. In Figure 2.6, we plot the elastic and anelastic parts of the potential of density and S-velocity heterogeneities to scatter an inhomogeneous

SI-wave into an inhomogeneous SI-wave. Comparing the P-P, P-SI and SI-SI modes altogether, we conclude that the anelasticity of a scatterer has a more pronounced effect on the outgoing wave for the converted wave modes. We can see by comparing Figures 2.4, 2.5 and 2.6 that only for the P-SI mode is the anelastic part of the scattering potential comparable to the elastic part.

2.5.4 Viscoelastic scattering of SII-waves

Borcherdt (2009) proved that for an infinite planar boundary between viscoelastic media in welded contact, neither an incident P- nor an SI-wave can convert through reflection or transmission into an SII-wave, and vice-versa. In the case of viscoelastic scattering from multidimensional heterogeneities we will show likewise that to first order (i.e., under the Born approximation) an incident SII-wave can only scatter into another SII-wave. For example let us consider the scattering of P-wave to SII-wave, in this case we have

$$\overset{\mathrm{P}}{\underset{\mathrm{SII}}{\mathcal{F}}} = \mathbf{n} \cdot \boldsymbol{\xi}_{\mathrm{P}i} = 0 \tag{2.112}$$

$$\overset{\mathrm{P}}{\underset{\mathrm{SII}}{\mathcal{G}_\alpha}} = \alpha_0^2 (\mathbf{n} \cdot \mathbf{k}_{\mathrm{S}r})(\boldsymbol{\xi}_{\mathrm{P}i} \cdot \mathbf{k}_{\mathrm{P}i}) = 0 \tag{2.113}$$

$$\overset{\mathrm{P}}{\underset{\mathrm{SII}}{\mathcal{G}_\beta}} = \beta_0^2 \left\{ (\mathbf{n} \cdot \boldsymbol{\xi}_{\mathrm{P}i})(\mathbf{k}_{\mathrm{S}r} \cdot \mathbf{k}_{\mathrm{P}i}) - 2(\mathbf{n} \cdot \mathbf{k}_{\mathrm{S}r})(\boldsymbol{\xi}_{\mathrm{P}i} \cdot \mathbf{k}_{\mathrm{P}i}) + (\boldsymbol{\xi}_{\mathrm{P}i} \cdot \mathbf{k}_{\mathrm{S}r})(\mathbf{n} \cdot \mathbf{k}_{\mathrm{P}i}) \right\} = 0, \tag{2.114}$$

where we have used the fact that polarization direction for SII wave is perpendicular to the plane constructed by the attenuation and propagation vectors. In a similar manner it is seen that the scattering elements for SI-SII, SII-P, P-SII, SII-SI and SI-SII are identically zero.

To analyse SII-SII scattering we calculate the second diagonal element of the scattering matrix, namely $\overset{\mathrm{SII}}{\underset{\mathrm{SII}}{\mathbb{V}}}_{\mathrm{VE}}$, obtaining

$$\overset{\mathrm{SII}}{\underset{\mathrm{SII}}{\mathbb{V}}}_{\mathrm{VE}} = \overset{\mathrm{SII}}{\underset{\mathrm{SII}}{\mathbb{V}}}_{\mathrm{E}} + i \overset{\mathrm{SII}}{\underset{\mathrm{SII}}{\mathbb{V}}}_{\mathrm{AE}} \tag{2.115}$$

where the elastic part of the scattering potential is given by

$$\overset{\mathrm{SII}}{\underset{\mathrm{SII}}{\mathbb{V}}}_{\mathrm{E}} = (1 + \cos\sigma) A_\rho + (2\cos\sigma) A_\beta \tag{2.116}$$

and the anelastic part by

$$\overset{\mathrm{SII}}{\underset{\mathrm{SII}}{\mathbb{V}}}_{\mathrm{AE}} = -Q_{\mathrm{S}0}^{-1} \sin\sigma \tan\delta_{\mathrm{S}} (2A_\beta + A_\rho) - Q_{\mathrm{S}0}^{-1} \cos\sigma A_{Q_{\mathrm{S}}} \tag{2.117}$$

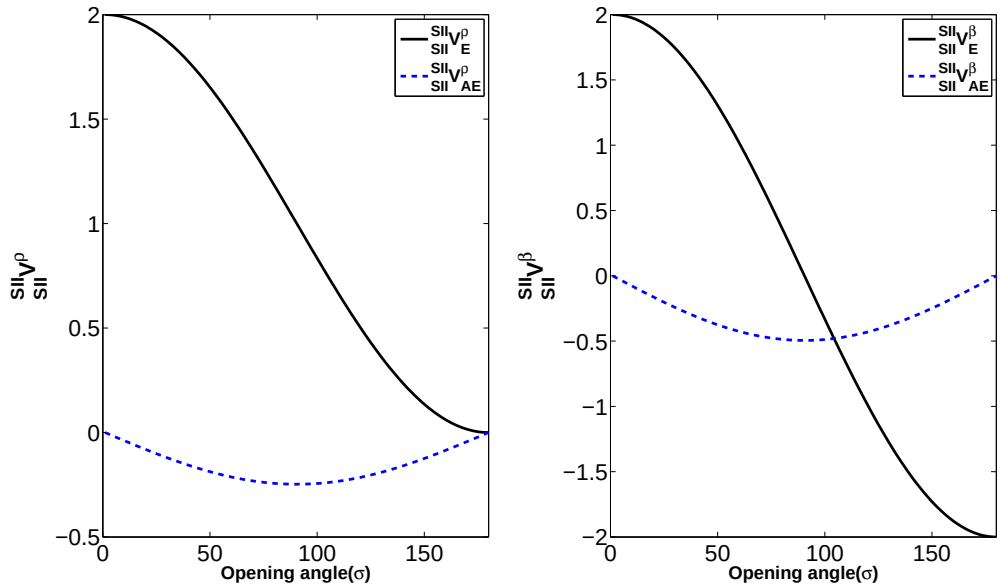

Figure 2.7: Elastic and anelastic density(left) and S-velocity(right) components of the viscoelastic potential for scattering of incident inhomogeneous SII-wave to inhomogeneous reflected SII-wave versus of reflected wave angle σ, for $\delta_S = 60°$. Quality factor for S-wave is 7. Also the S-to P-velocity ratio for reference medium is chosen to be 1/2. Dash line is for anelastic part and solid line for elastic part.

In Figure 2.7 we plot the elastic and anelastic parts of the potential of density and S-wave velocity perturbations to scatter an inhomogeneous SII-wave into an inhomogeneous SII-wave.

2.6 Summary and conclusion

The seismic response of the real earth deviates from the elastic-isotropic model often used to frame the seismic wave propagation problem. Here we investigate viscoelasticity in its capacity to reproduce the effect of dissipation on the propagation of a wave. Full formal theory for viscoelastic seismic waves exists, but the most powerful versions of it have largely been restricted to layered media. Exact, closed-form solutions for viscoelastic waves in arbitrary multidimensional media are not in general available, but, to first order, scattering formulations can provide interpretable approximate forms. These forms are important for obtaining physical insight into interactions of seismic waves with dissipative media, but also for posing and solving inverse scattering and full waveform inversion problems.

In a viscoelastic medium generally the directions of maximum attenuation and wave propagation are not aligned, in which case the wave is considered inhomogeneous. Allowing for inhomogeneity, there are three types of waves that propagate in a viscoelastic medium. P and SI-waves with elliptical motion in the plane defined by propagation and attenuation directions, and SII with linear polarization perpendicular to that plane.

To make a scattering matrix whose elements refer to the scattering of viscoelastic wave modes, we first define the polarization vectors for P, SI and SII-waves. For P-wave the polarization vector is a complex vector in the plane of attenuation-propagation. This polarization involves the elliptical particle motion. For SI-waves, polarization vector is also a complex vector, this time perpendicular to the P-wave polarization. The particle motion for SI-wave is on an ellipse perpendicular to the P-wave particle motion ellipse. In the case that attenuation in medium goes to zero, SI-wave reduces to the SV-wave. Another S-wave is SII, which has a linear polarization and in the case of elastic reduces to the SH wave. We show that an SII-wave can only be scattered to an SII-wave. Also P- and SI-waves can not be converted to an SII-wave. So in the scattering matrix the only converted waves are P-SI and S-IP.

The scattering potential in displacement space is obtained by sandwiching the scattering operator between the incident and reflected polarization vectors. Since for the viscoelastic waves, polarizations are complex, the viscoelastic scattering potential we obtained is a complex function whose real part is elastic scattering potential and whose imaginary part is related to the anelasticity of the medium. In contrast to the elastic scattering potential that only alters the amplitude of the outgoing field, the viscoelastic scattering potential alters both amplitude and phase of the outgoing field. Anelasticity appears to have more significant effect on converted waves than on conserved modes.

Appendix A

Perturbation in complex domain

Consider to the complex velocity in a low-loss viscoelastic medium

$$V = V_{\mathrm{E}} \left(1 + \frac{i}{2} Q^{-1}\right), \tag{A.1}$$

the perturbation in V is given by

$$\Delta V = V - V_0 = V_{\mathrm{E}} - V_{\mathrm{E0}} + \frac{i}{2}\left(V_{\mathrm{E}} Q^{-1} - V_{\mathrm{E0}} Q_0^{-1}\right). \tag{A.2}$$

By inserting

$$V_{\mathrm{E}} = (1 + A_{V_{\mathrm{E}}}) V_{\mathrm{E0}}, \tag{A.3}$$

$$Q^{-1} = (1 - A_{Q_{\mathrm{P}}}) Q_0^{-1}, \tag{A.4}$$

into (A.2) we arrive at

$$\Delta V = \Delta V_{\mathrm{E}} + \frac{i}{2}(A_{V_{\mathrm{E}}} - A_Q) V_{\mathrm{E0}} Q_0^{-1}, \tag{A.5}$$

or in terms of fractional perturbations

$$A_V = A_{V_{\mathrm{E}}} - \frac{i}{2} Q_0^{-1} A_Q. \tag{A.6}$$

So the fractional perturbation of complex velocity is equal to perturbation in elastic velocity plus a complex term related to the perturbation in quality factor. Now let's consider to the amplitude and phase of the fractional perturbation in V, in this case amplitude and phase respectively are

$$\mathrm{Amp}(A_V) = |A_V| = \sqrt{A_{V_{\mathrm{E}}}^2 + \frac{1}{4} Q_0^{-2} A_Q^2} \approx |A_{V_{\mathrm{E}}}|, \tag{A.7}$$

$$\mathrm{Phase}(A_V) = \arctan\left(\frac{1}{2} Q_0^{-1} \frac{A_Q}{A_{V_{\mathrm{E}}}}\right) \approx \frac{1}{2} Q_0^{-1} \frac{A_Q}{A_{V_{\mathrm{E}}}}, \tag{A.8}$$

As a result, in linearized form of the scattering potential for a low-loss viscoelastic medium, the only change in the complex quantities appears in the phase of the fractional perturbation.

Chapter 3

Numerical analysis of scattering in a viscoelastic medium

3.1 Abstract

Recently we have developed a theoretical picture of viscoelastic scattering applicable to seismic waves propagating in arbitrary multidimensional geological volumes. The purpose of this paper is to begin to integrate this theoretical analysis with numerical analysis. That combination will permit very general versions of attenuation/Q related analysis, processing, and inversion in multicomponent seismic to be formulated. Here we used the code developed by Martin and Komatitsch (2009b) to simulate the reflections caused by general viscoelastic contrasts designed to be comparable to the results from the Born approximation. We apply the code to a viscoelastic geological model involving a contrast between two layers with different elastic and anelastic properties. We show that the anelastic contrasts generate reflection amplitudes which quantitatively are in agreement with those derived theoretically by Moradi and Innanen (2013).

3.2 Introduction

The goal of seismic inversion is estimation of physical properties of subsurface earth from recorded data. In an inverse problem recorded wavefield is known whereas the subsurface properties in which the wave field propagates are unknown. In order to solve the inverse problem, it is essential to understand the forward problem in which we model the the observed data from physical characteristics of subsurface.

The scattering of seismic waves in a heterogenous medium in the context of the Born approximation has been investigated by many authors (Beylkin and Burridge, 1990; Stolt and Weglein, 2012). Stolt and Weglein (2012) introduced a formal theory for the description of the multidimensional scattering of seismic waves based on an isotropic-elastic model. We

have elsewhere identified as a research priority the adaptation of this approach to incorporate other, more complete pictures of seismic wave propagation. We have progressed one of these, the extension to include anelasticity and/or viscoelasticity (Flugge, 1967), which brings to the wave model the capacity to transform elastic energy into heat. Anelasticity is generally held to be a key contributor to seismic attenuation, or "seismic Q", which has received several decades worth of careful attention in the literature (e.g., Aki and Richards, 2002; Futterman, 1962).

Wave propagation in linear viscoelastic media has been extensively studied numerically (Carcione et al., 1988b,a; Carcione, 1993). Borcherdt (2009) has presented a complete theory for seismic waves propagating in layered anelastic media, assuming a viscoelastic model to hold. Borcherdt in particular predicts a range of transverse inhomogeneous wave types unique to viscoelastic media (Type I and II S waves), and develops rules for conversion of one type to another during interactions with planar boundaries.

Motivated by the need to derive and characterize increasingly sophisticated seismic data analysis and inversion methods incorporating wave dissipation, the problem of scattering of homogeneous and inhomogeneous waves from perturbations in five viscoelastic parameters (density, P- and S-wave velocities, and P- and S-wave quality factors), formulated in the context of the Born approximation (Moradi and Innanen, 2013). In this report, we validate those formulation using existing numerical forward modeling schemes (Carcione, 1993).

The paper is organized as follows. In section 1 we review the physical models for viscoelastic medium based on the dash-pot spring systems and introduced the constitutive equation between stress and strain. In section 3.3, the wave equation for viscoelastic medium based on the memory variables are described. In section 3.4, we briefly describe the scattering potential components in Born approximation. In section 3.5, we simulate the wave propagation in a two layer medium with elastic and anelastic properties. Finally in section 3.6 we summarized the results and clarify the future directions for this research.

3.3 Review of common viscoelastic models

For a linear elastic medium the stress and strain has linear relationship. If the stress is removed, a linear elastic medium instantaneously returns to its original shape. Mathematically it is said that elastic medium behaviour is time-independent. In contrast, a viscoelastic medium has a time-dependent behaviour, when stress is loaded and unloaded. Such a medium has both viscosity and elasticity. For viscoelastic medium, stress not only is a function of strain but also time variation of strain (Flugge, 1967; Borcherdt, 2009).

To mimic the viscoelastic behaviour of medium, various combinations of springs and dashpots are used. Springs display the elastic properties and dashpots simulate the viscous characteristics. The simplest analogous model can by obtained by connecting springs and dashpots in parallel or in series. The first one called Kelvin-Voigt model and the second one Maxwell model. In Kelvin-Voigt, since the spring and dashpot are in parallel, the displacement is the same throughout the system but different stresses are experienced. A Maxwell model in which the spring and dashpot are in series, the stress is the same throughout the system but different displacements are experienced.

Springs represents the elastic properties of the medium and dashpots simulates the fluid behavior which are assumed to deform continuously. In the Maxwell model when stress applied to the system spring deformation is finite but continuous so long as the stress is maintained. Due to this the Maxwell model is said simulate a viscoelastic fluid. In contrast, in Kelvin-Voigt model when stress is applied to the model, since the dashpot is in parallel to the spring, the dashpot deformes as long as the spring keeps deforming. In other words, the dashpot can not deform continuously. As a result Kelvin-Voigt model behaves as a viscoelastic solid medium. Neither Kelvin-Voigt model nor Maxwell model represent a real viscoelastic model, however in combination with additional springs in series or in parallel can explain most properties of a viscoelastic medium. One example is referred to as the standard linear model.

Let us consider a one-dimensional viscoelastic model. In this case the relation between stress (σ) and strain(e) is given by a convolution (Borcherdt, 2009)

$$\sigma(t) = r * \dot{\varepsilon} = \int_{-\infty}^{t} r(t-\tau) \left[\frac{d\varepsilon}{dt}\right]_{t=\tau} d\tau, \tag{3.1}$$

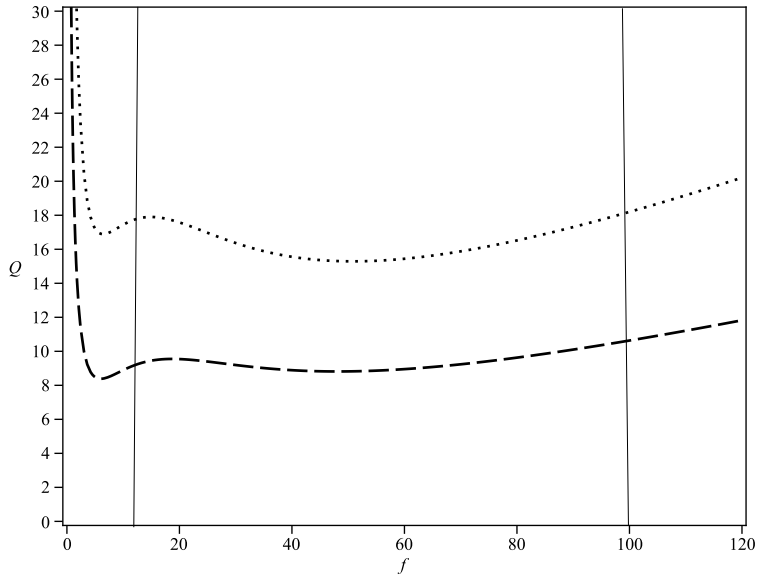

Figure 3.1: Quality factor Q for different numbers of relaxation mechanisms in the frequency band from 0 to 120 Hz. The frequency band from 30 to 100 Hz, for which Q is constructed to be approximately constant, is separated by vertical lines. Dot line is for Q_p and dash line for Q_s

where r is relaxation function. Equation (3.1) implies that the stress at any time t is determined by the entire history of the strain until time t. The inverse of this equation which relates the strain to stress also can be written as a convolution

$$\varepsilon(t) = c * \sigma_{,t} = \int_{-\infty}^{\infty} c(t-\tau) \left[\frac{d\sigma}{dt}\right]_{t=\tau} d\tau, \tag{3.2}$$

where c is the creep function and,t denotes the derivative respect to time. The complex modulus M is next defined as

$$M(\omega) = i\omega R(\omega), \tag{3.3}$$

where $R(\omega)$ is Fourier transform of the relaxation function. The fractional energy loss expressed in terms of the ratio of the imaginary and real parts of the complex modulus (Borcherdt, 2009) is then used to define the reciprocal of the Q factor

$$Q^{-1} = \frac{\Im M}{\Re M} = \frac{M_I}{M_R}. \tag{3.4}$$

The relaxation and creep functions for standard linear model are given by (Flugge, 1967)

$$r(t) = M_r \left[1 - \left(1 - \frac{\tau_\varepsilon}{\tau_\sigma}\right) e^{-t/\tau_\sigma}\right] H(t), \tag{3.5}$$

$$c(t) = \frac{1}{M_r}\left[1 - \left(1 - \frac{\tau_\sigma}{\tau_\varepsilon}\right)e^{-t/\tau_\varepsilon}\right]H(t). \tag{3.6}$$

Here $H(t)$ is step function and τ_ε and τ_σ stand for relaxation times for strain and stress respectively

$$\tau_\sigma = \frac{\eta}{k_1 + k_2}, \qquad \tau_\varepsilon = \frac{\eta}{k_2}. \tag{3.7}$$

In addition M_r refers to the relaxed elastic modulus

$$M_r = \frac{k_1 k_2}{k_1 + k_2}, \tag{3.8}$$

where k is a constant relating stress and strain in Hooke's law for a spring and η is the viscosity of the dashpot component. It can be seen that elastic limit is recovered by setting $\tau_\sigma = \tau_\varepsilon$. By applying the Fourier transform to (3.5) and inserting in (3.3) we obtain the complex modulus

$$M(\omega) = M_r \frac{1 + i\omega\tau_\varepsilon}{1 + i\omega\tau_\sigma}. \tag{3.9}$$

Unrelaxed or high-frequency modulus is an instantaneous elastic response of the viscoelastic material which is given by

$$M_u = \lim_{\omega\to\infty} M(\omega) = M_r \frac{\tau_\varepsilon}{\tau_\sigma}. \tag{3.10}$$

On the other side, low-frequency or relaxed modulus is a long term equilibrium response

$$M_r = \lim_{\omega\to 0} M(\omega). \tag{3.11}$$

Finally using the definition of quality factor in (3.4) we arrive at

$$Q^{-1} = \frac{\omega(\tau_\varepsilon - \tau_\sigma)}{1 + \omega^2\tau_\varepsilon\tau_\sigma}. \tag{3.12}$$

We can see that for $\tau_\sigma = \tau_\varepsilon$ the attenuation factor goes to zero. The above analysis can be generalized to the l-mechanism system. In this case complex modulus takes the following form (Flugge, 1967)

$$M(\omega) = M_r\left(1 - L + \sum_{l=1}^{L} \frac{1 + i\omega\tau_{\varepsilon l}}{1 + i\omega\tau_{\sigma l}}\right). \tag{3.13}$$

Similar to the one-mechanism case, the unrelaxed modulus is

$$M_u = M_r + \sum_{l=1}^{L} M_l, \tag{3.14}$$

where

$$M_l = M_r \left(\frac{\tau_{\varepsilon l}}{\tau_{\sigma l}} - 1 \right). \tag{3.15}$$

In this case the quality factor is given by

$$Q(\omega) = \frac{1 - L + \sum_{l=1}^{L} \frac{1+\omega^2 \tau_{\varepsilon l}\tau_{\sigma l}}{1+\omega^2 \tau_{\sigma l}^2}}{\sum_{l=1}^{L} \frac{\omega(\tau_{\varepsilon l} - \tau_{\sigma l})}{1+\omega^2 \tau_{\varepsilon l}\tau_{\sigma l}}}. \tag{3.16}$$

There is a method to extract the desired Q-constant model for given values of relaxation times called τ-model (Blanch et al., 1995). To describe this method first we define a dimensionless parameter τ

$$\tau = \frac{\tau_{\varepsilon l}}{\tau_{\sigma l}} - 1. \tag{3.17}$$

For real materials $\tau \ll 1$, so we can approximate (3.16) as

$$Q^{-1}(\omega, \tau_{\sigma l}, \tau) \approx \sum_{l=1}^{L} \frac{\omega \tau_{\sigma l} \tau}{1 + \omega^2 \tau_{\sigma l}^2}. \tag{3.18}$$

Using the least-squares inversion, the optimization variables $\tau_{\sigma l}$ and τ are determined. The following function is minimized numerically in a least-squares sense

$$J(\tau_{\sigma l}, \tau) = \int_{\omega_a}^{\omega_b} \left[Q^{-1}(\omega, \tau_{\sigma l}, \tau) - Q_0^{-1} \right]^2 d\omega. \tag{3.19}$$

In Figure 3.1, we plot the quality factor for P- and S-waves versus frequency for a two-mechanism model. We observe that frequency in the range of $30Hz < f < 100Hz$, quality factor is nearly constant. In can be shown that a larger number of relaxation mechanisms gives better constant-Q approximations, especially for higher frequencies.

3.3.1 Equation of Motion

In one dimension, say in x-direction, the particle velocity is given by

$$\dot{u}_x = v_x = \dot{\varepsilon}. \tag{3.20}$$

where u is displacement in x-direction, v is the particle velocity. Now, the equation of motion for 1-D viscoelastic medium is given by

$$\rho \dot{v} = \sigma_{,x}, \tag{3.21}$$

$$\dot{\sigma} = \dot{r} * v_{,x}, \tag{3.22}$$

where $', x'$ denotes the partial derivative respect to x. To eliminate the convolution term in Eq. (3.22), memory variables are defined (Carcione, 1993). Differentiating equation (3.1) with respect to t

$$\dot{\sigma}(t) = \left(\left\{ M_r + \sum_{l=1}^{L} M_l e^{-t/\tau_{\sigma l}} \right\} \delta(t) + \sum_{l=1}^{L} \frac{M_l}{\tau_{\sigma l}} e^{-t/\tau_{\sigma l}} H(t) \right) * v_{,x}. \tag{3.23}$$

By definition of the L-memory variable we have

$$m_l = \left[\frac{M_l}{\tau_{\sigma l}} e^{-t/\tau_{\sigma l}} H(t) \right] * v_{,x} \tag{3.24}$$

In which case equation Eq.(3.23) reduces to

$$\dot{\sigma}(t) = M_u v_{,x} + \sum_{l=1}^{L} m_l. \tag{3.25}$$

The only convolutional term that left is in equation (3.24). To remove that we take the time derivative and obtain

$$\dot{m}_l = \left[\frac{M_l}{\tau_{\sigma l}} e^{-t/\tau_{\sigma l}} \delta(t) - \frac{1}{\tau_{\sigma l}} \left\{ \frac{M_l}{\tau_{\sigma l}} e^{-t/\tau_{\sigma l}} \right\} H(t) \right] * v_{,x}, \tag{3.26}$$

finding that the memory variables satisfy in a first order differential equation

$$\dot{m}_l = \frac{m_l}{\tau_{\sigma l}} + \frac{M_l}{\tau_{\sigma l}} v_{,x}. \tag{3.27}$$

Equations (3.21),(3.25), and (3.27) comprise a set of $2 + L$ equations, referred to 1-D viscoelastic wave propagation in a medium with L sets of standard linear solids.

3.4 Viscoelastic scattering amplitude

Allowing for inhomogeneity, there are three types of waves that propagate in a viscoelastic medium. P and SI waves with elliptical motion in the plane defined by propagation and attenuation directions, and SII with linear polarization perpendicular to that plane. If the two half-space medium are very similar we can define the linearized reflectivity functions in terms of changes in density, velocities and quality factors. The fractional perturbation in property τ is defined as

$$A_\tau = \frac{\Delta\tau}{\bar{\tau}}, \tag{3.28}$$

where $\tau = \rho, \alpha, \beta, Q_p, Q_s$ and

$$\Delta\tau = \tau_2 - \tau_1, \tag{3.29}$$

and

$$\bar{\tau} = \frac{\tau_2 + \tau_1}{2}. \tag{3.30}$$

Frequency independent scattering potential for scattering of P-wave to P-wave is given by(Moradi and Innanen, 2013)

$$\begin{aligned} {}^{P}_{P}\mathbb{V}_{visco} = \left({}^{P}_{P}\mathbb{V}^{\alpha}_{e}\right) A_\alpha + \left({}^{P}_{P}\mathbb{V}^{\rho}_{e} + i{}^{P}_{P}\mathbb{V}^{\rho}_{ane}\right) A_\rho + \left({}^{P}_{P}\mathbb{V}^{\beta}_{e} + i{}^{P}_{P}\mathbb{V}^{\beta}_{ane}\right) A_\beta \\ + i\left({}^{P}_{P}\mathbb{V}^{Q_{hs}}_{ane}\right) A_{Q_s} + i\left({}^{P}_{P}\mathbb{V}^{Q_p}_{ane}\right) A_{Q_p}. \end{aligned} \tag{3.31}$$

The term corresponds to the P-wave velocity is real and terms related to S-wave and density are complex. In addition contributions for perturbation in quality factors of P- and S-wave are purely imaginary. Scattering potentials for P to SI and SI to SI are give by

$${}^{P}_{SI}\mathbb{V}_{visco} = \left({}^{P}_{SI}\mathbb{V}^{\rho}_{e} + i{}^{P}_{SI}\mathbb{V}^{\rho}_{ane}\right) A_\rho + \left({}^{P}_{SI}\mathbb{V}^{\beta}_{e} + i{}^{P}_{SI}\mathbb{V}^{\beta}_{ane}\right) A_\beta + i\left({}^{P}_{SI}\mathbb{V}^{Q_{hs}}_{ane}\right) A_{Q_s}, \tag{3.32}$$

$${}^{SI}_{SI}\mathbb{V}_{visco} = \left({}^{SI}_{SI}\mathbb{V}^{\rho}_{e} + i{}^{SI}_{SI}\mathbb{V}^{\rho}_{ane}\right) A_\rho + \left({}^{SI}_{SI}\mathbb{V}^{\beta}_{e} + i{}^{SI}_{SI}\mathbb{V}^{\beta}_{ane}\right) A_\beta + i\left({}^{SI}_{SI}\mathbb{V}^{Q_{hs}}_{ane}\right) A_{Q_s}. \tag{3.33}$$

$${}^{SI}_{P}\mathbb{V}_{visco} = \left({}^{SI}_{P}\mathbb{V}^{\rho}_{e} + i{}^{SI}_{P}\mathbb{V}^{\rho}_{ane}\right) A_\rho + \left({}^{SI}_{P}\mathbb{V}^{\beta}_{e} + i{}^{SI}_{P}\mathbb{V}^{\beta}_{ane}\right) A_\beta + i\left({}^{SI}_{P}\mathbb{V}^{Q_{hs}}_{ane}\right) A_{Q_s}. \tag{3.34}$$

It can be seen from (3.32) and (3.34) that only relative differences in density, S-wave velocity and it's quality factor influence the scattered waves. On the other hand fractional perturbations in P-wave velocity and it's quality factor has no contributions in these cases. In the next section we numerically examine the effects of changing in elastic and anelastic properties of medium on the scattered wave.

3.5 Numerical implementation

In two dimensions we have $8 + 7L$ dynamic variables; three stress values $\sigma_{xx}, \sigma_{xy}, \sigma_{yy}$, and corresponding $3L$ memory variables $m_{xxl}; m_{yyl}; m_{xyl}$, $4L$ relaxation times, $\tau^{p}_{\varepsilon l}; \tau^{p}_{\sigma l}; \tau^{s}_{\varepsilon l}; \tau^{s}_{\sigma l}$, two components of particle velocity $v_x; v_y$ and three material parameters $\mu; \pi; \rho$. Where π is the

relaxation modulus corresponding to P-wave analogues to $\lambda + 2\mu$ in the elastic case where λ and μ are Lame parameters. Stress, memory variables and velocity are the wave variables, and relaxation times and material parameters define the and make-up of the viscoelastic medium.

Figure 3.2 is a simple two layer model that uses 900×200 grid with spacing $D_x = D_y = 5m$. We put the layer boundary at the depth of 400m to set up the contrasts in elastic and anelastic properties of medium. In addition, we buried the source in depth 50m by injecting a vertical displacement wavelet with a central frequency of 45Hz. We expect not only to see P-to-P modes, but to record the SI-to-P and SI-to-SI modes as well as the surface effects.

Contributions of perturbations in elasic and anelastic properties to the scattered waves are numerically examined as follows. First the viscoelastic code (Martin and Komatitsch (2009a)) is run with the perturbations in density, velocities and quality factors on a homogeneous background model in place. Second, we isolate the upgoing scattered wave field by re-running the code without the perturbations and subtracting the resulting direct wave field. The results are displayed in figures 3.3 to 3.7.

Figures 3.3, 3.4 and 3.5 illustrate the reflections caused by $\Delta\alpha$, $\Delta\beta$ and $\Delta\rho$. Similar to the elastic medium changing in the P-wave velocity produced only PP scattered wave, which is expected as we have one term in P-to-P scattering potential Eq. (3.31). However, perturbation in density and S-velocity generate all modes (figures 3.4).

According to Eq.(3.16), in order to simulate the contrast in Q, we changed the corresponding relaxation times of stress and strain for P- and S-waves, and left all other properties constant. Figure 3.6 displays the scattering of P-to-P wave for contrast in Q_p. As seen, there is one reflection which corresponds to only one perturbation term in Q_p in scattering potential. Figure 3.7 shows the influence of perturbation in Qs on scattered waves. Perturbation in Q_p only influence the P-to-P mode according to Eq. (3.31). However contribution of perturbation in Q_s exists in all modes in Eq.(3.31) to (3.34). The consistency of the derived scattering potentials with numerical modeling of the radiation patterns generated by perturbations in density, P- and S-wave velocities and quality factors is shown in figures (3.8)-(3.11).

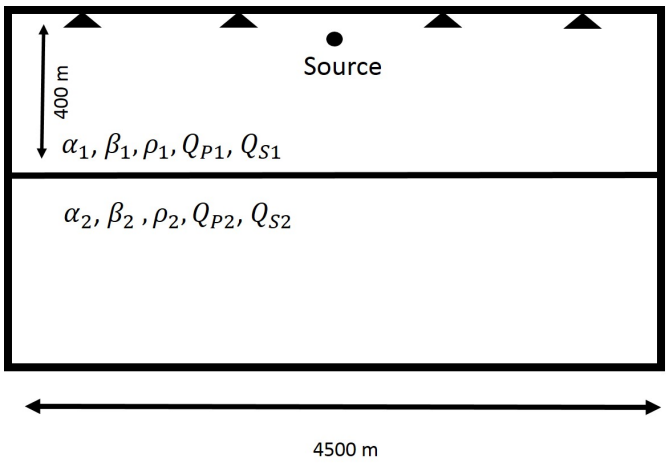

Figure 3.2: Model description of two layer viscoelastic medium.

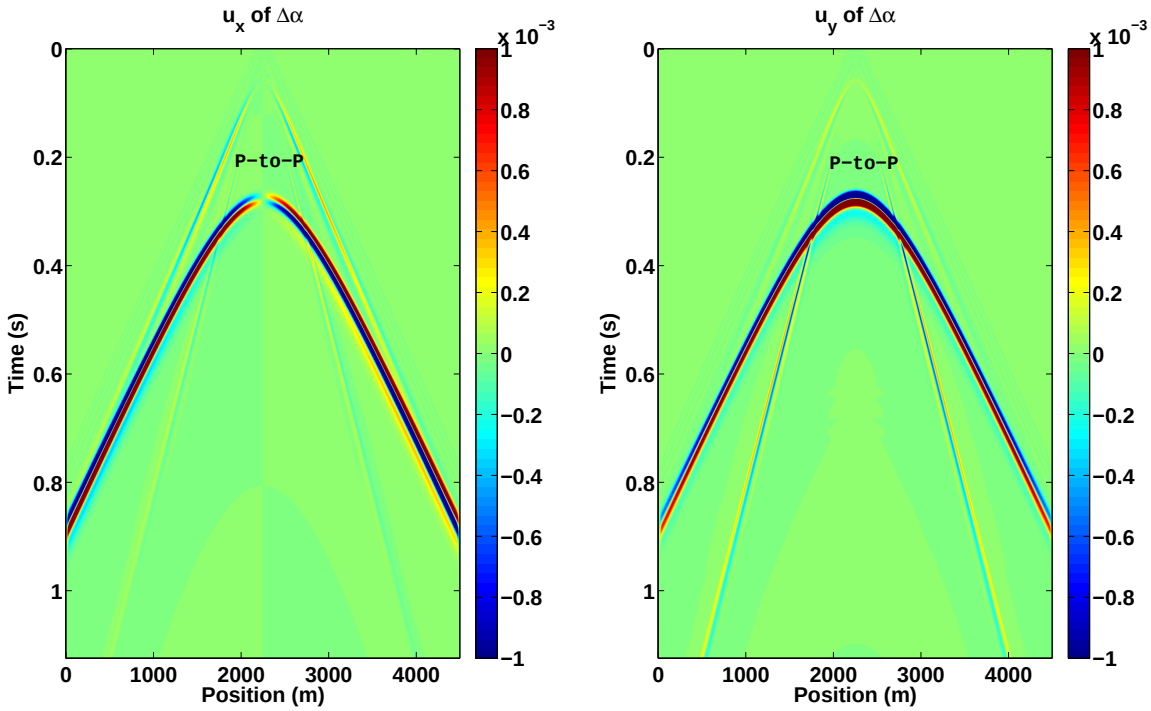

Figure 3.3: Simulated seismic data corresponding to the contrast in P-wave velocity α. The left figure is the x-component of displacement and right is the y-component of displacement.

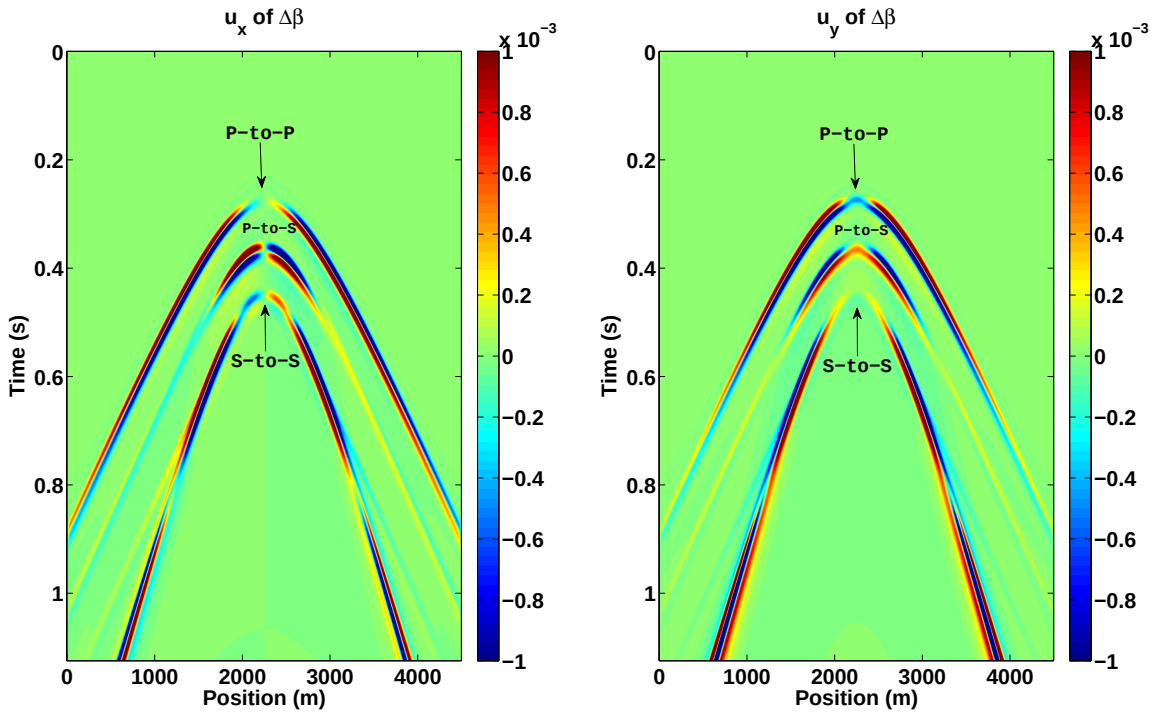

Figure 3.4: Simulated seismic data corresponding to the contrast in S-wave velocity β. The left figure is the x-component of displacement and right is the y-component of displacement.

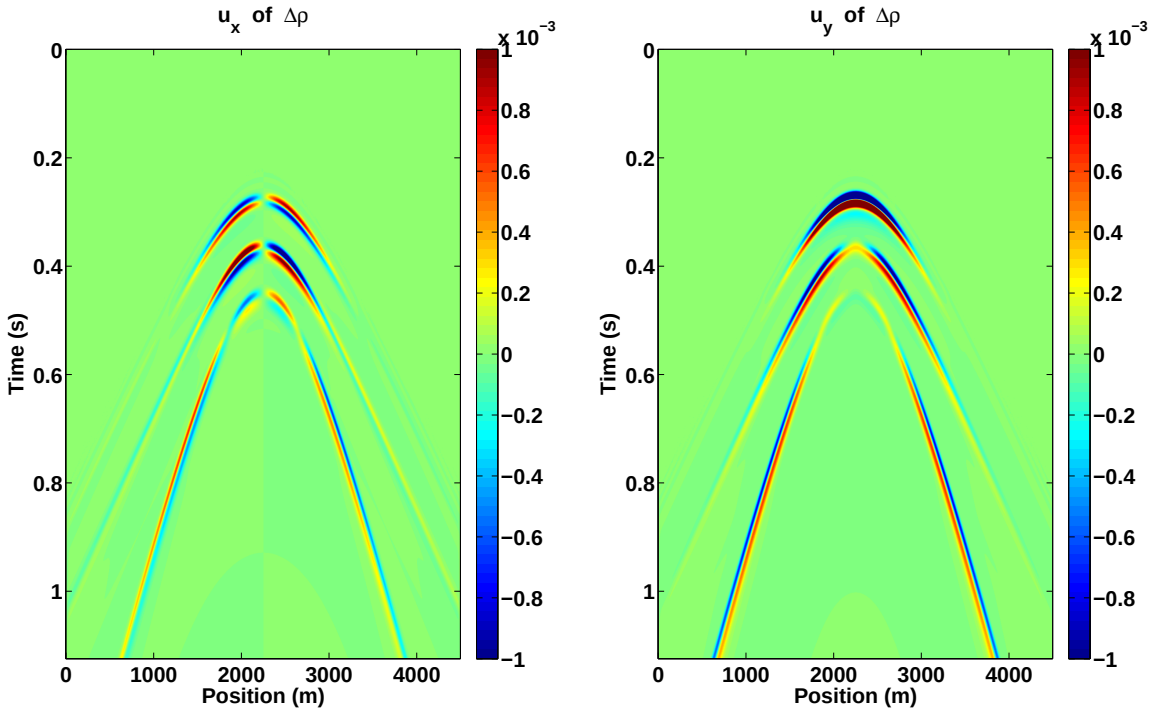

Figure 3.5: Simulated seismic data corresponding to the contrast in density ρ.The left figure is the x-component of displacement and right is the y-component of displacement.

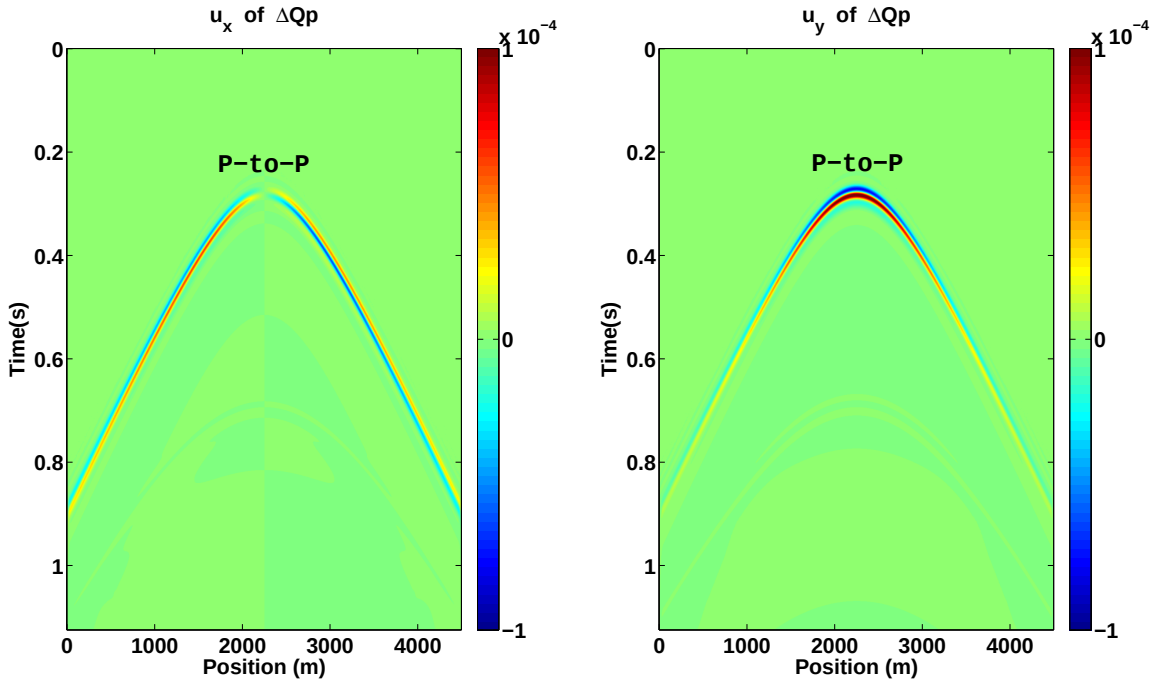

Figure 3.6: Simulated seismic data corresponding to the contrast in quality factor for P-wave velocity Q_p. The left figure is the x-component of displacement and right is the y-component of displacement.

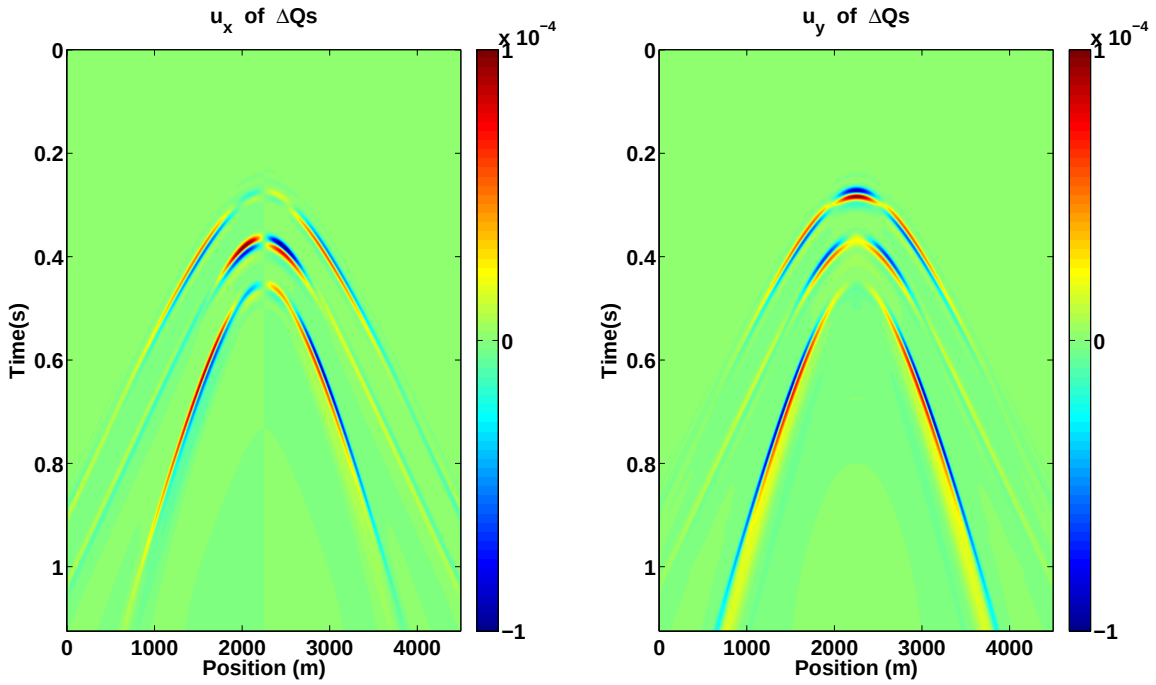

Figure 3.7: Simulated seismic data corresponding to the contrast in quality factor for S-wave velocity Q_s. The left figure is the x-component of displacement and right is the y-component of displacement.

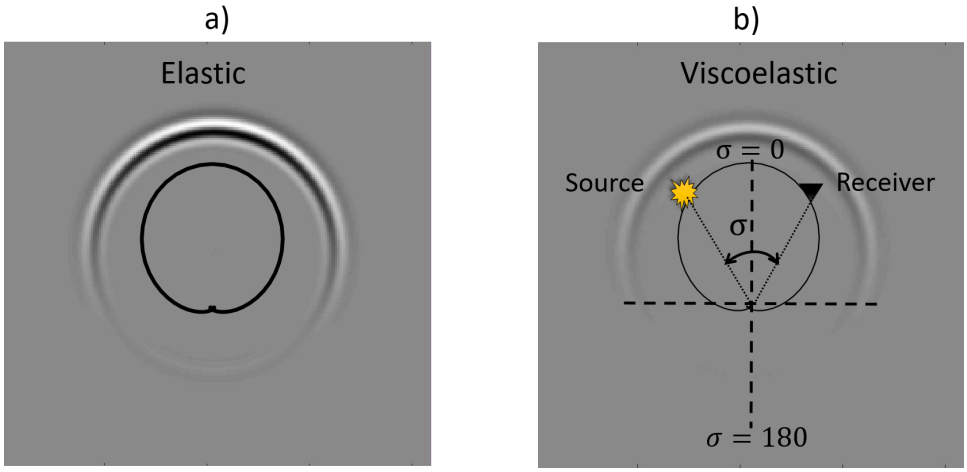

Figure 3.8: Comparison of theoretical results for PP scattering potential with numerical simulation of wave scattering from density scatter point in a) elastic background and b) viscoelastic background medium. σ is the opening angle between the incident and reflected (scattered) wave.

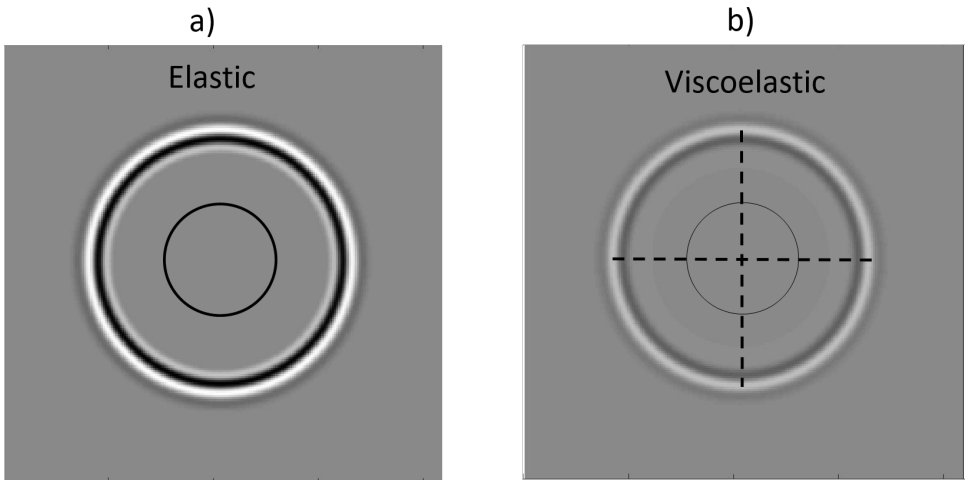

Figure 3.9: The same explanation as figure 3.8 for P-wave scatter point.

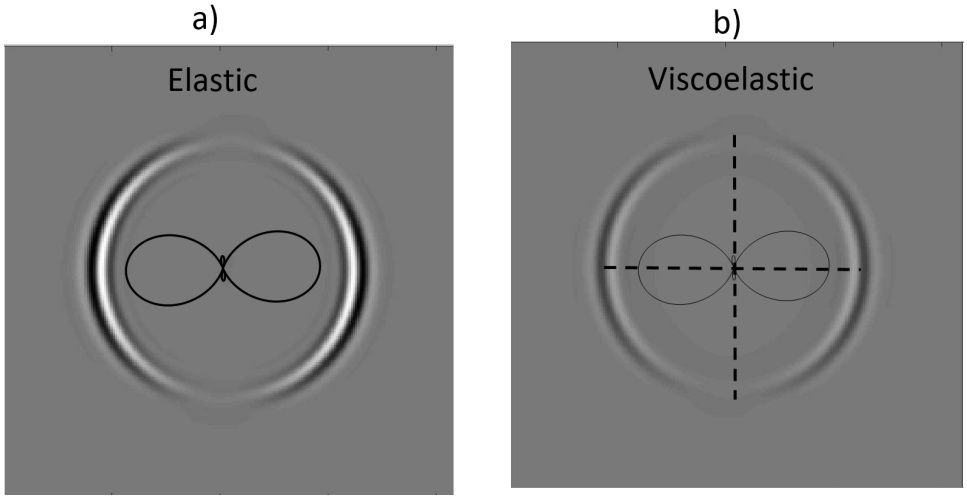

Figure 3.10: The same explanation as figure 3.8 for S-wave scatter point.

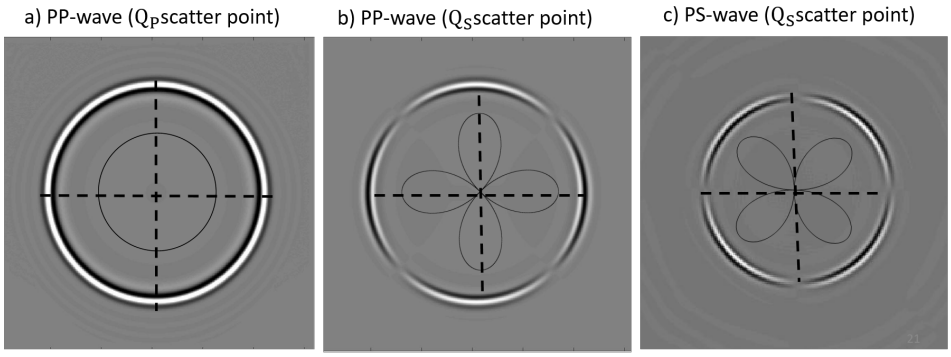

Figure 3.11: The same explanation as figure 3.8 for P- and S-wave quality factor scatter points.

3.6 Summary and future direction

In summary, the numerical analysis of scattering in viscoelastic medium in the context of Born approximation is investigated. Scattering potential in the presence of anelasticity has been studied in (Moradi and Innanen, 2013). There are two important features, first the perturbation in the quality factors of P- and S-waves has contribution in scattering potential. Second, scattering potential is a complex function in which the real part is elastic scattering potential and imaginary part corresponds to anelasticity in medium. In this report numerically we examine the first feature. We show that perturbation in quality factor for P-wave between two layers generate only P-to-P reflection. The latter result is concordance with the viscoelastic scattering potential, which indicate that there is one term due to perturbation in Q_p.

The consistency of our theoretical/scattering treatment with the numerical results obtained by an independent modeling code (based on the framework of Carcione et al. (1988b)) is a significant step towards the development of several processing and inversion applications for data with nonneglible P and S wave attenuation. These in include standard Q estimation techniques, but also viscoelastic extensions of land seismic reflection full waveform inversion.

Additionally, we can investigate the second feature of scattering amplitude, which is related to complex terms induced by anelasticity. From equation (3.31) to (3.34) we can see that scattering potential elements corresponds to perturbation in density and S-velocity

have imaginary parts. So comparing to the elastic case we expect the changes not only in amplitude of scattered wave but also in the phase behaviour.

Appendix B

Appendixe: 3-D viscoelastic medium

The constitutive equation for a 2-D(or 3D) linear isotropic homogeneous viscoelastic medium is given by

$$\sigma_{ij} = \dot{\Lambda} * \delta_{ij}\varepsilon_{kk} + 2\dot{M} * \varepsilon_{ij}, \tag{B.1}$$

Time derivative of the strain tensor can be written as

$$\dot{\varepsilon}_{ij} = \frac{1}{2}(\partial_i v_j + \partial_j v_i). \tag{B.2}$$

Where v is particle velocity. For a standard linear model of viscoelastic medium we can define

$$\Pi = \Lambda + 2M = \pi\Gamma^p(t)H(t), \tag{B.3}$$

and

$$M = \mu\Gamma^s(t)H(t), \tag{B.4}$$

where $\tau^p_{\varepsilon l}$ is relaxation time of strain for P-wave, $\tau^s_{\varepsilon l}$ is relaxation time of strain for S-wave and $\tau_{\sigma l}$ is relaxation time of stress for both P- and S-wave. In addition we define

$$\Gamma^k(t) = 1 - \sum_{l=1}^{L}\left(1 - \frac{\tau^k_{\varepsilon l}}{\tau_{\sigma l}}\right)e^{-t/\tau_{\sigma l}}, \qquad k = p, s \tag{B.5}$$

After some algebra we arrive at

$$\dot{\sigma}_{ij} = \left(\pi\Gamma^p_0 - 2\mu\Gamma^s_0\right)\partial_k v_k + 2\mu\Gamma^s_0\partial_i v_j + \sum_{l=1}^{L} m_{ijl}, \qquad i = j \tag{B.6}$$

and

$$\dot{\sigma}_{ij} = \mu\Gamma^s_0(\partial_i v_j + \partial_j v_i) + \sum_{l=1}^{L} r_{ijl}, \qquad i \neq j \tag{B.7}$$

Where $\Gamma_0 = \Gamma(t = 0)$ and m_{ijl} is a memory tensor for mechanism-l, which satisfies in the following differential equation

$$\dot{m}_{ijl} = -\frac{1}{\tau_{\sigma l}}\left[m_{ijl} + \left\{\pi\left(\frac{\tau^p_{\varepsilon l}}{\tau_{\sigma l}}\right) - 2\mu\left(\frac{\tau^s_{\varepsilon l}}{\tau_{\sigma l}}\right)\right\}\partial_k v_k + 2\mu\left(\frac{\tau^s_{\varepsilon l}}{\tau_{\sigma l}}\right)\partial_i v_j\right], \quad i = j \tag{B.8}$$

for diagonal terms, and

$$\dot{m}_{ijl} = -\frac{1}{\tau_{\sigma l}} \left[r_{ijl} + \left(\frac{\tau^s_{\varepsilon l}}{\tau_{\sigma l}} \right) (\partial_i v_j + \partial_j v_i) \right], \quad i \neq j \tag{B.9}$$

The linearized equation for wave propagation in absence of body forces is given by

$$\rho \ddot{u}_i = \sigma_{ij,j} \quad i = x, y. \tag{B.10}$$

Where $, j$ is spacial derivative, ρ is density, u denotes the displacement and σ refers to the stress.

Chapter 4

Viscoelastic amplitude variation with offset equations with account taken of jumps in attenuation angle

4.1 Abstract

Anelastic properties of reservoir rocks are important and sensitive indicators of fluid saturation and viscosity changes due (for instance) to steam injection. The description of seismic waves propagating through viscoelastic continua is quite complex, involving a range of unique homogeneous and inhomogeneous modes. This is true even in the relatively simple theoretical environment of amplitude-variation-with-offset (AVO) analysis. For instance, a complete treatment of the problem of linearizing the solutions of the low-loss viscoelastic Zoeppritz equations, to obtain an extended Aki-Richards equations (one that is in accord with the appropriate complex Snell's law) is lacking in the literature. Also missing is a clear analytical path allowing such forms to be reconciled with more general volume scattering pictures of viscoelastic seismic wave propagation. Our analysis, which provides these two missing elements, leads to approximate reflection and transmission coefficients for the P-, types-I and II S-waves. These involve additional, complex, terms alongside those of the standard isotropic-elastic Aki-Richards equations. The extra terms are shown to have a significant influence on reflection strengths, particularly when the degree of inhomogeneity is high. The particular AVO forms we present are finally shown to be special cases of potentials for volume scattering from viscoelastic inclusions.

4.2 Introduction

Recently a volume scattering picture of viscoelastic seismic waves has been developed for the purposes of modeling, processing and inversion of seismic data exhibiting non-negligible intrinsic attenuation (Moradi and Innanen, 2015b). That work, which culminates in the derivation of the mathematical form of the viscoelastic scattering potential, can be under-

stood as the extension of the exact layered-medium result of (Borcherdt, 2009) to a linearized but fully multidimensional framework. It adds, to the toolbox for the quantitative analysis of homogeneous and inhomogeneous anelastic waves, a perturbation-based approach, to sit alongside complex ray-based techniques (Hearn and Krebes, 1990) and numerical techniques (Carcione et al., 1988a,b; Carcione, 1993; Robertsson et al., 1994; Carcione, 2007).

From the point of view of practical exploration and monitoring geophysics, the consequences of the scattering result are twofold. First, all direct inverse scattering target identification/inversion methods are formulated beginning with the framing of an appropriate scattering potential (Weglein et al., 2003, 2009). So, the new framework permits a range of viscoacoustic inverse scattering results (Innanen and Weglein, 2007; Innanen and Lira, 2010) now to be posed for the more complete attenuating elastic case. Second, the scattering potential is also a useful starting point in the construction of Frechet kernels for full waveform inversion (Fichtner, 2010; Fichtner and van Driel, 2014). If it is desirable to include some particular observable viscoelastic phenomenon (e.g., inhomogeneous wave modes) in a full waveform inversion procedure, the Frechet kernel must be general enough to admit that phenomenon. So, the new viscoelastic result also makes possible the derivation of general full waveform inversion formulas for attenuating media.

There remain several outstanding questions regarding the relationship between the newer viscoelastic volume scattering picture and the older stratified medium picture. The purpose of this paper is to address those questions.

In exploration and monitoring geophysics, backscattered seismic amplitudes from stratified media fit into processing flows through AVO/AVA technology (Castagna and Backus, 1993; Foster et al., 2010). The workhorse formula within this technology is the Aki-Richards approach (Aki and Richards, 2002), wherein exact displacement reflection coefficients R_{PP}, R_{PS}, R_{SP} and R_{SS} are linearized with respect to perturbations in elastic properties across a reflecting boundary. Stolt and Weglein (2012) have shown that there is a close relationship between the isotropic-elastic scattering potentials and the Aki-Richards equations, the former reducing to the latter for small contrasts and small opening angles. It follows that a similar reduction of the viscoelastic case should lead to formulas corresponding to a viscoelastic-type Aki-Richards equations. A confirmation of this expectation, and the detailed process

by which it occurs, are outstanding issues.

Anelastic reflection coefficients have been discussed analytically (White, 1965; Krebes, 1984; Ursin and Stovas, 2002; Zhao et al., 2014) and numerically (Samec and Blangy, 1992), and in the context of a variety of linear approximations, both in isotropic and anisotropic settings (Behura and Tsvankin, 2009b,a; Innanen, 2011). These latter formulas are examples of anelastic Aki-Richards equations, and so they belong to the same class of formulas in which we expect the reduced version of the general viscoelastic scattering potential to belong. Formulas of this kind can be used to drive anelastic inversion procedures, both linear and nonlinear (Innanen, 2011); or, alternatively, via examination of the frequency rate of change of reflection coefficients (Innanen, 2012). Techniques of this kind become increasingly relevant as evidence accrues that anelastic amplitude signatures provide direct information about reservoir fluids (Ostrander, 1984; Chapman et al., 2006; Odebeatu et al., 2006; Schmalholz and Podladchikov, 2009; Ren et al., 2009; Wu et al., 2014)

The general process of an inhomogeneous viscoelastic plane wave interacting with a planar horizontal boundary is quite complicated. Thus far no linearization of the exact equations for this reflection and transmission problem has been presented in the literature wherein general inhomogeneity is accommodated. A key result in this paper is the provision of such a linearization (i.e., viscoelastic Aki-Richards equations), and the demonstration that the viscoelastic volume scattering model reduces to it.

A full linearization procedure must take into account in detail both specialized anelastic Zoeppritz equations and the complex ray parameter/vertical slowness vector as input to those equations. We begin with the latter wave quantities, determining the relationship between perturbations in elastic P- and S-wave velocities and quality factors across a reflecting boundary and the resulting perturbations in the P- and S-wave attenuation angles (i.e., the angles between planes of constant phase and planes of constant amplitude). We then write down the Zoeppritz equations, formulated for reflection, transmission and conversion of plane anelastic P and type-I S waves (see Borcherdt, 2009 for a complete discussion of P, SI and SII modes). These lead to exact, though rather complicated, expressions for all requisite reflection and transmission coefficients. Next, the P-P, P-SI, and SI-SI coefficients are linearized by considering the effect of weak contrasts on both the complex Snell's law and

the Zoeppritz equations. Finally we demonstrate the consistency between the linearized viscoelastic reflection coefficient expressions and the viscoelastic scattering potentials as derived in the general volume scattering framework (Moradi and Innanen, 2015b).

4.3 Viscoelastic ray parameters and slownesses

Linearized AVO analysis requires the definition of polarization and slowness vectors. In a viscoelastic medium, the wavenumber vector is a complex vector whose real part characterizes the direction of wave propagation and imaginary part characterizes the attenuation of the wave. The wavenumber vector of an inhomogeneous wave is represented by

$$\mathbf{K} = \mathbf{P} - i\mathbf{A}. \tag{4.1}$$

Here $\mathbf{P}$ is the propagation vector perpendicular to the constant phase plane $\mathbf{P}\cdot\mathbf{r} = constant$, and $\mathbf{A}$ is the attenuation vector perpendicular to the amplitude constant plane $\mathbf{A}\cdot\mathbf{r} = constant$. The attenuation vector $\mathbf{A}$ is in the direction of maximum decrease of amplitude. In the case that attenuation and propagation vectors are in the same direction, the wave is said to be homogeneous. An elastic media is represented by $\mathbf{A} = 0$. If we represent the angle between $\mathbf{P}$ and $\mathbf{A}$ by δ, for inhomogeneous waves: $0 < \delta < \pi/2$. Throughout the paper we assume the media is low-loss, which means that inverse of quality factors Q_{P}^{-1} and Q_{S}^{-1} are much less than unity. In this case, complex P- and S-wave velocities in viscoelastic media are generalized to the elastic P- and S-velocities V_{PE} and V_{SE}:

$$V_{\mathrm{P}} = V_{\mathrm{PE}}\left(1 + i\frac{Q_{\mathrm{P}}^{-1}}{2}\right), \tag{4.2}$$

$$V_{S} = V_{\mathrm{SE}}\left(1 + i\frac{Q_{\mathrm{S}}^{-1}}{2}\right). \tag{4.3}$$

There are three types of waves in viscoelastic media, P-, Type-I and -II S waves. Inhomogeneous P- and SI- waves have the elliptical polarization which reduce to the linear in the limit of homogenous wave. An SII wave is always linearly polarized. The displacement vectors for P- and SI-waves are (Borcherdt, 2009)

$$\mathbf{U}_{\mathrm{P}} = \boldsymbol{\xi}_{\mathrm{P}}\Phi_0 \exp\left[-i(\mathbf{K}_{\mathrm{P}}\cdot\mathbf{r} - \omega t)\right], \tag{4.4}$$

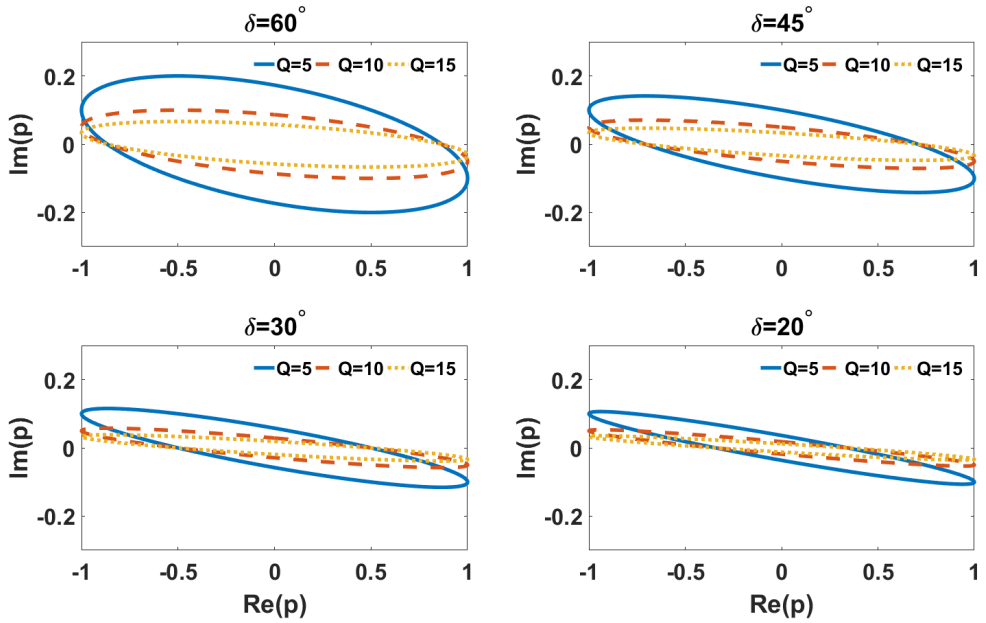

Figure 4.1: Diagram illustrating the complex ray parameter for various values of reciprocal quality factor Q and attenuation angle δ.

$$\mathbf{U}_S = \boldsymbol{\zeta}_S \Psi_0 \exp\left[-i(\mathbf{K}_S \cdot \mathbf{r} - \omega t)\right], \tag{4.5}$$

where Φ_0 and Ψ_0 are complex scalar constants and $\boldsymbol{\xi}_{\mathrm{P}}$ and $\boldsymbol{\zeta}_S$ are, respectively, the polarization vectors for P- and SI-waves

$$\begin{aligned} \boldsymbol{\xi}_{\mathrm{P}} &= \frac{1}{\omega} V_{\mathrm{P}} \mathbf{K}_{\mathrm{P}} = \frac{V_{\mathrm{PE}}}{\omega} \left\{ \mathbf{K}_{\mathrm{P}} + \frac{i}{2} Q_{\mathrm{P}}^{-1} \mathbf{P}_{\mathrm{P}} \right\}, \\ \boldsymbol{\zeta}_S &= \frac{1}{\omega} V_S \mathbf{K}_S \times \mathbf{n} = \frac{V_{\mathrm{SE}}}{\omega} \left\{ \mathbf{K}_S + \frac{i}{2} Q_{\mathrm{S}}^{-1} \mathbf{P}_S \right\} \times \mathbf{n}, \end{aligned} \tag{4.6}$$

where $\mathbf{n}$ is a unit vector orthogonal to the plane formed by $\mathbf{P}_{\mathrm{S}}$ and $\mathbf{A}_{\mathrm{S}}$. Simple analysis shows that the particle motion related to the displacement for P and SI waves is elliptical.

The above results apply for viscoelastic plane waves propagating in an isotropic homogeneous medium. What happens if an inhomogeneous wave with elliptical polarization hits the boundary between two half-spaces? To answer this question we define two half-spaces with different physical properties separated by a planar boundary. The analysis of the Zoeppritz equations and the continuity of displacements and stresses across the boundary is similar to the elastic case. The difference is that ray parameters and vertical slownesses are complex.

Let us consider a wave number vector corresponding to an incident P-wave (figure 4.3):

$$\begin{aligned}\mathbf{P}_{\mathrm{P}} &= \frac{\omega}{V_{\mathrm{PE}}}(\mathbf{z}\cos\theta_{\mathrm{P}} + \mathbf{x}\sin\theta_{\mathrm{P}}),\\ \mathbf{A}_{\mathrm{P}} &= Q_{\mathrm{P}}^{-1}\frac{\omega}{2V_{\mathrm{PE}}}\left(\mathbf{z}[\cos\theta_{\mathrm{P}} + \sin\theta_{\mathrm{P}}\tan\delta_{\mathrm{P}}] + \mathbf{x}[\sin\theta_{\mathrm{P}} - \cos\theta_{\mathrm{P}}\tan\delta_{\mathrm{P}}]\right).\end{aligned} \tag{4.7}$$

The displacement for this wave field is

$$\mathbf{U}_{\mathrm{P}}^{\downarrow} \simeq (\xi_x\mathbf{x} + \xi_z\mathbf{z})\exp\left\{-i\omega(px + q_{\mathrm{P}}z - t)\right\}, \tag{4.8}$$

where $\downarrow$ indicates the direction of the vertical component of the incident wave propagation vector, and where the complex ray parameter p and vertical slowness q_{P} are defined as

$$\begin{aligned}p &= \frac{1}{\omega}(\mathrm{P}_x - i\mathrm{A}_x) = \frac{1}{V_{\mathrm{PE}}}\left[\sin\theta_{\mathrm{P}}\left(1 - i\frac{Q_{\mathrm{P}}^{-1}}{2}\right) + \frac{i}{2}Q_{\mathrm{P}}^{-1}\cos\theta_{\mathrm{P}}\tan\delta_{\mathrm{P}}\right],\\ q_{\mathrm{P}} &= \frac{1}{\omega}(\mathrm{P}_z - i\mathrm{A}_z) = \frac{1}{V_{\mathrm{PE}}}\left[\cos\theta_{\mathrm{P}}\left(1 - i\frac{Q_{\mathrm{P}}^{-1}}{2}\right) - \frac{i}{2}Q_{\mathrm{P}}^{-1}\sin\theta_{\mathrm{P}}\tan\delta_{\mathrm{P}}\right].\end{aligned} \tag{4.9}$$

In addition we define the x- and z-components of the polarization vectors as

$$\begin{aligned}\xi_x &= pV_{\mathrm{P}} = \sin\theta_{\mathrm{P}} + \frac{i}{2}Q_{\mathrm{P}}^{-1}\cos\theta_{\mathrm{P}}\tan\delta_{\mathrm{P}},\\ \xi_z &= q_{\mathrm{P}}V_{\mathrm{P}} = \cos\theta_{\mathrm{P}} - \frac{i}{2}Q_{\mathrm{P}}^{-1}\sin\theta_{\mathrm{P}}\tan\delta_{\mathrm{P}}.\end{aligned} \tag{4.10}$$

Analogous expressions hold for the case of an incident S-wave. We confirm our results by observing that the complex ray parameter, vertical slowness and polarization components satisfy the following relations

$$\begin{aligned}p^2 + q_{\mathrm{P}}^2 &= \frac{1}{V_{\mathrm{PE}}^2}(1 + iQ_{\mathrm{P}}^{-1}) = \frac{1}{V_{\mathrm{P}}^2},\\ \xi_x^2 + \xi_z^2 &= 1.\end{aligned} \tag{4.11}$$

In Figure 4.1, we plot the complex ray parameter versus phase and attenuation angles for various values of quality factor Q in the complex plane. It can be seen that the ray parameter for a viscoelastic medium is an ellipse whose eccentricity grows for smaller values of attenuation angle.

4.4 Viscoelastic Snell's law in the low-contrast approximation

Consider two homogeneous viscoelastic half spaces separated by a plane interface. All properties and quantities related to the upper and lower half spaces are labeled respectively by

subscripts 1 and 2. Snell's law expresses the relationship between incident and transmitted angles and velocities before and after the reflection or transmission of waves. The study of Snell's law in viscoelastic media is required for several reasons: first among them is that we can analyze the homogeneity or inhomogeneity of the reflected and transmitted waves relative to the homogeneity or inhomogeneity of the incident wave. Secondly, in the process of linearization we need to obtain the perturbation in phase and attenuation angles in terms of perturbations in physical properties. Snell's law for viscoelastic materials is discussed by Wennerberg (1985) and Borcherdt (2009). Since the ray parameter in a viscoelastic medium is complex, the generalized Snell's law has two parts, real and imaginary.

Snell's law is based on the fact that the horizontal slowness (ray parameter) is conserved during the reflection and transmission from a boundary. For a viscoelastic medium, the ray parameter not only depends on the phase angle but also on the attenuation angle. Also it is a complex quantity whose real part is the elastic ray parameter given by

$$p_E = \frac{\sin\theta_{P1}}{V_{PE1}} = \frac{\sin\theta_{P2}}{V_{PE2}} = \frac{\sin\theta_{S1}}{V_{SE1}} = \frac{\sin\theta_{S2}}{V_{SE2}}, \tag{4.12}$$

and whose imaginary part is:

$$\begin{aligned} p_A &= \frac{Q_{P1}^{-1}}{2}(p_E - q_{PE1}\tan\delta_{P1}) = \frac{Q_{P2}^{-1}}{2}(p_E - q_{PE2}\tan\delta_{P2}), \\ &= \frac{Q_{S1}^{-1}}{2}(p_E - q_{SE1}\tan\delta_{S1}) = \frac{Q_{S2}^{-1}}{2}(p_E - q_{SE2}\tan\delta_{S2}), \end{aligned} \tag{4.13}$$

where

$$q_{SE} = \frac{\cos\theta_S}{V_{SE}}, \qquad q_{PE} = \frac{\cos\theta_P}{V_{PE}}, \tag{4.14}$$

are the elastic vertical slownesses. Here θ_{P1} is the angle for incident P-wave, θ_{P2} the angle for transmitted P-wave, θ_{S1} the angle of reflected S-wave and θ_{S2} the angle of transmitted S-wave. Using the imaginary part of Snell's law we can analyze the conditions for homogeneity and inhomogeneity of the reflected and transmitted waves (Borcherdt, 2009, 1982). For example, for an incident P-wave, the angle of incidence is equal to the angle of the reflected P-wave, which is confirmed using the real part of Snell's law. In this case the imaginary part of Snell's law ensures that the attenuation angle for incident and reflected waves are equal. As a result the reflected P-wave is homogeneous if and only if the incident wave is homogeneous. Let us consider the case where we have an incident inhomogeneous P-wave. Using the first

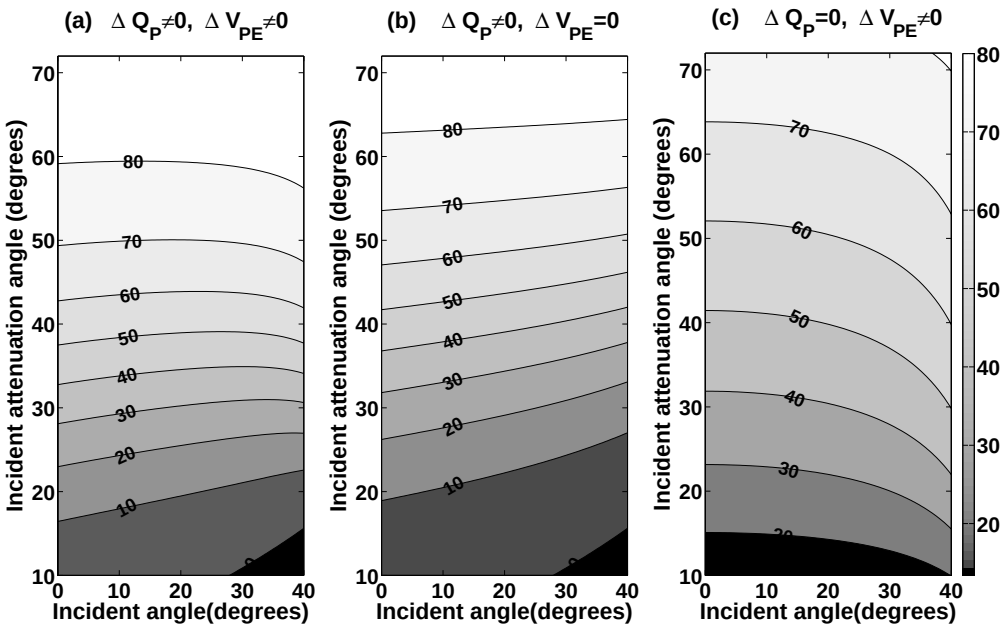

Figure 4.2: Diagram illustrating the transmitted attenuation angle δ_{P2} versus incident angle θ_{P1} and incident attenuation angle δ_{P1}(a) contract in both velocity and quality factor (b) contrast in quality factor with constant velocity (c) contrast in velocity with constant quality factor.

two terms in (4.13) and equations (4.12) and (4.14), the transmitted attenuation angle for the P-wave, in terms of incident attenuation angle and incident phase angle, is given by

$$\tan\delta_{P2} = \left(\frac{V_{PE2}}{V_{PE1}}\right)\frac{\sin\theta_{P1} - \frac{Q_{P2}}{Q_{P1}}\left[\sin\theta_{P1} - \cos\theta_{P1}\tan\delta_{P1}\right]}{\sqrt{1-\left(\frac{V_{PE2}}{V_{PE1}}\right)^2\sin^2\theta_{P1}}}. \tag{4.15}$$

For reflected and transmitted S-wave, respectively we have

$$\begin{aligned}\tan\delta_{S1} &= \left(\frac{V_{SE1}}{V_{PE1}}\right)\frac{\sin\theta_{P1} - \frac{Q_{S1}}{Q_{P1}}\left[\sin\theta_{P1} - \cos\theta_{P1}\tan\delta_{P1}\right]}{\sqrt{1-\left(\frac{V_{SE1}}{V_{PE1}}\right)^2\sin^2\theta_{P1}}},\\ \tan\delta_{S2} &= \left(\frac{V_{SE2}}{V_{PE1}}\right)\frac{\sin\theta_{P1} - \frac{Q_{S2}}{Q_{P1}}\left[\sin\theta_{P1} - \cos\theta_{P1}\tan\delta_{P1}\right]}{\sqrt{1-\left(\frac{V_{SE2}}{V_{PE1}}\right)^2\sin^2\theta_{P1}}}.\end{aligned} \tag{4.16}$$

For an incident P-wave, if $V_{PE2} > V_{SE2} > V_{PE1}$, when $\theta_{P1} \to 90°$, the wave is refracted rather than transmitted. In this case Snell's law predicts two critical angles, one for the refracted P-wave and the other for the refracted S-wave.

Let us consider the special case in which there is no contrast in P-wave quality factors

$Q_{P1} = Q_{P2}$. In this case

$$\tan\delta_{P2} = \frac{\left(\frac{V_{PE2}}{V_{PE1}}\right)\cos\theta_{P1}}{\sqrt{1-\left(\frac{V_{PE2}}{V_{PE1}}\right)^2\sin^2\theta_{P1}}}\tan\delta_{P1}. \tag{4.17}$$

This equation shows that even if there is no contrast in the P-wave quality factor, the incident and transmitted attenuation angles are different. In other words, a P-wave velocity contrast alone can cause a change in the attenuation angle. Figure 4.2, illustrates the transmitted attenuation angle versus incident angle and incident attenuation angle. It can be seen that for a contrast in P-wave velocity the incident and transmitted attenuation angles are not the same. At normal incidence, $\theta_{P1} = 0$, we have

$$\tan\delta_{P2} = \left(\frac{V_{\mathrm{PE2}}Q_{P2}}{V_{\mathrm{PE1}}Q_{P1}}\right)\tan\delta_{P1}, \tag{4.18}$$

$$\tan\delta_{S1} = \left(\frac{V_{\mathrm{SE1}}Q_{S1}}{V_{\mathrm{PE1}}Q_{P1}}\right)\tan\delta_{P1}, \tag{4.19}$$

$$\tan\delta_{S2} = \left(\frac{V_{\mathrm{SE2}}Q_{S2}}{V_{\mathrm{PE1}}Q_{P1}}\right)\tan\delta_{P1}. \tag{4.20}$$

So at normal incidence, if the incident P-wave is an (in)homogeneous wave, the reflected or transmitted S- and P-waves are (in)homogenous.

To analyze the contributions of the jumps in elastic and anelastic properties to the reflectivities, in an environment familiar to AVO theorists and practitioners, we next linearize the reflection amplitudes. To calculate the approximate reflectivities for a low contrast model, and to write the physical quantities in medium 1, and medium 2 in terms of fractional perturbations, we must express the phase and attenuation angles in perturbed form. This in turn requires us to linearize the generalized Snell's law in eqs. (4.12) and (4.13).

The main assumption required to extract the approximate form of the reflectivities is that the physical properties in the two layers are only slightly different. In other words, we can define fractional changes in properties as perturbations which are much smaller than one. This procedure is straightforward for properties of the medium like density, velocities and quality factors. For example the density of the layer above the reflector is given by

$$\rho_1 = \bar{\rho}\left(1 - \frac{1}{2}\frac{\Delta\rho}{\bar{\rho}}\right), \tag{4.21}$$

while the density in the layer below the reflector is

$$\rho_2 = \bar{\rho}\left(1 + \frac{1}{2}\frac{\Delta\rho}{\bar{\rho}}\right). \tag{4.22}$$

Similar expressions are valid for V_{P}, V_S, Q_{P} and Q_{S}. In the above relations, Δ refers to the difference in the lower and upper layers and bar indicates the average of the quantities. In the final form of the linearized reflectivity we shouldn't have any quantities related explicitly to either the upper or lower medium. Hence we need to express the phase and attenuation angles in terms of corresponding perturbations. This can be done by linearization of Snell's law. In the previous section we saw that Snell's law has both real and imaginary parts. By applying the linearization to the real part we obtain the perturbation in phase angle in terms of the perturbation in the corresponding velocity, weighted by the average of the phase angle. Using the linearization of the imaginary part, we obtain the perturbation in the attenuation angle in terms of the perturbations in the corresponding velocities and quality factors. In what follows any quantity related to the material property, slowness vector or angles without subscripts 1 or 2, stands for the average of that quantity. The real part of Snell's law for P-wave results in:

$$\frac{\sin\theta_{P1}}{V_{PE1}} = \frac{\sin\theta_{P2}}{V_{PE2}}. \tag{4.23}$$

Using the expressions (4.21) and (4.22) for incidence phase angle for P-wave, θ_{P1}, and transmitted phase angle θ_{P2}, we expand the sin functions as

$$\sin\theta_{P1} = \sin\theta_{\mathrm{P}}\left(1 - \frac{1}{2}\frac{\Delta\theta_{\mathrm{P}}}{\tan\theta_{\mathrm{P}}}\right), \tag{4.24}$$

$$\sin\theta_{P2} = \sin\theta_{\mathrm{P}}\left(1 + \frac{1}{2}\frac{\Delta\theta_{\mathrm{P}}}{\tan\theta_{\mathrm{P}}}\right). \tag{4.25}$$

Inserting (4.24) and (4.25) and corresponding expressions for V_{PE1} and V_{PE2} in terms of average and differences in the P-wave velocity, we obtain the difference in the incidence and transmitted angles in terms of the fractional perturbation in the P-wave velocity

$$\Delta\theta_{\mathrm{P}} \approx \frac{\Delta V_{\mathrm{PE}}}{V_{\mathrm{PE}}}\tan\theta_{\mathrm{P}}. \tag{4.26}$$

A similar expression holds for the θ_S. Consider the imaginary part of the Snell's law as

$$\frac{Q_{P2}}{Q_{P1}}\frac{V_{PE2}}{V_{PE1}}\frac{\cos\delta_{P2}}{\cos\delta_{P1}} = \frac{\sin\left(\theta_{P2} - \delta_{P2}\right)}{\sin\left(\theta_{P1} - \delta_{P1}\right)}. \tag{4.27}$$

By expansion of the cosine functions in terms of differences and averages in attenuation angle we arrive at

$$\cos\delta_{P1} = \cos\delta_{\mathrm{P}}\left(1+\frac{1}{2}\tan\delta_{\mathrm{P}}\Delta\delta_{\mathrm{P}}\right), \tag{4.28}$$

$$\cos\delta_{P2} = \cos\delta_{\mathrm{P}}\left(1-\frac{1}{2}\tan\delta_{\mathrm{P}}\Delta\delta_{\mathrm{P}}\right). \tag{4.29}$$

Using the equations (4.24) and (4.25) for sin of δ_{P1}, δ_{P2}, θ_{P1}, θ_{P2} and the corresponding relation for velocities and quality factors in terms of perturbations we arrive at

$$\Delta\delta_{\mathrm{P}} = \frac{1}{2}\sin 2\delta_{\mathrm{P}}\left\{\frac{\Delta V_{\mathrm{PE}}}{V_{\mathrm{PE}}}\frac{1}{\cos^2\theta_{\mathrm{P}}}+\left(1-\frac{\tan\theta_{\mathrm{P}}}{\tan\delta_{\mathrm{P}}}\right)\frac{\Delta Q_{\mathrm{P}}}{Q_{\mathrm{P}}}\right\}, \tag{4.30}$$

and similarly for the S-wave

$$\Delta\delta_{S} = \frac{1}{2}\sin 2\delta_{S}\left\{\frac{\Delta V_{\mathrm{SE}}}{V_{\mathrm{SE}}}\frac{1}{\cos^2\theta_{S}}+\left(1-\frac{\tan\theta_{S}}{\tan\delta_{S}}\right)\frac{\Delta Q_{\mathrm{S}}}{Q_{\mathrm{S}}}\right\}. \tag{4.31}$$

As a result, perturbation in attenuation angle can be expressed in terms of perturbation in elastic velocities and quality factors. Also perturbation in attenuation angle depends to the average angle θ.

4.5 Exact reflection/transmission coefficients

It has been shown that waves with elliptical polarization can not be converted to waves with the linear polarizations (Borcherdt, 2009; Moradi and Innanen, 2015b). For example SII wave that has a linear polarization does not convert to P or SI waves. As a result we can write the reflection transmission for P- and SI-waves as a 4×4 matrix given by

$$\mathrm{R} = \begin{pmatrix} {}^{\downarrow}\mathrm{PP}^{\uparrow} & {}^{\downarrow}\mathrm{SIP}^{\uparrow} & {}^{\uparrow}\mathrm{PP}^{\uparrow} & {}^{\uparrow}\mathrm{SIP}^{\uparrow} \\ {}^{\downarrow}\mathrm{PSI}^{\uparrow} & {}^{\downarrow}\mathrm{SISI}^{\uparrow} & {}^{\uparrow}\mathrm{PSI}^{\uparrow} & {}^{\uparrow}\mathrm{SISI}^{\uparrow} \\ {}^{\downarrow}\mathrm{PP}^{\downarrow} & {}^{\downarrow}\mathrm{SIP}^{\downarrow} & {}^{\uparrow}\mathrm{PP}^{\downarrow} & {}^{\uparrow}\mathrm{SIP}^{\downarrow} \\ {}^{\downarrow}\mathrm{PSI}^{\downarrow} & {}^{\downarrow}\mathrm{SISI}^{\downarrow} & {}^{\uparrow}\mathrm{PSI}^{\downarrow} & {}^{\uparrow}\mathrm{SISI}^{\downarrow} \end{pmatrix}. \tag{4.32}$$

In this notation, the first letter refers the type of incident wave, and the second letter denotes the type of reflected or transmitted wave. The downward arrow $\downarrow$ indicates a wave traveling downward and $\uparrow$ indicates a wave traveling upward. So that a combination $\downarrow\uparrow$ refers a reflection coefficient, and a combination $\uparrow\uparrow$ indicates a transmission coefficient. The

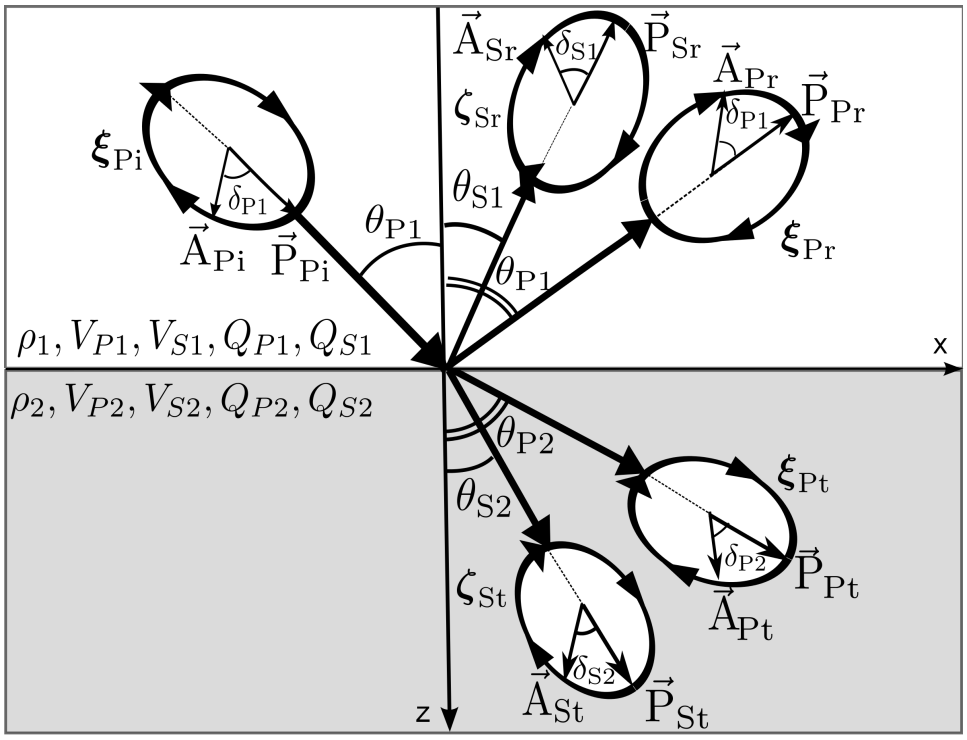

Figure 4.3: Schematic diagram showing definitions of the phase and attenuation angles of the incident, reflected, and transmitted rays of an incident P-wave with non-normal incidence. Medium 1 is defined by its P-wave velocity V_{P1}, S-wave velocity V_{S1}, P-wave quality factor Q_{P1}, S-wave quality factor Q_{S1} and its density ρ_1; and for medium 2, by $V_{\mathrm{P2}}, V_{\mathrm{S2}}, Q_{\mathrm{P2}}, Q_{\mathrm{S2}}$ and ρ_2. Angles are defined as, θ_{P1} for the incident and reflected P-wave in medium 1, θ_{S1} for the reflected SI-wave, and θ_{P2} and θ_{S2} respectively for transmitted P- and SI-waves. Attenuation angle for incident and reflected P-wave is given by δ_{P1}, also attenuation angles for reflected SI-wave, transmitted P- and SI-waves respectively are given by δ_{S1}, δ_{S2} and δ_{P2}. ξ_{Pi}, ξ_{Pr} and ξ_{Pt} respectively denotes the complex polarization vectors for incident, reflected and transmitted P-waves and ζ_{Sr} and ζ_{St} are the polarizations for the reflected and transmitted SI-waves respectively.

diagonal elements of the reflection-transmission matrix represents the reflections that preserve the type of the waves. For example ${}^{\downarrow}\mathrm{PP}^{\uparrow}$ refers to the reflected upgoing P-wave from downgoing incidence P-wave and similar explanations for other diagonal elements. On the other hand some off-diagonal elements indicate converted waves. For instance, ${}^{\downarrow}\mathrm{SIP}^{\uparrow}$ denotes a reflected upgoing P from incidence downgoing SI wave. Other off-diagonal elements refer to transmitted waves either converted modes or preserved modes. For example ${}^{\downarrow}\mathrm{SISI}^{\downarrow}$ is related to the transmitted downgoing SI wave from a downgoing incidence SI wave and ${}^{\downarrow}\mathrm{SIP}^{\downarrow}$ is a downgoing transmitted P wave from a downgoing incidence SI wave. For non-normal incidence, an incident P-wave generates reflected P- and SI-waves and transmitted P- and SI-waves. The reflection and transmission coefficients depend on the angle of incidence and attenuation as well as on the material properties of the two layers. Fig. 4.3, is a schematic description of the reflection/transmission problem for an incident inhomogeneous P-wave. The displacements for incident, reflected and transmitted waves are

$$\mathbf{U}^{\downarrow}_{\mathrm{Pi}} \simeq \boldsymbol{\xi}_{\mathrm{Pi}} \exp\left(i\mathbf{K}_{\mathrm{Pi}} \cdot \mathbf{r}\right) = \left(\xi_{\mathrm{P}1x}\mathbf{x} + \xi_{\mathrm{P}1z}\mathbf{z}\right) \exp\left\{i\omega(\mathrm{p}x + \mathrm{q}_{\mathrm{P}1}z)\right\}, \tag{4.33}$$

$$\mathbf{U}^{\uparrow}_{\mathrm{Pr}} \simeq ({}^{\downarrow}\mathrm{PP}^{\uparrow})\boldsymbol{\xi}_{\mathrm{Pr}} \exp\left(i\mathbf{K}_{\mathrm{Pr}} \cdot \mathbf{r}\right) = ({}^{\downarrow}\mathrm{PP}^{\uparrow})\left(\xi_{\mathrm{P}1x}\mathbf{x} - \xi_{\mathrm{P}1z}\mathbf{z}\right) \exp\left\{i\omega(\mathrm{p}x - \mathrm{q}_{\mathrm{P}1}z)\right\}, \tag{4.34}$$

$$\mathbf{U}^{\downarrow}_{\mathrm{Pt}} \simeq ({}^{\downarrow}\mathrm{PP}^{\downarrow})\boldsymbol{\xi}_{\mathrm{Pt}} \exp\left(i\mathbf{K}_{\mathrm{Pt}} \cdot \mathbf{r}\right) = ({}^{\downarrow}\mathrm{PP}^{\downarrow})\left(\xi_{\mathrm{P}2x}\mathbf{x} + \xi_{\mathrm{P}2z}\mathbf{z}\right) \exp\left\{i\omega(\mathrm{p}x + \mathrm{q}_{\mathrm{P}2}z)\right\}, \tag{4.35}$$

$$\mathbf{U}^{\uparrow}_{\mathrm{Sr}} \simeq ({}^{\downarrow}\mathrm{PSI}^{\uparrow})\boldsymbol{\zeta}_{\mathrm{Sr}} \exp\left(i\mathbf{K}_{\mathrm{Sr}} \cdot \mathbf{r}\right) = ({}^{\downarrow}\mathrm{PSI}^{\uparrow})\left(\xi_{\mathrm{S}1z}\mathbf{x} + \xi_{\mathrm{S}1x}\mathbf{z}\right) \exp\left\{i\omega(\mathrm{p}x - \mathrm{q}_{\mathrm{S}1}z)\right\}, \tag{4.36}$$

$$\mathbf{U}^{\downarrow}_{\mathrm{St}} \simeq ({}^{\downarrow}\mathrm{PSI}^{\downarrow})\boldsymbol{\zeta}_{\mathrm{St}} \exp\left(i\mathbf{K}_{\mathrm{St}} \cdot \mathbf{r}\right) = ({}^{\downarrow}\mathrm{PSI}^{\downarrow})\left(\xi_{\mathrm{S}2z}\mathbf{x} - \xi_{\mathrm{S}2x}\mathbf{z}\right) \exp\left\{i\omega(\mathrm{p}x + \mathrm{q}_{\mathrm{S}2}z)\right\}, \tag{4.37}$$

Here the angle of incidence and reflection for the P-wave is defined by $\theta_{\mathrm{P}1}$, the angle of the reflected SI-wave defined by $\theta_{\mathrm{S}1}$, and $\theta_{\mathrm{P}2}$, and $\theta_{\mathrm{S}2}$ are the angles respectively for transmitted P- and SI waves. After solving the Zoeppritz equations, the reflection coefficients are given by (Ikelle and Amundsen, 2005)

$$({}^{\downarrow}\mathrm{PP}^{\uparrow}) = \frac{c_1 d_2 - c_3 d_4}{d_1 d_2 + d_3 d_4}, \tag{4.38}$$

$$({}^{\downarrow}\mathrm{PSI}^{\uparrow}) = -\left(\frac{V_{P1}}{V_{S1}}\right)\frac{c_3 d_1 + c_1 d_3}{d_1 d_2 + d_3 d_4}, \tag{4.39}$$

$$({}^{\downarrow}\mathrm{SISI}^{\uparrow}) = -\frac{c_2 d_1 + c_4 d_3}{d_1 d_2 + d_3 d_4}, \tag{4.40}$$

where

$$d_1 = -2p^2\Delta M(q_{P1} - q_{P2}) + (\rho_1 q_{P2} + \rho_2 q_{P1}), \tag{4.41}$$

$$d_2 = -2p^2\Delta M(q_{S1} - q_{S2}) + (\rho_1 q_{S2} + \rho_2 q_{S1}), \tag{4.42}$$

$$d_3 = -p\left[2\Delta M(q_{P1}q_{S2} + p^2) - \Delta\rho\right], \tag{4.43}$$

$$d_4 = -p\left[2\Delta M(q_{P2}q_{S1} + p^2) - \Delta\rho\right], \tag{4.44}$$

$$c_1 = -2p^2\Delta M(q_{P1} + q_{P2}) - (\rho 1 q_{P2} - \rho_2 q_{P_1}), \tag{4.45}$$

$$c_2 = -2p^2\Delta M(q_{S1} + q_{S2}) - (\rho_1 q_{S2} - \rho_2 q_{S1}), \tag{4.46}$$

$$c_3 = p\left[2\Delta M(q_{P1}q_{S2} - p^2) + \Delta\rho\right], \tag{4.47}$$

$$c_4 = p\left[2\Delta M(q_{P2}q_{S1} - p^2) + \Delta\rho\right]. \tag{4.48}$$

We can write the differences in complex moduli M as a sum of the differences in elastic shear modulus plus an imaginary part

$$\Delta M = \Delta\mu_E + i\Delta\mu_A, \tag{4.49}$$

where the real part is given by

$$\Delta\mu_E = \mu_{E2} - \mu_{E1} = \rho_2 V_{SE2}^2 - \rho_1 V_{SE1}^2, \tag{4.50}$$

and imaginary part by

$$\Delta\mu_A = Q_{S2}^{-1}\mu_{E2} - Q_{S1}^{-1}\mu_{E1} = \rho_2 V_{SE2}^2 Q_{S2}^{-1} - \rho_1 V_{SE1}^2 Q_{S1}^{-1}. \tag{4.51}$$

By having the exact reflection coefficients, and the linearization tools for viscoelastic properties, we are ready to calculate the AVO equations.

4.6 Linearization of reflectivity

In this section we derive the linearized form of the P-to-P, P-to-SI and SI-to-SI reflection coefficients. For a low-loss viscoelastic medium we follow the Aki and Richards (2002) approach which is based on the assumption of low contrasts in both elastic and anelastic properties.

For a viscoelastic medium, linearized coefficients are functions of the averages of elastic and anelastic properties across the interface and fractional changes in properties. Amplitude variation with offset (AVO) analysis is based on expressions for reflection coefficients in elastic media. If anelasticity is present it is modified to a complex quantity whose real part is the elastic reflection coefficients. The exact form of the reflectivities are too complicated to provide much intuitive information about the physical properties of the subsurface and their relationship with seismic amplitudes. Fortunately, for most reflecting interfaces in seismology the change in the elastic and anelastic properties are small, so that we can linearize the reflectivities in terms of perturbations of earth properties, defined as the ratio of the difference to the average of the properties of the contiguous layers. The resulting equations are much more straightforward to analyze, and form a stable platform for inversion.

4.6.1 P-to-P reflection coefficient

In this section we derive the first order approximation to the P-to-P reflection coefficient. Let us consider the case that an inhomogeneous P-wave hits the boundary of a slightly different low-loss viscoelastic medium (Figure 4.4). In this case the reflected P-wave is also an inhomogeneous wave. All complex quantities and expressions we have defined thus far include a first order contribution from the attenuation factor Q^{-1}. As a result, in the low-loss approximation any term in (4.38) which includes two imaginary parts in a product is negligible.

From Eqs. (4.43), (4.44) and (4.47) we notice that $c_3 d_4$ and $d_3 d_4$ are in second order in the perturbations, which can be ignored in the first order approximation. If we keep first order terms only, the P-to-P reflection (4.38) reduces to

$$({}^{\downarrow}\mathrm{PP}^{\uparrow}) = \frac{c_1}{d_1} = \frac{2p^2\Delta M(q_{P_1} + q_{P_2}) + (\rho_1 q_{P_2} - \rho_2 q_{P_1})}{2p^2\Delta M(q_{P_1} - q_{P_2}) - (\rho_1 q_{P_2} + \rho_2 q_{P_1})}. \tag{4.52}$$

From the above equation we can not determine intuitively the influence of the change in a particular elastic or anelastic parameter on the reflectivity. We next linearize the above reflection coefficient according to the low contrast approximation. First if we expand (4.52) in terms of ΔM to first order we have

$$({}^{\downarrow}\mathrm{PP}^{\uparrow}) = ({}^{\downarrow}\mathrm{PP}^{\uparrow})^{\mathrm{FF}} + ({}^{\downarrow}\mathrm{PP}^{\uparrow})^{\mathrm{M}}, \tag{4.53}$$

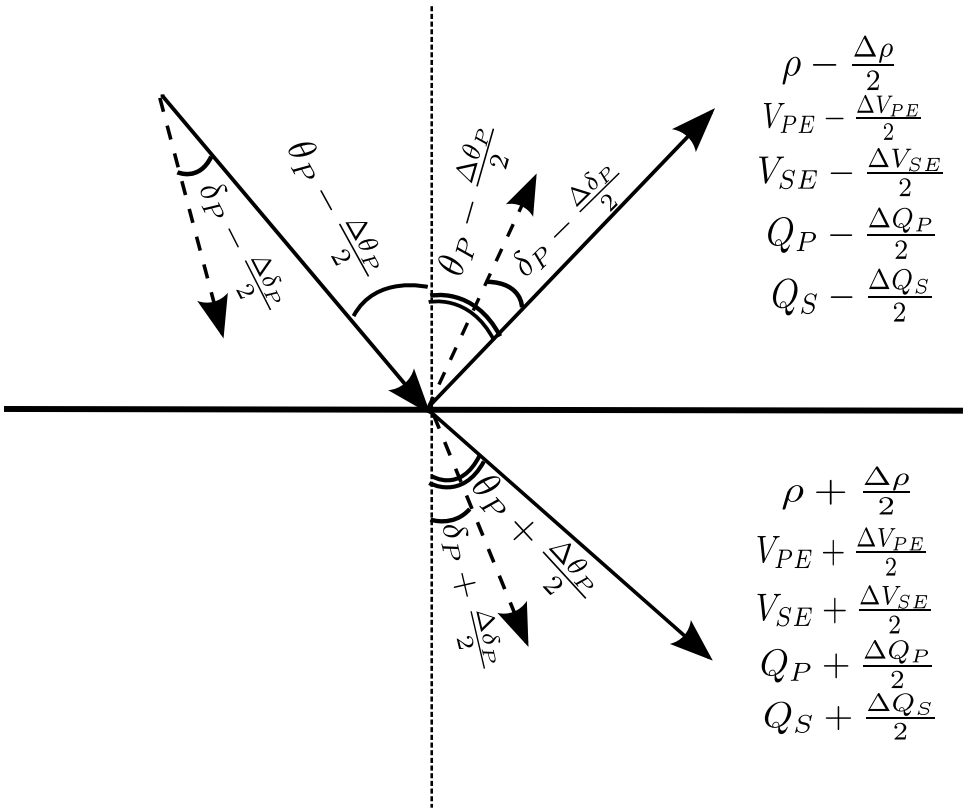

Figure 4.4: Schematic diagram illustrating the terms in linearized P-to-P reflectivity. Incident, reflected and transmitted phase and attenuation angles can be expressed in terms of averages and differences in angles. Same interpretation is valid for SI-wave.

where the first term is related to the reflectivity of the fluid-fluid interface

$$({}^{\downarrow}\mathrm{PP}^{\uparrow})^{\mathrm{FF}} = \frac{1}{2}\left(\frac{\Delta\rho}{\rho} - \frac{\Delta q_{\mathrm{P}}}{q_{\mathrm{P}}}\right), \tag{4.54}$$

and the second term is related to the change in complex modulus M

$$({}^{\downarrow}\mathrm{PP}^{\uparrow})^{\mathrm{M}} = -2p^2\frac{\Delta M}{\rho}. \tag{4.55}$$

The linearization of the fluid-fluid reflectivity results

$$({}^{\downarrow}\mathrm{PP}^{\uparrow})^{\mathrm{FF}} = ({}^{\downarrow}\mathrm{PP}^{\uparrow})^{\mathrm{FF}}_{\mathrm{E}} + i({}^{\downarrow}\mathrm{PP}^{\uparrow})^{\mathrm{FF}}_{\mathrm{A}}, \tag{4.56}$$

where the first term, which is the real part of the $({}^{\downarrow}\mathrm{PP}^{\uparrow})^{\mathrm{FF}}$, is the reflectivity for a fluid-fluid interface for a non attenuative medium

$$({}^{\downarrow}\mathrm{PP}^{\uparrow})^{\mathrm{FF}}_{\mathrm{E}} = \frac{1}{2}\frac{\Delta\rho}{\rho} + \frac{1}{2\cos^2\theta_{\mathrm{P}}}\frac{\Delta V_{\mathrm{PE}}}{V_{\mathrm{PE}}}, \tag{4.57}$$

and the anelastic part which induced by the change in P-wave velocity and P-wave quality factor is given by

$$({}^{\downarrow}\mathrm{PP}^{\uparrow})^{\mathrm{FF}}_{\mathrm{A}} = \frac{1}{2\cos^2\theta_{\mathrm{P}}}Q_{\mathrm{P}}^{-1}\left(\tan\theta_{\mathrm{P}}\tan\delta_{\mathrm{P}}\frac{\Delta V_{\mathrm{PE}}}{V_{\mathrm{PE}}} - \frac{1}{2}\frac{\Delta Q_{\mathrm{P}}}{Q_{\mathrm{P}}}\right). \tag{4.58}$$

Comparing the fluid-fluid reflectivity for elastic and viscoelastic media it can be seen that, in the elastic case, when the contrast in P-wave velocity is zero, reflectivity depends only upon the change in the density and is independent of the incidence angle. On the other hand for a viscoelastic medium, even if the contrast in P-wave velocity is zero, the reflectivity is angle dependent. Consider the term in equation (4.55), which is the contribution of the change of complex moduli M to the reflectivity. The real and imaginary parts of the perturbation in complex moduli are given by

$$\Delta\mu_E = \rho V_{\mathrm{SE}}^2\left[\frac{\Delta\rho}{\rho} + 2\frac{\Delta V_{\mathrm{SE}}}{V_{\mathrm{SE}}}\right], \tag{4.59}$$

$$\Delta\mu_A = \rho Q_{\mathrm{S}}^{-1}V_{\mathrm{SE}}^2\left(\frac{\Delta\rho}{\rho} + 2\frac{\Delta V_{\mathrm{SE}}}{V_{\mathrm{SE}}} - \frac{\Delta Q_{\mathrm{S}}}{Q_{\mathrm{S}}}\right). \tag{4.60}$$

Inserting the above relations in (4.55), we arrive at

$$({}^{\downarrow}\mathrm{PP}^{\uparrow})^{\mathrm{M}} = ({}^{\downarrow}\mathrm{PP}^{\uparrow})^{\mathrm{M}}_{\mathrm{E}} + i({}^{\downarrow}\mathrm{PP}^{\uparrow})^{\mathrm{M}}_{\mathrm{A}}. \tag{4.61}$$

Where the real part, which is related to the case where the attenuation is zero in the medium, is given by

$$({}^{\downarrow}\mathrm{PP}^{\uparrow})_{\mathrm{E}}^{\mathrm{M}} = -2\sin^2\theta_P \left(\frac{V_{\mathrm{SE}}}{V_{\mathrm{PE}}}\right)^2 \left[\frac{\Delta\rho}{\rho} + 2\frac{\Delta V_{\mathrm{SE}}}{V_{\mathrm{SE}}}\right], \tag{4.62}$$

and the imaginary part by

$$\begin{aligned}({}^{\downarrow}\mathrm{PP}^{\uparrow})_{\mathrm{A}}^{\mathrm{M}} = &-2\sin^2\theta_P \left(\frac{V_{\mathrm{SE}}}{V_{\mathrm{PE}}}\right)^2 \times \\ &\left\{\left[\frac{\Delta\rho}{\rho} + 2\frac{\Delta V_{\mathrm{SE}}}{V_{\mathrm{SE}}}\right]\left(Q_{\mathrm{S}}^{-1} - Q_{\mathrm{P}}^{-1}\left[1 - \frac{\tan\delta_{\mathrm{P}}}{\tan\theta_{\mathrm{P}}}\right]\right) - Q_{\mathrm{S}}^{-1}\frac{\Delta Q_{\mathrm{S}}}{Q_{\mathrm{S}}}\right\}.\end{aligned} \tag{4.63}$$

Evidently contrasts in complex moduli M affect the reflectivity only for nonzero offsets. Finally, the P-to-P reflectivity can be rewritten into

$$({}^{\downarrow}\mathrm{PP}^{\uparrow}) = ({}^{\downarrow}\mathrm{PP}^{\uparrow})_{\mathrm{E}} + i({}^{\downarrow}\mathrm{PP}^{\uparrow})_{\mathrm{A}}, \tag{4.64}$$

where the imaginary part is given by

$$({}^{\downarrow}\mathrm{PP}^{\uparrow})_{\mathrm{A}} = ({}^{\downarrow}\mathrm{PP}^{\uparrow})_{\mathrm{A}}^{\rho} + ({}^{\downarrow}\mathrm{PP}^{\uparrow})_{\mathrm{A}}^{\mathrm{V_{PE}}} + ({}^{\downarrow}\mathrm{PP}^{\uparrow})_{\mathrm{A}}^{\mathrm{V_{SE}}} + ({}^{\downarrow}\mathrm{PP}^{\uparrow})_{\mathrm{A}}^{\mathrm{Q_P}} + ({}^{\downarrow}\mathrm{PP}^{\uparrow})_{\mathrm{A}}^{\mathrm{Q_S}}, \tag{4.65}$$

with the density component

$$({}^{\downarrow}\mathrm{PP}^{\uparrow})_{\mathrm{A}}^{\rho} = -\left(\frac{V_{\mathrm{SE}}}{V_{\mathrm{PE}}}\right)^2 \left(2(Q_{\mathrm{S}}^{-1} - Q_{\mathrm{P}}^{-1})\sin^2\theta_P + Q_{\mathrm{P}}^{-1}\tan\delta_{\mathrm{P}}\sin 2\theta_{\mathrm{P}}\right)\frac{\Delta\rho}{\rho}, \tag{4.66}$$

the P-wave velocity component

$$({}^{\downarrow}\mathrm{PP}^{\uparrow})_{\mathrm{A}}^{\mathrm{V_{PE}}} = Q_{\mathrm{P}}^{-1}\frac{\tan\theta_{\mathrm{P}}\tan\delta_{\mathrm{P}}}{2\cos^2\theta_{\mathrm{P}}}\frac{\Delta V_{\mathrm{PE}}}{V_{\mathrm{PE}}}, \tag{4.67}$$

the S-wave velocity component

$$({}^{\downarrow}\mathrm{PP}^{\uparrow})_{\mathrm{A}}^{\mathrm{V_{SE}}} = -2\left(\frac{V_{\mathrm{SE}}}{V_{\mathrm{PE}}}\right)^2 \left(2(Q_{\mathrm{S}}^{-1} - Q_{\mathrm{P}}^{-1})\sin^2\theta_P + Q_{\mathrm{P}}^{-1}\tan\delta_{\mathrm{P}}\sin 2\theta_{\mathrm{P}}\right)\frac{\Delta V_{\mathrm{SE}}}{V_{\mathrm{SE}}}, \tag{4.68}$$

the P-wave quality factor component

$$({}^{\downarrow}\mathrm{PP}^{\uparrow})_{\mathrm{A}}^{\mathrm{Q_P}} = -\frac{1}{4\cos^2\theta_{\mathrm{P}}}Q_{\mathrm{P}}^{-1}\frac{\Delta Q_{\mathrm{P}}}{Q_{\mathrm{P}}}, \tag{4.69}$$

and the S-wave quality factor component

$$({}^{\downarrow}\mathrm{PP}^{\uparrow})_{\mathrm{A}}^{\mathrm{Qs}} = 2\sin^2\theta_{\mathrm{P}}\left(\frac{V_{\mathrm{SE}}}{V_{\mathrm{PE}}}\right)^2 Q_{\mathrm{S}}^{-1}\frac{\Delta Q_{\mathrm{S}}}{Q_{\mathrm{S}}}. \tag{4.70}$$

$$\tag{4.71}$$

The real part is

$$({}^{\downarrow}\mathrm{PP}^{\uparrow})_{\mathrm{E}} = \frac{1}{2}\left(\frac{\Delta\rho}{\rho} + \frac{1}{\cos^2\theta_{\mathrm{P}}}\frac{\Delta V_{\mathrm{PE}}}{V_{\mathrm{PE}}}\right) - 2\sin^2\theta_P\left(\frac{V_{\mathrm{SE}}}{V_{\mathrm{PE}}}\right)^2\left(\frac{\Delta\rho}{\rho} + 2\frac{\Delta V_{\mathrm{SE}}}{V_{\mathrm{SE}}}\right). \tag{4.72}$$

$({}^{\downarrow}\mathrm{PP}^{\uparrow})_{\mathrm{E}}$ is the P-to-P reflection coefficient for a low contrast interface between two isotropic elastic layered media. The real part of the linearized P-to-P reflectivity for two slightly different low-loss viscoelastic media is the P-to-P reflection coefficient induced by a contrast in elastic properties. The imaginary part is caused by both elastic and/or anelastic contrasts between the two layeres. As a consequence, even if the quality factors for P- and S-waves do not change between the two layers, the contrasts in elastic properties can still contribute an imaginary part. At normal incidence,

$$({}^{\downarrow}\mathrm{PP}^{\uparrow}) = \frac{\Delta\rho}{2\rho} + \frac{\Delta V_{\mathrm{PE}}}{2V_{\mathrm{PE}}} - \frac{i}{4}Q_{\mathrm{P}}^{-1}\frac{\Delta Q_{\mathrm{P}}}{Q_{\mathrm{P}}}. \tag{4.73}$$

So, at normal incidence the reflectivity is affected by the by contrast in the P-wave quality factor. The relative change in density and P-wave velocity have similar influence on the normal incidence reflection coefficient.

4.7 Linearized P-to-SI reflection

In this section we derive the converted P-to-SI reflection coefficient for a two-layered low-loss viscoelastic medium with small contrast in material properties across the boundary. For an isotropic viscoelastic medium, the converted P-to-SI wave amplitude variation patterns reveal the changes in density, S-wave velocity and quality factor. When the incidence wave is an inhomogeneous P-wave, the reflected wave can be either an inhomogeneous P- or SI-wave. In contrast to the elastic case, the linearization is more complicated and the linearized result includes the terms related to the change in S-wave quality factor. Under the low-contrast and low-loss medium assumptions, the P-to-SI reflection coefficient in equation (4.39) reduces to

$$({}^{\downarrow}\mathrm{PSI}^{\uparrow}) = -\left(\frac{V_{\mathrm{P1}}}{V_{\mathrm{S1}}}\right)\frac{c_1d_3 + c_3d_1}{d_1d_2} = -\left(\frac{V_{\mathrm{P1}}}{V_{\mathrm{S1}}}\right)\frac{p}{q_S}\frac{[2(q_{\mathrm{P}}q_S - p^2)\Delta M + \Delta\rho]}{2\rho}. \tag{4.74}$$

In the low-loss approximation we have

$$\frac{p}{q_{\mathrm{S}}} = \tan\theta_S \left(1 + iQ_{\mathrm{S}}^{-1}\frac{\tan\delta_S}{\sin 2\theta_S}\right), \tag{4.75}$$

where q_S, is the average of the vertical slowness for S-wave. To produce a form of the reflectivity that explicitly shows its dependency upon medium property perturbations, we first consider the multiplication of the P- and S-wave vertical slowness vectors

$$\begin{aligned} q_{\mathrm{P}}q_{\mathrm{S}} =& \frac{1}{V_{\mathrm{PE}}V_{\mathrm{SE}}}\left[\cos\theta_{\mathrm{P}}\cos\theta_S\left(1 - \frac{i}{2}(Q_{\mathrm{P}}^{-1} + Q_{\mathrm{S}}^{-1})\right) - \right. \\ & \left. \frac{i}{2}(Q_{\mathrm{S}}^{-1}\tan\delta_S\cos\theta_{\mathrm{P}}\sin\theta_S + Q_{\mathrm{P}}^{-1}\tan\delta_{\mathrm{P}}\cos\theta_S\sin\theta_{\mathrm{P}})\right], \end{aligned} \tag{4.76}$$

and square of the ray parameter

$$\begin{aligned} p^2 =& \frac{1}{V_{\mathrm{PE}}V_{\mathrm{SE}}}\left[\sin\theta_{\mathrm{P}}\sin\theta_S\left(1 - \frac{i}{2}(Q_{\mathrm{P}}^{-1} + Q_{\mathrm{S}}^{-1})\right) + \right. \\ & \left. \frac{i}{2}(Q_{\mathrm{S}}^{-1}\tan\delta_S\cos\theta_S\sin\theta_{\mathrm{P}} + Q_{\mathrm{P}}^{-1}\tan\delta_{\mathrm{P}}\cos\theta_{\mathrm{P}}\sin\theta_S)\right]. \end{aligned} \tag{4.77}$$

Using the perturbation in complex moduli in equations (4.50) and (4.51), we arrive at the linearized P-to-SI reflectivity function

$$({}^{\downarrow}\mathrm{PSI}^{\uparrow}) = ({}^{\downarrow}\mathrm{PSI}^{\uparrow})_{\mathrm{E}} + i({}^{\downarrow}\mathrm{PSI}^{\uparrow})_{\mathrm{A}}, \tag{4.78}$$

where the imaginary part is related to the change in S-wave quality factor, density and S-wave velocity

$$({}^{\downarrow}\mathrm{PSI}^{\uparrow})_{\mathrm{A}} = ({}^{\downarrow}\mathrm{PSI}^{\uparrow})_{\mathrm{A}}^{\rho} + ({}^{\downarrow}\mathrm{PSI}^{\uparrow})_{\mathrm{A}}^{\mathrm{V_{SE}}} + ({}^{\downarrow}\mathrm{PSI}^{\uparrow})_{\mathrm{A}}^{\mathrm{Q_S}}, \tag{4.79}$$

$$\tag{4.80}$$

with the density component

$$\begin{aligned} ({}^{\downarrow}\mathrm{PSI}^{\uparrow})_{\mathrm{A}}^{\rho} =& -\frac{1}{2}\tan\theta_S\left[\frac{1}{2}(Q_P^{-1} - Q_S^{-1}) + Q_S^{-1}\frac{\tan\delta_S}{\sin 2\theta_S}\right]\frac{V_{PE}}{V_{SE}}\frac{\Delta\rho}{\rho} \\ & - \tan\theta_S\cos(\theta_P + \theta_S)\left[Q_S^{-1}\frac{\tan\delta_S}{\sin 2\theta_S}\right]\frac{\Delta\rho}{\rho} \\ & + \frac{1}{2}\tan\theta_S\sin(\theta_P + \theta_S)(Q_S^{-1}\tan\delta_S + Q_P^{-1}\tan\delta_P)\frac{\Delta\rho}{\rho}, \end{aligned} \tag{4.81}$$

the S-wave velocity component

$$
\begin{aligned}
({}^{\downarrow}\mathrm{PSI}^{\uparrow})_{\mathrm{A}}^{\mathrm{V_{SE}}} = & -2\tan\theta_S\cos(\theta_P+\theta_S)\left[Q_S^{-1}\frac{\tan\delta_S}{\sin 2\theta_S}\right]\frac{\Delta V_{SE}}{V_{SE}} \\
& +\tan\theta_S\sin(\theta_P+\theta_S)(Q_S^{-1}\tan\delta_S+Q_P^{-1}\tan\delta_P)\frac{\Delta V_{SE}}{V_{SE}},
\end{aligned}
\tag{4.82}
$$

and the S-wave quality factor component

$$
({}^{\downarrow}\mathrm{PSI}^{\uparrow})_{\mathrm{A}}^{\mathrm{Qs}} = Q_S^{-1}\tan\theta_S\cos(\theta_P+\theta_S)\frac{\Delta Q_S}{Q_S}. \tag{4.83}
$$

In addition, $({}^{\downarrow}\mathrm{PSI}^{\uparrow})_{\mathrm{E}}$ is the reflectivity for non-attenuative medium or the P-to-SV reflectivity. It is given by

$$
({}^{\downarrow}\mathrm{PSI}^{\uparrow})_{\mathrm{E}} = -\tan\theta_S\left(\cos(\theta_{\mathrm{P}}+\theta_S)+\frac{1}{2}\frac{V_{\mathrm{PE}}}{V_{\mathrm{SE}}}\right)\frac{\Delta\rho}{\rho}-2\tan\theta_S\cos(\theta_{\mathrm{P}}+\theta_S)\frac{\Delta V_{\mathrm{SE}}}{V_{\mathrm{SE}}}. \tag{4.84}
$$

In the above expressions, $\theta_{\mathrm{P}}(\theta_{\mathrm{S}})$ is the average of angles of incidence and transmission for P(SI)-wave; θ_{S} can be calculated from θ_{P} using Snell's law; ρ, V_{PE}, V_{SE}, $\mathrm{Q_S}$, $\mathrm{Q_P}$, δ_{P} and δ_{S} are the average quantities. Unlike the P-to-P reflection coefficient, the P-to-SI reflection coefficient does not depend on the contrasts in the P-wave velocity and its quality factor.

Similarly to the P-to-P reflection case, $({}^{\downarrow}\mathrm{PSI}^{\uparrow})_{\mathrm{E}}$ denotes the low contrast reflection coefficient at an interface separating two elastic media. Equation (4.78) represents the P-to-SI reflection coefficient for a low contrast interface separating two arbitrary low-loss viscoelastic media. By inspecting the above equations, at normal incidence, the reflection coefficient is evidently not affected by either elasticity or anelasticity. Approximate SI-to-P reflection coefficient is similar to that of the P-to-SI coefficient; the only difference is that the exchange of rule between P and SI waves.

4.8 SI-to-SI reflection

It has been shown that an SI-wave can be reflected or scattered to either P- or SI-waves, but can not be converted to an SII-wave with a linear polarization. SI-to-P reflectivity is very similar to the P-to-SI case, so we will not consider this case here. Let us consider the SI-to-SI reflectivity. In the first order approximation the exact SI-to-SI reflectivity in equation (4.40) reduces to

$$
({}^{\downarrow}\mathrm{SISI}^{\uparrow}) = \frac{c_2}{d_2} = \frac{2p^2\Delta M(q_{S_1}+q_{S_2})+(\rho_1 q_{S_2}-\rho_2 q_{S_1})}{2p^2\Delta M(q_{S_1}-q_{S_2})-(\rho_1 q_{S_2}+\rho_2 q_{S_1})}. \tag{4.85}
$$

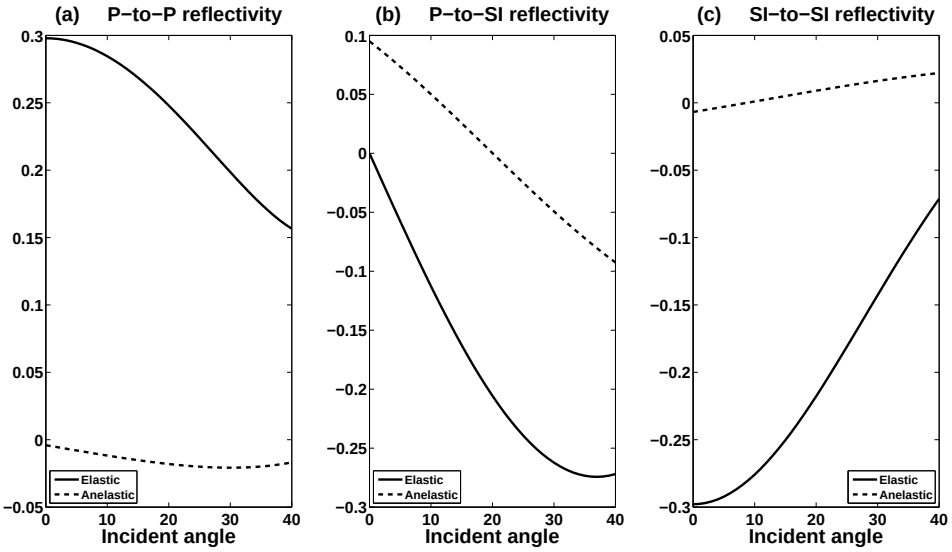

Figure 4.5: Elastic and anelastic parts of linearized reflectivities versus incident angle for $\rho_2/\rho_1 = V_{\rm SE2}/V_{\rm SE1} = V_{\rm PE2}/V_{\rm PE1} = Q_{\rm P2}/Q_{\rm P1} = Q_{\rm S2}/Q_{\rm S1} = 1.35$ and average attenuation angles $\delta_{\rm S} = \delta_{\rm P} = 60^\circ$. Dash line is for anelastic part and solid line for elastic part.

After applying the linearization procedure we arrive at

$$({}^{\downarrow}\mathrm{SISI}^{\uparrow}) = ({}^{\downarrow}\mathrm{SISI}^{\uparrow})_E + i({}^{\downarrow}\mathrm{SISI}^{\uparrow})_A, \tag{4.86}$$

$$\tag{4.87}$$

where the elastic part is given by

$$({}^{\downarrow}\mathrm{SISI}^{\uparrow})_E = \frac{1}{2}\left(1 - 4\sin^2\theta_S\right)\frac{\Delta\rho}{\rho} + \frac{1}{2\cos^2\theta_{\rm S}}(1 - 2\sin^2 2\theta_S)\frac{\Delta V_{\rm SE}}{V_{\rm SE}}, \tag{4.88}$$

and the anelastic term is

$$({}^{\downarrow}\mathrm{SISI}^{\uparrow})_A = ({}^{\downarrow}\mathrm{SISI}^{\uparrow})_A^{\rho} + ({}^{\downarrow}\mathrm{SISI}^{\uparrow})_A^{V_{\rm SE}} + ({}^{\downarrow}\mathrm{SISI}^{\uparrow})_A^{Q_S}, \tag{4.89}$$

with the density component being

$$({}^{\downarrow}\mathrm{SISI}^{\uparrow})_A^{\rho} = -Q_{\rm S}^{-1}\sin 2\theta_S \tan\delta_{\rm S}\frac{\Delta\rho}{\rho}, \tag{4.90}$$

the S-wave velocity component

$$({}^{\downarrow}\mathrm{SISI}^{\uparrow})_A^{V_{\rm SE}} = -\frac{\tan\theta_S}{2\cos^2\theta_S}\left(1 - 8\cos^4\theta_S\right)\tan\delta_S Q_{\rm S}^{-1}\frac{\Delta V_{\rm SE}}{V_{\rm SE}}, \tag{4.91}$$

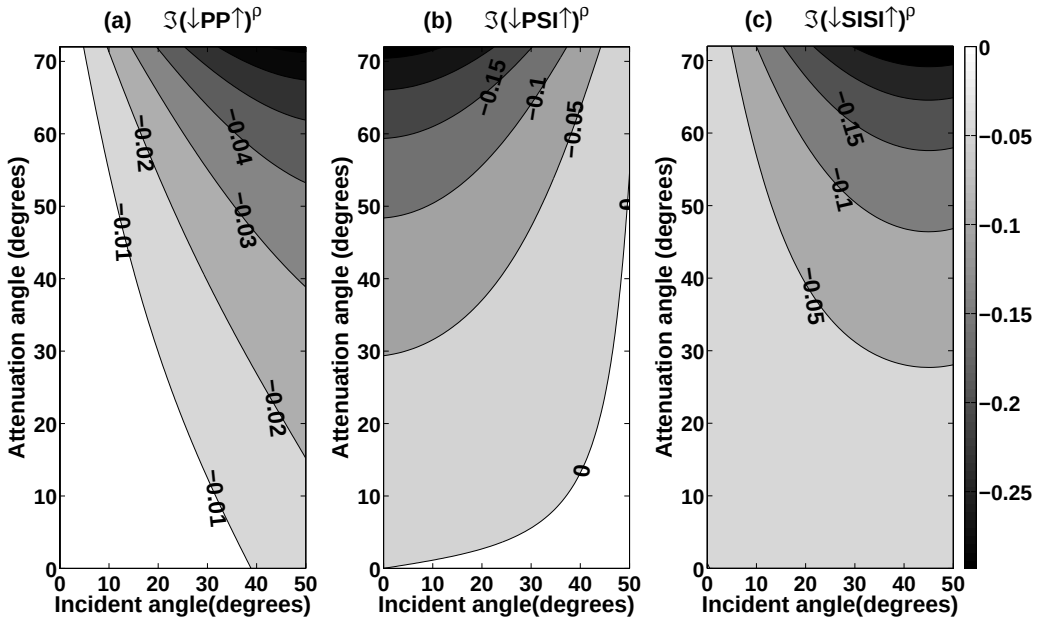

Figure 4.6: The maps of imaginary part of density component of the linearized reflectivities. The vertical axis indicates the attenuation angle and horizontal axis incident angle. Physical proprieties of layers are the same as figure 4.5. We assumed that attenuation angles for P- and S-waves are the same.

and the S-wave quality factor component being

$$({}^{\downarrow}\mathrm{SISI}^{\uparrow})_A^{Q_S} = \frac{1}{4\cos^2\theta_S} Q_{\mathrm{S}}^{-1} \left(2\sin^2 2\theta_S - 1\right) \frac{\Delta Q_{\mathrm{S}}}{Q_{\mathrm{S}}}. \tag{4.92}$$

Figure 4.5 shows the elastic (real) and anelastic (imaginary) parts of amplitude variation with angle equations for P-to-P, P-to-SI and SI-to-SI modes. It can be seen that the anelacticity has a greater influence on the converted wave P-to-SI than conserved modes P-to-P and SI-to-SI. To display the effects of attenuation angles on AVO equations, the maps for density component of P-to-P, P-to-SI and SI-to-SI reflectivities versus phase and attenuation angles are plotted in figure 4.6.

4.9 The relationship between the reflectivity and the viscoelastic scattering potential

Here we relate the linearized forms for viscoelastic reflection and conversion to recent results concerning the general problem of scattering of viscoelastic waves. The reflectivity model

and the volume scattering model are not precisely equivalent (see Figure 4.7); however under the assumption of small angle and small contrasts across the reflecting boundary the two are consistent, and indeed are mathematically equivalent.

The scattering potential (see, e.g., (Stolt and Weglein, 2012; Weglein et al., 2003; Beylkin and Burridge, 1990)) enters into a modeling of wave interaction with heterogenous media either through the Born approximation which neglects nonlinearity in the wave/medium relationship, or through the full scattering series, in which amplitudes and phases of waves accommodate large and extended perturbation (e.g.,(Weglein et al., 2003; Innanen, 2009)), and events whose propagation histories have introduced more that one subsurface reflection, like multiples are incorporated (Weglein and Dragoset, 2005). One instance of the scattering potential arises in the Born approximation, thus analysis of the potential in isolation qualitatively "feels like" analysis of the Born approximation. It can be this, but we emphasize the potential is description of the full, nonlinear problem also.

Generally the relationship between the scattering potential and reflectivity function is given by (Beylkin and Burridge, 1990)

$$({}^{\downarrow}\mathrm{IR}^{\uparrow}) = -\frac{1}{2V_{\mathrm{R}}^2 q_{\mathrm{R}}(q_{\mathrm{R}}+q_{\mathrm{I}})}\,{}^{\mathrm{I}}_{\mathrm{R}}\mathbb{V}, \tag{4.93}$$

where index I refers to the type of the incidence wave and R indicates the type of reflected wave and V_{R} is the wave velocity corresponding to the wave type R. A similar relation applies to the vertical slownesses, q_{R} and q_{I}. Additionally ${}^{\mathrm{I}}_{\mathrm{R}}\mathbb{V}$, is the scattering potential for the incidence wave type I and scattered type R. In the elastic case we have

$$({}^{\downarrow}\mathrm{IR}^{\uparrow})_{\mathrm{E}} = -\frac{\sin\theta_{\mathrm{I}}}{2\cos\theta_{\mathrm{R}}\sin(\theta_{\mathrm{I}}+\theta_{\mathrm{R}})}\,{}^{\mathrm{I}}_{\mathrm{R}}\mathbb{V}_{\mathrm{E}}. \tag{4.94}$$

Where θ_{I} is the phase angle for wave type I and θ_{R} is the phase angle for wave type R. For example if the reflected wave is a P-wave, $\theta_{\mathrm{R}} \equiv \theta_{\mathrm{P}}$, which can be interpreted either as a phase angle for the incidence P-wave or as a average of incidence and transmitted P-waves. In the next section we obtain one-to-one relationships between the scattering potential and reflectivity functions.

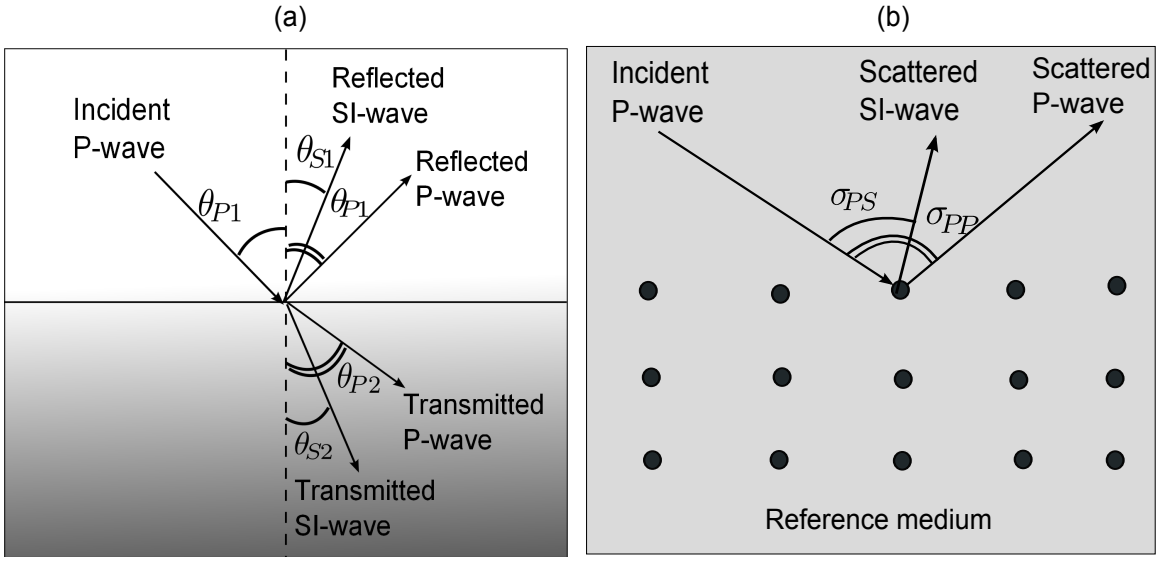

Figure 4.7: The reflectivity model vs volume scattering model. (a) The boundary is assumed to involved welded contact between two media whose properties differ only slightly. Incident, reflected and transsmited rays are related by Snell's law;interface normal helps define ray angles. (b) Reference medium is perturbed by one or more volume scattering inclusions; ray angles are defined in terms of the opening angle between incident and scattered rays. $\sigma_{\mathrm{PP}} = 2\theta_{\mathrm{P}}$, is the opening angle between the incident and scattered P-waves, where θ_{P} is the average of incident and transmitted angles. $\sigma_{\mathrm{PS}} = \theta_{\mathrm{P}} + \theta_{\mathrm{S}}$, is the opening angle between the incident P-wave and scattered SI-wave, where θ_{S} is the average of incident and transmitted SI-waves.

4.9.1 P-to-P scattering potential

In this case the incidence and reflected waves are P-type; as a result, $\theta_{\mathrm{I}} = \theta_{\mathrm{R}} = \theta_{\mathrm{P}}$. θ_{P} is interpreted as the average of phase angles of the incident and transmitted P-waves. Since for the low contrast there is only a small difference between the incident and transmitted angles, we can say that θ_{P} is the phase angle of the incidence wave. However in the development of linearization for the reflectivity we assumed that their difference is not zero. For elastic case the relationship between reflectivity and scattering potential reduces to

$$({}^{\downarrow}\mathrm{PP}^{\uparrow})_{\mathrm{E}} = -\frac{1}{4\cos^2\theta_{\mathrm{P}}}{}^{\mathrm{P}}_{\mathrm{P}}\mathbb{V}_{\mathrm{E}}. \tag{4.95}$$

Let us now consider to the viscoelastic case, specifically one in which an inhomogeneous P-wave reflects to an inhomogeneous P-wave. In this case the relation between the reflectivity and scattering potential is given by

$${}^{\mathrm{P}}_{\mathrm{P}}\mathbb{V} = -4V_{\mathrm{P}}^2 q_{\mathrm{P}}^2({}^{\downarrow}\mathrm{PP}^{\uparrow}), \tag{4.96}$$

or

$${}^{\mathrm{P}}_{\mathrm{P}}\mathbb{V} = -4\cos^2\theta_{\mathrm{P}}(1 - iQ_{\mathrm{P}}^{-1}\tan\theta_{\mathrm{P}}\tan\delta_{\mathrm{P}})({}^{\downarrow}\mathrm{PP}^{\uparrow}). \tag{4.97}$$

After doing some algebra we find that the reflectivity of P-to-P mode we derived, upon substitution into equation (4.97), results in a scattering potential

$${}^{\mathrm{P}}_{\mathrm{P}}\mathbb{V} = {}^{\mathrm{P}}_{\mathrm{P}}\mathbb{V}_{\mathrm{E}} + i{}^{\mathrm{P}}_{\mathrm{P}}\mathbb{V}_{\mathrm{A}}, \tag{4.98}$$

where the elastic scattering potential for PP-mode is

$$\begin{aligned} {}^{\mathrm{P}}_{\mathrm{P}}\mathbb{V}_{\mathrm{E}} = &\left[-1 - \cos\sigma_{\mathrm{PP}} + 2\left(\frac{V_{\mathrm{SE}}}{V_{\mathrm{PE}}}\right)^2 \sin^2\sigma_{\mathrm{PP}}\right]\frac{\Delta\rho}{\rho} \\ &- 2\frac{\Delta V_{\mathrm{PE}}}{V_{\mathrm{PE}}} + 4\left(\frac{V_{\mathrm{SE}}}{V_{\mathrm{PE}}}\right)^2 \sin^2\sigma_{\mathrm{PP}}\frac{\Delta V_{\mathrm{SE}}}{V_{\mathrm{SE}}}, \end{aligned} \tag{4.99}$$

and the anelastic part

$$
\begin{aligned}
{}^{\mathrm{P}}_{\mathrm{P}}\mathbb{V}_{\mathrm{A}} = & Q_{\mathrm{P}}^{-1} \sin\sigma_{\mathrm{PP}} \tan\delta_{\mathrm{P}} \frac{\Delta\rho}{\rho} \\
& + 2\left(\frac{V_{\mathrm{SE}}}{V_{\mathrm{PE}}}\right)^2 \left[\sin^2\sigma_{\mathrm{PP}}(Q_{\mathrm{S}}^{-1} - Q_{\mathrm{P}}^{-1}) + Q_{\mathrm{P}}^{-1}\sin 2\sigma_{\mathrm{PP}}\tan\delta_{\mathrm{P}}\right]\frac{\Delta\rho}{\rho} \\
& + 4\left(\frac{V_{\mathrm{SE}}}{V_{\mathrm{PE}}}\right)^2 \left[\sin^2\sigma_{\mathrm{PP}}(Q_{\mathrm{S}}^{-1} - Q_{\mathrm{P}}^{-1}) + Q_{\mathrm{P}}^{-1}\sin 2\sigma_{\mathrm{PP}}\tan\delta_{\mathrm{P}}\right]\frac{\Delta V_{\mathrm{SE}}}{V_{\mathrm{SE}}} \\
& - 2Q_{\mathrm{S}}^{-1}\left(\frac{V_{\mathrm{SE}}}{V_{\mathrm{PE}}}\right)^2 \sin^2\sigma_{\mathrm{PP}}\frac{\Delta Q_{\mathrm{S}}}{Q_{\mathrm{S}}} \\
& + Q_{\mathrm{P}}^{-1}\frac{\Delta Q_{\mathrm{P}}}{Q_{\mathrm{P}}},
\end{aligned}
\tag{4.100}
$$

Where, $\sigma_{\mathrm{PP}} = 2\theta_{\mathrm{P}}$, is the opening angle between the incidence and reflected waves. The above expression is the same as that obtained using the volume scattering formalism (Moradi and Innanen, 2015b). Thus our current linearization of reflectivity is consistent with the more general scattering picture.

4.9.2 SI-to-SI scattering potential

Similar to the P-to-P case, the relation between the scattering potential for SI-to-SI wave and its corresponding linearized reflection is given by

$$
{}^{\mathrm{SI}}_{\mathrm{SI}}\mathbb{V} = -4\cos^2\theta_S(1 - iQ_{\mathrm{S}}^{-1}\tan\theta_{\mathrm{S}}\tan\delta_{\mathrm{S}})({}^{\downarrow}\mathrm{SISI}^{\uparrow}). \tag{4.101}
$$

The scattering potential for the scattering of the SI-wave to SI-wave is determined to be

$$
{}^{\mathrm{SI}}_{\mathrm{SI}}\mathbb{V} = {}^{\mathrm{SV}}_{\mathrm{SV}}\mathbb{V}_{\mathrm{E}} + i{}^{\mathrm{SI}}_{\mathrm{SI}}\mathbb{V}_{\mathrm{A}}. \tag{4.102}
$$

The real part is the elastic scattering potential for scattering of SV-wave to SV-wave

$$
{}^{\mathrm{SV}}_{\mathrm{SV}}\mathbb{V}_{\mathrm{E}} = -\left(\cos(2\sigma_{\mathrm{SS}}) + \cos\sigma_{\mathrm{SS}}\right)\frac{\Delta\rho}{\rho} - 2\cos(2\sigma_{\mathrm{SS}})\frac{\Delta V_{\mathrm{SE}}}{V_{\mathrm{SE}}}, \tag{4.103}
$$

$$
\tag{4.104}
$$

and the anelastic part is given by

$$
\begin{aligned}
{}^{\mathrm{SI}}_{\mathrm{SI}}\mathbb{V}_{\mathrm{A}} = & Q_{\mathrm{S}}^{-1}\left(\sin\sigma_{\mathrm{SS}} + 2\sin(2\sigma_{\mathrm{SS}})\right)\tan\delta_S\frac{\Delta\rho}{\rho} \\
& + 4Q_{\mathrm{S}}^{-1}\sin(2\sigma_{\mathrm{SS}})\tan\delta_S\frac{\Delta V_{\mathrm{SE}}}{V_{\mathrm{SE}}} + \cos(2\sigma_{\mathrm{SS}})Q_{\mathrm{S}}^{-1}\frac{\Delta Q_{\mathrm{S}}}{Q_{\mathrm{S}}},
\end{aligned}
\tag{4.105}
$$

Where, $\sigma_{\mathrm{SS}} = 2\theta_{\mathrm{S}}$, is the opening angle between the incidence and scattered waves, which is the scattering potential obtained using the Born approximation.

4.9.3 P-to-SI scattering potential

First the relation between the reflectivity and scattering potential is given by

$$\overset{\mathrm{P}}{\underset{\mathrm{SI}}{}}\mathbb{V} = -2V_{\mathrm{S}}^2 q_{\mathrm{S}}(q_{\mathrm{S}} + q_{\mathrm{P}})(^{\downarrow}\mathrm{PSI}^{\uparrow}). \tag{4.106}$$

The scattering potential for P-to-SI is, consequently

$$\overset{\mathrm{P}}{\underset{\mathrm{SI}}{}}\mathbb{V} = \overset{\mathrm{P}}{\underset{\mathrm{SI}}{}}\mathbb{V}_{\mathrm{E}} + i\overset{\mathrm{P}}{\underset{\mathrm{SI}}{}}\mathbb{V}_{\mathrm{A}}. \tag{4.107}$$

where the elastic part of the scattering potential $\overset{\mathrm{P}}{\underset{\mathrm{SI}}{}}\mathbb{V}_{\mathrm{E}}$ is given by

$$\overset{\mathrm{P}}{\underset{\mathrm{SI}}{}}\mathbb{V}_{\mathrm{E}} = -\left[\sin\sigma_{\mathrm{PS}} + \left(\frac{V_{\mathrm{SE}}}{V_{\mathrm{PE}}}\right)\sin 2\sigma_{\mathrm{PS}}\right]\frac{\Delta\rho}{\rho} - 2\left[\left(\frac{V_{\mathrm{SE}}}{V_{\mathrm{PE}}}\right)\sin 2\sigma_{\mathrm{PS}}\right]\frac{\Delta V_{\mathrm{SE}}}{V_{\mathrm{SE}}}. \tag{4.108}$$

and the anelastic part is given by

$$\begin{aligned}
\overset{\mathrm{P}}{\underset{\mathrm{SI}}{}}\mathbb{V}_{\mathrm{A}} = &-\frac{1}{2}\left(\frac{V_{\mathrm{SE}}}{V_{\mathrm{PE}}}\right)\sin 2\sigma_{\mathrm{PS}}(Q_{\mathrm{S}}^{-1} - Q_{\mathrm{P}}^{-1})\frac{\Delta\rho}{\rho} \\
&-\frac{1}{2}\left(\frac{V_{\mathrm{SE}}}{V_{\mathrm{PE}}}\right)\left[2\cos 2\sigma_{\mathrm{PS}} + \left(\frac{V_{\mathrm{PE}}}{V_{\mathrm{SE}}}\right)\cos\sigma_{\mathrm{PS}}\right](Q_{\mathrm{S}}^{-1}\tan\delta_{\mathrm{S}} + Q_{\mathrm{P}}^{-1}\tan\delta_{\mathrm{P}})\frac{\Delta\rho}{\rho} \\
&-\left(\frac{V_{\mathrm{SE}}}{V_{\mathrm{PE}}}\right)\left[\sin 2\sigma_{\mathrm{PS}}(Q_{\mathrm{S}}^{-1} - Q_{\mathrm{P}}^{-1}) + 2\cos 2\sigma_{\mathrm{PS}}(Q_{\mathrm{S}}^{-1}\tan\delta_{\mathrm{S}} + Q_{\mathrm{P}}^{-1}\tan\delta_{\mathrm{P}})\right]\frac{\Delta V_{\mathrm{SE}}}{V_{\mathrm{SE}}} \\
&+\left(\frac{V_{\mathrm{SE}}}{V_{\mathrm{PE}}}\right)Q_{\mathrm{S}}^{-1}\sin 2\sigma_{\mathrm{PS}}\frac{\Delta Q_{\mathrm{S}}}{Q_{\mathrm{S}}}.
\end{aligned} \tag{4.109}$$

Here, the opening angle between the incidence P-wave and reflected SI-wave is $\sigma_{\mathrm{PS}} = \theta_{\mathrm{P}} + \theta_{\mathrm{S}}$. Also, θ_{P} for a welded boundary is the average of the incidence P-wave and transmitted P-wave; the same interpretation applies for θ_{S}.

4.10 Conclusion

Amplitude variation with offset (AVO) or amplitude variation with angle (AVA) analysis is a study of the effects of changes in medium properties and incident angles on the reflection coefficients as the contrast between two layer is weak. Even in the case of an isotropic

elastic medium the exact equations for the reflection coefficients are sufficiently complicated that the effects of changes in medium properties and dependency on the incidence angle is not explicitly clear. When attenuation is added to medium as in a viscoelastic case, the problem gets still more complicated. In this case, besides the elastic properties and phase angle, reflectivity is sensitive to change in the anelastic quantities and attenuation angles. Since in practical cases, attenuation is often weak, the reflection coefficient simplifies. In our linearization, besides the assumption of weak contrasts in elastic and anelastic properties, we applied the additional assumption of weak attenuation, i.e., what is termed a low-loss medium, in both half spaces. P-to-P, P-to-SI and SI-to-SI wave reflection coefficients in low-loss viscoelastic media for a weak contrast separating two isotropic viscoelastic media have been derived. These coefficients linearly depend on the fractional changes in elastic and anelastic properties. Our results indicate that the sensitivity of the reflected waves to change in P- and S-wave quality factors, which is the essence of AVO analysis. Reflectivities are split into two parts: a real part which is in terms of the elastic reflectivities, and an imaginary part, related to the anelasticity in the medium. The anelastic part itself is composed of two terms, one term being the anelastic-homogenous which is related to the case that waves are homogenous, this term is sensitive to changes in both elastic and anelastic properties. In the case that waves are inhomogeneous another term is added to the reflectivity, this one is sensitive to changes in elastic properties; however for the homogenous case when the attenuation angle is zero this term vanishes. Let us consider to the linearized P-to-P reflectivity. It can be written as

$$\mathrm{R_{PP}}(\theta_{\mathrm{P}}, \delta_{\mathrm{P}}) = \mathrm{R^{E}_{PP}}(\theta_{\mathrm{P}}) + i\mathrm{R^{AH}_{PP}}(\theta_{\mathrm{P}}) + i\mathrm{R^{AIH}_{PP}}(\theta_{\mathrm{P}}, \delta_{\mathrm{P}}). \tag{4.110}$$

The real part with superscript E refers to the elastic reflectivity, the second term is the contribution of the elastic and anelastic contrasts, and the third term is the contribution of the contrast in elastic properties in presence of an inhomogeneous wave. The anelastic homogenous term is sensitive to the fractional changes in density, S-wave velocity, S- and P-wave quality factors. The anelastic inhomogeneous term only depends on the change in density, P- and S-wave velocity. At normal incidence the inhomogeneous term is zero.

There exist some techniques to invert the anelastic parameters from linearized reflection

coefficients using such a model. However, these techniques neglect the possible inhomogeneity of the wave. Although the inhomogeneity angle is one of the characteristics of an attenuative medium, the linearized AVO equations are not directly depend on the change in it. However using the Snell's law, we show that perturbations in the attenuation angle can be expressed in terms of changes in velocity, quality factor and phase angle. Although experimental measurements of inhomogeneity are very limited, and have, so far, only been reported potentially on laboratory scales (Deschamps and Assouline, 2000; Huang et al., 1994), our analysis points to significant effects may be visited on AVO in its presence.

4.11 Summary

Linearized forms of PP, PSI and SISI reflection coefficients for low contrast interfaces separating two arbitrary low-loss viscoelastic media were derived. The linearized viscoelastic reflection coefficient we derived relate the AVO response to the anelastic parameters. It is shown that the reflectivity not only depends upon the perturbations in elastic properties, but also on perturbations in quality factors for P- and S-waves. Also using the viscoelastic Snell's law we show that the transmitted and reflected P- and S-waves attenuation angles can be expressed in terms of incidence angle and incidence attenuation angles. To derive the reflectivities, we linearized Snell's law for a two layer viscoelastic media and show that in the linearized reflectivity only the average of attenuation angle affects the reflectivity. Also we showed that the linearized reflectivities can be transformed to the scattering potential obtained using the Born approximation.

To model the anelasticity in a medium linear viscoelasticity is used. Plane waves are generally inhomogeneous, where the attenuation and propagation are not in the same direction. The elastic reflectivity can be obtained in the limit that attenuation quantities Q go to zero. If all parameters related to the anelasticity go to zero the viscoelastic reflections reduces to the linearized elastic isotropic reflection coefficients obtained by Aki and Richards (2002).

The results we present are at present more theoretical than practical. Nevertheless the significance of inhomogeneity to reflection amplitudes as predicted by our and others analysis suggests that ultimately a real impact will be felt on AVO inversion in strongly attenuating

geological volumes.

Chapter 5

Significance and behaviour of the homogeneous and inhomogeneous components of linearized viscoelastic reflection coefficients

5.1 Abstract

In a recent paper (Moradi and Innanen, 2016), seismic amplitude-variation-with-offset (AVO) equations describing P-to-P and P-to-S reflections from boundaries separating low-loss viscoelastic media, with account taken for variation in attenuation angle, have been derived. We find that opportunities now present themselves to use these equations to expose a range of relationships between measured amplitudes and subsurface elastic and anelastic properties. This has significant applicability in quantitative interpretation of seismic data in, for instance, reservoir characterization. To facilitate the analysis we decompose the equations into three parts: elastic, homogeneous and inhomogeneous. We show that, for PP modes, the elastic part is sensitive to changes across a reflecting boundary in density and P- and S-wave velocities; the homogeneous part is sensitive to changes in density, S-wave velocity and the P- and S-wave quality factors; and the inhomogeneous part is sensitive to changes in density, and P-and S-wave velocities. The latter term is seen to vanish when the attenuation angle vanishes. For PP modes, elastic and homogeneous terms are linear with respect to $\sin^2\theta_{\rm P}$, where $\theta_{\rm P}$ is the P-wave incidence angle, however the inhomogeneous term is similarly linear only if normalized by dividing by $\tan\theta_{\rm P}$. For PS modes, the elastic part is sensitive to changes in density and S-wave velocity; the homogeneous part is sensitive to changes in density, S-wave velocity and the S-wave quality factor; and the inhomogeneous part is sensitive to changes in density and S-wave velocity. This term also vanishes for zero attenuation angle, i.e., in the homogenous limit. For PS modes, the inhomogeneous terms are linear with respect to $\sin^2\theta_{\rm P}$, however the elastic and homogeneous terms are first and third order in $\sin\theta_{\rm P}$. A further and key result of this expansion of the wave types allowable in AVO

analysis is that, for inhomogeneous PS scattering, the viscoelastic AVO equations predict a non-zero reflectivity at normal incidence. This is a significant deviation from common models of converted wave amplitude analysis.

5.2 Introduction

A primary aim of modern exploration and monitoring seismology is to determine geological and engineering-relevant properties of subsurface hydrocarbon reservoirs from the travel time, phase and amplitude information in seismic reflections. Amplitude-variation-with-offset (AVO) analysis and inversion, in its various forms (Castagna and Backus, 1993; Foster et al., 2010), is a key driving technology in this effort. The problem of robustly analyzing and inverting reflected seismic amplitudes is complex and incompletely solved, requiring (1) integrated seismic acquisition, data processing, and image-forming techniques to produce seismic amplitudes of appropriate fidelity, and (2) accurate, robust, and intelligible formulae and algorithms for modelling and inverting these amplitudes. In the latter domain, research has been active in recent years to understand the limits of standard approximate solutions for reflection amplitudes, connect them with auxiliary geological information to infer increasingly specific reservoir engineering properties (Chopra and Marfurt, 2007), and incorporate more complete physics, for instance the anisotropy and/or viscosity arising from the presence of fractures and fluids. In this paper we continue to address the problem of accommodating a maximal amount of the complexity and richness of viscoelastic wave propagation in AVO theory and practice.

Including wave physics beyond the elasticity and isotropy of standard AVO analysis and inversion brings benefit and difficulty. The benefit is an increase in the information derivable from the data. If, for instance, attenuation due to changes in reservoir viscosity influences seismic observations, an extended model will permit that information to be used and this extra rock/fluid property will be at least in principle inferrable. The difficulty is that, for each additional parameter we ask the seismic data to constrain, the more stress is placed on the acquisition-processing-imaging chain to provide accurate data over a wider range of angles and azimuths. As more "difficult" elastic properties are sought, examples of which

are density and various anisotropic parameters, often the limits of our mathematical models are reached, and the data variations needed to determine them increasingly tend to occur near the limits of our experimental apertures.

Thus when we extend the reach of seismic amplitude analysis by including a more complete model of wave physics, it is insufficient to simply write down new mathematics and leave it at that. An extension of (say) the Zoeppritz equations to incorporate a viscoelastic model, which is part of the work represented in this and the preceding papers, is a starting point only. To activate new technologies wherein attenuative properties of the subsurface can be inferred from seismic measurements requires (1) useable and interpretable approximations in addition to the complex exact equations, (2) an understanding of the behaviour and accuracy of approximations and exact solutions as the quantities related to seismic acquisition reach their limits (e.g., incidence angle and/or maximum source-receiver offset), (3) an understanding of regimes in which data variations caused by new and/or additional parameters are prevalent, and (4) an understanding of if, and how, these data variations can be used to determine simultaneous changes in all of the rock properties as they generally occur in the Earth. The mathematics of the viscoelastic AVO equations, exact and linearized, with attenuation angle incorporated, have been discussed in previous work (Moradi and Innanen, 2016); here we report on developments of these secondary but critical parts of the full problem.

Approximate reflection coefficients for weak contrast interfaces separating elastic isotropic media are well-established. These equations linearly depend on the fractional changes in density, P-wave and S-wave velocities weighted by trigonometric functions of incident angle (Aki and Richards, 2002). In the presence of anelasticity, in which the polarization vector and the ray parameter are complex-valued, reflection coefficients are complex functions (Ursin and Stovas, 2002; Moradi and Innanen, 2016, 2015a; Krebes, 1983, 1984). The corresponding linearized AVO equations not only depend on the changes in elastic properties across the boundary but also depend on the changes in P- and S-wave quality factors weighted by trigonometric functions of incident phase and attenuation angles. The problem of determining exact and approximate reflection and transmission coefficients at a plane interface between two viscoelastic media for homogenous waves was studied by (Ursin and

Stovas, 2002). The authors concluded that the approximate PP and PS reflectivities are very similar to the exact solutions of the associated Zoeppritz equations. The same authors generalized the problem to incorporate transversely isotropic viscoelastic problems (Stovas and Ursin, 2003). The effects of attenuation on PP- and PS-wave reflection coefficients for anisotropic viscoelastic media with the main emphasis on transversely isotropic models with a vertical symmetry axis has also been treated (Behura and Tsvankin, 2009a). These authors allowed for inhomogeneity in the waves, assuming that the attenuation angles across a reflecting boundary remain constant, but pointing out that the inhomogeneity angle can make a substantial contribution to the AVO response for strongly attenuative media (Behura and Tsvankin, 2009b).

The related but more general problem of scattering of seismic waves from viscoelastic inclusions in the context of Born approximation has also been recently investigated. A comprehensive mathematical framework for scattering, building from Borcherdt's layered-medium formalism has been developed for the purposes of modeling, processing, and inversion of seismic data exhibiting non-negligible intrinsic attenuation (Moradi and Innanen, 2015b). It was further shown that either independently or beginning from this scattering theory, linearized forms of PP, PS, and SS reflection coefficients for low-contrast interfaces separating two arbitrary low-loss viscoelastic media for arbitrary incident angle are derivable (Moradi and Innanen, 2016, 2015a). These equations relate the AVO response to anelastic parameters. In that work it was shown how the reflectivity depends upon perturbations in elastic properties and on perturbations in quality factors for P- and S-waves. These equations are expected to be of practical importance in the characterization of viscosity and viscosity changes in unconventional reservoirs. One feature of our approach in deriving the linearized AVO equation is that Snell's law and its linearized form is properly accounted for in the linearization, which has typically been assumed to be constant (Behura and Tsvankin, 2009a,b). AVO formulas of this kind represent physically more complete versions of those which underlie anelastic inversion procedures (Innanen, 2011, 2012). Updates to these inversion procedures making use of these more complete expressions is in progress.

In this paper we are concerned with a certain decomposition of the approximate viscoelastic reflection coefficients, and a qualitative and quantitative analysis of the results. Specif-

ically, effects of the attenuation angle and the quality factors will be focused on. We shall see that the attenuation angle has very significant qualitative effect on the AVO responses, and we offer some ideas of the relative importance of the AVO equations for homogeneous and inhomogeneous waves. Another result of this paper is that some insight into common alternative forms for the AVO equations (e.g., the Shuey approximation, (Shuey, 1985)), adjusted for attenuative media, is provided. Again incorporating into these re-written equations the change in attenuation angle across the boundary is unexplored territory. Because we develop results for P-to-S conversions as well as standard P-to-P reflections, our analysis is applicable to linear and nonlinear inversion of multicomponent seismic data (Margrave et al., 2001; Lehocki et al., 2014).

This paper is organized as follows. In section 5.3 we briefly introduce notation for the complex ray parameter and slowness vector for inhomogeneous waves in low-loss viscoelastic media. In section 5.4 we apply the Snell's law to decompose the vertical slowness for reflected and transmitted waves. It is shown that the vertical slowness for P- and S-wave is a function of incident attenuation angle. In section 5.5 we apply the method that we developed in previous section to the decomposition of the exact solutions of the viscoelastic Zoeppritz equations. In section 5.6 we lay out the viscoelastic version of the Shuey approximation for PP-reflection coefficients, and compare the decomposed exact reflectivities with the approximate ones for two reservoir rock models. Finally we produce some useful approximations for converted PS-wave.

5.3 Preliminaries

In viscoelastic media there are three types of waves: P, Type-I S, and Type-II S. These may be homogeneous or inhomogeneous, depending on whether their propagation and attenuation vectors are, respectively, parallel or not (Borcherdt, 2009). Polarization vectors for inhomogeneous P and SI-waves are elliptical; for homogeneous waves they are linear. The elliptical motion reduces to linear motion in the homogeneous limit. The SI-wave is the generalization of the elastic SV wave, and the SII-wave is the generalization of the elastic SH wave, with the former reducing to the latter as attenuation goes to zero. The SII-wave

involves linear particle motion perpendicular to the propagation-attenuation plane in both homogeneous and inhomogeneous cases. In reflection problems, if the incident wave is an inhomogeneous P-wave, the reflected wave can be an inhomogeneous P- or SI-wave. For an inhomogeneous wave, the ray parameter and slowness vector not only depend to the phase angle but also on the attenuation angle.

To properly compute linear solutions of the Zoeppritz equations, generalized to accommodate viscoelasticity, to facilitate AVO analysis in the presence of attenuation, we must define polarization and slowness vectors with some care. In a viscoelastic medium, the wavenumber vector is a complex vector whose real part characterizes the direction of wave propagation and whose imaginary part characterizes the attenuation of the wave. This is laid out by, e.g., (Borcherdt, 1971, 1973a,b, 1977, 1982; Borcherdt and Wennerberg, 1985; Borcherdt et al., 1986; Borcherdt, 1988, 2009) who presents a complete theory for seismic waves propagating in layered viscoelastic medium. Borcherdt's formulation predicts a range of transverse, inhomogeneous wave types unique to viscoelastic media (the Type I and II S waves discussed above), including rules for conversion of one type to another during interactions with planar boundaries. As a result of the complexity of the wavenumber vector, slowness and polarization vectors are complex functions. The complex wave-number vector is given by

$$\mathbf{K} = \mathbf{P} - i\mathbf{A}, \tag{5.1}$$

where the propagation vector $\mathbf{P}$ is perpendicular to the wavefront, and specifies the direction of propagation, and the attenuation vector $\mathbf{A}$ is perpendicular to the plane of constant amplitude, and specifies the direction of maximum attenuation. The angle between these two vectors is always less that 90° and is referred to as the attenuation angle (figure 5.1). If the attenuation and propagation vectors are parallel and $\delta = 0$ the wave is homogenous; otherwise it is inhomogeneous. In the case of low-loss viscoelastic media, in which the quality factor $Q^{-1} \ll 1$, the propagation and attenuation vectors can be written (Borcherdt, 2009)

$$\begin{aligned} \mathbf{P} &= \frac{\omega}{V_{\mathrm{E}}}(\mathbf{x}\sin\theta + \mathbf{z}\cos\theta), \\ \mathbf{A} &= \frac{\omega}{V_{\mathrm{E}}} Q^{-1} \sec\delta \left[\mathbf{x}\sin(\theta-\delta) + \mathbf{z}\cos(\theta-\delta)\right], \end{aligned} \tag{5.2}$$

where V_{E} is either P-wave or S-wave velocity, θ is the phase angle and δ is the attenuation

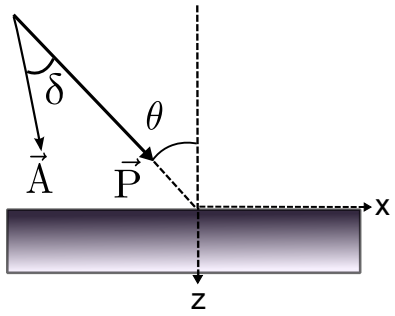

Figure 5.1: Incident inhomogeneous wave ($\delta \neq 0$). **P** is the propagation vector, **A** is the attenuation vector, θ is the incident phase angle and δ is the incident attenuation angle.

angle. For an inhomogeneous wave, the ray parameter and the vertical slowness are complex functions which depend on the quality factor and attenuation angles (Moradi and Innanen, 2016). These quantities can be split into elastic, homogeneous and inhomogeneous parts

$$\begin{aligned} p &= p_{\mathrm{E}} + ip_{\mathrm{H}} + ip_{\mathrm{IH}}, \\ q &= q_{\mathrm{E}} + iq_{\mathrm{H}} + iq_{\mathrm{IH}}, \end{aligned} \tag{5.3}$$

where the components are given by

$$\begin{aligned} p_{\mathrm{E}} &= \frac{\sin\theta}{V_{\mathrm{E}}}, & q_{\mathrm{E}} &= \sqrt{V_{\mathrm{E}}^{-2} - p_{\mathrm{E}}^2}, \\ p_{\mathrm{H}} &= -\frac{1}{2}Q^{-1}p_{\mathrm{E}}, & q_{\mathrm{H}} &= -\frac{1}{2}Q^{-1}q_{\mathrm{E}}, \\ p_{\mathrm{IH}} &= \frac{1}{2}Q^{-1}q_{\mathrm{E}}\tan\delta, & q_{\mathrm{IH}} &= -\frac{1}{2}Q^{-1}p_{\mathrm{E}}\tan\delta. \end{aligned}$$

In the above relations the indexes E, H and IH respectively refer to the elastic, homogeneous and inhomogeneous parts. Reflected and transmitted angles can be obtained in terms of the incident angle from Snell's law. For a low-contrast, two layered medium, the deviation of transmitted angle away from the incident angle is small. Consequently, we can linearize Snell's law to obtain a simple expression of the difference between the incident and transmitted wave in terms of changes in velocity between the layers. Snell's law for viscoelastic materials is discussed by (Wennerberg, 1985) and (Borcherdt, 2009). Importantly for our purposes, since the attenuation angle changes across the boundary, the linearized form of Snell's law also gives us in a simple form the difference in attenuation angle in terms of changes in velocity and quality factor (Moradi and Innanen, 2016).

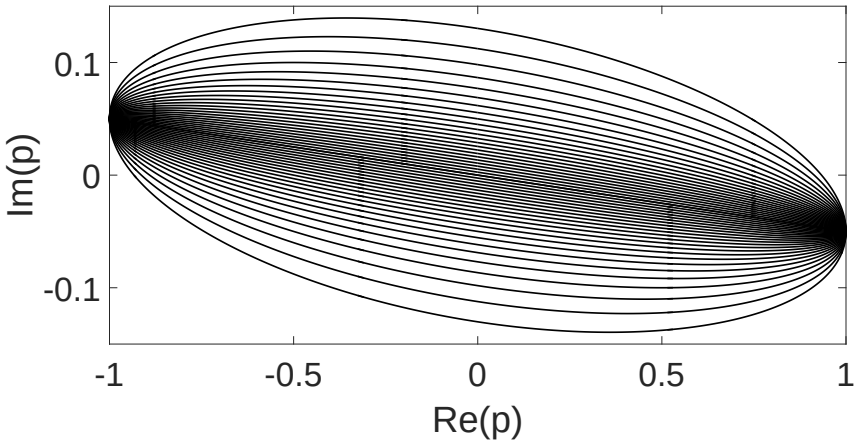

Figure 5.2: Plots of the viscoelastic ray parameter p in the complex plane for $Q = 10$ over a range of attenuation angles, from 0° to 70°.

5.4 Homogeneous and inhomogeneous parts of the slownesses

To decompose the reflectivity into the contributions from inhomogeneity of wave, first we need to split the slowness vector to elastic, homogeneous and inhomogeneous parts. Let an inhomogeneous P-wave be incident in medium 1 on a horizontal interface. The P-wave transmitted through the interface has vertical slowness

$$q_{\mathrm{P}2} = q_{\mathrm{PE}2} + iq_{\mathrm{PA}2}, \tag{5.4}$$

where the elastic and anelastic parts, $q_{\mathrm{PE}2}$ and $q_{\mathrm{PA}2}$ respectively, are given by

$$q_{\mathrm{PE}2} = \sqrt{V_{\mathrm{PE}2}^{-2} - p_{\mathrm{E}}^2}, \tag{5.5}$$

$$q_{\mathrm{PA}2} = -\frac{Q_{\mathrm{P}2}^{-1}}{2}(q_{\mathrm{PE}2} + p_{\mathrm{E}} \tan \delta_{\mathrm{P}2}). \tag{5.6}$$

In equation (5.6), subscript A labels the anelastic part of the vertical slowness. In the same way, for the reflected S-wave we have

$$q_{\mathrm{SE}1} = \sqrt{V_{\mathrm{SE}1}^{-2} - p_{\mathrm{E}}^2}, \tag{5.7}$$

$$q_{\mathrm{SA}1} = -\frac{Q_{\mathrm{S}1}^{-1}}{2}(q_{\mathrm{SE}1} + p_{\mathrm{E}} \tan \delta_{\mathrm{S}1}), \tag{5.8}$$

and for the transmitted S-wave

$$q_{\mathrm{SE}2} = \sqrt{V_{\mathrm{SE}2}^{-2} - p_{\mathrm{E}}^2}, \tag{5.9}$$

$$q_{\mathrm{SA}2} = -\frac{Q_{\mathrm{S}2}^{-1}}{2}(q_{\mathrm{SE}2} + p_{\mathrm{E}} \tan \delta_{\mathrm{S}2}). \tag{5.10}$$

To separate the homogeneous and inhomogeneous components of these relations we must invoke Snell's law, because the transmitted and reflected attenuation angles are functions of the incident attenuation angle (see appendix C). We have

$$\tan\delta_{P2} = \frac{1}{q_{\mathrm{PE2}}}\left[p_{\mathrm{E}} - \frac{Q_{P2}}{Q_{P1}}\left(p_{\mathrm{E}} - q_{\mathrm{PE1}}\tan\delta_{P1}\right)\right], \tag{5.11}$$

where δ_{P2} is the attenuation angle for the transmitted P-wave, and δ_{P1} is the attenuation angle for the incident P-wave. For the reflected S-wave, the attenuation angle δ_{S1} is

$$\tan\delta_{S1} = \frac{1}{q_{\mathrm{SE1}}}\left[p_{\mathrm{E}} - \frac{Q_{S1}}{Q_{P1}}\left(p_{\mathrm{E}} - q_{\mathrm{SE1}}\tan\delta_{P1}\right)\right],, \tag{5.12}$$

and for the transmitted S-wave the attenuation angle δ_{S2} is

$$\tan\delta_{S2} = \frac{1}{q_{\mathrm{SE2}}}\left[p_{\mathrm{E}} - \frac{Q_{S2}}{Q_{P1}}\left(p_{\mathrm{E}} - q_{\mathrm{SE2}}\tan\delta_{P1}\right)\right],. \tag{5.13}$$

By substituting equation (5.11) into (5.6), and (5.12) into (5.8), and finally (5.13) into (5.10) we can decompose the transmitted P-wave slowness vector into homogenous and inhomogeneous parts,

$$q_{\mathrm{PAH2}} = -\frac{1}{2}Q_{\mathrm{P2}}^{-1}\frac{\cos\theta_{\mathrm{P2}}}{V_{\mathrm{P2}}} - \frac{1}{2}\frac{\sin\theta_{\mathrm{P2}}}{V_{P2}}\tan\theta_{\mathrm{P2}}(Q_{\mathrm{P2}} - Q_{\mathrm{P1}}), \tag{5.14}$$

$$q_{\mathrm{PAIH2}} = -\frac{1}{2}Q_{\mathrm{P1}}^{-1}\frac{\cos\theta_{P1}}{V_{\mathrm{P1}}}\tan\theta_{P2}\tan\delta_{P1}. \tag{5.15}$$

Similarly for the reflected S-wave we obtain

$$q_{\mathrm{SAH1}} = -\frac{1}{2}Q_{\mathrm{S1}}^{-1}\frac{\cos\theta_{\mathrm{S1}}}{V_{\mathrm{S1}}} - \frac{1}{2}\frac{\sin\theta_{\mathrm{S1}}}{V_{S1}}\tan\theta_{\mathrm{S1}}(Q_{\mathrm{S1}} - Q_{\mathrm{P1}}) \tag{5.16}$$

$$q_{\mathrm{SAIH1}} = -\frac{1}{2}Q_{\mathrm{P1}}^{-1}\frac{\cos\theta_{P1}}{V_{\mathrm{P1}}}\tan\theta_{S1}\tan\delta_{P1}, \tag{5.17}$$

and for the transmitted S-wave

$$q_{\mathrm{SAH2}} = -\frac{1}{2}Q_{\mathrm{S2}}^{-1}\frac{\cos\theta_{\mathrm{S2}}}{V_{\mathrm{S2}}} - \frac{1}{2}\frac{\sin\theta_{\mathrm{S2}}}{V_{P2}}\tan\theta_{\mathrm{S2}}(Q_{\mathrm{S2}} - Q_{\mathrm{P1}}) \tag{5.18}$$

$$q_{\mathrm{PAIH2}} = -\frac{1}{2}Q_{\mathrm{P1}}^{-1}\frac{\cos\theta_{P1}}{V_{\mathrm{P1}}}\tan\theta_{S2}\tan\delta_{P1}. \tag{5.19}$$

These relations separate the homogeneous from the inhomogeneous components of the slownesses, in the sense that for a purely homogeneous P-wave, with zero attenuation angle $\delta_{P1} = 0$, the components labelled inhomogeneous vanish. Let us next use this complex Snell's law decomposition procedure for viscoelastic ray parameters and vertical slownesses to analyze the viscoelastic reflectivity.

5.5 Decomposition of solutions of the viscoelastic Zoeppritz equations

Our interest is to be able to separately analyze and predict behaviour of the homogeneous versus inhomogeneous components of viscoelastic waves having reflected from and transmitted through a planar boundary. Consider two homogeneous viscoelastic half-spaces, in which the upper half-space is characterized by the density ρ_1, P-wave velocity V_{PE}, S-wave velocity V_{SE}, P-wave quality factor Q_{P} and S-wave quality factor Q_{S}. Each of these experiences a jump in transitioning to the lower half-space, where the parameters are labelled with the subscript 2. A plane P-wave incident on the boundary between the two half-spaces generates reflected and transmitted P- and S-waves. Solutions of the purely elastic-isotropic Zoeppritz equations can be straightforwardly extended to correspond to exact PP and PS reflection coefficients in this viscoelastic case. This is done by substituting the complex ray parameter, slowness vector and velocities discussed in the previous section.

These solutions are complicated nonlinear functions of the changes in both elastic and anelastic parameters (Aki and Richards, 2002; Ikelle and Amundsen, 2005; Moradi and Innanen, 2016):

$$\mathrm{R_{PP}} = \frac{c_1 d_2 - c_3 d_4}{d_1 d_2 + d_3 d_4}, \tag{5.20}$$

$$\mathrm{R_{PS}} = -\left(\frac{V_{\mathrm{P1}}}{V_{\mathrm{S1}}}\right)\frac{c_3 d_1 + c_1 d_3}{d_1 d_2 + d_3 d_4} \tag{5.21}$$

where

$$d_1 = -2p^2\Delta M(q_{P1} - q_{P2}) + (\rho_1 q_{P2} + \rho_2 q_{P1}), \tag{5.22}$$

$$d_3 = -p\left[2\Delta M(q_{P1}q_{S2} + p^2) - \Delta\rho\right], \tag{5.23}$$

and where $d_2 = d_1$ (but with $q_P \to q_S$), $d_4 = d_3$ (with $q_P \leftrightarrow q_S$), $c_1 = d_1$ (with $q_{P2} \to -q_{P2}$), $c_2 = d_2$ (with $q_{S2} \to -q_{S2}$), $c_3 = d_3$ (with $q_{P1} \to -q_{P1}$), and $c_4 = d_4$ (with $q_{S1} \to -q_{S1}$). In above equations $\Delta\rho = \rho_2 - \rho_1$ is the difference between the density in lower and upper media and $\Delta M = \Delta\mu + i\Delta\mu_A$ is the change in the complex modulus across the boundary:

$$\Delta\mu_E = \rho_2 V_{SE2}^2 - \rho_1 V_{SE1}^2 = \mu_{E2} - \mu_{E1}, \tag{5.24}$$

and

$$\Delta\mu_A = \rho_2 V_{SE2}^2 Q_{S2}^{-1} - \rho_1 V_{SE1}^2 Q_{S1}^{-1} = Q_{S2}^{-1}\mu_{E2} - Q_{S1}^{-1}\mu_{E1}. \tag{5.25}$$

	Shale	Salt	Limestone	Limestone(gas)
$V_{\rm PE}$(km/s)	3.811	4.537	5.335	5.043
$V_{\rm SE}$(km/s)	2.263	2.729	2.957	2.957
ρ(gm/cm^3)	2.40	2.005	2.65	2.49

Table 5.1: Density, P and S-wave velocity used in the numerical tests for shale, salt, limestone and limestone(gas). For all models we assumed the P- and S-wave quality factors as $Q_{S1} = 5$, $Q_{S2} = 7$, $Q_{P1} = 9$ and $Q_{P2} = 11$.

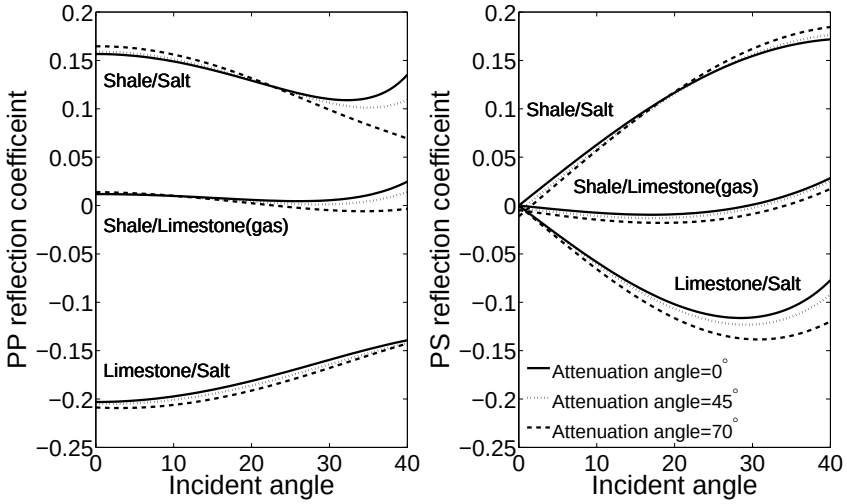

Figure 5.3: Comparing the real part of the exact viscoelastic PP and PS-reflectivity for $\delta_P = 0°, 45°, 70°$ for four selected models from table 5.1.

In figure 5.3 the real parts of reflection coefficients for PP and PS modes at boundaries between two viscoelastic half-spaces, with quality factors near and below 10, are plotted. The elastic properties are selected to correspond with natural geological boundaries as discussed below. The coefficients are plotted three times each, with attenuation angle varying from 0°, to 45°, and to 70°; and angles of incidence up to 40° are included. The solid line refers to the homogeneous wave with zero attenuation angle; the dotted line is the inhomogeneous wave with moderate incident attenuation angle $\delta_P = 45°$ and the dashed line is the highly attenuative wave with $\delta_P = 70°$. The reflectivity curves for converted wave in the homogeneous and moderate attenuation cases approach each other near normal incidence, but in general the attenuation angle can be seen to have a significant impact on reflection amplitudes. For the PP-reflection coefficients and shale/salt and shale/limestone models, the attenuation angle has its largest influence for angles greater than 20°.

The influence of anelastic parameters and attenuation angles on the reflection coefficients in equations (5.20) and (5.21) is not easy to analyze in this unaltered form. To address this we decompose the reflectivity into three components, elastic, anelastic homogeneous and anelastic inhomogeneous. We insert the decomposed ray and slowness parameters calculated in previous section into d_i and c_i, obtaining

$$\mathrm{d}_j = \mathrm{d}_{Ej} + i\mathrm{d}_{Hj} + i\mathrm{d}_{IHj}, \tag{5.26}$$

$$\mathrm{c}_j = \mathrm{c}_{Ej} + i\mathrm{c}_{H4} + i\mathrm{c}_{IHj}, \quad j = 1, 2, 3, 4. \tag{5.27}$$

The detailed form of d_1, for instance, is

$$\begin{aligned}
d_1^{\mathrm{E}} =& -2p_E^2\Delta\mu_E(q_{\mathrm{P1}}^{\mathrm{E}} - q_{\mathrm{P2}}^{\mathrm{E}}) + (\rho_2 q_{\mathrm{P1}}^{\mathrm{E}} + \rho_1 q_{\mathrm{P2}}^{\mathrm{E}}) \\
d_1^{\mathrm{H}} =& -2p_E^2\Delta\mu_E(q_{\mathrm{P1}}^{\mathrm{H}} - q_{\mathrm{P2}}^{\mathrm{H}}) - 2(p_E^2\Delta\mu_A + 2p_E p_{\mathrm{H}}\Delta\mu_E)(q_{\mathrm{P1}}^{\mathrm{E}} - q_{\mathrm{P2}}^{\mathrm{E}}) + \rho_2 q_{\mathrm{P1}}^{\mathrm{H}} + \rho_1 q_{\mathrm{P2}}^{\mathrm{H}} \\
d_1^{\mathrm{IH}} =& -2p_E^2\Delta\mu_E(q_{\mathrm{P1}}^{\mathrm{IH}} - q_{\mathrm{P2}}^{\mathrm{IH}}) - 4p_E p_{\mathrm{IH}}\Delta\mu_E(q_{\mathrm{P1}}^{\mathrm{E}} - q_{\mathrm{P2}}^{\mathrm{E}}) + \rho_2 q_{\mathrm{P1}}^{\mathrm{IH}} + \rho_1 q_{\mathrm{P2}}^{\mathrm{IH}}.
\end{aligned}$$

More detail of dependency of this parameters to the medium properties can be found in appendix A. To compute the decomposed reflectivity we note that in low-loss viscoelastic media all terms involving the product of homogeneous and inhomogeneous terms are negligible (for instance, $d^H d^{IH} \approx (d^H)^2 \approx (d^{IH})^2 \approx 0$). Taking into account the low-loss aspect of the media, and inserting (5.26) and (5.27) into the (5.20) and (5.21), we arrive at

$$\mathrm{R_{PP}} = \mathrm{R_{PP}^{E}} + i\mathrm{R_{PP}^{H}} + i\mathrm{R_{PP}^{IH}}, \tag{5.28}$$

$$\mathrm{R_{PS}} = \mathrm{R_{PS}^{E}} + i\mathrm{R_{PS}^{H}} + i\mathrm{R_{PS}^{IH}}, \tag{5.29}$$

where $\mathrm{R_{PP}^{E}}$ is the elastic reflectivity, i.e., the reflectivity in the absence of attenuation:

$$\mathrm{R_{PP}^{E}} = \frac{\mathrm{c}_{E1}\mathrm{d}_{E2} - \mathrm{c}_{E3}\mathrm{d}_{E_4}}{\mathrm{d}_{E_1}\mathrm{d}_{E_2} + \mathrm{d}_{E_3}\mathrm{d}_{E_4}},$$

$\mathrm{R_{PP}^{H}}$ is the homogeneous anelastic term, i.e., the term which remains when the attenuation angle is zero,

$$\begin{aligned}
\mathrm{R_{PP}^{H}} =& -\mathrm{R_{PP}^{E}}\frac{\mathrm{d}_{E2}\mathrm{d}_{H1} + \mathrm{d}_{E1}\mathrm{d}_{H2} + \mathrm{d}_{E3}\mathrm{d}_{H4} + \mathrm{d}_{E4}\mathrm{d}_{H3}}{\mathrm{d}_{E1}\mathrm{d}_{E2} + \mathrm{d}_{E3}\mathrm{d}_{E4}} \\
& - \frac{\mathrm{c}_{E3}\mathrm{d}_{H4} + \mathrm{c}_{H3}\mathrm{d}_{E4} - \mathrm{c}_{H1}\mathrm{d}_{E2} - \mathrm{c}_{E1}\mathrm{d}_{H2}}{\mathrm{d}_{E1}\mathrm{d}_{E2} + \mathrm{d}_{E3}\mathrm{d}_{E4}}
\end{aligned}$$

and finally $\mathrm{R}^{\mathrm{IH}}_{\mathrm{PP}}$, the inhomogeneous term which appears with non-zero attenuation angle,

$$\begin{aligned}\mathrm{R}^{\mathrm{IH}}_{\mathrm{PP}} = &- \mathrm{R}^{\mathrm{E}}_{\mathrm{PP}} \frac{\mathrm{d}_{E2}\mathrm{d}_{IH1} + \mathrm{d}_{E1}\mathrm{d}_{IH2} + \mathrm{d}_{E3}\mathrm{d}_{IH4} + \mathrm{d}_{E4}\mathrm{d}_{IH3}}{\mathrm{d}_{E1}\mathrm{d}_{E2} + \mathrm{d}_{E3}\mathrm{d}_{E4}} \\ &- \frac{\mathrm{c}_{E3}\mathrm{d}_{IH4} + \mathrm{c}_{IH3}\mathrm{d}_{E4} - \mathrm{c}_{IH1}\mathrm{d}_{E2} - \mathrm{c}_{E1}\mathrm{d}_{IH2}}{\mathrm{d}_{E1}\mathrm{d}_{E2} + \mathrm{d}_{E3}\mathrm{d}_{E4}}.\end{aligned}$$

In the same way three components of PS-reflectivity are

$$\mathrm{R}^{\mathrm{E}}_{\mathrm{PS}} = - \left(\frac{V_{\mathrm{PE1}}}{V_{\mathrm{SE1}}}\right) \frac{\mathrm{c}_{E3}\mathrm{d}_{E1} + \mathrm{c}_{E1}\mathrm{d}_{E3}}{\mathrm{d}_{E1}\mathrm{d}_{E2} + \mathrm{d}_{E3}\mathrm{d}_{E4}} \tag{5.30}$$

$$\mathrm{R}^{\mathrm{H}}_{\mathrm{PS}} = \frac{1}{2}\left(Q^{-1}_{P1} - Q^{-1}_{S1}\right)\mathrm{R}^{\mathrm{E}}_{\mathrm{PS}} \tag{5.31}$$

$$- \mathrm{R}^{\mathrm{E}}_{\mathrm{PS}} \frac{\mathrm{d}_{E1}\mathrm{d}_{H2} + \mathrm{d}_{E3}\mathrm{d}_{H4} + \mathrm{d}_{H1}\mathrm{d}_{E2} + \mathrm{d}_{H3}\mathrm{d}_{E4}}{\mathrm{d}_{E1}\mathrm{d}_{E2} + \mathrm{d}_{E3}\mathrm{d}_{E4}} \tag{5.32}$$

$$- \left(\frac{V_{\mathrm{PE1}}}{V_{\mathrm{SE1}}}\right) \frac{\mathrm{c}_{E3}\mathrm{d}_{H1} + \mathrm{c}_{E1}\mathrm{d}_{H3} + \mathrm{c}_{H3}\mathrm{d}_{E1} + \mathrm{c}_{H1}\mathrm{d}_{E3}}{\mathrm{d}_{E1}\mathrm{d}_{E2} + \mathrm{d}_{E3}\mathrm{d}_{E4}} \tag{5.33}$$

$$\mathrm{R}^{\mathrm{IH}}_{\mathrm{PS}} = -\mathrm{R}^{\mathrm{E}}_{\mathrm{PS}} \frac{\mathrm{d}_{E1}\mathrm{d}_{IH2} + \mathrm{d}_{E3}\mathrm{d}_{IH4} + \mathrm{d}_{IH1}\mathrm{d}_{E2} + \mathrm{d}_{IH3}\mathrm{d}_{E4}}{\mathrm{d}_{E1}\mathrm{d}_{E2} + \mathrm{d}_{E3}\mathrm{d}_{E4}} \tag{5.34}$$

$$- \left(\frac{V_{\mathrm{PE1}}}{V_{\mathrm{SE1}}}\right) \frac{\mathrm{c}_{E3}\mathrm{d}_{IH1} + \mathrm{c}_{E1}\mathrm{d}_{IH3} + \mathrm{c}_{IH3}\mathrm{d}_{E1} + \mathrm{c}_{IH1}\mathrm{d}_{E3}}{\mathrm{d}_{E1}\mathrm{d}_{E2} + \mathrm{d}_{E3}\mathrm{d}_{E4}}. \tag{5.35}$$

In summary, the viscoelastic reflection coefficients have real and imaginary parts, with the real part being identical to the solutions of the elastic Zoeppritz equations, and the imaginary part with a more complicated structure, depending on the elastic, anelastic terms as well as the attenuation angle.

5.6 The viscoelastic Shuey approximation

Linearized approximate forms of the solutions to the Zoeppritz equations are typically used in AVO analysis and inversion (Aki and Richards, 2002; Castagna and Backus, 1993; Foster et al., 2010). A range of linearized forms are available, distinguished by their treatment of the plane wave incidence angle and their parameterization of elastic properties and their variation across the reflecting interface; amongst these the Shuey approximation (Shuey, 1985) is one of the most frequently used. Ideally a linearized form (1) only differs from the exact solution by a small amount in the regions (e.g., angle-range) it is employed, (2) provides an intuitive interpretability , (3) leads to stable inversion algorithms, and (4) correctly predicts the main reflection phenomena observed in seismic data. In this section we review and decompose

the viscoelastic version of this approximation. There are two main assumptions made in deriving the equations of linear AVO analysis, firstly, that the relative changes in properties (elastic or anelastic) across the interface are small, and secondly, that the incident angle is well below the critical angle. The small-offset linearized P-to-P reflection coefficient for an inhomogeneous seismic wave reflected from boundary of two isotropic viscoelastic media under the assumption of small contrast interface is given by (Moradi and Innanen, 2016)

$$\mathrm{R_{PPL}} = \mathrm{R^{E}_{PPL}} + i\mathrm{R^{H}_{PPL}} + i\mathrm{R^{IH}_{PPL}}, \tag{5.36}$$

where the real part is

$$\mathrm{R^{E}_{PPL}} = \frac{1}{2}\left(\frac{\Delta\rho}{\rho} + \frac{1}{\cos^2\theta_{\mathrm{P}}}\frac{\Delta V_{\mathrm{P}}}{V_{\mathrm{P}}}\right) - 2\sin^2\theta_P\left(\frac{V_{\mathrm{S}}}{V_{\mathrm{P}}}\right)^2\left(\frac{\Delta\rho}{\rho} + 2\frac{\Delta V_{\mathrm{S}}}{V_{\mathrm{S}}}\right) \tag{5.37}$$

the homogeneous-imaginary part $\mathrm{R^{H}_{PP}}$ is

$$\mathrm{R^{H}_{PPL}} = -2\left(\frac{V_{\mathrm{S}}}{V_{\mathrm{P}}}\right)^2(Q_{\mathrm{S}}^{-1} - Q_{\mathrm{P}}^{-1})\sin^2\theta_{\mathrm{P}}\left(\frac{\Delta\rho}{\rho} + 2\frac{\Delta V_{\mathrm{S}}}{V_{\mathrm{S}}}\right) \tag{5.38}$$

$$- \frac{1}{4\cos^2\theta_{\mathrm{P}}}Q_{\mathrm{P}}^{-1}\frac{\Delta Q_{\mathrm{P}}}{Q_{\mathrm{P}}} + 2\sin^2\theta_{\mathrm{P}}\left(\frac{V_{\mathrm{S}}}{V_{\mathrm{P}}}\right)^2 Q_{\mathrm{S}}^{-1}\frac{\Delta Q_{\mathrm{S}}}{Q_{\mathrm{S}}}. \tag{5.39}$$

and the inhomogeneous-imaginary part $\mathrm{R^{IH}_{PP}}$ is

$$\mathrm{R^{IH}_{PPL}} = -Q_{\mathrm{P}}^{-1}\tan\delta_{\mathrm{P}}\left[\sin 2\theta_{\mathrm{P}}\left(\frac{V_{\mathrm{S}}}{V_{\mathrm{P}}}\right)^2\left(\frac{\Delta\rho}{\rho} + 2\frac{\Delta V_{\mathrm{S}}}{V_{\mathrm{S}}}\right) - \frac{\tan\theta_{\mathrm{P}}}{2\cos^2\theta_{\mathrm{P}}}\frac{\Delta V_{\mathrm{P}}}{V_{\mathrm{P}}}\right]. \tag{5.40}$$

Here $\Delta\rho/\rho$ is fractional change in density, with $\Delta\rho = \rho_2 - \rho_1$ and $\rho = (\rho_2 + \rho_1)/2$; $\Delta V_{\mathrm{P}}/V_{\mathrm{P}}$ is fractional change in P-wave velocity, with $\Delta V_{\mathrm{P}} = V_{\mathrm{P2}} - V_{\mathrm{P1}}$ and $V_{\mathrm{P}} = (V_{\mathrm{P2}} + V_{\mathrm{P1}})/2$; $\Delta V_{\mathrm{S}}/V_{\mathrm{S}}$ is fractional change in S-wave velocity, with $\Delta V_{\mathrm{S}} = V_{\mathrm{S2}} - V_{\mathrm{S1}}$ and $V_{\mathrm{S}} = (V_{\mathrm{S2}} + V_{\mathrm{S1}})/2$; $\Delta Q_{\mathrm{P}}/Q_{\mathrm{P}}$ is fractional change in P-wave quality factor, with $\Delta Q_{\mathrm{P}} = Q_{\mathrm{P2}} - Q_{\mathrm{P1}}$ and $Q_{\mathrm{P}} = (Q_{\mathrm{P2}} + Q_{\mathrm{P1}})/2$; $\Delta Q_{\mathrm{S}}/Q_{\mathrm{S}}$ is fractional change in S-wave quality factor, with $\Delta Q_{\mathrm{S}} = Q_{\mathrm{S2}} - Q_{\mathrm{S1}}$ and $Q_{\mathrm{S}} = (Q_{\mathrm{S2}} + Q_{\mathrm{S1}})/2$. In addition $\theta_{\mathrm{P}} = (\theta_{\mathrm{P2}} + \theta_{\mathrm{P1}})/2$ where θ_{P1} is the incident phase angle and θ_{P2} is the transmitted phase angle; $\delta_{\mathrm{P}} = (\delta_{\mathrm{P2}} + \delta_{\mathrm{P1}})/2$ where δ_{P1} is the incident attenuation angle and δ_{P2} is the transmitted attenuation angle. Subscript 1 refers to the upper layer and subscript 2 refers to the lower layer. It can be seen that the anelastic-inhomogeneous term is a function of the fractional changes in density, P- and S-wave velocities.

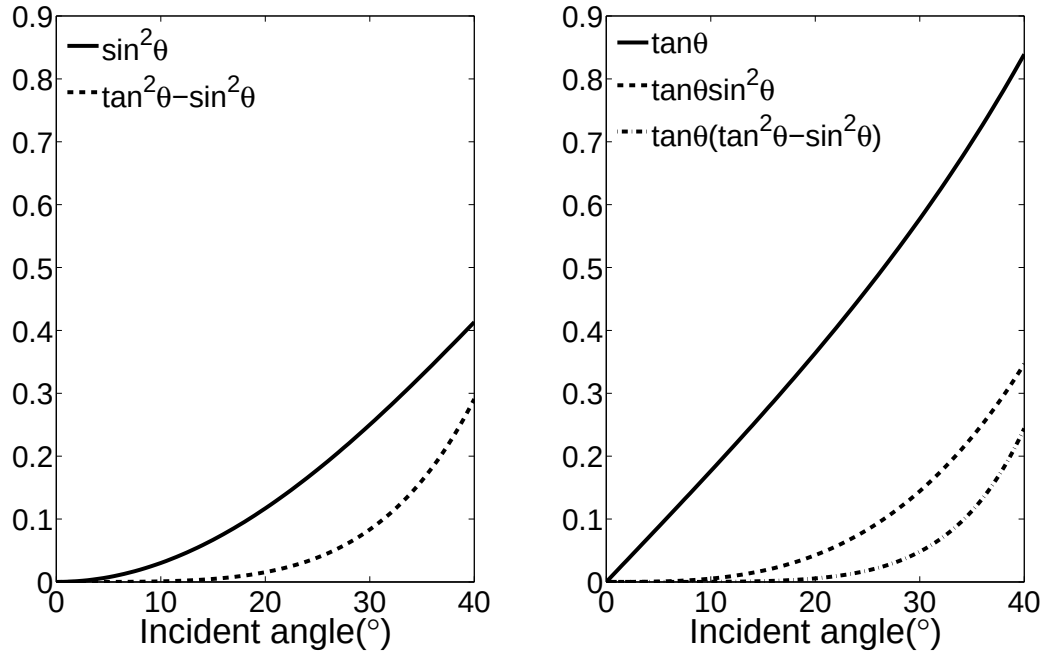

Figure 5.4: Comparing the two and three term AVO responses for the decomposed PP reflectivity.

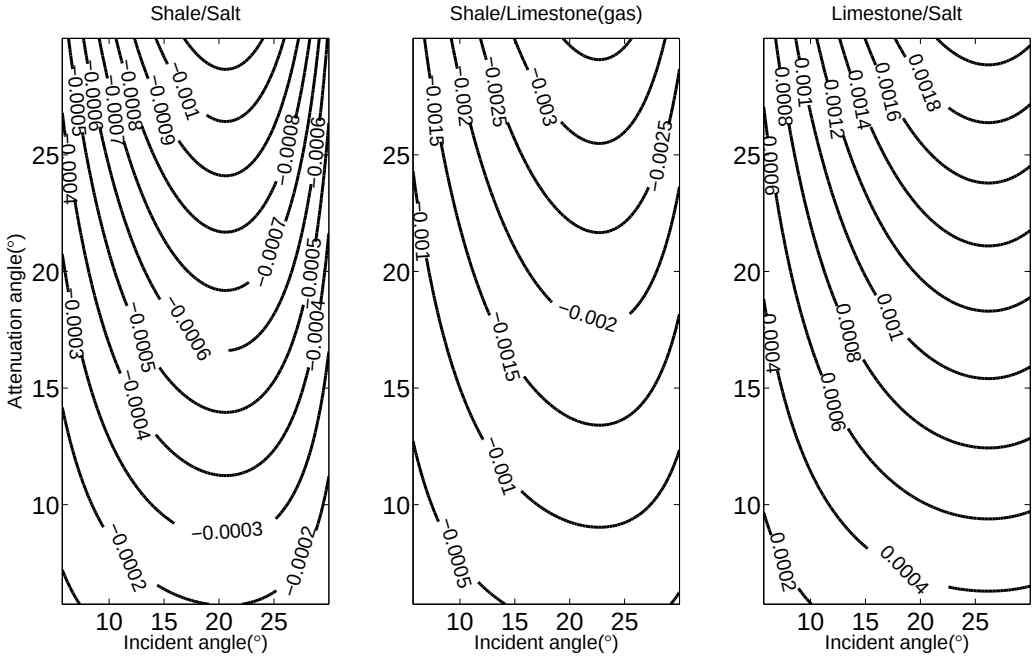

Figure 5.5: The maps of the inhomogeneous part of the PP-reflectivity for three models in table 1. The vertical axis indicates the attenuation angle and horizontal axis incident angle.

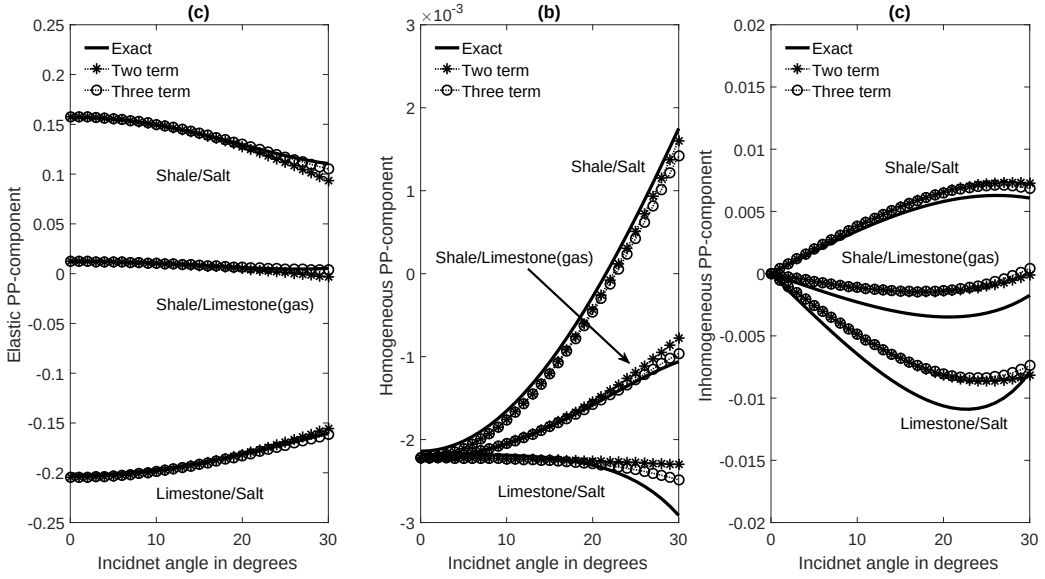

Figure 5.6: Components of the PP-reflection coefficients versus incident angle $\theta_{\rm P}$ for three two layer mineral models introduced in table 5.1. Solid line represent the exact reflectivity calculated from the Zoeppritz equation (Eq. 5.20), star and circle-dot lines respectively are related to the two and three terms (Figures 5.6b and 5.6c). Reflectivity components corresponding to the interface models of Shale/salt, Shale/Limestone(gas) and Limestone/Salt.

Equations (5.37-5.40) can be rearranged in powers of $\sin\theta_{\rm P}$ and $\tan\theta_{\rm P}$

$$\mathrm{R_{PPL}}(\theta_{\rm P},\delta_{\rm P}) = \mathrm{R^{E}_{PP}}(\theta_{\rm P}) + i\mathrm{R^{H}_{PPL}}(\theta_{\rm P}) + i\mathrm{R^{IH}_{PPL}}(\theta_{\rm P},\delta_{\rm P}), \tag{5.41}$$

with elastic, anelastic-homogenous and anelastic-inhomogeneous terms given by

$$\mathrm{R^{E}_{PPL}}(\theta_{\rm P}) = A^{\rm E}_{\rm PP} + B^{\rm E}_{\rm PP}\sin^2\theta_{\rm P} + C^{\rm E}_{\rm PP}(\tan^2\theta_{\rm P} - \sin^2\theta_P), \tag{5.42}$$

$$\mathrm{R^{H}_{PPL}}(\theta_{\rm P}) = A^{\rm H}_{\rm PP} + B^{\rm H}_{\rm PP}\sin^2\theta_{\rm P} + A^{\rm H}_{\rm PP}(\tan^2\theta_{\rm P} - \sin^2\theta_P), \tag{5.43}$$

$$\mathrm{R^{IH}_{PPL}}(\theta_{\rm P},\delta_{\rm P}) = A^{\rm IH}_{\rm PP}\tan\theta_P + B^{\rm IH}_{\rm PP}\tan\theta_{\rm P}\sin^2\theta_{\rm P} + C^{\rm IH}_{\rm PP}\tan\theta_{\rm P}(\tan^2\theta_{\rm P} - \sin^2\theta_{\rm P}), \tag{5.44}$$

where the elastic constants are

$$A^{\rm E}_{\rm PP} = \frac{1}{2}\left[\frac{\Delta\rho}{\rho} + \frac{\Delta V_{\rm P}}{V_{\rm P}}\right],$$
$$B^{\rm E}_{\rm PP} = \frac{1}{2}\frac{\Delta V_{\rm P}}{V_{\rm P}} - 2\left(\frac{V_{\rm S}}{V_{\rm P}}\right)^2\left[\frac{\Delta\rho}{\rho} + 2\frac{\Delta V_{\rm S}}{V_{\rm S}}\right],$$
$$C^{\rm E}_{\rm PP} = \frac{1}{2}\frac{\Delta V_{\rm P}}{V_{\rm P}},$$

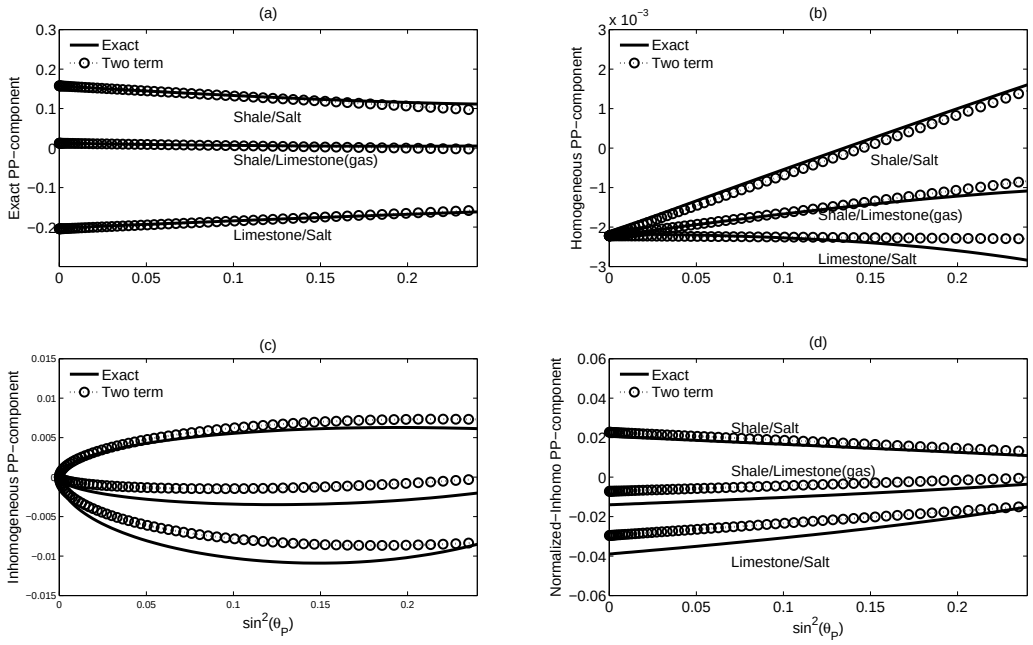

Figure 5.7: Components of the PP-reflection coefficients versus $\sin^2\theta_{\mathrm{P}}$ for three two layer mineral models introduced in table 5.1. Solid line represent the exact reflectivity calculated from the Zoeppritz equation (Eq. 5.20)and circle-dot lines corresponds to the two term approximation. Reflectivity components corresponding to the interface models of Shale/salt, Shale/Limestone(gas) and Limestone/Salt. Figure(5.6d) corresponds to the inhomogeneous components normalized by dividing to $\tan\theta_{\mathrm{P}}$

the homogeneous constants are

$$A^{\mathrm{H}}_{\mathrm{PP}} = -\frac{1}{4}Q_{\mathrm{P}}^{-1}\frac{\Delta Q_{\mathrm{P}}}{Q_{\mathrm{P}}},$$
$$B^{\mathrm{H}}_{\mathrm{PP}} = -2\left(\frac{V_{\mathrm{S}}}{V_{\mathrm{P}}}\right)^2\left[(Q_{\mathrm{P}}^{-1}-Q_{\mathrm{S}}^{-1})\left(\frac{\Delta\rho}{\rho}+2\frac{\Delta V_{\mathrm{S}}}{V_{\mathrm{S}}}\right)+Q_{\mathrm{S}}^{-1}\frac{\Delta Q_{\mathrm{S}}}{Q_{\mathrm{S}}}\right]-\frac{1}{4}Q_{\mathrm{P}}^{-1}\frac{\Delta Q_{\mathrm{P}}}{Q_{\mathrm{P}}},$$

and the inhomogeneous constants are

$$A^{\mathrm{IH}}_{\mathrm{PP}} = Q_{\mathrm{P}}^{-1}\tan\delta_{\mathrm{P}}\left[\frac{1}{2}\frac{\Delta V_{\mathrm{P}}}{V_{\mathrm{P}}}-2\left(\frac{V_{\mathrm{S}}}{V_{\mathrm{P}}}\right)^2\left(\frac{\Delta\rho}{\rho}+2\frac{\Delta V_{\mathrm{S}}}{V_{\mathrm{S}}}\right)\right]$$
$$B^{\mathrm{IH}}_{\mathrm{PP}} = Q_{\mathrm{P}}^{-1}\tan\delta_{\mathrm{P}}\left[\frac{1}{2}\frac{\Delta V_{\mathrm{P}}}{V_{\mathrm{P}}}+2\left(\frac{V_{\mathrm{S}}}{V_{\mathrm{P}}}\right)^2\left(\frac{\Delta\rho}{\rho}+2\frac{\Delta V_{\mathrm{S}}}{V_{\mathrm{S}}}\right)\right]$$
$$C^{\mathrm{IH}}_{\mathrm{PP}} = Q_{\mathrm{P}}^{-1}\tan\delta_{\mathrm{P}}\frac{1}{2}\left[\frac{\Delta V_{\mathrm{P}}}{V_{\mathrm{P}}}\right].$$

Equations (5.42)-(5.44) are arranged in such a way that successive terms grow in importance as the angle of incidence grows. These equations are the generalization of the Shuey approximation to viscoelastic media. For each of the elastic, homogeneous and inhomogeneous parts, the first term corresponds to reflection coefficient at normal incidence. The second term is called the AVO gradient, and the third term, which becomes important for wide angles of incidence (roughly $\theta_{\mathrm{P}} > 30°$) is called the curvature. We note that the inhomogeneous term at normal incidence is zero, indicating that to leading order contributions from the attenuation angle should not be expected in the PP-reflectivity at normal incidence.

The linearized forms also make qualitatively clear aspects of the dependence of the reflection strengths on the physical properties above and below the interface. The elastic part of the reflectivity is sensitive to changes in density, P- and S-wave velocities and has a non zero value for waves at normal incidence. The anelastic-homogeneous term is sensitive to changes in density, S-wave velocity, P-wave quality factor and S-wave quality factor. At normal incidence this term is not zero, but, only a change in P-wave quality factor influences it. The inhomogeneous term is nonzero and sensitive to changes in density, P- and S-wave velocities; it is zero at normal incidence. We show later that the inhomogeneous term is a function of incidence angle, a property shared by the elastic and anelastic converted P-wave.

In Figure (5.4) we compare the relative importance of the three terms in the AVO responses expressed in equations (5.42) – (5.44). For elastic and homogeneous terms the

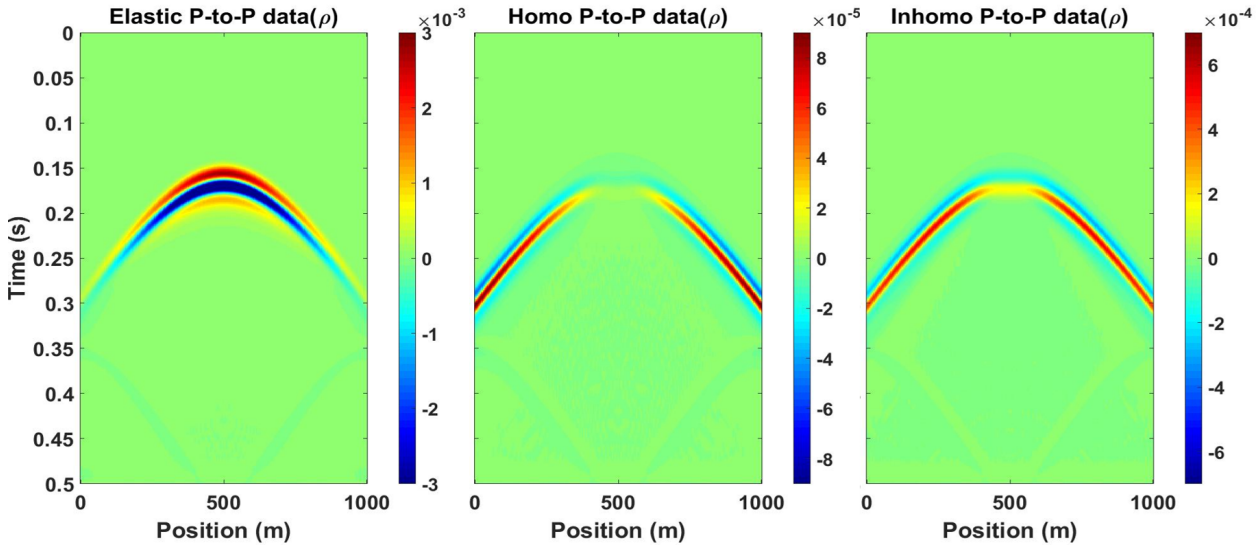

Figure 5.8: Numerical modeling of elastic, homogeneous and inhomogeneous terms in linearized P-to-P reflection coefficient for contrast in density.

contributions of the curvature at angles $\theta_P < 20°$ is negligible. Increasing the incidence angle, this term becomes relevant beyond $\theta_P > 30°$. The three components of the PP-reflection coefficient are illustrated in Figure (5.6). The elastic component shows a significant increase in accuracy moving from the two-term approximation (intercept and gradient) to the three-term approximation (including the curvature). The homogeneous component in isolation deviates only slightly from the exact solution for angles up to 20° except in the case of the limestone/salt model. In Figure (5.6c), we observe that the approximate form of the inhomogeneous component of the reflection coefficient deviates significantly from the exact result for all but the shale/salt model with incidence angles up to 20°. Figure 5.8 is the numerical comparison of elastic, homogeneous and inhomogeneous terms in P-to-P reflection coefficients for contrast in density.

In Figure 5.7 we plot the exact versus linearized P-to-P reflectivity for the three single-interface models in Table 1. For elastic and homogeneous parts of the reflectivity, the linearity with respect to $\sin^2\theta_{\rm P}$ can be seen explicitly. The inhomogeneous term $\mathrm{R}_{\rm PP}^{\rm IH}$ is not a linear function of $\sin^2\theta_{\rm P}$, but linearity can be enforced through the normalization

$$\mathrm{R}_{\rm PPN}^{\rm IH} = \frac{\mathrm{R}_{\rm PP}^{\rm IH}}{\tan\theta_{\rm P}}, \quad \theta_{\rm P} \neq 0. \tag{5.45}$$

The exact and approximate inhomogeneous reflectivities, introduced in equation (5.45), are

plotted in Figure (5.7d). The $\mathrm{R}^{\mathrm{IH}}_{\mathrm{PPN}}$ term is evidently linear with respect to $\sin^2\theta_{\mathrm{P}}$ in the range $0 \leq \theta_{\mathrm{P}} \leq 25^{\circ}$. Using the decomposition defined in equation (5.36), and the terms plotted in Figure 5.9, we can obtain the zero offset coefficients A and gradient terms B from the exact reflectivity. Contour maps, illustrating the variability of the inhomogeneous component of the P-to-P reflectivity versus phase and attenuation angles, are plotted in Figure 5.5.

5.7 Converted wave approximations

By solving the Zoeppritz equation for two half-spaces involving low-loss viscoelastic media, we can obtain exact expressions for the PP- and PS-reflection coefficients (Moradi and Innanen, 2015a, 2016). To linearize the reflectivities in terms of changes in elastic and anelastic properties, we assume the incidence angle to be smaller that 30°, and also that the relative change in all elastic/anelastic properties are much less than one. In this paper, to treat the case of the converted wave, we use the appropriate version of Snell's law to obtain an expression for the S-wave attenuation angle, appropriate for small angles of incidence, which is written as a function of the incident phase and attenuation angles (appendix C). The weak-contrast converted-wave reflectivity is then given by

$$\mathrm{R}_{\mathrm{PS}} = \mathrm{R}^{\mathrm{E}}_{\mathrm{PS}} + i\mathrm{R}^{\mathrm{H}}_{\mathrm{PS}} + i\mathrm{R}^{\mathrm{IH}}_{\mathrm{PS}}, \tag{5.46}$$

where the real part is

$$\mathrm{R}^{\mathrm{E}}_{\mathrm{PS}} = -\tan\theta_S \frac{1}{2}\frac{V_{\mathrm{P}}}{V_{\mathrm{S}}}\frac{\Delta\rho}{\rho} - \tan\theta_S \cos(\theta_{\mathrm{P}} + \theta_S)\left(\frac{\Delta\rho}{\rho} + 2\frac{\Delta V_{\mathrm{S}}}{V_{\mathrm{S}}}\right), \tag{5.47}$$

the homogeneous-imaginary part $\mathrm{R}^{\mathrm{H}}_{\mathrm{PP}}$ is

$$\mathrm{R}^{\mathrm{H}}_{\mathrm{PS}} = -\frac{1}{4}\tan\theta_S(Q_P^{-1} - Q_S^{-1})\frac{V_P}{V_S}\frac{\Delta\rho}{\rho} + Q_S^{-1}\tan\theta_S\cos(\theta_P + \theta_S)\frac{\Delta Q_S}{Q_S}, \tag{5.48}$$

and the inhomogeneous-imaginary part $\mathrm{R}^{\mathrm{IH}}_{\mathrm{PP}}$ is

$$\mathrm{R}^{\mathrm{IH}}_{\mathrm{PS}} = -\frac{1}{4}Q_S^{-1}\tan\delta_S\frac{1}{\cos^2\theta_S}\frac{V_P}{V_S}\frac{\Delta\rho}{\rho} \tag{5.49}$$

$$-\frac{1}{2}Q_S^{-1}\tan\delta_S\frac{\cos(\theta_P + \theta_S)}{\cos^2\theta_S}\left(\frac{\Delta\rho}{\rho} + 2\frac{\Delta V_{\mathrm{S}}}{V_{\mathrm{S}}}\right) \tag{5.50}$$

$$+\frac{1}{2}\tan\theta_S\sin(\theta_P + \theta_S)(Q_S^{-1}\tan\delta_S + Q_P^{-1}\tan\delta_P)\left(\frac{\Delta\rho}{\rho} + 2\frac{\Delta V_{\mathrm{S}}}{V_{\mathrm{S}}}\right). \tag{5.51}$$

This approximate PS-reflectivity is a function of density, S-wave velocity and S-wave quality factors. Snell's law relates the reflected and transmitted phase and attenuation angles to the incident phase and attenuation angles. In order to analyze the converted-wave reflection coefficient properly in the lowest order, using the Snell's law the average S-wave attenuation angle for small angles of incidence is written as a function of incident phase and attenuation angles:

$$\begin{aligned} Q_S^{-1}\tan\delta_S = & \frac{V_S}{V_P}Q_P^{-1}\tan\delta_P \\ & + \frac{V_S}{V_P}(Q_S^{-1}-Q_P^{-1})\sin\theta_P \\ & - \frac{1}{2}\frac{V_S}{V_P}\left[1-\left(\frac{V_S}{V_P}\right)^2\right]Q_P^{-1}\tan\delta_P\sin^2\theta_{\mathrm{P}} \\ & + \frac{1}{2}\left(\frac{V_S}{V_P}\right)^3(Q_S^{-1}-Q_P^{-1})\sin^3\theta_P. \end{aligned} \tag{5.52}$$

Then, using standard approximations for trigonometric functions for small angles, and collecting the powers of $\sin\theta_{\mathrm{P}}$, we obtain

$$\mathrm{R_{PS}}(\theta_{\mathrm{P}},\delta_{\mathrm{P}}) = \mathrm{R^{E}_{PS}}(\theta_{\mathrm{P}}) + i\mathrm{R^{H}_{PS}}(\theta_{\mathrm{P}}) + i\mathrm{R^{IH}_{PS}}(\theta_{\mathrm{P}},\delta_{\mathrm{P}}), \tag{5.53}$$

where the elastic, homogenous and inhomogeneous terms are given by

$$\begin{aligned} \mathrm{R^{E}_{PS}}(\theta_{\mathrm{P}}) &= A^{\mathrm{E}}_{\mathrm{PS}}\sin\theta_{\mathrm{P}} + B^{\mathrm{E}}_{\mathrm{PS}}\sin^3\theta_{\mathrm{P}}, \\ \mathrm{R^{H}_{PS}}(\theta_{\mathrm{P}}) &= A^{\mathrm{H}}_{\mathrm{PS}}\sin\theta_{\mathrm{P}} + B^{\mathrm{H}}_{\mathrm{PS}}\sin^3\theta_{\mathrm{P}}, \\ \mathrm{R^{IH}_{PS}}(\theta_{\mathrm{P}},\delta_{\mathrm{P}}) &= A^{\mathrm{IH}}_{\mathrm{PS}} + B^{\mathrm{IH}}_{\mathrm{PS}}\sin^2\theta_P, \end{aligned}$$

with elastic constants

$$\begin{aligned} A^{\mathrm{E}}_{\mathrm{PS}} =& -\left(\frac{1}{2}+\frac{V_{\mathrm{S}}}{V_{\mathrm{P}}}\right)\frac{\Delta\rho}{\rho} - 2\frac{V_{\mathrm{S}}}{V_{\mathrm{P}}}\frac{\Delta V_{\mathrm{S}}}{V_{\mathrm{S}}}, \\ B^{\mathrm{E}}_{\mathrm{PS}} =& \frac{V_{\mathrm{S}}}{V_{\mathrm{P}}}\left[\left(\frac{1}{2}+\frac{3}{4}\frac{V_{\mathrm{S}}}{V_{\mathrm{P}}}\right)\frac{\Delta\rho}{\rho} + 2\left[\frac{1}{2}+\frac{V_{\mathrm{S}}}{V_{\mathrm{P}}}\right]\frac{\Delta V_{\mathrm{S}}}{V_{\mathrm{S}}}\right], \end{aligned}$$

homogeneous constants

$$
\begin{aligned}
A_{\mathrm{PS}}^{\mathrm{H}} =& \frac{V_{\mathrm{S}}}{V_{\mathrm{P}}}\left\{Q_S^{-1}\frac{\Delta Q_S}{Q_S} - \frac{1}{2}(Q_S^{-1} - Q_P^{-1})\left(\frac{\Delta\rho}{\rho} + 2\frac{\Delta V_{\mathrm{S}}}{V_{\mathrm{S}}}\right)\right\},\\
B_{\mathrm{PS}}^{\mathrm{H}} =& -\frac{V_{\mathrm{S}}}{V_{\mathrm{P}}}\left[\frac{1}{2} + \frac{V_{\mathrm{S}}}{V_{\mathrm{P}}}\right]Q_S^{-1}\frac{\Delta Q_S}{Q_S} - \frac{1}{4}\left(\frac{V_{\mathrm{S}}}{V_{\mathrm{P}}}\right)^2(Q_S^{-1} - Q_P^{-1})\frac{\Delta\rho}{\rho}\\
&+ \frac{1}{4}\frac{V_S}{V_P}\left(1 + 4\frac{V_{\mathrm{S}}}{V_{\mathrm{P}}}\right)(Q_S^{-1} - Q_P^{-1})\left(\frac{\Delta\rho}{\rho} + 2\frac{\Delta V_{\mathrm{S}}}{V_{\mathrm{S}}}\right),
\end{aligned}
$$

and inhomogeneous constants

$$
\begin{aligned}
A_{\mathrm{PS}}^{\mathrm{IH}} =& -\frac{1}{2}\frac{V_S}{V_P}\left[\left(1 + \frac{1}{2}\frac{V_P}{V_S}\right)\frac{\Delta\rho}{\rho} + 2\frac{\Delta V_{\mathrm{S}}}{V_{\mathrm{S}}}\right]Q_P^{-1}\tan\delta_P,\\
B_{\mathrm{PS}}^{\mathrm{IH}} =& \frac{1}{8}\left[1 - 3\left(\frac{V_S}{V_P}\right)^2\right]\frac{\Delta\rho}{\rho}Q_P^{-1}\tan\delta_P\\
&+ \frac{V_S}{V_P}\left(1 + \frac{3}{2}\frac{V_{\mathrm{S}}}{V_{\mathrm{P}}}\right)\left(\frac{\Delta\rho}{\rho} + 2\frac{\Delta V_{\mathrm{S}}}{V_{\mathrm{S}}}\right)Q_P^{-1}\tan\delta_P.
\end{aligned}
$$

The elastic term is seen to be sensitive to changes in density and S-wave velocity. The anelastic-homogeneous term is likewise seen to be sensitive to changes in density, S-wave velocity and its quality factor. These two terms are zero at normal incidence. The anelastic-inhomogeneous term is affected only by changes in density and S-wave velocity. This term also depends on the incident attenuation angle and is non zero at the normal incidence case; we note that this makes it quite singular in the standard converted wave AVO problem, wherein no contribution at normal incidence is ever predicted. Figure 5.10 is the numerical comparison of elastic, homogeneous and inhomogeneous terms in P-to-S reflection coefficients for contrast in density.

In Figure (5.9), we plot the exact versus linearized elastic, anelastic homogeneous and anelastic inhomogeneous terms for converted wave for the three models in Table (5.1). We observe that the elastic and homogenous terms are not linear in $\sin^2\theta_P$, and the inhomogeneous terms is. Thus we also define normalized elastic and homogeneous reflectivities by dividing them by $\sin\theta_{\mathrm{P}}$.

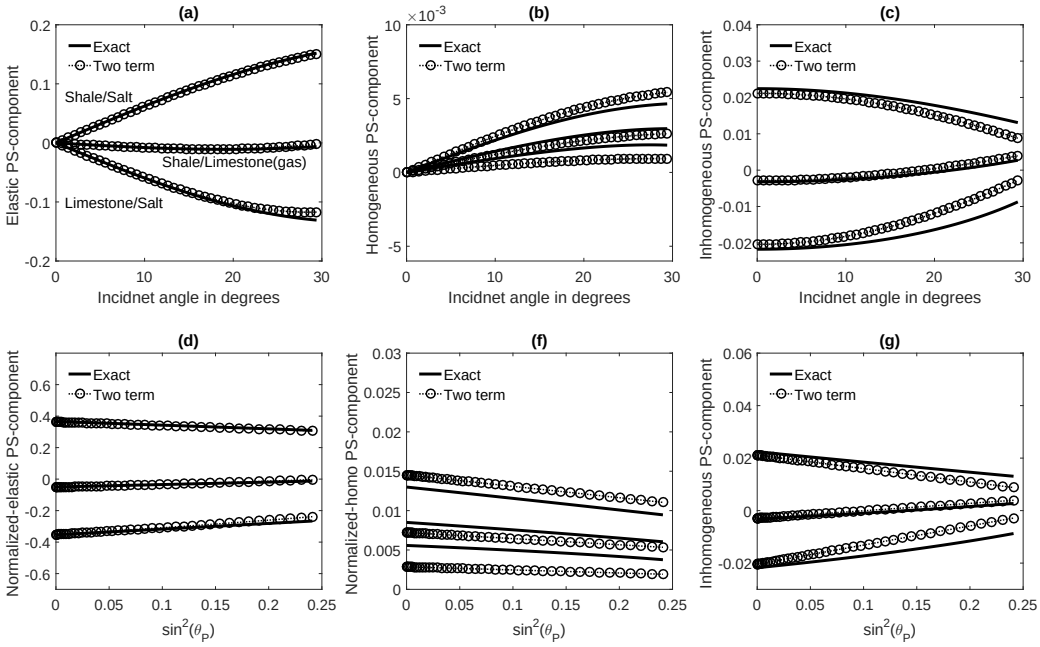

Figure 5.9: Components of the PS-reflection coefficients versus incident angle and $\sin^2\theta_{\mathrm{P}}$ for three two layer mineral models introduced in table 5.1. Solid line represent the exact reflectivity calculated from the Zoeppritz equation (Eq. 5.21)and circle-dot lines corresponds to the two term approximation. Reflectivity components corresponding to the interface models of Shale/salt, Shale/Limestone(gas) and Limestone/Salt. Figures (5.9d,f) to corresponds to the components normalized by dividing to $\sin\theta_{\mathrm{P}}$

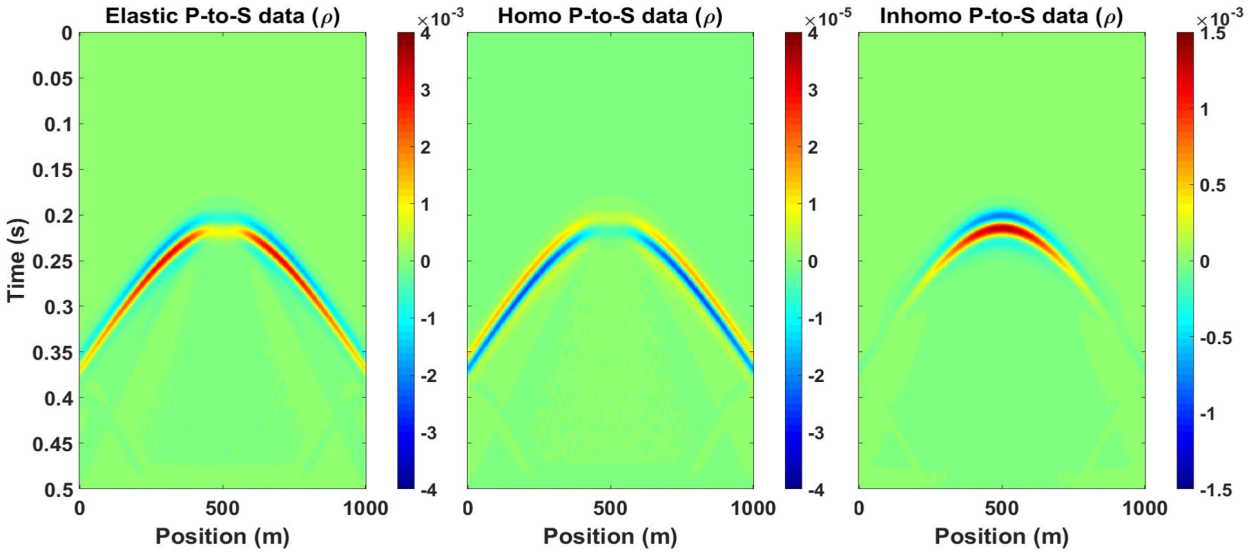

Figure 5.10: Numerical modeling of elastic, homogeneous and inhomogeneous terms in linearized P-to-S reflection coefficient for contrast in density.

5.8 Conclusions

The formulation of the amplitude-versus-offset equations for viscoelastic media is of increasing interest and importance, with quantitative interpretation of seismic data being deployed to characterize fluid presence, type, and viscosity in hydrocarbon reservoirs, CO_2 injection sites, and other exploration and monitoring settings. Properly formulated, these equations also provide insights into the character of eventual viscoelastic full waveform inversion algorithms. To date, investigations and analysis of anelastic reflection coefficients have been constructed on the assumption that the attenuation angle is unchanged across the boundary, which cannot be generally justified. We believe that a more fruitful approach approach is to apply an appropriate version of Snell's law in such way that transmitted and reflected attenuation angles are expressed in terms of the incident attenuation angle. This approach allows changes in attenuation angle to be expressed in terms of changes in velocity and quality factors, leading to new terms in the relevant AVO equations with a wider capture of anelastic reflection and transmission phenomena incorporated.

We show how Snell's law can be put to work in order to learn about the homogeneous and inhomogeneous components of complex vertical slowness. We have presented a decomposition of the exact and approximate viscoelastic reflection coefficients to expose the above discussed of the attenuation angle, demonstrating the possibly significant errors resulting from its neglect, in particular in cases of for highly attenuative media.

Linearization of reflection coefficients in viscoelastic media is more complicated than in elastic media in two ways. First, because of seismic amplitude damping, the polarization and slowness vectors are complex, and therefore so is the reflectivity. Second, we have as discussed the perturbation of the attenuation angle across the boundary, as predicted by the viscoelastic Snell's law. Taking into account these facts, the linearized AVO equations include the terms related to the changes in S-wave quality factors and the attenuation angle.

To to understand quantitatively and qualitatively the importance and influence of the attenuation angle, we decompose the reflectivity into three terms, elastic, homogeneous and inhomogeneous. Linearity of the elastic and homogeneous parts are visible; the inhomogeneous part must be normalized to share this feature. In terms of powers of $\sin\theta_{\mathrm{P}}$, the

converted PS-wave has four contributions, from zeroth to third order. The extra terms are due to the inhomogeneity of the waves. We examine our AVO equation with three two-half space models. Numerically, we find that the elastic and homogeneous terms are not linear with respect to $\sin^2\theta_{\mathrm{P}}$, however the inhomogeneous term for small angles ($\theta_{\mathrm{P}} < 30^{\circ}$) is perfectly linear for both exact and approximate cases. The most striking feature of this model of reflections from viscoelastic targets is that a non-zero converted wave at normal incidence is predicted, connected to the attenuation angle.

The result presented in this research indicate that linearized reflection coefficients for inhomogeneous PP-wave match for most inverse schemes the exact reflection coefficients with adequate accuracy. More important, the new approximations and the decomposition of reflectivity into three terms indicate that intercepts and gradients can be used in future research to determine the quality factor and attenuation angle in an appropriate inversion strategy.

Appendix C

Complex coefficients

Decomposition of the complex coefficients in reflection functions (5.20) and (5.21) are given by

$$\mathrm{d}_1 = d_1^{\mathrm{E}} + i d_1^{\mathrm{H}} + i d_1^{\mathrm{IH}},$$

where

$$\begin{aligned}
d_1^{\mathrm{E}} =& -2p_E^2\Delta\mu_E(q_{\mathrm{P1}}^{\mathrm{E}} - q_{\mathrm{P2}}^{\mathrm{E}}) + (\rho_2 q_{\mathrm{P1}}^{\mathrm{E}} + \rho_1 q_{\mathrm{P2}}^{\mathrm{E}}) \\
d_1^{\mathrm{H}} =& -2p_E^2\Delta\mu_E(q_{\mathrm{P1}}^{\mathrm{H}} - q_{\mathrm{P2}}^{\mathrm{H}}) - 2(p_E^2\Delta\mu_A + 2p_E p_{\mathrm{H}}\Delta\mu_E)(q_{\mathrm{P1}}^{\mathrm{E}} - q_{\mathrm{P2}}^{\mathrm{E}}) + \rho_2 q_{\mathrm{P1}}^{\mathrm{H}} + \rho_1 q_{\mathrm{P2}}^{\mathrm{H}} \\
d_1^{\mathrm{IH}} =& -2p_E^2\Delta\mu_E(q_{\mathrm{P1}}^{\mathrm{IH}} - q_{\mathrm{P2}}^{\mathrm{IH}}) - 4p_E p_{\mathrm{IH}}\Delta\mu_E(q_{\mathrm{P1}}^{\mathrm{E}} - q_{\mathrm{P2}}^{\mathrm{E}}) + \rho_2 q_{\mathrm{P1}}^{\mathrm{IH}} + \rho_1 q_{\mathrm{P2}}^{\mathrm{IH}}
\end{aligned}$$

also

$$\mathrm{d}_2 = d_2^{\mathrm{E}} + i d_2^{\mathrm{H}} + i d_2^{\mathrm{IH}},$$

where

$$\begin{aligned}
d_2^{\mathrm{E}} =& -2p_E^2\Delta\mu_E(q_{\mathrm{S}}^{\mathrm{E}} - q_{\mathrm{S2}}^{\mathrm{E}}) + (\rho_2 q_{\mathrm{S1}}^{\mathrm{E}} + \rho_1 q_{\mathrm{S2}}^{\mathrm{E}}) \\
d_2^{\mathrm{H}} =& -2p_E^2\Delta\mu_E(q_{\mathrm{P1}}^{\mathrm{H}} - q_{\mathrm{P2}}^{\mathrm{H}}) - 2(p_E^2\Delta\mu_A + 2p_E p_{\mathrm{H}}\Delta\mu_E)(q_{\mathrm{S1}}^{\mathrm{E}} - q_{\mathrm{S2}}^{\mathrm{E}}) + \rho_2 q_{\mathrm{S1}}^{\mathrm{H}} + \rho_1 q_{\mathrm{S2}}^{\mathrm{H}} \\
d_2^{\mathrm{IH}} =& -2p_E^2\Delta\mu_E(q_{\mathrm{S1}}^{\mathrm{IH}} - q_{\mathrm{S2}}^{\mathrm{IH}}) - 4p_E p_{\mathrm{IH}}\Delta\mu_E(q_{\mathrm{S1}}^{\mathrm{E}} - q_{\mathrm{S2}}^{\mathrm{E}}) + \rho_2 q_{\mathrm{S1}}^{\mathrm{IH}} + \rho_1 q_{\mathrm{S2}}^{\mathrm{IH}}
\end{aligned}$$

also

$$\mathrm{d}_3 = d_3^{\mathrm{E}} + i d_3^{\mathrm{H}} + i d_3^{\mathrm{IH}},$$

where

$$\begin{aligned}
d_3^{\mathrm{E}} =& -p_E\left[2\Delta\mu_E(q_{\mathrm{P1}}^{\mathrm{E}} q_{\mathrm{S2}}^{\mathrm{E}} + p^2) - \Delta\rho\right] \\
d_3^{\mathrm{H}} =& -2(p_{\mathrm{E}}\Delta\mu_A + p_{\mathrm{H}}\Delta\mu_E)(q_{\mathrm{P1}}^{\mathrm{E}} q_{\mathrm{S2}}^{\mathrm{E}} + p_E^2) - 2p_E\Delta\mu_E(2p_{\mathrm{E}}p_{\mathrm{H}} + q_{\mathrm{P1}}^{\mathrm{H}} q_{\mathrm{S2}}^{\mathrm{E}} + q_{\mathrm{P1}}^{\mathrm{E}} q_{\mathrm{S2}}^{\mathrm{H}}) + p_{\mathrm{H}}\Delta\rho \\
d_3^{\mathrm{IH}} =& -2p_{\mathrm{IH}}\Delta\mu_E(q_{\mathrm{P1}}^{\mathrm{E}} q_{\mathrm{S2}}^{\mathrm{E}} + p_E^2) - 2p_E\Delta\mu_E(q_{\mathrm{P1}}^{\mathrm{IH}} q_{\mathrm{S2}}^{\mathrm{E}} + q_{\mathrm{P1}}^{\mathrm{E}} q_{\mathrm{S2}}^{\mathrm{IH}}) + p_{\mathrm{IH}}\Delta\rho
\end{aligned}$$

also

$$\mathrm{d}_4 = d_4^{\mathrm{E}} + i d_4^{\mathrm{H}} + i d_4^{\mathrm{IH}},$$

where

$$\begin{aligned}
d_4^{\mathrm{E}} &= -\, p_E \left[2\Delta\mu_E (q_{\mathrm{P}2}^{\mathrm{E}} q_{\mathrm{S}1}^{\mathrm{E}} + p^2) - \Delta\rho \right] \\
d_4^{\mathrm{H}} &= -\, 2(p_{\mathrm{E}}\Delta\mu_A + p_{\mathrm{H}}\Delta\mu_E)(q_{\mathrm{P}2}^{\mathrm{E}} q_{\mathrm{S}1}^{\mathrm{E}} + p_E^2) - 2p_E\Delta\mu_E(2p_{\mathrm{E}}p_{\mathrm{H}} + q_{\mathrm{P}2}^{\mathrm{H}} q_{\mathrm{S}1}^{\mathrm{E}} + q_{\mathrm{P}2}^{\mathrm{E}} q_{\mathrm{S}1}^{\mathrm{H}}) + p_{\mathrm{H}}\Delta\rho \\
d_4^{\mathrm{IH}} &= -\, 2p_{\mathrm{IH}}\Delta\mu_E(q_{\mathrm{P}2}^{\mathrm{E}} q_{\mathrm{S}1}^{\mathrm{E}} + p_E^2) - 2p_E\Delta\mu_E(q_{\mathrm{P}2}^{\mathrm{IH}} q_{\mathrm{S}1}^{\mathrm{E}} + q_{\mathrm{P}2}^{\mathrm{E}} q_{\mathrm{S}1}^{\mathrm{IH}}) + p_{\mathrm{IH}}\Delta\rho
\end{aligned}$$

also

$$\mathrm{c}_1 = c_1^{\mathrm{E}} + i c_1^{\mathrm{H}} + i c_1^{\mathrm{IH}},$$

where

$$\begin{aligned}
c_1^{\mathrm{E}} &= -\, 2p_E^2\Delta\mu_E(q_{\mathrm{P}1}^{\mathrm{E}} + q_{\mathrm{P}2}^{\mathrm{E}}) + (\rho_2 q_{\mathrm{P}1}^{\mathrm{E}} - \rho_1 q_{\mathrm{P}2}^{\mathrm{E}}) \\
c_1^{\mathrm{H}} &= -\, 2p_E^2\Delta\mu_E(q_{\mathrm{P}1}^{\mathrm{H}} + q_{\mathrm{P}2}^{\mathrm{H}}) - 2(p_E^2\Delta\mu_A + 2p_E p_{\mathrm{H}}\Delta\mu_E)(q_{\mathrm{P}1}^{\mathrm{E}} + q_{\mathrm{P}2}^{\mathrm{E}}) + \rho_2 q_{\mathrm{P}1}^{\mathrm{H}} - \rho_1 q_{\mathrm{P}2}^{\mathrm{H}} \\
c_1^{\mathrm{IH}} &= -\, 2p_E^2\Delta\mu_E(q_{\mathrm{P}1}^{\mathrm{IH}} + q_{\mathrm{P}2}^{\mathrm{IH}}) - 4p_E p_{\mathrm{IH}}\Delta\mu_E(q_{\mathrm{P}1}^{\mathrm{E}} + q_{\mathrm{P}2}^{\mathrm{E}}) + \rho_2 q_{\mathrm{P}1}^{\mathrm{IH}} - \rho_1 q_{\mathrm{P}2}^{\mathrm{IH}}
\end{aligned}$$

also

$$\mathrm{c}_2 = c_2^{\mathrm{E}} + i c_2^{\mathrm{H}} + i c_2^{\mathrm{IH}},$$

where

$$\begin{aligned}
c_2^{\mathrm{E}} &= -\, 2p_E^2\Delta\mu_E(q_{\mathrm{S}}^{\mathrm{E}} + q_{\mathrm{S}2}^{\mathrm{E}}) + (\rho_2 q_{\mathrm{S}1}^{\mathrm{E}} - \rho_1 q_{\mathrm{S}2}^{\mathrm{E}}) \\
c_2^{\mathrm{H}} &= -\, 2p_E^2\Delta\mu_E(q_{\mathrm{P}1}^{\mathrm{H}} + q_{\mathrm{P}2}^{\mathrm{H}}) - 2(p_E^2\Delta\mu_A + 2p_E p_{\mathrm{H}}\Delta\mu_E)(q_{\mathrm{S}1}^{\mathrm{E}} + q_{\mathrm{S}2}^{\mathrm{E}}) + \rho_2 q_{\mathrm{S}1}^{\mathrm{H}} - \rho_1 q_{\mathrm{S}2}^{\mathrm{H}} \\
c_2^{\mathrm{IH}} &= -\, 2p_E^2\Delta\mu_E(q_{\mathrm{S}1}^{\mathrm{IH}} + q_{\mathrm{S}2}^{\mathrm{IH}}) - 4p_E p_{\mathrm{IH}}\Delta\mu_E(q_{\mathrm{S}1}^{\mathrm{E}} + q_{\mathrm{S}2}^{\mathrm{E}}) + \rho_2 q_{\mathrm{S}1}^{\mathrm{IH}} - \rho_1 q_{\mathrm{S}2}^{\mathrm{IH}}
\end{aligned}$$

also

$$\mathrm{c}_3 = c_3^{\mathrm{E}} + i c_3^{\mathrm{H}} + i c_3^{\mathrm{IH}},$$

where

$$
\begin{aligned}
c_3^{\mathrm{E}} =& p_E \left[2\Delta\mu_E(q_{\mathrm{P1}}^{\mathrm{E}} q_{\mathrm{S2}}^{\mathrm{E}} - p^2) + \Delta\rho\right] \\
c_3^{\mathrm{H}} =& 2(p_{\mathrm{E}}\Delta\mu_A + p_{\mathrm{H}}\Delta\mu_E)(q_{\mathrm{P1}}^{\mathrm{E}} q_{\mathrm{S2}}^{\mathrm{E}} - p_E^2) - 2p_E\Delta\mu_E(2p_{\mathrm{E}}p_{\mathrm{H}} - q_{\mathrm{P1}}^{\mathrm{H}} q_{\mathrm{S2}}^{\mathrm{E}} - q_{\mathrm{P1}}^{\mathrm{E}} q_{\mathrm{S2}}^{\mathrm{H}}) + p_{\mathrm{H}}\Delta\rho \\
c_3^{\mathrm{IH}} =& 2p_{\mathrm{IH}}\Delta\mu_E(q_{\mathrm{P1}}^{\mathrm{E}} q_{\mathrm{S2}}^{\mathrm{E}} - p_E^2) + 2p_E\Delta\mu_E(q_{\mathrm{P1}}^{\mathrm{IH}} q_{\mathrm{S2}}^{\mathrm{E}} + q_{\mathrm{P1}}^{\mathrm{E}} q_{\mathrm{S2}}^{\mathrm{IH}}) + p_{\mathrm{IH}}\Delta\rho
\end{aligned}
$$

also

$$
\mathrm{c}_4 = c_4^{\mathrm{E}} + ic_4^{\mathrm{H}} + ic_4^{\mathrm{IH}},
$$

where

$$
\begin{aligned}
c_4^{\mathrm{E}} =& p_E \left[2\Delta\mu_E(q_{\mathrm{P2}}^{\mathrm{E}} q_{\mathrm{S1}}^{\mathrm{E}} + p^2) + \Delta\rho\right] \\
c_4^{\mathrm{H}} =& 2(p_{\mathrm{E}}\Delta\mu_A + p_{\mathrm{H}}\Delta\mu_E)(q_{\mathrm{P2}}^{\mathrm{E}} q_{\mathrm{S1}}^{\mathrm{E}} - p_E^2) - 2p_E\Delta\mu_E(2p_{\mathrm{E}}p_{\mathrm{H}} - q_{\mathrm{P2}}^{\mathrm{H}} q_{\mathrm{S1}}^{\mathrm{E}} - q_{\mathrm{P2}}^{\mathrm{E}} q_{\mathrm{S1}}^{\mathrm{H}}) + p_{\mathrm{H}}\Delta\rho \\
c_4^{\mathrm{IH}} =& 2p_{\mathrm{IH}}\Delta\mu_E(q_{\mathrm{P2}}^{\mathrm{E}} q_{\mathrm{S1}}^{\mathrm{E}} - p_E^2) + 2p_E\Delta\mu_E(q_{\mathrm{P2}}^{\mathrm{IH}} q_{\mathrm{S1}}^{\mathrm{E}} + q_{\mathrm{P2}}^{\mathrm{E}} q_{\mathrm{S1}}^{\mathrm{IH}}) + p_{\mathrm{IH}}\Delta\rho
\end{aligned}
$$

Appendix D

Trigonometric functions for small angles

For small angle of incident θ_{P} we can write

$$\frac{1}{\cos^2\theta_{\mathrm{P}}} \approx 1 + \sin^2\theta_{\mathrm{P}} \tag{D.1}$$

$$\cos\theta_{\mathrm{P}} \approx 1 - \frac{1}{2}\sin^2\theta_{\mathrm{P}} \tag{D.2}$$

$$\frac{1}{\cos\theta_{\mathrm{P}}} \approx 1 + \frac{1}{2}\sin^2\theta_{\mathrm{P}} \tag{D.3}$$

$$\tan\theta_{\mathrm{P}} \approx \sin\theta_{\mathrm{P}} + \frac{1}{2}\sin^3\theta_{\mathrm{P}} \tag{D.4}$$

$$\sin 2\theta_{\mathrm{P}} \approx 2\sin\theta_{\mathrm{P}} - \sin^3\theta_{\mathrm{P}} \tag{D.5}$$

$$\frac{\tan\theta_{\mathrm{P}}}{\cos^2\theta_{\mathrm{P}}} \approx \sin\theta_{\mathrm{P}} + \frac{3}{2}\sin^3\theta_{\mathrm{P}} \tag{D.6}$$

$$\sin\theta_{\mathrm{S}} = \frac{V_{\mathrm{S}}}{V_{\mathrm{P}}}\sin\theta_{\mathrm{P}} \tag{D.7}$$

$$\cos\theta_{\mathrm{S}} \approx 1 - \frac{1}{2}\left(\frac{V_{\mathrm{S}}}{V_{\mathrm{P}}}\right)^2\sin^2\theta_{\mathrm{P}} \tag{D.8}$$

$$\frac{1}{\cos\theta_{\mathrm{S}}} \approx 1 + \frac{1}{2}\left(\frac{V_{\mathrm{S}}}{V_{\mathrm{P}}}\right)^2\sin^2\theta_{\mathrm{P}} \tag{D.9}$$

$$\frac{1}{\cos^2\theta_{\mathrm{S}}} \approx 1 + \left(\frac{V_{\mathrm{S}}}{V_{\mathrm{P}}}\right)^2\sin^2\theta_{\mathrm{P}} \tag{D.10}$$

$$\tan\theta_{\mathrm{S}} \approx \frac{V_{\mathrm{S}}}{V_{\mathrm{P}}}\sin\theta_{\mathrm{P}}\left(1 + \frac{1}{2}\left(\frac{V_{\mathrm{S}}}{V_{\mathrm{P}}}\right)^2\sin^2\theta_{\mathrm{P}}\right) \tag{D.11}$$

$$\cos(\theta_{\mathrm{S}} + \theta_{\mathrm{P}}) \approx 1 - \frac{1}{2}\sin^2\theta_{\mathrm{P}}\left[1 + \frac{V_{\mathrm{S}}}{V_{\mathrm{P}}}\right]^2 \tag{D.12}$$

$$\sin(\theta_{\mathrm{S}} + \theta_{\mathrm{P}}) \approx \left[1 + \frac{V_{\mathrm{S}}}{V_{\mathrm{P}}}\right]\sin\theta_{\mathrm{P}}\left(1 + \frac{1}{2}\frac{V_{\mathrm{S}}}{V_{\mathrm{P}}}\sin^2\theta_{\mathrm{P}}\right) \tag{D.13}$$

$$\tan\theta_{\mathrm{S}}\cos(\theta_{\mathrm{S}} + \theta_{\mathrm{P}}) \approx \frac{V_{\mathrm{S}}}{V_{\mathrm{P}}}\sin\theta_{\mathrm{P}}\left(1 - \left[\frac{1}{2} + \frac{V_{\mathrm{S}}}{V_{\mathrm{P}}}\right]\sin^2\theta_{\mathrm{P}}\right) \tag{D.14}$$

$$\frac{\cos(\theta_{\mathrm{S}} + \theta_{\mathrm{P}})}{\cos^2\theta_{\mathrm{S}}} \approx \frac{V_{\mathrm{S}}}{V_{\mathrm{P}}}\left[1 + \frac{V_{\mathrm{S}}}{V_{\mathrm{P}}}\right]\sin^2\theta_{\mathrm{P}} \tag{D.15}$$

Appendix E

Linearization procedure in viscoelastic media

First consider to the perturbations in elastic and anelastic properties. Subscript 1 refers to the upper layer(medium 1) and subscribe 2 refers to the lower layer (medium 2). Δ means difference between the properties in medium 2 and medium 1 and superscript L denotes the linearized form. In the linearization procedure $\Delta^2 = 0$. Properties without index means the average in properties.

Property	Layer 1	Layer2
Density	$\rho - \frac{\Delta\rho}{2}$	$\rho + \frac{\Delta\rho}{2}$
P-wave velocity	$V_{\mathrm{PE}} - \frac{\Delta V_{\mathrm{PE}}}{2}$	$V_{\mathrm{PE}} + \frac{\Delta V_{\mathrm{PE}}}{2}$
S-wave velocity	$V_{\mathrm{SE}} - \frac{\Delta V_{\mathrm{SE}}}{2}$	$V_{\mathrm{SE}} + \frac{\Delta V_{\mathrm{SE}}}{2}$
P-wave quality factor	$Q_{\mathrm{P}} - \frac{\Delta Q_{\mathrm{P}}}{2}$	$Q_{\mathrm{P}} + \frac{\Delta Q_{\mathrm{P}}}{2}$
S-wave quality factor	$Q_{\mathrm{S}} - \frac{\Delta Q_{\mathrm{S}}}{2}$	$Q_{\mathrm{S}} + \frac{\Delta Q_{\mathrm{S}}}{2}$
P-wave phase angle	$\theta_{\mathrm{P}} - \frac{\Delta\theta_{\mathrm{P}}}{2}$	$\theta_{\mathrm{P}} + \frac{\Delta\theta_{\mathrm{P}}}{2}$
S-wave phase angle	$\theta_{\mathrm{S}} - \frac{\Delta\theta_{\mathrm{S}}}{2}$	$\theta_{\mathrm{S}} + \frac{\Delta\theta_{\mathrm{S}}}{2}$
P-wave attenuation angle	$\delta_{\mathrm{P}} - \frac{\Delta\delta_{\mathrm{P}}}{2}$	$\delta_{\mathrm{P}} + \frac{\Delta\delta_{\mathrm{P}}}{2}$
S-wave attenuation angle	$\delta_{\mathrm{S}} - \frac{\Delta\delta_{\mathrm{S}}}{2}$	$\delta_{\mathrm{S}} + \frac{\Delta\delta_{\mathrm{S}}}{2}$

Trigonometric functions in this procedures for attenuation angle are given by

$$\cos\delta_n = \cos\delta_{\mathrm{P}}\left(1 + (-)^{n+1}\tan\delta\frac{\Delta\delta}{2}\right), \tag{E.1}$$

$$\sin\delta_n = \sin\delta_{\mathrm{P}}\left(1 - (-)^{n+1}\frac{1}{\tan\delta}\frac{\Delta\delta}{2}\right), \tag{E.2}$$

$$\tan\delta_n = \tan\delta_{\mathrm{P}}\left(1 - (-)^{n+1}\frac{1}{\tan\delta}\Delta\delta\right), \qquad n = 1, 2 \tag{E.3}$$

$$\tag{E.4}$$

The real part of the Snell's law for P-wave results

$$\frac{\sin\theta_{\mathrm{P1}}}{V_{\mathrm{P1}}} = \frac{\sin\theta_{\mathrm{P2}}}{V_{\mathrm{P2}}}, \tag{E.5}$$

where θ_{P1} is incident angle and θ_{P2} is transmitted phase angle, using the perturbed term, we obtain the change in P-wave phase angle across the boundary in terms of change in the P-wave velocity

$$\Delta\theta_{\mathrm{P}} = \frac{\Delta V_{\mathrm{P}}}{V_{\mathrm{P}}} \tan\theta_{\mathrm{P}}, \tag{E.6}$$

Imaginary part of the Snell's law for P-wave is given by

$$\frac{Q_{\mathrm{P1}}^{-1}}{V_{\mathrm{P1}}} \left(\sin\theta_{\mathrm{P1}} - \cos\theta_{\mathrm{P1}} \tan\delta_{\mathrm{P1}}\right) = \frac{Q_{\mathrm{P2}}^{-1}}{V_{\mathrm{P2}}} \left(\sin\theta_{\mathrm{P2}} - \cos\theta_{\mathrm{P2}} \tan\delta_{\mathrm{P2}}\right) \tag{E.7}$$

Using the perturbation terms in table (E), we obtain the changes in P-wave attenuation angle across the boundary in terms of changes in phase angle, P-wave velocity and P-wave quality factor

$$\Delta\delta_{\mathrm{P}} = \frac{1}{2} \sin 2\delta_{\mathrm{P}} \left\{ \frac{\Delta V_{\mathrm{P}}}{V_{\mathrm{P}}} \frac{1}{\cos^2\theta_{\mathrm{P}}} + \left(1 - \frac{\tan\theta_{\mathrm{P}}}{\tan\delta_{\mathrm{P}}}\right) \frac{\Delta Q_{\mathrm{P}}}{Q_{\mathrm{P}}} \right\}, \tag{E.8}$$

Let us consider to the linearization of the vertical slowness

$$q_{\mathrm{P}} = q_{\mathrm{PE}} + iq_{\mathrm{PAH}} + iq_{\mathrm{PAIH}},$$

where

$$\begin{aligned} q_{\mathrm{PE}} &= \frac{\cos\theta_{\mathrm{P}}}{V_{\mathrm{P}}} \\ q_{\mathrm{PAH}} &= -\frac{Q_{\mathrm{P}}^{-1}}{2} \frac{\cos\theta_{\mathrm{P}}}{V_{\mathrm{P}}} \\ q_{\mathrm{PAIH}} &= -\frac{1}{2} Q_{\mathrm{P}}^{-1} \tan\delta_{\mathrm{P}} \frac{\sin\theta_{\mathrm{P}}}{V_{\mathrm{P}}} \end{aligned}$$

To obtain the linearized form of vertical slownesses we note that we have to linearize the summation of homogeneous and inhomogeneous term

$$q_{\mathrm{PAH1}} + q_{\mathrm{PAIH1}} \longrightarrow q_{\mathrm{PAH1}}^{\mathrm{L}} + q_{\mathrm{PAIH1}}^{\mathrm{L}} \tag{E.9}$$

In other words

$$q_{\mathrm{PAH1}} \neq q_{\mathrm{PAH1}}^{\mathrm{L}}$$

$$q_{\mathrm{PAIH1}} \neq q_{\mathrm{PAIH1}}^{\mathrm{L}}$$

Now the vertical slowness for incident P-wave is given by

$$q_{\mathrm{P1}} = q_{\mathrm{PE1}} + iq_{\mathrm{PAH1}} + iq_{\mathrm{PAIH1}},$$

where

$$\begin{aligned} q_{\mathrm{PE1}} &= \frac{\cos\theta_{\mathrm{P1}}}{V_{\mathrm{P1}}} \\ q_{\mathrm{PAH1}} &= -\frac{Q_{\mathrm{P1}}^{-1}}{2}\frac{\cos\theta_{\mathrm{P1}}}{V_{\mathrm{P1}}} \\ q_{\mathrm{PAIH1}} &= -\frac{1}{2}Q_{\mathrm{P1}}^{-1}\tan\delta_{\mathrm{P1}}\frac{\sin\theta_{\mathrm{P1}}}{V_{\mathrm{P1}}} \end{aligned}$$

Using the linearized form of the angles and P-wave velocity and P-wave quality factor we have

$$\begin{aligned} q_{\mathrm{PE1}}^{\mathrm{L}} &= q_{\mathrm{PE}}\left(1 + \frac{1}{2\cos^2\theta_{\mathrm{P}}}\frac{\Delta V_{\mathrm{P}}}{V_{\mathrm{P}}}\right) \\ q_{\mathrm{PAH1}}^{\mathrm{L}} &= q_{\mathrm{PAH}}\left(1 + \frac{1}{2\cos^2\theta_{\mathrm{P}}}\left[\frac{\Delta V_{\mathrm{P}}}{V_{\mathrm{P}}} + \frac{\Delta Q_{\mathrm{P}}}{Q_{\mathrm{P}}}\right]\right) \\ q_{\mathrm{PAIH1}}^{\mathrm{L}} &= q_{\mathrm{PAIH}}\left(1 - \frac{1}{2\cos^2\theta_{\mathrm{P}}}\frac{\Delta V_{\mathrm{P}}}{V_{\mathrm{P}}}\right) \end{aligned}$$

Transmitted P-wave

$$\begin{aligned} q_{\mathrm{PE2}}^{\mathrm{L}} &= q_{\mathrm{PE}}\left(1 - \frac{1}{2\cos^2\theta_{\mathrm{P}}}\frac{\Delta V_{\mathrm{P}}}{V_{\mathrm{P}}}\right) \\ q_{\mathrm{PAH2}}^{\mathrm{L}} &= q_{\mathrm{PAH}}\left(1 - \frac{1}{2\cos^2\theta_{\mathrm{P}}}\left[\frac{\Delta V_{\mathrm{P}}}{V_{\mathrm{P}}} + \frac{\Delta Q_{\mathrm{P}}}{Q_{\mathrm{P}}}\right]\right) \\ q_{\mathrm{PAIH2}}^{\mathrm{L}} &= q_{\mathrm{PAIH}}\left(1 + \frac{1}{2\cos^2\theta_{\mathrm{P}}}\frac{\Delta V_{\mathrm{P}}}{V_{\mathrm{P}}}\right) \end{aligned}$$

Incident S-wave

$$
\begin{aligned}
q^{\mathrm{L}}_{\mathrm{SE1}} &= q_{\mathrm{SE}}\left(1+\frac{1}{2\cos^2\theta_{\mathrm{S}}}\frac{\Delta V_{\mathrm{S}}}{V_{\mathrm{S}}}\right)\\
q^{\mathrm{L}}_{\mathrm{SAH1}} &= q_{\mathrm{SAH}}\left(1+\frac{1}{2\cos^2\theta_{\mathrm{S}}}\left[\frac{\Delta V_{\mathrm{S}}}{V_{\mathrm{S}}}+\frac{\Delta Q_{\mathrm{S}}}{Q_{\mathrm{S}}}\right]\right)\\
q^{\mathrm{L}}_{\mathrm{SAIH1}} &= q_{\mathrm{SAIH}}\left(1-\frac{1}{2\cos^2\theta_{\mathrm{S}}}\frac{\Delta V_{\mathrm{S}}}{V_{\mathrm{S}}}\right)
\end{aligned}
$$

Transmitted S-wave

$$
\begin{aligned}
q^{\mathrm{L}}_{\mathrm{SE2}} &= q_{\mathrm{SE}}\left(1-\frac{1}{2\cos^2\theta_{\mathrm{S}}}\frac{\Delta V_{\mathrm{S}}}{V_{\mathrm{S}}}\right)\\
q^{\mathrm{L}}_{\mathrm{SAH2}} &= q_{\mathrm{SAH}}\left(1-\frac{1}{2\cos^2\theta_{\mathrm{S}}}\left[\frac{\Delta V_{\mathrm{S}}}{V_{\mathrm{S}}}+\frac{\Delta Q_{\mathrm{S}}}{Q_{\mathrm{S}}}\right]\right)\\
q^{\mathrm{L}}_{\mathrm{SAIH2}} &= q_{\mathrm{SAIH}}\left(1+\frac{1}{2\cos^2\theta_{\mathrm{S}}}\frac{\Delta V_{\mathrm{S}}}{V_{\mathrm{S}}}\right)
\end{aligned}
$$

The complex shear modulus can be written as a real and imaginary part

$$\mu = \mu_{\mathrm{E}} + i\mu_{\mathrm{A}}, \tag{E.10}$$

where $\mu_{\mathrm{E}} = \rho V_{\mathrm{S}}^2$ and $\mu_{\mathrm{A}} = \rho\, Q_{\mathrm{S}} V_{\mathrm{S}}^2$. Now we linearized the shear modulus

$$
\begin{aligned}
\mu_1 =& \mu_{\mathrm{E1}} + i\mu_{\mathrm{A1}}\\
\mu_2 =& \mu_{\mathrm{E2}} + i\mu_{\mathrm{A2}}
\end{aligned}
$$

where

$$
\begin{aligned}
\mu_{\mathrm{E1}} =& \mu_{\mathrm{E}}\left(1-\frac{1}{2}\left[\frac{\Delta\rho}{\rho}+2\frac{\Delta V_{\mathrm{S}}}{V_{\mathrm{S}}}\right]\right)\\
\mu_{\mathrm{E2}} =& \mu_{\mathrm{E}}\left(1+\frac{1}{2}\left[\frac{\Delta\rho}{\rho}+2\frac{\Delta V_{\mathrm{S}}}{V_{\mathrm{S}}}\right]\right)\\
\mu_{\mathrm{A1}} =& \mu_{\mathrm{A}}\left(1-\frac{1}{2}\left[\frac{\Delta\rho}{\rho}+2\frac{\Delta V_{\mathrm{S}}}{V_{\mathrm{S}}}-\frac{\Delta Q_{\mathrm{S}}}{Q_{\mathrm{S}}}\right]\right)\\
\mu_{\mathrm{A2}} =& \mu_{\mathrm{A}}\left(1+\frac{1}{2}\left[\frac{\Delta\rho}{\rho}+2\frac{\Delta V_{\mathrm{S}}}{V_{\mathrm{S}}}-\frac{\Delta Q_{\mathrm{S}}}{Q_{\mathrm{S}}}\right]\right)
\end{aligned}
$$

Now we have

$$\begin{aligned}\Delta\mu_{\mathrm{E}} =& \mu_{\mathrm{E}}\left[\frac{\Delta\rho}{\rho} + 2\frac{\Delta V_{\mathrm{S}}}{V_{\mathrm{S}}}\right] \\ \Delta\mu_{\mathrm{A}} =& \mu_{\mathrm{A}}\left[\frac{\Delta\rho}{\rho} + 2\frac{\Delta V_{\mathrm{S}}}{V_{\mathrm{S}}} - \frac{\Delta Q_{\mathrm{S}}}{Q_{\mathrm{S}}}\right]\end{aligned}$$

Chapter 6

Born scattering and inversion sensitivities in viscoelastic transversely isotropic media

6.1 Abstract

We analyze the volume scattering of seismic waves from anisotropic-viscoelastic inclusions using the Born approximation. We consider the specific case of Vertical Transverse Isotropic (VTI) media with low-loss attenuation and weak anisotropy such that second- and higher-order contributions from quality factors and Thomsen parameters are negligible. To accommodate the volume scattering approach, the viscoelastic VTI media is broken into a homogeneous viscoelastic reference medium with distributed inclusions in both viscoelastic and anisotropic properties. In viscoelastic reference media in which all propagations take place, wave modes are of P-wave type, SI-wave type and SII-wave type, all with complex slowness and polarization vectors. We generate expressions for P-to-P, P-to-SI, SI-to-SI and SII-to-SII scattering potentials, and demonstrate that they reduce to previously-derived isotropic results. These scattering potential expressions are, we end by pointing out, sensitivity kernels related to the Fréchet derivatives which provide the weights for multi-parameter full waveform inversion updates.

6.2 Introduction

Anisotropic and viscoelastic models of seismic wave propagation provide a link between measured amplitude/phase information and certain subsurface geological properties which are unaccounted for with isotropic-elastic models. These include viscosity and viscosity changes, stresses, fluid presence and type, and fracture density, weakness, and orientation. Such links are particularly important for evaluating production in unconventional hydrocarbon reservoirs (Fatti et al., 1994; Beretta et al., 2002; Tsvankin et al., 2010), and for environmental applications such as detection of CO_2 and monitoring of its storage (Bickle, 2009;

Lumley, 2010), and monitoring of migration of shallow gas (Grasso and Wittlinger, 1990), etc. Simultaneous determination of these properties (if and when it is practical to do so) requires analysis of very subtle variations in seismic data. All current methods for such determination, including amplitude-variation-with-offset, or AVO (Castagna and Backus, 1993), multi-parameter full waveform inversion, or FWI (Virieux and Operto, 2009), and inverse scattering (Weglein et al., 2003; Stolt and Weglein, 2012), are founded on mathematical expressions of the process of scattering, wherein an incoming wave is transformed into an outgoing wave of altered character after interaction with a point- or plane-perturbation. Parameterization of scattering from simultaneous variations in both viscoelastic and anisotropic properties, which has several somewhat complex features, is an important, and theoretically incomplete, step in formulating seismic inverse problems applicable in the above settings.

In the AVO problem (and related problems such as amplitude-variation-with-azimuth, or AVAz), scattering is expressed via linearized expressions for reflection coefficients. Weak contrast linearized reflection coefficient expressions, once derived, play a major role in inversion of seismic data as they contain unique information on sensitivity of the seismic data to the changes in earth properties (Beylkin and Burridge, 1990; Burridge et al., 1998; Tarantola, 1986). The traditional way to compute these linearized reflection coefficients is via approximate solution of the Zoeppritz equation in which it is assumed that properties across the boundary vary only slightly and that illumination occurs only at small incidence angles (Aki and Richards, 2002). Exact and approximate reflection and transmission coefficients have been derived for layered isotropic-viscoelastic media, taking into account the changes in the viscoelastic parameters but assuming that the incident plane wave is homogeneous (Ursin and Stovas, 2002). The same problem but with allowance made for an inhomogeneous viscoelastic plane wave interacting with a low-contrast variation in isotropic viscoelastic parameters, wherein jumps in the inhomogeneity angle are included, have recently been derived (Moradi and Innanen, 2016). A mapping between these linearized reflection coefficient expressions and viscoelastic volume scattering potentials was also provided in that work (Moradi and Innanen, 2015b). Earlier Cervený & Psencík have studied homogeneous and inhomogeneous plane waves propagating in an anisotropic-viscoelastic medium (Cervený and Psencík, 2005a,b, 2008). Linearized reflection coefficients for weak-contrast anisotropic-viscoelastic

media, including the inhomogeneity angle of the incident wave, have been derived based on the exact solutions of the Zoeppritz equations by Behura and Tsvankin (2009b,a). The main result of the current paper concerns the mathematical details of volume scattering from anisotropic-viscoelastic inclusions.

Understanding the scattering patterns induced by perturbations in medium properties is prerequisite for AVO inversion (Castagna and Backus, 1993) and full waveform inversion (FWI) (Virieux and Operto, 2009; Fichtner, 2010). This is particularly true for multiparameter FWI, in which cross-talk between simultaneous variations in several elastic properties produces issues comparable to those grappled with in AVO inversion (Innanen, 2014). Current and future practical FWI will likely require multiple parameters to be robustly accounted for, in spite of these issues. Specifically, multiple isotropic-elastic properties, P- and S-wave impedances and density are known from the history of AVO (Castagna and Backus, 1993; Foster et al., 2010) to be required to adequately describe precritical reflection amplitudes. Also, anisotropic parameters have been demonstrated to be critical for FWI in velocity model building (Warner et al., 2013), and also must play very important roles in FWI for characterization of fracturing and stress in reservoirs. Finally, strong anelastic attenuation in near surface environments, gas cloud environments, and many unconventional reservoir environments make simultaneous incorporation of attenuation parameters in FWI a major current subject of research (Métivier et al., 2015; Operto et al., 2013; Prieux et al., 2013). From a mathematical-geophysics point of view, quantitatively- and qualitatively-interpretable expressions of the quantities which relate weighting factors in seismic inversion with processes of scattering of seismic waves from changes in such parameters is a critical step. The purpose of this paper is to frame such expressions for quite general types of attenuating and anisotropic elastic problems.

The Born approximation method, based on perturbation theory, is an efficient approach to evaluate sensitivity kernels for many types of multi-parameter FWI (da Silva et al., 2016; Plessix and Cao, 2011). In this approach, the actual medium is considered as a reference medium (with slightly different properties from those of the actual medium) and randomly distributed perturbations. In the cases described in this paper, the vertically-attenuative isotropic medium perturbations are in: density, vertical P- and S-wave velocities, vertical P-

and S-wave quality factors, three anisotropic Thomsen parameters and three Q-dependent Thomsen parameters. Compared to elastic-isotropic versions of such approximations the mathematical expressions generated are complicated, so to make the results more easily interpretable we assume both weak anisotropy and low attenuation in the lower and upper media.

The rest of the paper is organized as follow. In section 6.3 we discuss the complex stiffness tensor for viscoelastic VTI media, then proceed assuming (a) the anisotropy is weak, and (b) the media is low-loss attenuative. In view of (a) and (b) we introduce the Q-dependent Thomsen parameters in terms of real stiffness tensor components and quality factor matrix components. In section 6.4 we describe the perturbations in the stiffness tensor from which we derive the approximate forms of the scattering potentials. In particular we will show how the perturbed VTI stiffness tensor is decomposed into contributions from the isotropic and anisotropic parameters. In section 6.5 we present the general form of scattering potential for scattering of P-wave to P wave, P-wave to SI-wave, SI-wave to SI-wave and SII-wave to SII-wave. We also describe the polarization and slowness vectors of the incident and scattered P- and SI-waves, which are essential to the evaluation of the scattering potentials. The results obtained for scattering potentials are discussed in more detail in section 6.6. There we show in particular that scattering potentials can be decomposed into terms interpretable as being contributions from isotropic-elastic, anisotropic-elastic, isotropic-viscoelastic and anisotropic-viscoelastic components of the medium.

6.3 The stiffness tensor for VTI-viscoelastic media and complex Thomsen parameters

A common and powerful anisotropic model often used in exploration seismology is that of transversely isotropic media with horizontal (HTI) or vertical (VTI) symmetry axes (Rüger, 2002). A VTI medium with its axis of symmetry along the vertical or depth (z) direction is for instance appropriate in geological media with thin, parallel bedding planes perpendicular

to z. The stiffness tensor in the form of a symmetric 6×6 matrix is given by

$$\mathrm{C}^{\mathrm{VTI}} = \begin{pmatrix} C_{11} & C_{11}-2C_{66} & C_{13} & 0 & 0 & 0 \\ C_{11}-2C_{66} & C_{11} & C_{13} & 0 & 0 & 0 \\ C_{13} & C_{13} & C_{33} & 0 & 0 & 0 \\ 0 & 0 & 0 & C_{55} & 0 & 0 \\ 0 & 0 & 0 & 0 & C_{55} & 0 \\ 0 & 0 & 0 & 0 & 0 & C_{66} \end{pmatrix}. \tag{6.1}$$

The P-wave phase velocity along the z axis is given by $V_{\mathrm{P}} = \sqrt{C_{33}/\rho}$, the S-wave velocity for shear wave polarized the z-direction along the vertical axis is given by $V_{\mathrm{S}} = \sqrt{C_{55}/\rho}$. The stiffness tensor in subscript notation can be written as (Ikelle and Amundsen, 2005):

$$\begin{aligned} \hat{C}^{\mathrm{VTI}}_{ijkl} &= (\hat{C}_{11}-2\hat{C}_{66})\delta_{ij}\delta_{kl} + \hat{C}_{66}(\delta_{ik}\delta_{jl}+\delta_{il}\delta_{jk}) \\ &+ (2\hat{C}_{66}-\hat{C}_{11}+\hat{C}_{13})(\delta_{ij}\delta_{k3}\delta_{l3}+\delta_{kl}\delta_{i3}\delta_{j3}) \\ &+ (\hat{C}_{55}-\hat{C}_{66})(\delta_{ik}\delta_{j3}\delta_{l3}+\delta_{jk}\delta_{i3}\delta_{l3}+\delta_{il}\delta_{j3}\delta_{k3}+\delta_{jl}\delta_{i3}\delta_{k3}) \\ &+ (\hat{C}_{11}-2\hat{C}_{13}+\hat{C}_{33}-4\hat{C}_{55})\delta_{i3}\delta_{j3}\delta_{k3}\delta_{l3}. \end{aligned} \tag{6.2}$$

The mark '^' distinguishes the complex stiffness tensor $\hat{C}_{ijkl}$ from the real elastic C_{ijkl}. This form of $\hat{C}_{ijkl}$ in eq.(6.2) helps express the scattering potential in terms of inner products of polarization and slowness vectors. It will also soon prove useful in the decomposition of the scattering potential into contributions from isotropic and anisotropic terms. In a viscoelastic medium, attenuation is often characterized by quality factors Q. The complex stiffness tensor is such that the real part is related to the elastic and anisotropic properties of the medium, and the imaginary part is related to the quality factors. Corresponding to each independent component of the stiffness tensor there is a quality factor defined by $Q_{mn} = C_{mn}/C^{\mathrm{I}}_{mn}$, where C_{mn} and C^{I}_{mn} are real and imaginary parts of the complex stiffness tensor $\hat{C}_{mn}$, using the Voigt notation in which $m = ij$ and $n = kl$. As a result $\hat{C}_{mn}$ can be written as a function of the quality factor tensor

$$\hat{C}_{mn} = C_{mn}\left(1 + iQ^{-1}_{mn}\right). \tag{6.3}$$

Thomsen's notation then enables us to separate the influence of anisotropy from the other properties (Thomsen, 1986). Complex Thomsen parameters are defined as

$$\hat{\varepsilon} = \frac{\hat{C}_{11} - \hat{C}_{33}}{2\hat{C}_{33}}, \tag{6.4}$$

$$\hat{\gamma} = \frac{\hat{C}_{66} - \hat{C}_{55}}{2\hat{C}_{55}}, \tag{6.5}$$

$$\hat{\delta} = \frac{(\hat{C}_{13} + \hat{C}_{55})^2 - (\hat{C}_{33} - \hat{C}_{55})^2}{2\hat{C}_{33}(\hat{C}_{33} - \hat{C}_{55})}. \tag{6.6}$$

Incorporating equation (6.3) into equations (6.4)-(6.6) and assuming the low-attenuation condition $Q_{ij}^{-1} \ll 1$, we obtain

$$\hat{\varepsilon} = \varepsilon + \frac{i}{2} Q_{33}^{-1} \varepsilon_Q, \tag{6.7}$$

$$\hat{\delta} = \delta + \frac{i}{2} Q_{33}^{-1} \delta_Q, \tag{6.8}$$

$$\hat{\gamma} = \gamma + \frac{i}{2} Q_{55}^{-1} \gamma_Q, \tag{6.9}$$

where $\varepsilon,\ \delta$ and γ are the standard elastic Thomsen parameters related to the phase velocities in VTI media. The quantity ε, which is the P-wave anisotropy parameter measuring the difference between the vertical and horizontal P-wave velocities, now refers to the *elastic* aspects of anisotropy of rock, i.e., in the attenuation-free limit. Meanwhile the parameter δ, the small-offset normal move-out (NMO) factor, controls the near-vertical anisotropy, and γ, which is the difference between the vertical and horizontal SH-wave velocities, is related to the SH-wave anisotropy (Thomsen, 1986). To these is added the Q-dependent Thomsen parameters, as defined by (Zhu and Tsvankin, 2006b)

$$\begin{aligned} \varepsilon_Q &= \frac{Q_{33} - Q_{11}}{Q_{11}} \\ \delta_Q &= 2\frac{C_{13}(C_{13} + C_{55})}{C_{33}(C_{33} - C_{55})} \frac{Q_{33} - Q_{13}}{Q_{13}} + \frac{C_{55}(C_{13} + C_{33})^2}{C_{33}(C_{33} - C_{55})^2} \frac{Q_{33} - Q_{55}}{Q_{55}}, \\ \gamma_Q &= \frac{Q_{55} - Q_{66}}{Q_{66}}. \end{aligned} \tag{6.10}$$

Now we write the components of $\hat{C}_{ij}$ in terms of Thomsen parameters and quality factors. Incorporating equations (6.7)-(6.9) we obtain

$$\begin{aligned}
\hat{C}_{33} =& C_{33}(1 + iQ_{33}^{-1}),\\
\hat{C}_{55} =& C_{55}(1 + iQ_{55}^{-1}),\\
\hat{C}_{11} =& C_{33}(1 + 2\varepsilon) + iQ_{33}^{-1}C_{33}(1 + 2\varepsilon + \varepsilon_Q),\\
\hat{C}_{66} =& C_{55}(1 + 2\gamma) + iQ_{55}^{-1}C_{55}(1 + 2\gamma + \gamma_Q),\\
\hat{C}_{13} =& C_{33}(1 + \delta) - 2C_{55} + iQ_{33}^{-1}C_{33}(1 + \delta + \delta_Q) - 2iQ_{55}^{-1}C_{55}.
\end{aligned} \tag{6.11}$$

Throughout the present work we will assume weak anisotropy $|\gamma|, |\delta|, |\varepsilon| \ll 1$ and weak attenuation $Q_{33}^{-1}, Q_{55}^{-1} \ll 1$. In what follows for notational simplicity we will use Q_{P} for the P-wave quality factor instead of Q_{33}, and Q_{S} for the S-wave quality factor instead of Q_{55}.

6.4 Perturbations in the stiffness tensor and the Born approximation

In this section we derive the main result of the paper, which is a form for the potential for scattering of P-, SI and SII waves. In figure 6.1, a volume-scattering model of wave interaction in anisotropic viscoelastic media is illustrated. The "actual" medium is divided into a homogeneous reference medium and perturbations in eleven medium properties. Here, the reference medium is an additional component of the model specially required by the anisotropic aspects of the wave propagation is the definition of a preferential direction z, which we will set as the vertical or depth axis, and the assumption that the incident wave approaches the scatter points in the positive z-direction. In this way we may further define θ_{In} as the angle between the direction of incident wave and the z-direction, and set the coordinate system in such a way that for non-converted waves $\theta_{\mathrm{In}} = \theta_{\mathrm{Sc}}$. In this coordinate system it will be true that for converted wave $\theta_{\mathrm{In}} \neq \theta_{\mathrm{Sc}}$. In this way the opening angle between incoming and outgoing wave vectors can be associated straightforwardly with both anisotropic medium characteristics and sums and differences of incidence/reflection/conversion angles. For example, for a P-to-P-scattered wave the opening angle can be expressed as $\theta_{\mathrm{In}} + \theta_{\mathrm{Sc}} = 2\theta_P$, and for converted PS-wave as $\theta_{\mathrm{In}} + \theta_{\mathrm{Sc}} = \theta_{\mathrm{P}} + \theta_{\mathrm{S}}$.

Within the Born approximation, the term $\Delta\rho = \rho - \rho_0$ represents the difference between the actual, or perturbed density ρ and the density of the reference medium ρ_0. In this case,

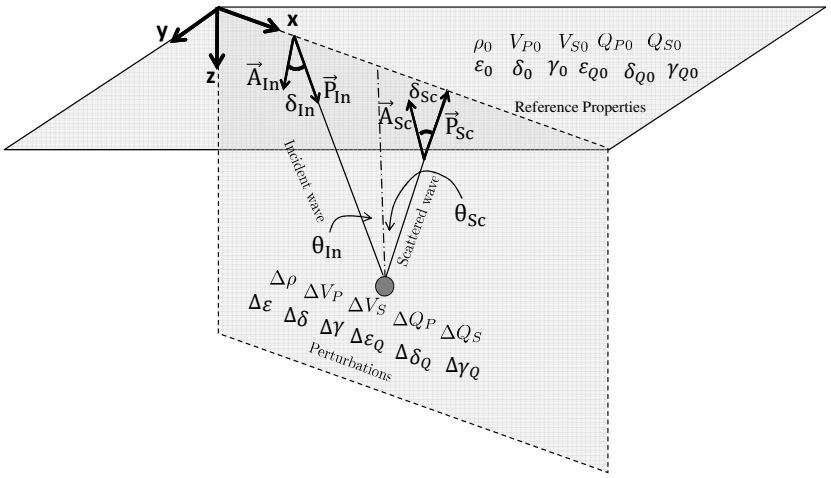

Figure 6.1: Schematic description of Born approximation based on the perturbation theory. The reference medium is characterized by its three elastic parameters P-wave velocity V_{P0}, S-wave velocity V_{S0} and density ρ_0; two viscoelastic parameters P-wave quality factor Q_{P0} and S-wave quality factor Q_{S0}; three anisotropic Thomsen parameters $(\varepsilon_0, \delta_0, \gamma_0)$ and corresponding Q-dependent Thomsen parameters $(\varepsilon_{Q0}, \delta_{Q0}, \gamma_{Q0})$. Perturbations are characterized by 11 components represented by $(\Delta\rho, \Delta V_{\mathrm{P}}, \Delta V_{\mathrm{S}}, \Delta\varepsilon, \Delta\delta, \Delta\gamma, \Delta Q_{\mathrm{P}}, \Delta Q_{\mathrm{S}}, \Delta\varepsilon_Q, \Delta\delta_Q, \Delta\gamma_Q)$. Other quantities are defined in table F.1.

fractional changes in properties can be represented by either $\Delta\rho/\rho_0$ or $\Delta\rho/\rho$, as under the single-scattering assumption both are much smaller than unity. In contrast, because in the case of weak anisotropy the Thomsen parameters are much smaller than unity, we can use the bare differences between the properties instead of the fractional changes. Consider first the perturbations in anisotropic parameters. Changes in the complex Thomsen parameters can be expressed in terms of changes in real and Q-dependent Thomsen parameters via

$$\Delta\hat{\varepsilon} = \left(\varepsilon + \frac{i}{2}Q_{\mathrm{P}}^{-1}\varepsilon_Q\right) - \left(\varepsilon_0 + \frac{i}{2}Q_{\mathrm{P}0}^{-1}\varepsilon_{Q0}\right), \tag{6.12}$$

$$\Delta\hat{\delta} = \left(\delta + \frac{i}{2}Q_{\mathrm{P}}^{-1}\delta_Q\right) - \left(\delta_0 + \frac{i}{2}Q_{\mathrm{P}0}^{-1}\delta_{Q0}\right), \tag{6.13}$$

$$\Delta\hat{\gamma} = \left(\gamma + \frac{i}{2}Q_{\mathrm{S}}^{-1}\gamma_Q\right) - \left(\gamma_0 + \frac{i}{2}Q_{\mathrm{S}0}^{-1}\gamma_{Q0}\right). \tag{6.14}$$

Quantities without the subscript '0' refer to the actual/perturbed medium. All quantities in the actual medium are next expressed in terms of their values in the reference medium and the perturbations. First, for the Thomsen parameters we have

$$\begin{aligned} \varepsilon &= \varepsilon_0 + \Delta\varepsilon, \qquad \varepsilon_Q = \varepsilon_{Q0} + \Delta\varepsilon_Q, \\ \delta &= \delta_0 + \Delta\delta, \qquad \delta_Q = \delta_{Q0} + \Delta\delta_Q, \\ \gamma &= \gamma_0 + \Delta\gamma, \qquad \gamma_Q = \gamma_{Q0} + \Delta\gamma_Q. \end{aligned} \tag{6.15}$$

For inverse P- and S-wave quality factors Q_{P}^{-1} and Q_{S}^{-1} we furthermore have

$$\begin{aligned} Q_{\mathrm{P}}^{-1} &= (Q_{\mathrm{P}0} + \Delta Q_{\mathrm{P}})^{-1} \approx Q_{\mathrm{P}0}^{-1}\left(1 - \frac{\Delta Q_{\mathrm{P}}}{Q_{\mathrm{P}}}\right), \\ Q_{\mathrm{S}}^{-1} &= (Q_{\mathrm{S}0} + \Delta Q_{\mathrm{S}})^{-1} \approx Q_{\mathrm{S}0}^{-1}\left(1 - \frac{\Delta Q_{\mathrm{S}}}{Q_{\mathrm{S}}}\right), \end{aligned} \tag{6.16}$$

where we taken advantage of both the low-loss attenuation and weak contrast assumptions, which are respectively given by $\left(Q_{\mathrm{P}0}^{-1}, Q_{\mathrm{P}0}^{-1}\right) \ll 1$ and $(\Delta Q_{\mathrm{P}}/Q_{\mathrm{P}}, \Delta Q_{\mathrm{S}}/Q_{\mathrm{S}}) \ll 1$. Incorporating equations (6.15) and (6.16) into equations (6.12)-(6.14) and considering terms up to first order in the perturbations, we arrive at

$$\Delta\hat{\varepsilon} = \Delta\varepsilon + \frac{i}{2}Q_{\mathrm{P}0}^{-1}\Delta\varepsilon_Q, \tag{6.17}$$

$$\Delta\hat{\delta} = \Delta\delta + \frac{i}{2}Q_{\mathrm{P}0}^{-1}\Delta\delta_Q, \tag{6.18}$$

$$\Delta\hat{\gamma} = \Delta\gamma + \frac{i}{2}Q_{\mathrm{S}0}^{-1}\Delta\gamma_Q. \tag{6.19}$$

For an elastic background, in which $Q_{\mathrm{P0}}^{-1} = Q_{\mathrm{S0}}^{-1} = 0$, the Q-dependent parameter vanishes as expected. We next expand the changes in $\hat{C}_{33}$ and $\hat{C}_{55}$ (isotropic part of changes in other components of the stiffness tensor can be expressed in terms of changes in these two components). The change in the $\hat{C}_{33}$ component is

$$\Delta\hat{C}_{33} = \hat{C}_{33} - \hat{C}_{33}^{(0)} = \rho\hat{V}_P^2 - \rho_0\hat{V}_{P0}^2, \tag{6.20}$$

where the complex $\hat{V}_P$ and $\hat{V}_{P0}$ are the P-wave velocities in the actual and reference media respectively. These in turn can be written in terms of elastic P-wave velocity and P-wave quality factors as

$$\begin{aligned} \hat{V}_{\mathrm{P}}^2 &= V_{\mathrm{P}}^2\left(1 + iQ_{\mathrm{P}}^{-1}/2\right)^2 \approx V_{\mathrm{P}}^2\left(1 + iQ_{\mathrm{P}}^{-1}\right), \\ \hat{V}_{\mathrm{P0}}^2 &= V_{\mathrm{P0}}^2\left(1 + iQ_{\mathrm{P0}}^{-1}/2\right)^2 \approx V_{\mathrm{P0}}^2\left(1 + iQ_{\mathrm{P0}}^{-1}\right). \end{aligned} \tag{6.21}$$

Inserting the expressions in (6.21) into equation (6.20) and using $\rho = \rho_0 + \Delta\rho$ and $V_{\mathrm{P}}^2 = V_{\mathrm{P0}}^2 + 2V_{\mathrm{P0}}\Delta V_{\mathrm{P}}$ we finally arrive at

$$\frac{\Delta\hat{C}_{33}}{\hat{C}_{33}^{(0)}} = \left(\frac{\Delta\rho}{\rho} + 2\frac{\Delta V_P}{V_P}\right) - iQ_{\mathrm{P0}}^{-1}\frac{\Delta Q_{\mathrm{P}}}{Q_{\mathrm{P}}}, \tag{6.22}$$

where $\hat{C}_{33}^{(0)} = \rho_0\hat{V}_{\mathrm{P0}}^2$. The fractional perturbation in $\hat{C}_{33}$ is thus decomposed into two components. The real part is influenced by perturbations in density and P-wave velocity, and the imaginary part by changes in P-wave quality factor. In a similar manner we calculate the fractional perturbation in C_{55} to be:

$$\frac{\Delta\hat{C}_{55}}{\hat{C}_{55}^{(0)}} = \left(\frac{\Delta\rho}{\rho} + 2\frac{\Delta V_S}{V_S}\right) - iQ_{\mathrm{S0}}^{-1}\frac{\Delta Q_{\mathrm{S}}}{Q_{\mathrm{S}}}, \tag{6.23}$$

where $\hat{C}_{55}^{(0)} = \rho_0\hat{V}_{\mathrm{S0}}^2$. Subsequently changes in other components of the stiffness tensor are

$$\begin{aligned} \Delta\hat{C}_{11} &= \hat{C}_{11} - \hat{C}_{11}^{(0)} = \Delta\hat{C}_{33} + 2\hat{C}_{33}^{(0)}\Delta\hat{\varepsilon}, \\ \Delta\hat{C}_{13} &= \hat{C}_{13} - \hat{C}_{13}^{(0)} = \Delta\hat{C}_{33} - 2\Delta\hat{C}_{55} + \hat{C}_{33}^{(0)}\Delta\hat{\delta}, \\ \Delta\hat{C}_{66} &= \hat{C}_{66} - \hat{C}_{66}^{(0)} = \Delta\hat{C}_{55} + 2\hat{C}_{55}^{(0)}\Delta\hat{\gamma}. \end{aligned} \tag{6.24}$$

Perturbations in the above components of the stiffness tensor are functions of changes in elastic and anelastic parameters, Thomsen parameters and Q-dependent Thomsen parameters. These are the basic elements from which scattering potentials will now be constructed in terms of variations in medium properties. Finally, we observe that changes in $\hat{C}_{ijkl}^{\mathrm{VTI}}$ can be

decomposed into isotropic and anisotropic terms. Such expressions will turn out to enable comparisons between our results and previously-derived scattering potentials for elastic and viscoelastic media (Stolt and Weglein, 2012; Moradi and Innanen, 2015b). Using equations (6.2) and (6.24), it follows now that the changes in the complex stiffness tensor can be written as

$$\Delta\hat{C}^{\mathrm{VTI}}_{ijkl} = \Delta\hat{C}^{\mathrm{Iso}}_{ijkl} + \Delta\hat{C}^{\varepsilon}_{ijkl} + \Delta\hat{C}^{\delta}_{ijkl} + \Delta\hat{C}^{\gamma}_{ijkl}, \tag{6.25}$$

where the isotropic part of the perturbation is given by

$$\Delta\hat{C}^{\mathrm{Iso}}_{ijkl} = \Delta\hat{C}_{33}\delta_{ij}\delta_{kl} + \Delta\hat{C}_{55}(\delta_{ik}\delta_{jk} - 2\delta_{ij}\delta_{kl} + \delta_{il}\delta_{jk}), \tag{6.26}$$

and the perturbations related to the Thomsen parameters are

$$\begin{aligned}
\Delta\hat{C}^{\varepsilon}_{ijkl} &= 2\hat{C}^{(0)}_{33}\Delta\hat{\varepsilon}\,(\delta_{ij}\delta_{kl})_{[1,2]}\,, \\
\Delta\hat{C}^{\delta}_{ijkl} &= \hat{C}^{(0)}_{33}\Delta\hat{\delta}(\delta_{ij}\delta_{k3}\delta_{l3} + \delta_{kl}\delta_{i3}\delta_{j3} - 2\delta_{i3}\delta_{j3}\delta_{k3}\delta_{l3}), \\
\Delta\hat{C}^{\gamma}_{ijkl} &= 2\hat{C}^{(0)}_{55}\Delta\hat{\gamma}(\delta_{ik}\delta_{jl} + \delta_{il}\delta_{jk} - 2\delta_{ij}\delta_{kl})_{[1,2]} \\
&\quad - 2\hat{C}^{(0)}_{55}\Delta\hat{\gamma}(\delta_{jk}\delta_{i3}\delta_{l3} + \delta_{jl}\delta_{i3}\delta_{k3} - 2\delta_{kl}\delta_{i3}\delta_{j3}).
\end{aligned} \tag{6.27}$$

By $[1,2]$ we mean that the subscripts only take on the values 1 and 2. This form will in the next section be combined with definitions of the polarization and slowness vectors to formulate the scattering potentials.

6.5 Scattering potentials

The Born approximation yields an expression for the scattered wave which is linear in fractional changes in medium properties. In the previous section, perturbations in the complex anisotropic-viscoelastic stiffness tensor were set out: in the isotropic-elastic limit we have perturbations in density, P- and S-wave velocity, and to add in effects of attenuation and anisotropy, perturbations in P- and S-wave quality factors, three elastic Thomsen parameters and three Q-related Thomsen parameters are included. Within any realization of the Born approximation appear forms for the scattering potential. The scattering potential is a central concept both in FWI, being closely related to the sensitivity kernels which weight data residuals in creating Gauss-Newton and Newton updates (Virieux and Operto, 2009),

and in wave modelling in general, as all of the information of scattering radiation pattern are contained therein.

Let us first consider the case that the reference medium and the perturbations are both anisotropic-viscoelastic, with weak anisotropy and weak attenuation. All parameters related to the reference medium are labelled with a subscript 0; unlabelled parameters are related to the actual medium. The general expression for the scattering potential is given by (Beylkin and Burridge, 1990)

$$\mathrm{S} = (\boldsymbol{\mathcal{S}} \cdot \boldsymbol{\mathcal{I}})\Delta\rho - \eta_{mn}\Delta\hat{C}_{mn} = (\boldsymbol{\mathcal{S}} \cdot \boldsymbol{\mathcal{I}})\Delta\rho - (\mathcal{S}_i \mathrm{k}_j^{\mathrm{Sc}} \mathcal{I}_k \mathrm{k}_l^{\mathrm{In}})\Delta\hat{C}_{ijkl}, \tag{6.28}$$

where the Voigt notation $m = ij$ and $n = kl$ has been invoked and $\Delta C_{ijkl} = C_{ijkl} - C^{(0)}_{ijkl}$ is the difference between the non-zero components of the stiffness tensor in the actual and the reference media. Additionally, $\boldsymbol{\mathcal{S}}$ and $\boldsymbol{\mathcal{I}}$ respectively are the polarization vectors of the scattered and incident waves; $\mathbf{k}^{\mathrm{Sc}}$ is the scattered slowness vector and $\mathbf{k}^{\mathrm{In}}$ is the incident slowness vector.

By incorporating equations (6.26) and (6.27) into (6.28) and rearranging the scattering potential in terms involving isotropic versus anisotropic parameters, we obtain

$$\mathrm{S} = \mathrm{S}^{\mathrm{Iso}} + \mathrm{S}^{\mathrm{Ani}}, \tag{6.29}$$

with isotropic and anisotropic parts respectively given by

$$\begin{aligned}
\mathrm{S}^{\mathrm{Iso}} =& (\boldsymbol{\mathcal{S}} \cdot \boldsymbol{\mathcal{I}})\Delta\rho \\
&- (\boldsymbol{\mathcal{S}} \cdot \mathbf{k}^{\mathrm{Sc}})(\boldsymbol{\mathcal{I}} \cdot \mathbf{k}^{\mathrm{In}})\Delta\hat{C}_{33} \\
&- \left\{(\boldsymbol{\mathcal{S}} \cdot \boldsymbol{\mathcal{I}})(\mathbf{k}^{\mathrm{Sc}} \cdot \mathbf{k}^{\mathrm{In}}) + (\boldsymbol{\mathcal{S}} \cdot \mathbf{k}^{\mathrm{In}})(\boldsymbol{\mathcal{I}} \cdot \mathbf{k}^{\mathrm{Sc}}) - 2(\boldsymbol{\mathcal{S}} \cdot \mathbf{k}^{\mathrm{Sc}})(\boldsymbol{\mathcal{I}} \cdot \mathbf{k}^{\mathrm{In}})\right\}\Delta\hat{C}_{55}, \\
\mathrm{S}^{\mathrm{Ani}} =& -2\hat{C}^{(0)}_{33}\left\{(\boldsymbol{\mathcal{S}} \cdot \mathbf{k}^{\mathrm{Sc}})(\boldsymbol{\mathcal{I}} \cdot \mathbf{k}^{\mathrm{In}})\right\}_{[1,2]}\Delta\hat{\varepsilon} \\
&- \hat{C}^{(0)}_{33}\left\{(\boldsymbol{\mathcal{S}} \cdot \mathbf{k}^{\mathrm{Sc}})_{[1,2]}\mathcal{I}_{\mathrm{z}}\mathrm{k}_{\mathrm{z}}^{\mathrm{In}} + (\boldsymbol{\mathcal{I}} \cdot \mathbf{k}^{\mathrm{In}})_{[1,2]}\mathcal{S}_{\mathrm{z}}\mathrm{k}_{\mathrm{z}}^{\mathrm{Sc}}\right\}\Delta\hat{\delta} \\
&- 2\hat{C}^{(0)}_{55}\left\{(\boldsymbol{\mathcal{S}} \cdot \boldsymbol{\mathcal{I}})(\mathbf{k}^{\mathrm{Sc}} \cdot \mathbf{k}^{\mathrm{In}}) + (\boldsymbol{\mathcal{S}} \cdot \mathbf{k}^{\mathrm{In}})(\boldsymbol{\mathcal{I}} \cdot \mathbf{k}^{\mathrm{Sc}}) - 2(\boldsymbol{\mathcal{S}} \cdot \mathbf{k}^{\mathrm{Sc}})(\boldsymbol{\mathcal{I}} \cdot \mathbf{k}^{\mathrm{In}})\right\}_{[1,2]}\Delta\hat{\gamma}.
\end{aligned} \tag{6.30}$$

Superscripts 'Sc' and 'In' refer to the scattered and incident waves respectively. As before the square brackets $[1, 2]$ restrict consideration to certain directions, in this case the x and y components in the expression; for example $(\boldsymbol{\mathcal{S}} \cdot \boldsymbol{\mathcal{I}})_{[1,2]} = \mathcal{S}_1\mathcal{I}_1 + \mathcal{S}_2\mathcal{I}_2$. The unique decomposition of the scattering potential into isotropic and anisotropic parts in equation (6.30) is significant to our forthcoming discussions.

To evaluate the scattering potential, we must next determine the slowness and polarization vectors for scattered and incident waves. In a viscoelastic medium, the wave number vector is complex, in other words it is of the form $\mathbf{K} = \mathbf{P} - i\mathbf{A}$, where $\mathbf{P}$ is the propagation vector and $\mathbf{A}$, the attenuation vector, further determines the direction of maximum attenuation. If propagation and maximum attenuation point in the same direction, the wave is called homogeneous, otherwise the wave is called inhomogeneous (Borcherdt, 2009). In what follows we will consider the general case in which inhomogeneous incident waves are scattered into inhomogeneous outgoing waves. In this case the polarization and slowness vectors for scattered and incident P-waves are given by

$$\begin{aligned}
\boldsymbol{\mathcal{I}}_{\mathrm{P}} &= \hat{V}_{\mathrm{P0}}\mathbf{k}_{\mathrm{P}}^{\mathrm{In}}, \\
\boldsymbol{\mathcal{S}}_{\mathrm{P}} &= \hat{V}_{\mathrm{P0}}\mathbf{k}_{\mathrm{P}}^{\mathrm{Sc}}, \\
\mathbf{k}_{\mathrm{P}}^{\mathrm{In}} &= \frac{\mathbf{K}_{\mathrm{P}}^{\mathrm{In}}}{\omega} = \frac{1}{\omega}\left(\mathbf{P}_{\mathrm{P}}^{\mathrm{In}} - i\mathbf{A}_{\mathrm{P}}^{\mathrm{In}}\right), \\
\mathbf{k}_{\mathrm{P}}^{\mathrm{Sc}} &= \frac{\mathbf{K}_{\mathrm{P}}^{\mathrm{Sc}}}{\omega} = \frac{1}{\omega}\left(\mathbf{P}_{\mathrm{P}}^{\mathrm{Sc}} - i\mathbf{A}_{\mathrm{P}}^{\mathrm{Sc}}\right),
\end{aligned} \tag{6.31}$$

where $\boldsymbol{\mathcal{I}}_{\mathrm{P}}$ and $\boldsymbol{\mathcal{S}}_{\mathrm{P}}$ respectively are the incident and scattered P-wave polarization vectors, and $\mathbf{k}_{\mathrm{P}}^{\mathrm{In}}$ and $\mathbf{k}_{\mathrm{P}}^{\mathrm{Sc}}$ respectively are the incident and scattered P-wave slowness vectors. The incident P-wave propagation and attenuation vectors are defined by $\mathbf{P}_{\mathrm{P}}^{\mathrm{In}}$ and $\mathbf{A}_{\mathrm{P}}^{\mathrm{In}}$ respectively, and the scattered wave vectors by $\mathbf{P}_{\mathrm{P}}^{\mathrm{Sc}}$ and $\mathbf{A}_{\mathrm{P}}^{\mathrm{Sc}}$ respectively (see Appendix F). The complex P-wave velocity in the reference medium is defined by $\hat{V}_{\mathrm{P0}} = V_{\mathrm{P0}}(1 + \frac{i}{2}Q_{\mathrm{P0}}^{-1})$ with elastic P-wave velocity V_{P0} and P-wave quality factor Q_{P0}. For the SI-wave we have

$$\begin{aligned}
\boldsymbol{\mathcal{I}}_{\mathrm{S}} &= \hat{V}_{\mathrm{S0}}\left(\mathbf{y} \times \mathbf{k}_{\mathrm{S}}^{\mathrm{In}}\right), \\
\boldsymbol{\mathcal{S}}_{\mathrm{S}} &= \hat{V}_{\mathrm{S0}}\left(\mathbf{y} \times \mathbf{k}_{\mathrm{S}}^{\mathrm{Sc}}\right), \\
\mathbf{k}_{\mathrm{S}}^{\mathrm{In}} &= \frac{\mathbf{K}_{\mathrm{S}}^{\mathrm{In}}}{\omega} = \frac{1}{\omega}\left(\mathbf{P}_{\mathrm{S}}^{\mathrm{In}} - i\mathbf{A}_{\mathrm{S}}^{\mathrm{In}}\right), \\
\mathbf{k}_{\mathrm{S}}^{\mathrm{Sc}} &= \frac{\mathbf{K}_{\mathrm{S}}^{\mathrm{Sc}}}{\omega} = \frac{1}{\omega}\left(\mathbf{P}_{\mathrm{S}}^{\mathrm{Sc}} - i\mathbf{A}_{\mathrm{S}}^{\mathrm{Sc}}\right).
\end{aligned} \tag{6.32}$$

Here $\mathbf{y}$ is a unit vector in y-direction. $\boldsymbol{\mathcal{I}}_{\mathrm{S}}$ and $\boldsymbol{\mathcal{S}}_{\mathrm{S}}$ respectively are the incident and scattered S-wave polarization vectors; $\mathbf{k}_{\mathrm{S}}^{\mathrm{In}}$ and $\mathbf{k}_{\mathrm{S}}^{\mathrm{Sc}}$ are the incident and scattered S-wave slowness vectors respectively. The complex S-wave velocity in the reference medium is defined by $\hat{V}_{\mathrm{S0}} = V_{\mathrm{S0}}(1 + \frac{i}{2}Q_{\mathrm{S0}}^{-1})$ with elastic S-wave velocity V_{S0} and S-wave quality factor Q_{S0} . The

incident S-wave propagation and attenuation vectors are defined by $\mathbf{P}_{\mathrm{S}}^{\mathrm{In}}$ and $\mathbf{A}_{\mathrm{S}}^{\mathrm{In}}$ respectively, and the scattered S-wave vectors by $\mathbf{P}_{\mathrm{S}}^{\mathrm{Sc}}$ and $\mathbf{A}_{\mathrm{S}}^{\mathrm{Sc}}$ respectively (see again Appendix F). Inserting the polarization/slowness components in equations (6.31) into (6.30), the potential for scattering of a P-wave to a P-wave is given by

$$\begin{aligned}
\mathrm{S}_{\mathrm{PP}} &= (\boldsymbol{\mathcal{S}}_{\mathrm{P}} \cdot \boldsymbol{\mathcal{I}}_{\mathrm{P}})\Delta\rho \\
&- (\boldsymbol{\mathcal{S}}_{\mathrm{P}} \cdot \mathbf{k}_{\mathrm{P}}^{\mathrm{Sc}})(\boldsymbol{\mathcal{I}}_{\mathrm{P}} \cdot \mathbf{k}_{\mathrm{P}}^{\mathrm{In}})\Delta\hat{C}_{33} \\
&- \left[(\boldsymbol{\mathcal{S}}_{\mathrm{P}} \cdot \boldsymbol{\mathcal{I}}_{\mathrm{P}})(\mathbf{k}_{\mathrm{P}}^{\mathrm{Sc}} \cdot \mathbf{k}_{\mathrm{P}}^{\mathrm{In}}) - 2(\boldsymbol{\mathcal{S}}_{\mathrm{P}} \cdot \mathbf{k}_{\mathrm{P}}^{\mathrm{Sc}})(\boldsymbol{\mathcal{I}}_{\mathrm{P}} \cdot \mathbf{k}_{\mathrm{P}}^{\mathrm{In}}) + (\boldsymbol{\mathcal{S}}_{\mathrm{P}} \cdot \mathbf{k}_{\mathrm{P}}^{\mathrm{In}})(\boldsymbol{\mathcal{I}}_{\mathrm{P}} \cdot \mathbf{k}_{\mathrm{P}}^{\mathrm{Sc}})\right]\Delta\hat{C}_{55} \\
&- 2\hat{C}_{33}^{(0)}(\mathcal{S}_{\mathrm{Px}}\mathrm{k}_{\mathrm{Px}}^{\mathrm{Sc}}\mathcal{I}_{\mathrm{Px}}\mathrm{k}_{\mathrm{Px}}^{\mathrm{In}})\Delta\hat{\varepsilon} \\
&- \hat{C}_{33}^{(0)}(\mathcal{S}_{\mathrm{Px}}\mathrm{k}_{\mathrm{Px}}^{\mathrm{Sc}}\mathcal{I}_{\mathrm{Pz}}\mathrm{k}_{\mathrm{Pz}}^{\mathrm{In}} + \mathcal{S}_{\mathrm{Pz}}\mathrm{k}_{\mathrm{Pz}}^{\mathrm{Sc}}\mathcal{I}_{\mathrm{Px}}\mathrm{k}_{\mathrm{Px}}^{\mathrm{In}})\Delta\hat{\delta},
\end{aligned} \tag{6.33}$$

The P-to-P scattering potential is thus sensitive to changes in all of the properties in this model, except changes in γ and γ_Q. The potential for a conversion upon scattering from P-wave to S-wave is

$$\begin{aligned}
\mathrm{S}_{\mathrm{PSI}} &= (\boldsymbol{\mathcal{S}}_{\mathrm{S}} \cdot \boldsymbol{\mathcal{I}}_{\mathrm{P}})\Delta\rho \\
&- \left[(\boldsymbol{\mathcal{S}}_{\mathrm{S}} \cdot \boldsymbol{\mathcal{I}}_{\mathrm{P}})(\mathbf{k}_{\mathrm{S}}^{\mathrm{Sc}} \cdot \mathbf{k}_{\mathrm{P}}^{\mathrm{In}}) + (\boldsymbol{\mathcal{S}}_{\mathrm{S}} \cdot \mathbf{k}_{\mathrm{P}}^{\mathrm{In}})(\boldsymbol{\mathcal{I}}_{\mathrm{P}} \cdot \mathbf{k}_{\mathrm{S}}^{\mathrm{Sc}})\right]\Delta\hat{C}_{55} \\
&- 2\hat{C}_{33}^{(0)}(\mathcal{S}_{\mathrm{Sx}}\mathrm{k}_{\mathrm{Sx}}^{\mathrm{Sc}}\mathcal{I}_{\mathrm{Px}}\mathrm{k}_{\mathrm{Px}}^{\mathrm{In}})\Delta\hat{\varepsilon} \\
&- \hat{C}_{33}^{(0)}(\mathcal{S}_{\mathrm{Sx}}\mathrm{k}_{\mathrm{Sx}}^{\mathrm{Sc}}\mathcal{I}_{\mathrm{Pz}}\mathrm{k}_{\mathrm{Pz}}^{\mathrm{In}} + \mathcal{S}_{\mathrm{Sz}}\mathrm{k}_{\mathrm{Sz}}^{\mathrm{Sc}}\mathcal{I}_{\mathrm{Px}}\mathrm{k}_{\mathrm{Px}}^{\mathrm{In}})\Delta\hat{\delta}.
\end{aligned} \tag{6.34}$$

In contrast to the P-to-P mode, the $\Delta\hat{C}_{33}$ terms does not appear here, and as a result changes in the P-wave velocity and P-wave quality factors have no contribution in P-to-SI scattering potential. For scattering of an SI-wave to another SI-wave the potential is

$$\begin{aligned}
\mathrm{S}_{\mathrm{SISI}} &= (\boldsymbol{\mathcal{S}}_{\mathrm{S}} \cdot \boldsymbol{\mathcal{I}}_{\mathrm{S}})\Delta\rho \\
&- \left[(\boldsymbol{\mathcal{S}}_{\mathrm{S}} \cdot \boldsymbol{\mathcal{I}}_{\mathrm{S}})(\mathbf{k}_{\mathrm{S}}^{\mathrm{Sc}} \cdot \mathbf{k}_{\mathrm{S}}^{\mathrm{In}}) + (\boldsymbol{\mathcal{S}}_{\mathrm{S}} \cdot \mathbf{k}_{\mathrm{S}}^{\mathrm{In}})(\boldsymbol{\mathcal{I}}_{\mathrm{S}} \cdot \mathbf{k}_{\mathrm{S}}^{\mathrm{Sc}})\right]\Delta\hat{C}_{55} \\
&- 2\hat{C}_{33}^{(0)}(\mathcal{S}_{\mathrm{Sx}}\mathrm{k}_{\mathrm{Sx}}^{\mathrm{Sc}}\mathcal{I}_{\mathrm{Sx}}\mathrm{k}_{\mathrm{Sx}}^{\mathrm{In}})\Delta\hat{\varepsilon} \\
&- \hat{C}_{33}^{(0)}(\mathcal{S}_{\mathrm{Sx}}\mathrm{k}_{\mathrm{Sx}}^{\mathrm{Sc}}\mathcal{I}_{\mathrm{Sz}}\mathrm{k}_{\mathrm{Sz}}^{\mathrm{In}} + \mathcal{S}_{\mathrm{Sz}}\mathrm{k}_{\mathrm{Sz}}^{\mathrm{Sc}}\mathcal{I}_{\mathrm{Sx}}\mathrm{k}_{\mathrm{Sx}}^{\mathrm{In}})\Delta\hat{\delta}.
\end{aligned} \tag{6.35}$$

The dependency of the potential for SI-to-SI scattering on parameter changes is the same as that of P-to-SI scattering. Finally potential for scattering of an SII-wave to another SII-wave is

$$\mathrm{S}_{\mathrm{SIISII}} = \Delta\rho - (\mathbf{k}_{\mathrm{S}}^{\mathrm{In}} \cdot \mathbf{k}_{\mathrm{S}}^{\mathrm{Sc}})\Delta\hat{C}_{55} - 2C_{55}^{(0)}(\mathrm{k}_{\mathrm{Sx}}^{\mathrm{Sc}}\mathrm{k}_{\mathrm{Sx}}^{\mathrm{In}})\Delta\hat{\gamma}. \tag{6.36}$$

These expressions for scattering potentials demonstrate the roles played by changes in anisotropic parameters in the scattering process. Changes in $\hat{\varepsilon}$ and $\hat{\delta}$ affect the P-to-P, P-to-SI and SI-to-SI scattering modes meanwhile changes in $\hat{\gamma}$ occur only for SII to SII scattering mode.

6.6 Anisotropic-viscoelastic scattering processes and inversion sensitivities

In this section we will analyze the scattering potentials, as derived in the previous section, in greater detail. Our assumption of low-loss attenuation, in which the higher orders of inverse quality factors Q_{P}^{-1} and Q_{S}^{-1} are negligible, will allow the scattering potential to be decomposed into the following components:

- **Isotropic Elastic (IE)**: terms which are sensitive to changes in density, and P- and S-wave velocities. This term as a whole is consistent with the scattering potential as derived for purely isotropic-elastic media.

- **Anisotropic Elastic (AE)**: terms which are sensitive to changes in the elastic Thomsen parameters. In the case that the medium under study is purely isotropic this term goes to zero. The combined (IE+AE)-terms represent the scattering potential for elastic waves in an anisotropic-elastic medium.

- **Isotropic Viscoelastic (IV)**: terms which are sensitive to changes in density, P-and S-wave velocities, and P- and S-wave quality factors. In the non-attenuating limit this term vanishes. The combined (IE+IV)-terms represent the scattering potential for viscoelastic waves in an isotropic-viscoelastic medium.

- **Anisotropic Viscoelastic (AV)**: terms which are sensitive to changes in Q-dependent Thomsen parameters. In the case that the medium under study is either isotropic or elastic this term is zero.

Quantitatively and qualitatively interpretable decompositions of this kind are of significance in part because they lead directly to the sensitivities which weight multiparameter FWI

algorithms, and permit characterization of issues such as parameter cross-talk (Plessix et al., 2013; Innanen, 2014; Pan et al., 2016). Let us consider the reference medium to be a isotropic viscoelastic medium perturbed by small (though possibly many) inclusions associated with viscoelastic and anisotropic parameter changes. Let us furthermore define for convenience a density-normalized scattering potential $\rho_0^{-1}\mathrm{S}$. The scattering potential now decomposes into four components:

$$[\mathrm{PP}] = [\mathrm{PP}]_{\mathrm{IE}} + [\mathrm{PP}]_{\mathrm{AE}} + i\,[\mathrm{PP}]_{\mathrm{IV}} + i\,[\mathrm{PP}]_{\mathrm{AV}}\,, \tag{6.37}$$

with elastic, anisotropic, viscoelastic and viscoelastic anisotropic changes and/or fractional changes, weighted by sensitivities, being:

$$\begin{aligned}
[\mathrm{PP}]_{\mathrm{IE}} &= [\mathrm{PP}]^{\rho}_{\mathrm{IE}}\,\frac{\Delta\rho}{\rho} + [\mathrm{PP}]^{\mathrm{Vp}}_{\mathrm{IE}}\,\frac{\Delta V_P}{V_P} + [\mathrm{PP}]^{\mathrm{Vs}}_{\mathrm{IE}}\,\frac{\Delta V_{\mathrm{S}}}{V_{\mathrm{S}}},\\
[\mathrm{PP}]_{\mathrm{AE}} &= [\mathrm{PP}]^{\varepsilon}_{\mathrm{AE}}\,\varepsilon + [\mathrm{PP}]^{\delta}_{\mathrm{AE}}\,\delta,\\
[\mathrm{PP}]_{\mathrm{IV}} &= [\mathrm{PP}]^{\rho}_{\mathrm{IV}}\,\frac{\Delta\rho}{\rho} + [\mathrm{PP}]^{\mathrm{Vs}}_{\mathrm{IV}}\,\frac{\Delta V_{\mathrm{S}}}{V_{\mathrm{S}}} + [\mathrm{PP}]^{\mathrm{Qp}}_{\mathrm{IV}}\,\frac{\Delta Q_{\mathrm{P}}}{Q_{\mathrm{P}}} + [\mathrm{PP}]^{\mathrm{Qs}}_{\mathrm{IV}}\,\frac{\Delta Q_{\mathrm{S}}}{Q_{\mathrm{S}}},\\
[\mathrm{PP}]_{\mathrm{AV}} &= [\mathrm{PP}]^{\varepsilon}_{\mathrm{AV}}\,\varepsilon + [\mathrm{PP}]^{\delta}_{\mathrm{AV}}\,\delta + [\mathrm{PP}]^{\varepsilon_{\mathrm{Q}}}_{\mathrm{AV}}\,\varepsilon_{\mathrm{Q}} + [\mathrm{PP}]^{\delta_{\mathrm{Q}}}_{\mathrm{AV}}\,\delta_{\mathrm{Q}},
\end{aligned} \tag{6.38}$$

where the sensitivities are, explicitly,

$$
\begin{aligned}
[\mathrm{PP}]^{\rho}_{\mathrm{IE}} &= -2 + 2\sin^2\theta_{\mathrm{P}} + 2V_{\mathrm{SP}}^2\sin^2 2\theta_{\mathrm{P}},\\
[\mathrm{PP}]^{\mathrm{Vp}}_{\mathrm{IE}} &= -2,\\
[\mathrm{PP}]^{\mathrm{Vs}}_{\mathrm{IE}} &= 4V_{\mathrm{PS}}^2\sin^2 2\theta_{\mathrm{P}},\\
[\mathrm{PP}]^{\varepsilon}_{\mathrm{AE}} &= -2\sin^4\theta_{\mathrm{P}},\\
[\mathrm{PP}]^{\delta}_{\mathrm{AE}} &= -\frac{1}{2}\sin^2 2\theta_{\mathrm{P}},\\
[\mathrm{PP}]^{\rho}_{\mathrm{IV}} &= 2V_{\mathrm{SP}}^2\sin^2 2\theta_{\mathrm{P}}(Q_{\mathrm{S0}}^{-1} - Q_{\mathrm{P0}}^{-1}) + Q_{\mathrm{P0}}^{-1}\left(\sin 2\theta_{\mathrm{P}} + 2V_{\mathrm{SP}}^2\sin 4\theta_{\mathrm{P}}\right)\tan\delta_{\mathrm{P}},\\
[\mathrm{PP}]^{\mathrm{Vs}}_{\mathrm{IV}} &= 4V_{\mathrm{SP}}^2\sin^2 2\theta_{\mathrm{P}}(Q_{\mathrm{S0}}^{-1} - Q_{\mathrm{P0}}^{-1}) + 4Q_{\mathrm{P0}}^{-1}V_{\mathrm{SP}}^2\sin 4\theta_{\mathrm{P}}\tan\delta_{\mathrm{P}},\\
[\mathrm{PP}]^{\mathrm{Qp}}_{\mathrm{IV}} &= Q_{\mathrm{P0}}^{-1},\\
[\mathrm{PP}]^{\mathrm{Qs}}_{\mathrm{IV}} &= -2Q_{\mathrm{S0}}^{-1}V_{\mathrm{SP}}^2\sin^2 2\theta_{\mathrm{P}},\\
[\mathrm{PP}]^{\varepsilon}_{\mathrm{AV}} &= -2Q_{\mathrm{P0}}^{-1}\sin 2\theta_{\mathrm{P}}\sin^2\theta_{\mathrm{P}}\tan\delta_{\mathrm{P}},\\
[\mathrm{PP}]^{\delta}_{\mathrm{AV}} &= -\frac{1}{2}Q_{\mathrm{P0}}^{-1}\sin 4\theta_{\mathrm{P}}\tan\delta_{\mathrm{P}},\\
[\mathrm{PP}]^{\varepsilon_{\mathrm{Q}}}_{\mathrm{AV}} &= -Q_{\mathrm{P0}}^{-1}\sin^4\theta_{\mathrm{P}},\\
[\mathrm{PP}]^{\delta_{\mathrm{Q}}}_{\mathrm{AV}} &= -\frac{1}{4}Q_{\mathrm{P0}}^{-1}\sin^2 2\theta_{\mathrm{P}}.
\end{aligned}
\tag{6.39}
$$

In the above equations, θ_P is the P-wave incident angle, the angle that the direction of the incident P-wave makes with the z-axis; δ_{P} is the average of the incident attenuation angle $\delta_{\mathrm{P}}^{\mathrm{In}}$ and scatter attenuation angle $\delta_{\mathrm{P}}^{\mathrm{Sc}}$ and $V_{\mathrm{SP}} = V_{\mathrm{S0}}/V_{\mathrm{P0}}$ is the reference medium reciprocal ratio. The quantity $[\mathrm{PP}]_{\mathrm{IE}}$ is the potential for scattering from a P-wave to a P-wave in an isotropic elastic medium. It has three components: $[\mathrm{PP}]^{\rho}_{\mathrm{IE}}$ is the sensitivity of the scattered wavefield to a local density variation, $[\mathrm{PP}]^{\mathrm{Vp}}_{\mathrm{IE}}$ is the sensitivity to variation of the P-wave velocity and $[\mathrm{PP}]^{\mathrm{Vs}}_{\mathrm{IE}}$ is the sensitivity to variation of the S-wave velocity.

The anisotropic component $[\mathrm{PP}]_{\mathrm{AE}}$ is a function of Thomsen parameters ε and δ. The viscoelastic component is a function of the fractional changes in density, P- and S-wave quality factors and the S-wave velocity. Viscoelastic anisotropic components are functions of the Q-dependent Thomsen parameters ε_Q and δ_Q. In the limit of normal incidence, where incident and reflected propagation vectors are in the opposite direction, contributions from anisotropic and viscoelastic anisotropic parameters vanish. In the $[\mathrm{PP}]_{\mathrm{AE}}$ and $[\mathrm{PP}]_{\mathrm{AV}}$ components no influence of changes in vertical P- and S-wave velocities and corresponding

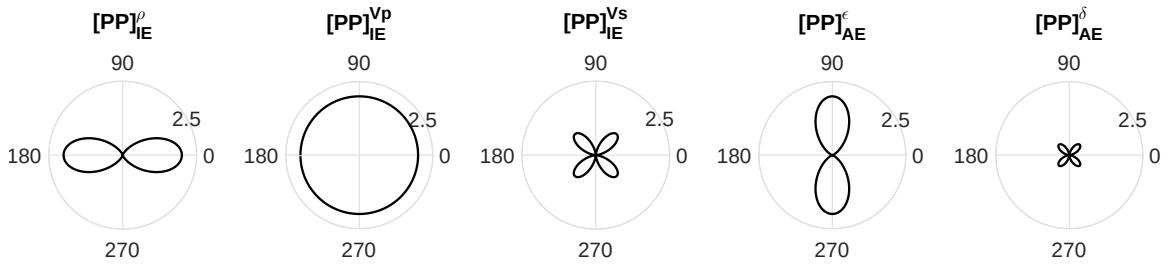

Figure 6.2: Sensitivity of the elastic part of the P-to-P scattering potential to the changes in properties versus incident P-wave angle θ_{P}. The S- to P-wave velocity ratio for reference medium is chosen to be 1/2.

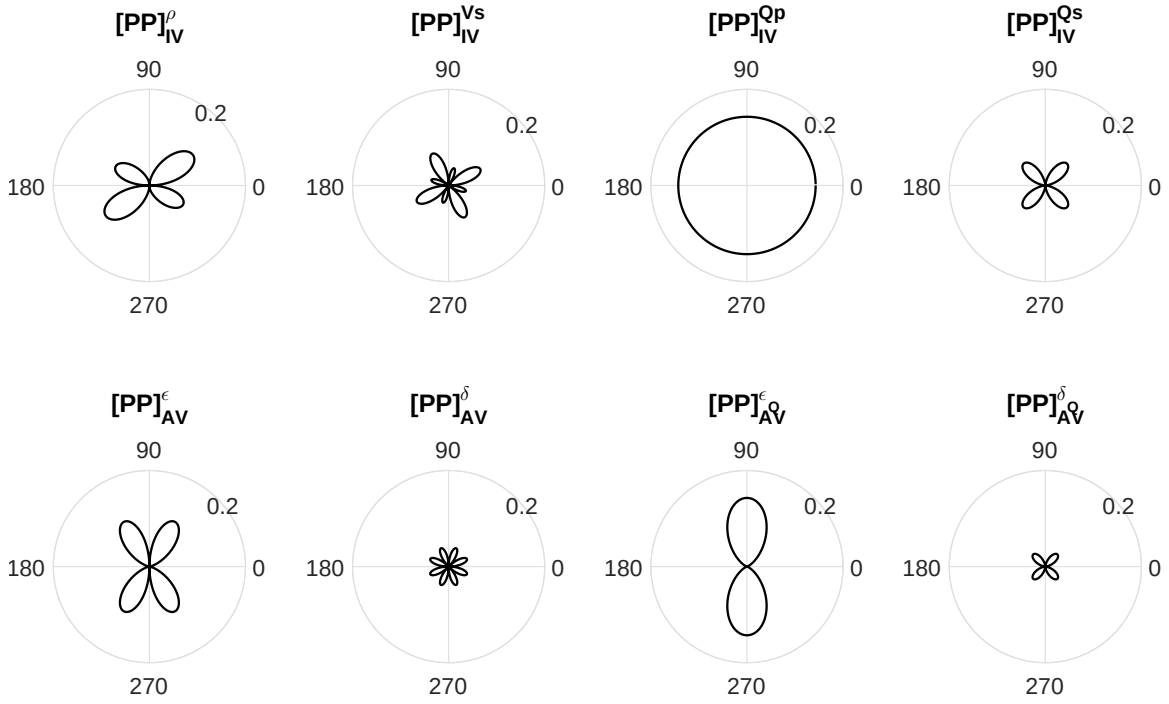

Figure 6.3: Sensitivity of the viscoelastic part of the P-to-P scattering potential to the changes in properties versus incident P-wave angle θ_{P}. Top plots are the sensitivity of the isotropic viscoelastic components and lower plots are the sensitivity of the anisotropic viscoelastic components. Quality factor of P-wave for reference medium is to be 10 and for S-wave is 7. Also the S- to P-wave velocity ratio for reference medium is chosen to be 1/2. P-wave attenuation angle is chosen to be $\delta_{\mathrm{P}} = \pi/6$.

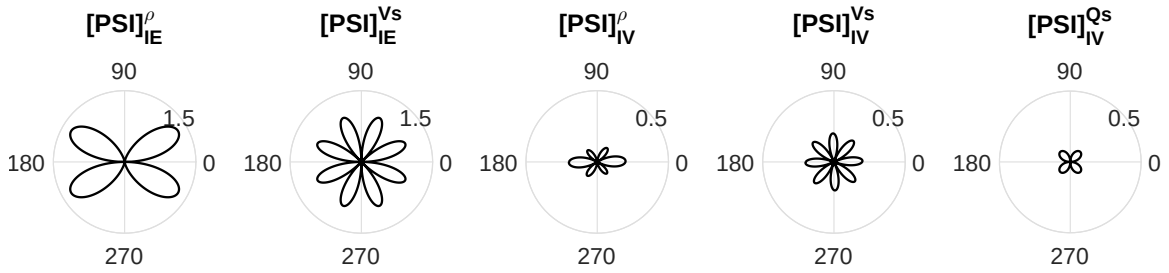

Figure 6.4: Sensitivity of the isotropic elastic and isotropic viscoelastic parts of the P-to-SI scattering potential to the changes in properties versus the average of incident P-wave angle θ_{P} and scattered S-wave angle θ_{S}. S-to-P velocity ratio, quality factor and attention angle same as figure 6.3.

quality factors is felt. For small incident angle only δ and δ_Q influence the anisotropic part of the scattering potential. If the actual medium is anisotropic-viscoelastic, but with zero ε and δ parameters, the scattering potential is seen to be nevertheless sensitive to the Q-dependent Thomsen parameters. If the perturbed media is non-attenuative VTI-anisotropic, the scattering potential is given by $([\mathrm{PP}]_{\mathrm{IE}} + [\mathrm{PP}]_{\mathrm{AE}})$.

Our results are in agreement with previously-derived scattering potential expressions (i.e., for what are here special cases), namely isotropic-elastic and isotropic-viscoelastic media. For instance, $[\mathrm{PP}]_{\mathrm{IE}}$ is the scattering potential for the case in which both the reference medium and the perturbing inclusions are purely isotropic-elastic (Stolt and Weglein, 2012) and $([\mathrm{PP}]_{\mathrm{IE}} + i\,[\mathrm{PP}]_{\mathrm{IV}})$ is the potential for scattering of an inhomogeneous P-wave to another P-wave in isotropic viscoelastic media (Moradi and Innanen, 2015b).

In Figure 6.2 we plot the elastic isotropic and anisotropic sensitivities for scattering of a P-wave to a P-wave versus the incident P-wave angle θ_{P}. The angle of incidence is considered to range across $(0°, 360°)$. The incident inhomogeneous P-wave propagates in an isotropic viscoelastic reference medium, and can be scattered to either an inhomogeneous P-wave or SI-wave. The sensitivity of the elastic scattering potential, $[\mathrm{PP}]^{\rho}_{\mathrm{IE}}$, to the density has two lobes reaching maximum absolute values at 0° and 180°. The radiation pattern of the sensitivity to P-wave velocity changes, $[\mathrm{PP}]^{\mathrm{V_P}}_{\mathrm{IE}}$, is circle independent of incidence angle. A similar interpretation applies to the radiation patterns as plotted in Figure 6.3 for viscoelastic components of the P-to-P scattering potential. Figures 6.4-6.8 illustrate

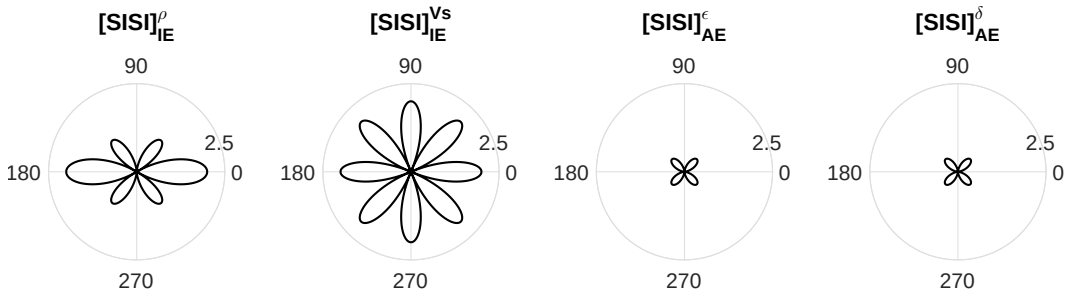

Figure 6.5: Sensitivity of the elastic part of the SI-to-SI scattering potential to the changes in properties versus incident S-wave angle θ_{S}.

the radiation patterns for elastic and viscoelastic components of the P-to-SI, SI-to-SI and SII-to-SII scattering potentials.

We next consider the converted wave, discussion of which can be carried out similar to that of the P-wave to P-wave scattering potential. The potential for scattering of a P-wave to an SI wave is given by

$$[\mathrm{PSI}] = [\mathrm{PSI}]_{\mathrm{IE}} + [\mathrm{PSI}]_{\mathrm{AE}} + i\,[\mathrm{PSI}]_{\mathrm{IV}} + i\,[\mathrm{PSI}]_{\mathrm{AV}}\,, \tag{6.40}$$

with the components defined by

$$\begin{aligned}
[\mathrm{PSI}]_{\mathrm{IE}} &= [\mathrm{PSI}]^{\rho}_{\mathrm{IE}}\,\frac{\Delta\rho}{\rho} + [\mathrm{PSI}]^{\mathrm{Vs}}_{\mathrm{IE}}\,\frac{\Delta V_{\mathrm{S}}}{V_{\mathrm{S}}} \\
[\mathrm{PSI}]_{\mathrm{AE}} &= [\mathrm{PSI}]^{\varepsilon}_{\mathrm{AE}}\,\varepsilon + [\mathrm{PSI}]^{\delta}_{\mathrm{AE}}\,\delta \\
[\mathrm{PSI}]_{\mathrm{IV}} &= [\mathrm{PSI}]^{\rho}_{\mathrm{IV}}\,\frac{\Delta\rho}{\rho} + [\mathrm{PSI}]^{\mathrm{Vs}}_{\mathrm{IV}}\,\frac{\Delta V_{\mathrm{S}}}{V_{\mathrm{S}}} + [\mathrm{PSI}]^{\mathrm{Qs}}_{\mathrm{IV}}\,\frac{\Delta Q_{\mathrm{S}}}{Q_{\mathrm{S}}} \\
[\mathrm{PSI}]_{\mathrm{AV}} &= [\mathrm{PSI}]^{\varepsilon}_{\mathrm{AV}}\,\varepsilon + [\mathrm{PSI}]^{\delta}_{\mathrm{AV}}\,\delta + [\mathrm{PSI}]^{\varepsilon_{\mathrm{Q}}}_{\mathrm{AV}}\,\varepsilon_{\mathrm{Q}} + [\mathrm{PSI}]^{\delta_{\mathrm{Q}}}_{\mathrm{AV}}\,\delta_{\mathrm{Q}}
\end{aligned} \tag{6.41}$$

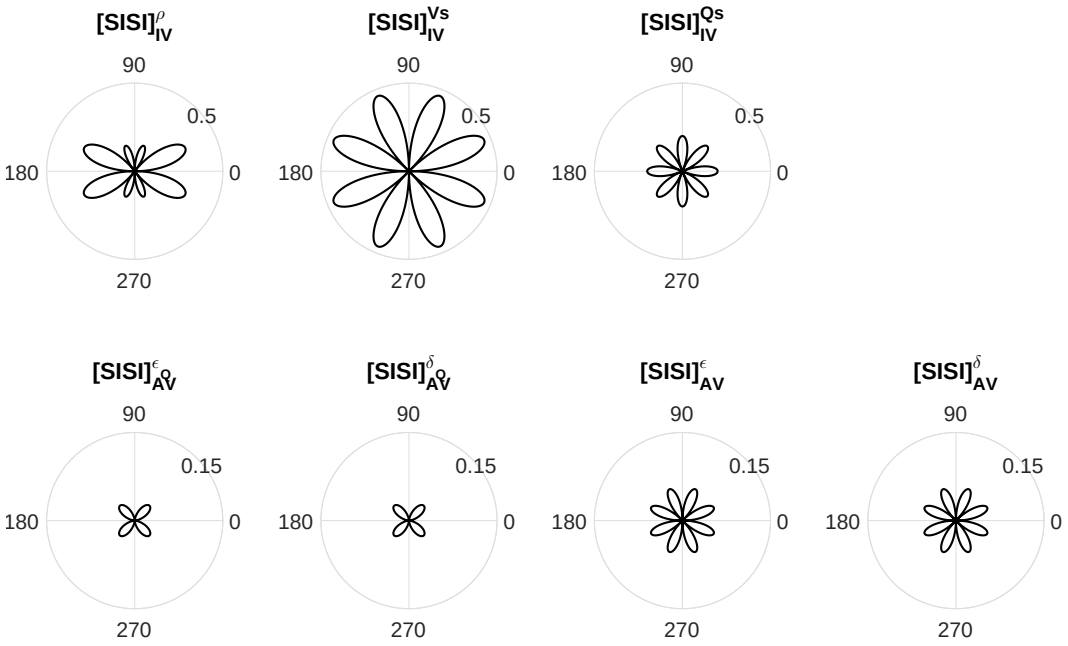

Figure 6.6: Sensitivity of the viscoelastic part of the SI-to-SI scattering potential to the changes in properties versus incident S-wave angle θ_S. Top plots are the sensitivity of the isotropic viscoelastic components and lower plots are the sensitivity of the anisotropic viscoelastic components. S-to-P velocity ratio, quality factor and attention angle same as figure 6.3.

where

$$
\begin{aligned}
[\mathrm{PSI}]^{\rho}_{\mathrm{IE}} &= -\sin(\theta_{\mathrm{P}}+\theta_{\mathrm{S}}) - V_{\mathrm{SP}}\sin 2(\theta_{\mathrm{P}}+\theta_{\mathrm{S}}) \\
[\mathrm{PSI}]^{\mathrm{Vs}}_{\mathrm{IE}} &= -2V_{\mathrm{SP}}\sin 2(\theta_{\mathrm{P}}+\theta_{\mathrm{S}}) \\
[\mathrm{PSI}]^{\varepsilon}_{\mathrm{AE}} &= V_{\mathrm{PS}}\sin 2\theta_{\mathrm{S}}\sin^2\theta_{\mathrm{P}} \\
[\mathrm{PSI}]^{\delta}_{\mathrm{AE}} &= \frac{1}{2}V_{\mathrm{PS}}\cos 2\theta_{\mathrm{P}}\sin 2\theta_{\mathrm{S}} \\
[\mathrm{PSI}]^{\rho}_{\mathrm{IV}} &= -\frac{1}{2}V_{\mathrm{SP}}(Q_{\mathrm{S0}}^{-1}-Q_{\mathrm{P0}}^{-1})\sin 2(\theta_{\mathrm{P}}+\theta_{\mathrm{S}}) \\
&\quad -\frac{1}{2}\left[\cos(\theta_{\mathrm{P}}+\theta_{\mathrm{S}})+2V_{\mathrm{SP}}\cos 2(\theta_{\mathrm{P}}+\theta_{\mathrm{S}})\right]\left(Q_{\mathrm{S0}}^{-1}\tan\delta_{\mathrm{S}}+Q_{\mathrm{P0}}^{-1}\tan\delta_{\mathrm{P}}\right) \\
[\mathrm{PSI}]^{\mathrm{Vs}}_{\mathrm{IV}} &= -V_{\mathrm{SP}}(Q_{\mathrm{S0}}^{-1}-Q_{\mathrm{P0}}^{-1})\sin 2(\theta_{\mathrm{P}}+\theta_{\mathrm{S}}) \\
&\quad -2V_{\mathrm{SP}}\cos 2(\theta_{\mathrm{P}}+\theta_{\mathrm{S}})\left(Q_{\mathrm{S0}}^{-1}\tan\delta_{\mathrm{S}}+Q_{\mathrm{P0}}^{-1}\tan\delta_{\mathrm{P}}\right) \\
[\mathrm{PSI}]^{\mathrm{Qs}}_{\mathrm{IV}} &= V_{\mathrm{SP}}Q_{\mathrm{S0}}^{-1}\sin 2(\theta_{\mathrm{P}}+\theta_{\mathrm{S}})\frac{\Delta Q_{\mathrm{S}}}{Q_{\mathrm{S}}} \\
[\mathrm{PSI}]^{\varepsilon}_{\mathrm{AV}} &= -\frac{1}{2}V_{\mathrm{PS}}(Q_{\mathrm{S0}}^{-1}-Q_{\mathrm{P0}}^{-1})\sin 2\theta_{\mathrm{S}}\sin^2\theta_{\mathrm{P}} \\
&\quad +V_{\mathrm{PS}}\left(Q_{\mathrm{S0}}^{-1}\cos 2\theta_{\mathrm{S}}\sin\theta_{\mathrm{P}}\tan\delta_{\mathrm{S}}+Q_{\mathrm{P0}}^{-1}\sin 2\theta_{\mathrm{S}}\cos\theta_{\mathrm{P}}\tan\delta_{\mathrm{P}}\right)\sin\theta_{\mathrm{P}} \\
[\mathrm{PSI}]^{\delta}_{\mathrm{AV}} &= -\frac{1}{4}V_{\mathrm{PS}}(Q_{\mathrm{S0}}^{-1}-Q_{\mathrm{P0}}^{-1})\cos 2\theta_{\mathrm{P}}\sin 2\theta_{\mathrm{S}} \\
&\quad +\frac{1}{2}V_{\mathrm{PS}}\left(Q_{\mathrm{S0}}^{-1}\cos 2\theta_{\mathrm{S}}\cos 2\theta_{\mathrm{P}}\tan\delta_{\mathrm{S}}-Q_{\mathrm{P0}}^{-1}\sin 2\theta_{\mathrm{S}}\sin 2\theta_{\mathrm{P}}\tan\delta_{\mathrm{P}}\right) \\
[\mathrm{PSI}]^{\varepsilon_{\mathrm{Q}}}_{\mathrm{AV}} &= \frac{1}{2}V_{\mathrm{PS}}Q_{\mathrm{P0}}^{-1}\sin 2\theta_{\mathrm{S}}\sin^2\theta_{\mathrm{P}} \\
[\mathrm{PSI}]^{\delta_{\mathrm{Q}}}_{\mathrm{AV}} &= \frac{1}{4}V_{\mathrm{PS}}Q_{\mathrm{P0}}^{-1}\cos 2\theta_{\mathrm{P}}\sin 2\theta_{\mathrm{S}}.
\end{aligned}
\tag{6.42}
$$

Here we have defined θ_S as the S-wave incident angle and $V_{\mathrm{PS}} = V_{\mathrm{P0}}/V_{\mathrm{S0}}$. The elastic and viscoelastic components of the scattering potential $[\mathrm{PSI}]_{\mathrm{IE}}, [\mathrm{PSI}]_{\mathrm{IV}}$ are sensitive to the fractional changes in the density, the vertical S-wave velocity and the S-wave quality factor. Changes in the vertical P-wave velocity and the P-wave quality factor do not have any effect on these two terms. $([\mathrm{PSI}]_{\mathrm{IE}} + i\,[\mathrm{PSI}]_{\mathrm{IV}})$ is the potential for scattering of an incident inhomogeneous P-wave into an inhomogenous SI-wave in an isotropic viscoelastic medium. The anisotropic and anisotropic viscoelastic terms, for small angles of incidence, are sensitive only to δ and δ_Q. For large incidence angles, the effects of P-wave Thomsen parameters ε and ε_Q become influential. The scattering potential for SI to SI waves is

$$
[\mathrm{SISI}] = [\mathrm{SISI}]_{\mathrm{IE}} + [\mathrm{SISI}]_{\mathrm{AE}} + i\,[\mathrm{SISI}]_{\mathrm{IV}} + i\,[\mathrm{SISI}]_{\mathrm{AV}}\,, \tag{6.43}
$$

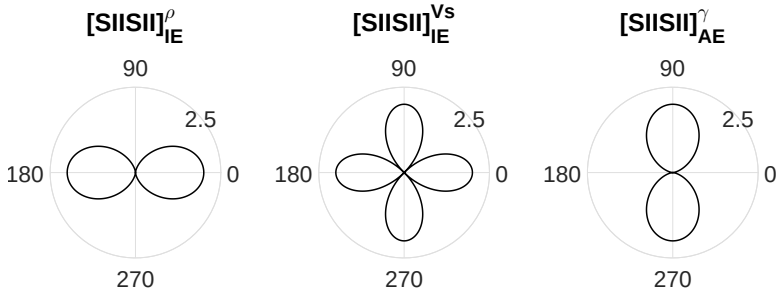

Figure 6.7: Sensitivity of the elastic part of the SII-to-SII scattering potential to the changes in properties.

where

$$
\begin{aligned}
[\mathrm{SISI}]_{\mathrm{IE}} &= -(\cos 2\theta_{\mathrm{S}} + \cos 4\theta_{\mathrm{S}})\frac{\Delta\rho}{\rho} - 2\cos 4\theta_{\mathrm{S}}\frac{\Delta V_{\mathrm{S}}}{V_{\mathrm{S}}},\\
[\mathrm{SISI}]_{\mathrm{AE}} &= \frac{1}{2}\sin^2 2\theta_{\mathrm{S}}(\delta - \varepsilon),\\
[\mathrm{SISI}]_{\mathrm{IV}} &= Q_{\mathrm{S0}}^{-1}\cos 4\theta_{\mathrm{S}}\frac{\Delta Q_S}{Q_S} + Q_{\mathrm{S0}}^{-1}\tan\delta_{\mathrm{S}}(\sin 2\theta_{\mathrm{S}} + 2\sin 4\theta_{\mathrm{S}})\frac{\Delta\rho}{\rho} + 4Q_{S0}^{-1}\sin 4\theta_{\mathrm{S}}\tan\delta_{\mathrm{S}}\frac{\Delta V_S}{V_S},\\
[\mathrm{SISI}]_{\mathrm{AV}} &= \frac{1}{4}Q_{\mathrm{S0}}^{-1}\sin^2 2\theta_{\mathrm{S}}(\delta_Q - \varepsilon_Q) + \frac{1}{2}Q_{\mathrm{S0}}^{-1}\sin 4\theta_{\mathrm{S}}\tan\delta_{\mathrm{S}}(\delta - \varepsilon).
\end{aligned}
\tag{6.44}
$$

Here $[\mathrm{SISI}]_{\mathrm{IE}}$ is the potential for scattering of an SV-wave to another SV-wave in an isotropic elastic background, i.e., where neither attenuation nor anisotropy is present. This term is sensitive to changes in density and S-wave velocity only; in other words to leading order a perturbation in the P-wave velocity does not scatter an incident SV-wave. $([\mathrm{SISI}]_{\mathrm{IE}} + i\,[\mathrm{SISI}]_{\mathrm{IV}})$ describes scattering of inhomogeneous SI-waves in an isotropic viscoelastic background. In the presence of attenuation, an incident SI-wave not influenced by changes in the P-wave quality factor Q_{P}. In total, in viscoelastic anisotropic media, to leading order, changes in seven parameters can cause scattering, $(\rho, V_{\mathrm{S}}, Q_{\mathrm{S}}, \delta, \varepsilon, \delta_Q, \varepsilon_Q)$.

Finally, the scattering potential for SII-to-SII scattering is

$$
[\mathrm{SIISII}] = [\mathrm{SIISII}]_{\mathrm{IE}} + [\mathrm{SIISII}]_{\mathrm{AE}} + i\,[\mathrm{SIISII}]_{\mathrm{IV}} + i\,[\mathrm{SIISII}]_{\mathrm{AV}}\,, \tag{6.45}
$$

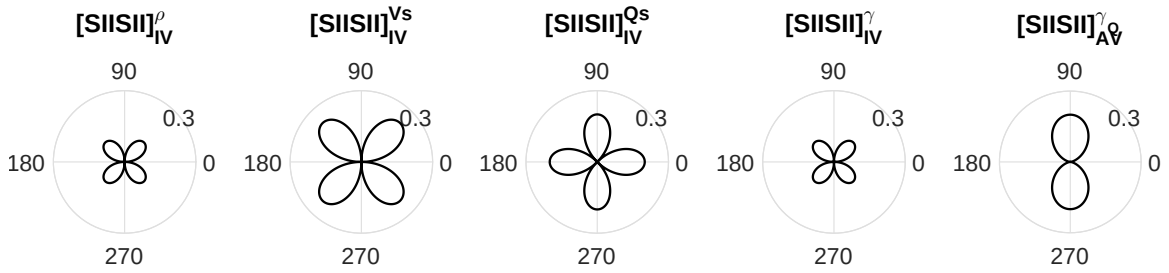

Figure 6.8: Sensitivity of the viscoelastic part of the SII-to-SII scattering potential to the changes in properties versus incident S-wave angle $\theta_{\rm S}$. S-to-P velocity ratio, quality factor and attention angle same as figure 6.3.

where

$$\begin{aligned}
[\text{SIISII}]_{\text{IE}} &= (1+\cos 2\theta_{\rm S})\frac{\Delta\rho}{\rho} + 2\cos 2\theta_{\rm S}\frac{\Delta V_S}{V_S},\\
[\text{SIISII}]_{\text{AE}} &= -2\sin^2\theta_{\rm S}\gamma,\\
[\text{SIISII}]_{\text{IV}} &= -Q_{\rm S0}^{-1}\sin 2\theta_{\rm S}\tan\delta_{\rm S}\left(\frac{\Delta\rho}{\rho}+2\frac{\Delta V_S}{V_S}\right) - Q_{\rm S0}^{-1}\cos 2\theta_{\rm S}\frac{\Delta Q_{\rm S}}{Q_{\rm S}},\\
[\text{SIISII}]_{\text{AV}} &= -Q_{\rm S0}^{-1}\sin^2\theta_{\rm S}\gamma_Q - Q_{\rm S0}^{-1}\sin 2\theta_S\tan\delta_{\rm S}\gamma.
\end{aligned} \tag{6.46}$$

In the absence of anisotropy the above expression reduces to the potential for the scattering of a standard inhomogeneous viscoelastic SII waves into another inhomogeneous SII wave.

6.7 Conclusion and summary

In this paper a detailed analysis has been performed to expose how seismic wave scattering radiation patterns depend on fractional and absolute changes in the anisotropic and viscoelastic properties of the medium. In particular we have shown how to decompose the P-to-P, P-to-SI, SI-to-SI and SII-to-SII scattering potentials into isotropic-elastic, anisotropic-elastic, isotropic-viscoelastic and anisotropic-viscoelastic components.

In an anisotropic medium when attenuation is included (by, for instance, adding an appropriately parameterized imaginary part to the stiffness tensor) there arise additional terms associated with the quality factors and anelastic Thomsen parameters. In calculations made assuming that the medium is weakly anisotropic and weakly attenuative, all inverse quality factors and Thomsen parameters are much smaller than unity, so that orders of

scattering in the fractional changes in all properties can be neglected, and relatively simple forms for scattering potentials emerge. In our formulation the complex Thomsen parameters are so written that the real part separately characterizes the medium anisotropy and the imaginary part characterizes the combined anisotropy-viscoelasticity of the medium. We also assumed that reference medium in which all wave propagation take place is a homogeneous isotropic viscoelastic. In this case, we can use the isotropic polarization and slowness vectors for reference medium. This greatly simplifies the analytical expressions, which is complicated by using the analytical form of the polarization and slowness vectors in anisotropic media.

These results have the benefit of accommodating multidimensional geological structures, and providing the key quantity needed compute seismic full waveform inversion sensitivities for multi-parameter anisotropic-viscoelastic models. The sensitivity analysis for scattered waves can using these results be carried out in detail, suggesting, for instance, optimal model parametrizations for FWI. This is a key step in developing and appraising the FWI problem in anisotropic-viscoelastic media.

Appendix F

Propagation and attenuation vectors

Propagation and attenuation vectors for incident P-wave are

$$\mathbf{P}_{\mathrm{P}}^{\mathrm{In}} = \frac{\omega}{V_{\mathrm{P}}}(\mathbf{z}\cos\theta_{\mathrm{P}} + \mathbf{x}\sin\theta_{\mathrm{P}}), \tag{F.1}$$

$$\mathbf{A}_{\mathrm{P}}^{\mathrm{In}} = \frac{\omega}{2V_{\mathrm{P}}} Q_{\mathrm{P0}}^{-1} \sec\delta_{\mathrm{P}}^{\mathrm{In}}(\mathbf{z}\cos(\theta_{\mathrm{P}} - \delta_{\mathrm{P}}^{\mathrm{In}}) + \mathbf{x}\sin(\theta_{\mathrm{P}} - \delta_{\mathrm{P}}^{\mathrm{In}})), \tag{F.2}$$

scattered P-wave

$$\mathbf{P}_{\mathrm{P}}^{\mathrm{Sc}} = \frac{\omega}{V_{\mathrm{P}}}(\mathbf{x}\sin\theta_{\mathrm{P}} - \mathbf{z}\cos\theta_{\mathrm{P}}), \tag{F.3}$$

$$\mathbf{A}_{\mathrm{P}}^{\mathrm{Sc}} = \frac{\omega}{2V_{\mathrm{P}}} Q_{\mathrm{P0}}^{-1} \sec\delta_{\mathrm{P}}^{\mathrm{Sc}}(\mathbf{x}\sin(\theta_{\mathrm{P}} - \delta_{\mathrm{P}}^{\mathrm{Sc}}) - \mathbf{z}\cos(\theta_{\mathrm{P}} - \delta_{\mathrm{P}}^{\mathrm{Sc}})), \tag{F.4}$$

incident S-wave

$$\mathbf{P}_{\mathrm{S}}^{\mathrm{In}} = \frac{\omega}{V_{\mathrm{S}}}(\mathbf{z}\cos\theta_{\mathrm{S}} + \mathbf{x}\sin\theta_{\mathrm{S}}), \tag{F.5}$$

$$\mathbf{A}_{\mathrm{S}}^{\mathrm{In}} = \frac{\omega}{2V_{\mathrm{S}}} Q_{\mathrm{S0}}^{-1} \sec\delta_{\mathrm{S}}^{\mathrm{In}}(\mathbf{z}\cos(\theta_{\mathrm{S}} - \delta_{\mathrm{S}}^{\mathrm{In}}) + \mathbf{x}\sin(\theta_{\mathrm{S}} - \delta_{\mathrm{S}}^{\mathrm{In}})), \tag{F.6}$$

scattered S-wave

$$\mathbf{P}_{\mathrm{S}}^{\mathrm{Sc}} = \frac{\omega}{V_{\mathrm{S}}}(\mathbf{x}\sin\theta_{\mathrm{S}} - \mathbf{z}\cos\theta_{\mathrm{S}}), \tag{F.7}$$

$$\mathbf{A}_{\mathrm{S}}^{\mathrm{Sc}} = \frac{\omega}{2V_{\mathrm{S}}} Q_{\mathrm{S0}}^{-1} \sec\delta_{\mathrm{S}}^{\mathrm{Sc}}(\mathbf{x}\sin(\theta_{\mathrm{S}} - \delta_{\mathrm{S}}^{\mathrm{Sc}}) - \mathbf{z}\cos(\theta_{\mathrm{S}} - \delta_{\mathrm{S}}^{\mathrm{Sc}})). \tag{F.8}$$

Table F.1: Notation

Symbol	Explanation	Symbol	Explanation
$\mathbf{P}_{\mathrm{P}}^{\mathrm{In}}$	Incident P-wave propagation vector	$\mathbf{A}_{\mathrm{P}}^{\mathrm{In}}$	Incident P-wave attenuation vector
$\mathbf{P}_{\mathrm{S}}^{\mathrm{In}}$	Incident S-wave propagation vector	$\mathbf{A}_{\mathrm{S}}^{\mathrm{In}}$	Incident S-wave attenuation vector
$\mathbf{P}_{\mathrm{P}}^{\mathrm{Sc}}$	Scattered P-wave propagation vector	$\mathbf{A}_{\mathrm{P}}^{\mathrm{Sc}}$	Scattered P-wave attenuation vector
$\mathbf{P}_{\mathrm{S}}^{\mathrm{Sc}}$	Scattered S-wave propagation vector	$\mathbf{A}_{\mathrm{S}}^{\mathrm{Sc}}$	Scattered S-wave attenuation vector
$\mathbf{K}_{\mathrm{P}}^{\mathrm{In}}$	Incident P-wave wavnumber vector	$\mathbf{K}_{\mathrm{S}}^{\mathrm{In}}$	Incident S-wave wavnumber vector
$\mathbf{K}_{\mathrm{P}}^{\mathrm{Sc}}$	Scattered P-wave wavnumber vector	$\mathbf{K}_{\mathrm{S}}^{\mathrm{Sc}}$	Scattered S-wave wavnumber vector
$\mathbf{k}_{\mathrm{P}}^{\mathrm{In}}$	Incident P-wave slowness vector	$\mathbf{k}_{\mathrm{S}}^{\mathrm{In}}$	Incident S-wave slowness vector
$\mathbf{k}_{\mathrm{P}}^{\mathrm{Sc}}$	Scattered P-wave slowness vector	$\mathbf{k}_{\mathrm{S}}^{\mathrm{Sc}}$	Scattered S-wave slowness vector
$\boldsymbol{\mathcal{I}}_{\mathrm{P}}$	Incident P-wave polarization vector	$\boldsymbol{\mathcal{S}}_{\mathrm{P}}$	Scattered P-wave polarization vector
$\boldsymbol{\mathcal{I}}_{\mathrm{S}}$	Incident S-wave polarization vector	$\boldsymbol{\mathcal{S}}_{\mathrm{S}}$	Scattered S-wave polarization vector
θ_{P}	Incident/Scattered P-wave phase angle	θ_{S}	Incident/Scattered S-wave phase angle
$\delta_{\mathrm{P}}^{\mathrm{In}}$	Incident P-wave attenuation angle	$\delta_{\mathrm{S}}^{\mathrm{In}}$	Incident S-wave attenuation angle
$\delta_{\mathrm{P}}^{\mathrm{Sc}}$	Scattered P-wave attenuation angle	$\delta_{\mathrm{S}}^{\mathrm{Sc}}$	Scattered S-wave attenuation angle
V_{P}	P-wave velocity	V_{S}	S-wave velocity
Q_{P}	P-wave quality factor	Q_{S}	S-wave quality factor

Chapter 7

Compressional wave scattering potentials and linearized reflection coefficients in elastic and low-loss viscoelastic orthorhombic media

7.1 Abstract

Amplitude variation with offset is usually described using the approximate solutions of Zoeppritz equation for a low contrast medium. Calculations require determination of slowness and polarization vectors. Exact solutions yield complicated functions in terms of medium properties in upper and lower medium as well as incident and transmitted phase angles. Similar results hold using the Born approximations based on the first order perturbation theory. In this paper taking advantages of using Born approximation, scattering potential and linearized reflection coefficients for a weak anisotropic, low-loss viscoelastic orthorhombic media are derived for P-to-P, P-to-SV and P-to-SH waves. An elastic orthorhombic stiffness tensor is described by nine real independent parameters including vertical P- and S-wave velocities and seven generalized Thompson parameters characterize the weak anisotropy in medium. If attenuation taken into account, the stiffness tensor components become complex whose imaginary parts are connected to the quality factors and Q-Thompson parameters. In deriving our results we assume that the reference medium is isotropic (visco)elastic however the perturbations are both in anisotropic and isotropic-(visco)elastic properties.

Comparing to the previously derived converted wave AVAz equations our derivations are new in two ways. Firstly, we avoid the complications of solution of Zoeppritz equations by using the Born approximation based on the first order perturbation theory. Secondly, we obtained the extra terms in AVAZ equations due to both anelasticity in medium and inhomogeneity of the wave.

7.2 Introduction

Amplitude variation with offset (AVO) and amplitude-variation-with-azimuth (AVAz) play a key role in exploration seismology, particularly in reservoir characterization, parameter imaging and migration/inversion (Tsvankin et al., 2010; Castagna and Backus, 1993). The generalization of the AVO equations to encompass volume/point scattering (Stolt and Weglein, 2012) connects them, furthermore, to multi-parameter sensitivity calculations in full waveform inversion, or FWI (Innanen, 2014). The management and use of seismic attenuation in both AVO-AVAz (Chapman et al., 2006; Innanen, 2011; Wu et al., 2014; Behura and Tsvankin, 2009b) and elastic-anisotropic FWI (Causse et al., 1999; Charara et al., 2000; Fichtner, 2010; Fichtner and van Driel, 2014; Hak and Mulder, 2011; Métivier et al., 2015; Yang et al., 2016; Kamei and Pratt, 2013; Keating and Innanen, 2017) is an important and complicating issue. Media which exhibit both viscoelastic and anisotropic features simultaneously are significantly more challenging to quantitatively describe than their elastic-anisotropic counterparts, and are only beginning to receive the attention they warrant (Carcione et al., 1998; Bai and Tsvankin, 2016; Bai et al., 2017).

Analysis of the seismic compressional wave (P-wave) in isolation, as opposed to the full multicomponent problem, while approximate, captures a significant fraction of the information content of the seismic signal (Ostrander, 1984). Approximate compressional wave-to-compressional wave (hereafter PP) reflection coefficients for weak-contrast interfaces separating elastic, weakly transversely isotropic media for vertical and horizontal axis of symmetry were derived by Rüger (1997, 1998, 2002). These results were obtained through linearization of exact reflection coefficient expressions in parameter perturbations and angle quantities, and by assuming weak anisotropy. Rüger (1997) modified linearized PP reflection coefficients previously derived by Thomsen (1993), admitting larger angles of incidence. PP reflection coeffients for weak-contrast interfaces separating two weakly, but arbitrarily, anisotropic media were derived by Cervený and Psencík (1998).

In isotropic viscoelastic media, reflection/transmission coefficients have been widely expressed and analyzed (Hearn and Krebes, 1990; Krebes, 1983, 1984; Ursin and Stovas, 2002; Stovas and Ursin, 2003; Borcherdt, 2009). For isotropic-over-anisotropic viscoelastic media,

linearized reflection coefficients based on exact solutions of the plane-wave Zoeppritz equations are generally adopted to carry out the associated AVO-type inversion/modelling. An effort has recently been made to generate practical linearized forms for reflection coefficients in viscoelastic-anisotropic media. This is a relatively complicated undertaking, primarily because of the complexity of the slownesses and polarizations in the presence of anisotropy. Moradi and Innanen (2016) derived AVO equations taking into account jumps across the reflecting boundary in the attenuation angle for inhomogeneous waves. The value of these is quantitive, but also qualitative, in our view, as a means of interpreting the expected impact on AVO signatures of perturbations in the five viscoelastic parameters.

In the presence of both anelasticity and anisotropy, PP reflections near and beyond the critical angle are affected by attenuation. Both quality factors and anisotropic parameters has no effect on the zero offset P-wave reflection coefficients and anisotropy has more influence on small angle reflectivity than the attenuation (Carcione et al., 1998). The reflection and transmission problem in viscoelastic transversely isotropic media for a homogeneous incident wave was studied by Carcione (1997) and Stovas and Ursin (2003). The effect on the AVO-VTI equations of incorporating inhomogeneity within the incident wave has subsequently also been comprehensively analyzed (Zhu and Tsvankin, 2006b; Behura and Tsvankin, 2009b,a).

The research summarized in this paper is part of an effort to derive interpretable and useable formulas for both AVO-AVAz and full waveform inversion (FWI) sensitivity analysis, in the presence of anisotropy and attenuation. The FWI and AVO goals can be accomplished more or less simultaneously because of the close connections that can be found between linearized reflection coefficients, e.g., the Aki-Richards approximation (Aki and Richards, 2002), scattering potentials (Stolt and Weglein, 2012), and FWI sensitivity kernels (Tarantola, 1986; Fichtner, 2010). The problem of volume scattering from viscoelastic-anisotropic inclusions alone is of interest, and contains some almost entirely unexplored features, but it lends itself well to the double task of AVO/FWI sensitivity determination. We begin by setting up a scattering framework to describe the interaction of seismic waves with arbitrary perturbations in viscoelastic orthorhombic media. We consider two cases. First, we assume that the reference wave field propagates in an isotropic-elastic reference medium, and is scattered by general viscoelastic-orthorhombic perturbations. The planar interface/specular reflection

analog of this involves an isotropic-elastic upper half-space and an orthorhombic lower half-space. Second, we assume that the reference medium is isotropic-viscoelastic, and that waves scatter from viscoelastic-orthorhombic perturbations. In both cases we analytically examine the relationship between the scattering potentials and the results of linearization of the exact anisotropic-viscoelastic Zoeppritz equations. We show that the former reduce to the latter.

7.3 Viscoelastic orthorhombic media

The most common model of orthorhombic symmetry involves parallel vertical fractures embedded in a vertical transversely isotropic (VTI) background (figure 7.1). The stiffness matrix for an elastic orthorhombic medium is given by (Ikelle and Amundsen, 2005)

$$C_{\text{orth}} = \begin{pmatrix} C_{11} & C_{12} & C_{13} & 0 & 0 & 0 \\ C_{12} & C_{22} & C_{23} & 0 & 0 & 0 \\ C_{13} & C_{23} & C_{33} & 0 & 0 & 0 \\ 0 & 0 & 0 & C_{44} & 0 & 0 \\ 0 & 0 & 0 & 0 & C_{55} & 0 \\ 0 & 0 & 0 & 0 & 0 & C_{66} \end{pmatrix}. \tag{7.1}$$

If the medium is attenuative, the stiffness tensor is complex, with an imaginary part related to attenuation. The imaginary part is parameterized by a set of quality factors, $Q_{ij} = C_{ij}/C_{ij}^{\text{I}}$, where C_{ij} and C_{ij}^{I} are real and imaginary parts of the stiffness tensor components; each independent component of the stiffness tensor has a corresponding quality factor. Model parametrization has a strong influence on full waveform inversion (Prieux et al., 2013; Gholami et al., 2013; Oh and Alkhalifah, 2016; Masmoudi and Alkhalifah, 2016). Orthorhombic-viscoelastic models can be expressed through at least three different parameterizations, each with between 15 and 18 independent parameters. Which, and how many, of these parameters can be practically constrained in FWI or AVO settings is presently unclear. But, in both cases, quantification of scattering, whether from point or planar perturbations, is the first step in providing answers to such questions.

The first of the three directly involves the real and imaginary parts of the stiffness tensor in equation (7.1). This parameterization is useful primarily for forward modelling of the

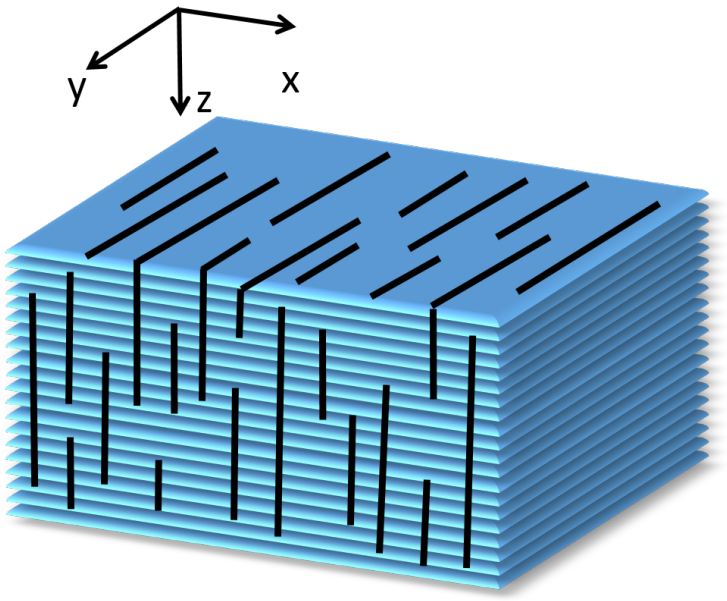

Figure 7.1: Schematic representation of orthorhombic media.

wave propagation.

The second involves 15 parameters in total, including the real part of the stiffness tensor, which can be described by 6 P- and S-wave velocity parameters with different polarizations, three off-diagonal elements, C_{12}, C_{13} and C_{23}, and 6 attenuation terms. The P-wave phase velocity along the vertical axis z is given by $V_{\mathrm{P}} = \sqrt{\rho^{-1}C_{33}}$, the horizontal P-wave velocity along the x-direction is given by $\sqrt{\rho^{-1}C_{11}}$ and along the y-direction by $\sqrt{\rho^{-1}C_{22}}$. The vertical S-wave velocity polarized in the x-direction is given by $V_{\mathrm{S}} = \sqrt{\rho^{-1}C_{55}}$, and the same velocity polarized in the y direction is given by $\sqrt{\rho^{-1}C_{44}}$. The horizontal S-wave velocity polarized in x-direction is given by $\sqrt{\rho^{-1}C_{66}}$. Rather than through the imaginary parts of the stiffness tensor, attenuation is characterized by the components of a quality factor tensor (Červeny̌ and Pšenčík, 2008). The components of this tensor are the quality factors emerging from the forms of the complex P-wave velocities. Q_{11}, Q_{22} and Q_{33} are the P-wave quality factors related to the P-wave velocities in the x, y and z-directions respectively. Similarly, Q_{44} can be interpreted as the SV-wave quality factor, and Q_{55} and Q_{66} are the SH-wave quality factors for velocities polarized in the z- and y-directions respectively. The full details of the phase velocity and quality factor scheme is summarized in Table 7.1.

The anisotropic-viscoelastic components deponed to the nine velocity parameters and

Symmetry-plane / Wave property		xy θ respect to y-axis		xz θ respect to z-axis		yz θ respect to z-axis	
		Vertical $\theta = 0°$	Horizental $\theta = 90°$	Vertical $\theta = 0°$	Horizental $\theta = 90°$	Vertical $\theta = 0°$	Horizental $\theta = 90°$
P-wave	Phase velocity	$\sqrt{C_{22}/\rho}$	$\sqrt{C_{11}/\rho}$	$\sqrt{C_{33}/\rho}$	$\sqrt{C_{11}/\rho}$	$\sqrt{C_{33}/\rho}$	$\sqrt{C_{22}/\rho}$
	Quality factor	Q_{22}	Q_{11}	Q_{33}	Q_{11}	Q_{33}	Q_{22}
SV-wave	Phase velocity	$\sqrt{C_{66}/\rho}$	$\sqrt{C_{66}/\rho}$	$\sqrt{C_{55}/\rho}$	$\sqrt{C_{55}/\rho}$	$\sqrt{C_{44}/\rho}$	$\sqrt{C_{44}/\rho}$
	Quality factor	Q_{66}	Q_{66}	Q_{55}	Q_{55}	Q_{44}	Q_{44}
SH-wave	Phase velocity	$\sqrt{C_{44}/\rho}$	$\sqrt{C_{55}/\rho}$	$\sqrt{C_{44}/\rho}$	$\sqrt{C_{66}/\rho}$	$\sqrt{C_{55}/\rho}$	$\sqrt{C_{66}/\rho}$
	Quality factor	Q_{44}	Q_{55}	Q_{44}	Q_{66}	Q_{55}	Q_{66}

Table 7.1: Phase velocity for P-, SV and SH waves in terms of diagonal componenets of stiffness tensor.

VTI anisotropic parameters		
	Thomsen parameters	Q-dependent Thomsen parameters
xy-plane	$\varepsilon^{(1)} = \frac{C_{22}-C_{33}}{2C_{33}}$	$\varepsilon_Q^{(1)} = \frac{Q_{33}-Q_{22}}{Q_{22}}$
	$\delta^{(1)} = \frac{(C_{23}+C_{44})^2-(C_{33}-C_{44})^2}{2C_{33}(C_{33}-C_{44})}$	$\delta_Q^{(1)} = \frac{C_{23}}{C_{33}}\frac{Q_{33}-Q_{23}}{Q_{23}} + 2\frac{C_{44}}{C_{33}}\frac{Q_{33}-Q_{44}}{Q_{44}}$
	$\gamma^{(1)} = \frac{C_{66}-C_{55}}{2C_{55}}$	$\gamma_Q^{(1)} = \frac{Q_{55}-Q_{66}}{Q_{66}}$
zy-plane	$\varepsilon^{(2)} = \frac{C_{11}-C_{33}}{2C_{33}}$	$\varepsilon_Q^{(2)} = \frac{Q_{33}-Q_{11}}{Q_{11}}$
	$\delta^{(2)} = \frac{(C_{13}+C_{55})^2-(C_{33}-C_{55})^2}{2C_{33}(C_{33}-C_{55})}$	$\delta_Q^{(2)} = \frac{C_{13}}{C_{33}}\frac{Q_{33}-Q_{13}}{Q_{13}} + 2\frac{C_{55}}{C_{33}}\frac{Q_{33}-Q_{55}}{Q_{55}}$
	$\gamma^{(2)} = \frac{C_{66}-C_{44}}{2C_{44}}$	$\gamma_Q^{(2)} = \frac{Q_{44}-Q_{66}}{Q_{66}}$
xz-plane	$\delta^{(3)} = \frac{(C_{12}+C_{66})^2-(C_{11}-C_{66})^2}{2C_{11}(C_{11}-C_{66})}$	$\delta_Q^{(3)} = \frac{C_{12}}{C_{11}}\frac{Q_{11}-Q_{12}}{Q_{12}} + 2\frac{C_{66}}{C_{11}}\frac{Q_{11}-Q_{66}}{Q_{66}}$

Table 7.2: Generalized Thomsen parameters for orthorhombic media in terms of VTI parameters in xz, xy and zy planes.

nine quality factors based on the assumption of both weak anisotropy and attenuation(Zhu and Tsvankin, 2006a).

7.4 Scattering potential

The scattering potential is a complete description of the difference between a background, or reference medium, and a perturbed medium (Sato et al., 2012). It is a core quantity in all scattering descriptions of waves, including the linearized single-scattering or Born approximation. Alone it bears a close connection with linearized reflection coefficient approximations, and within the Born approximation it leads directly to forms for FWI sensitivities. We suppose that the values of density and stiffness tensor components change slightly from their reference values, $\rho^{(0)}$ and $C^{(0)}_{ijkl}$, to their perturbed values (the viscoelastic model remains embedded in the complex stiffness components in this section):

$$\rho = \rho_0 + \Delta\rho, \tag{7.2}$$

$$C_{ijkl} = C^{(0)}_{ijkl} + \Delta C_{ijkl}, \tag{7.3}$$

where reference medium properties are labelled with the superscript '(0)'. Wave propagation is described by the Green's function or propagator. The scattered wave, which is the difference between the waves propagating in the reference and perturbed media, is expanded as a series. The first term of the series describes the sum of all instances of single scattering from the given by (Beylkin and Burridge, 1990):

$$\mathbb{S} = (\boldsymbol{\mathcal{S}} \cdot \boldsymbol{\mathcal{I}})\Delta\rho - \eta_{mn}\Delta C_{mn} = (\boldsymbol{\mathcal{S}} \cdot \boldsymbol{\mathcal{I}})\Delta\rho - (\mathcal{S}_i \mathrm{k}^{\mathrm{Sc}}_j \mathcal{I}_k \mathrm{k}^{\mathrm{I}}_l)\Delta C_{ijkl}, \tag{7.4}$$

where $\boldsymbol{\mathcal{S}}$ and $\boldsymbol{\mathcal{I}}$ are the scattered and incident polarizations, and $\mathbf{k}^{\mathrm{Sc}}$ and $\mathbf{k}^{\mathrm{In}}$ are the scattered and incident slowness vectors. In addition, $m = ij$ and $n = kl$ are the Voigt indices, with $11 \to 1, 22 \to 2, 33 \to 3, (23, 32) \to 4, (13, 31) \to 5, (12, 21) \to 6$.

To expose the effects of anisotropy on scattering radiation patterns, we express the perturbation in the stiffness tensor in terms of the perturbations in both viscoelastic and anisotropic parameters. In the case of a reference medium that is isotropic and elastic (Figure 7.2) we

have

$$
\begin{aligned}
\Delta C_{11} &= \Delta C_{33} + 2C_{33}^{(0)}\varepsilon^{(2)},\\
\Delta C_{22} &= \Delta C_{33} + 2C_{33}^{(0)}\varepsilon^{(1)},\\
\Delta C_{66} &= \frac{1}{2}(\Delta C_{55} + \Delta C_{44}) + C_{55}^{(0)}\left[\gamma^{(1)} + \gamma^{(2)}\right],\\
\Delta C_{23} &= \Delta C_{33} - 2\Delta C_{44} + C_{33}^{(0)}\delta^{(1)},\\
\Delta C_{13} &= \Delta C_{33} - 2\Delta C_{55} + C_{33}^{(0)}\delta^{(2)},\\
\Delta C_{12} &= \Delta C_{33} - (\Delta C_{55} + \Delta C_{44}) + C_{33}^{(0)}\left[\delta^{(3)} + 2\varepsilon^{(2)}\right] - 2C_{55}^{(0)}\left[\gamma^{(1)} + \gamma^{(2)}\right].
\end{aligned}
\tag{7.5}
$$

Inserting equation (7.5) into equation (7.4), we obtain the general form of the scattering potential in terms of the inner products of polarization and slowness vectors:

$$
\mathbb{S} = [\rho]\Delta\rho - [C_{33}]\Delta C_{33} - [C_{44}]\Delta C_{44} - [C_{55}]\Delta C_{55} - \sum_{A}[A]A, \tag{7.6}
$$

where A refers to the anisotropic parameters. In addition sensitivities are

$$
\begin{aligned}
[\rho] =& \boldsymbol{\mathcal{S}} \cdot \boldsymbol{\mathcal{I}},\\
[C_{33}] =& (\boldsymbol{\mathcal{S}} \cdot \mathbf{k}^{\mathrm{Sc}})(\boldsymbol{\mathcal{I}} \cdot \mathbf{k}^{\mathrm{I}}),\\
[C_{55}] =& -(\mathcal{S}_1\mathrm{k}_1^{\mathrm{Sc}}\mathcal{I}_2\mathrm{k}_2^{\mathrm{I}} + \mathcal{S}_2\mathrm{k}_2^{\mathrm{Sc}}\mathcal{I}_1\mathrm{k}_1^{\mathrm{I}}) - 2(\mathcal{S}_1\mathrm{k}_1^{\mathrm{Sc}}\mathcal{I}_3\mathrm{k}_3^{\mathrm{I}} + \mathcal{S}_3\mathrm{k}_3^{\mathrm{Sc}}\mathcal{I}_1\mathrm{k}_1^{\mathrm{I}})\\
&+ (\mathcal{S}_1\mathrm{k}_3^{\mathrm{Sc}} + \mathcal{S}_3\mathrm{k}_1^{\mathrm{Sc}})(\mathcal{I}_1\mathrm{k}_3^{\mathrm{I}} + \mathcal{I}_3\mathrm{k}_1^{\mathrm{I}}) + \frac{1}{2}(\mathcal{S}_1\mathrm{k}_2^{\mathrm{Sc}} + \mathcal{S}_2\mathrm{k}_1^{\mathrm{Sc}})(\mathcal{I}_1\mathrm{k}_2^{\mathrm{I}} + \mathcal{I}_2\mathrm{k}_1^{\mathrm{I}})\\
[C_{44}] =& -(\mathcal{S}_1\mathrm{k}_1^{\mathrm{Sc}}\mathcal{I}_2\mathrm{k}_2^{\mathrm{I}} + \mathcal{S}_2\mathrm{k}_2^{\mathrm{Sc}}\mathcal{I}_1\mathrm{k}_1^{\mathrm{I}}) - 2(\mathcal{S}_2\mathrm{k}_2^{\mathrm{Sc}}\mathcal{I}_3\mathrm{k}_3^{\mathrm{I}} + \mathcal{S}_3\mathrm{k}_3^{\mathrm{Sc}}\mathcal{I}_2\mathrm{k}_2^{\mathrm{I}}),\\
&+ (\mathcal{S}_2\mathrm{k}_3^{\mathrm{Sc}} + \mathcal{S}_3\mathrm{k}_2^{\mathrm{Sc}})(\mathcal{I}_2\mathrm{k}_3^{\mathrm{I}} + \mathcal{I}_3\mathrm{k}_2^{\mathrm{I}}) + \frac{1}{2}(\mathcal{S}_1\mathrm{k}_2^{\mathrm{Sc}} + \mathcal{S}_2\mathrm{k}_1^{\mathrm{Sc}})(\mathcal{I}_1\mathrm{k}_2^{\mathrm{I}} + \mathcal{I}_2\mathrm{k}_1^{\mathrm{I}}),\\
[\gamma^{(1)}] =& [\gamma^{(2)}] = \mathrm{V}_{\mathrm{S0}}^2\left[(\mathcal{S}_1\mathrm{k}_2^{\mathrm{Sc}} + \mathcal{S}_2\mathrm{k}_1^{\mathrm{Sc}})(\mathcal{I}_1\mathrm{k}_2^{\mathrm{I}} + \mathcal{I}_2\mathrm{k}_1^{\mathrm{I}}) - 2\mathcal{S}_1\mathrm{k}_1^{\mathrm{Sc}}\mathcal{I}_2\mathrm{k}_2^{\mathrm{I}} - 2\mathcal{S}_2\mathrm{k}_2^{\mathrm{Sc}}\mathcal{I}_1\mathrm{k}_1^{\mathrm{I}}\right],\\
[\varepsilon^{(1)}] =& 2\mathrm{V}_{\mathrm{P0}}^2\mathcal{S}_2\mathrm{k}_2^{\mathrm{Sc}}\mathcal{I}_2\mathrm{k}_2^{\mathrm{I}},\\
[\varepsilon^{(2)}] =& 2\mathrm{V}_{\mathrm{P0}}^2\left(\mathcal{S}_1\mathrm{k}_1^{\mathrm{Sc}}\mathcal{I}_1\mathrm{k}_1^{\mathrm{I}} + \mathcal{S}_1\mathrm{k}_1^{\mathrm{Sc}}\mathcal{I}_2\mathrm{k}_2^{\mathrm{I}} + \mathcal{S}_2\mathrm{k}_2^{\mathrm{Sc}}\mathcal{I}_1\mathrm{k}_1^{\mathrm{I}}\right),\\
[\delta^{(1)}] =& \mathrm{V}_{\mathrm{P0}}^2\left(\mathcal{S}_2\mathrm{k}_2^{\mathrm{Sc}}\mathcal{I}_3\mathrm{k}_3^{\mathrm{I}} + \mathcal{S}_3\mathrm{k}_3^{\mathrm{Sc}}\mathcal{I}_2\mathrm{k}_2^{\mathrm{I}}\right),\\
[\delta^{(2)}] =& \mathrm{V}_{\mathrm{P0}}^2\left(\mathcal{S}_1\mathrm{k}_1^{\mathrm{Sc}}\mathcal{I}_3\mathrm{k}_3^{\mathrm{I}} + \mathcal{S}_3\mathrm{k}_3^{\mathrm{Sc}}\mathcal{I}_1\mathrm{k}_1^{\mathrm{I}}\right),\\
[\delta^{(3)}] =& \mathrm{V}_{\mathrm{P0}}^2\left(\mathcal{S}_1\mathrm{k}_1^{\mathrm{Sc}}\mathcal{I}_2\mathrm{k}_2^{\mathrm{I}} + \mathcal{S}_2\mathrm{k}_2^{\mathrm{Sc}}\mathcal{I}_1\mathrm{k}_1^{\mathrm{I}}\right).
\end{aligned}
\tag{7.7}
$$

As anisotropy vanishes, the above equation reduces to the scattering potential for an elastic wave traveling in an isotropic elastic medium interacting with perturbations in density and P- and S-wave velocities.

We have now seen that it is not too hard to measure the sensitivity of the scatter wave to the changes in stiffness tensor components. This simplicity and the high efficiency are the main reasons why Born approximation appear more attractive than the approach based on the solution of the Zoeppritz equation. Table 7.1 is an illustration of parametrization for the model of viscoelastic-orthorhombic media that we used for volume scattering versus low-contrast reflection. We divide the medium parameters into four parts: isotropic-elastic properties including density, vertical P- and S-wave velocities;isotropic-viscoelastic properties including vertical P- and S-wave quality factors; anisotropic-elastic properties characterized by seven weak Thomsen parameters and anisotropic-viscoelastic parameters characterized by seven Q-Thomsen parameters. We assumed that in volume scattering model, actual medium is anisotropic with isotropic reference medium which is equivalent to a low-contrast medium with isotropic upper(incident) layer above an anisotropic medium.

7.5 Scattering of P-wave to P-wave

First we restrict ourselves to the case of isotropic elastic background filled with perturbations in both elastic and anisotropic properties (Figure 7.2a), i.e., use the results of the previous section neglecting imaginary components of the stiffness tensor. The isotropic reference medium is described by $(\rho_0, V_{\mathrm{P}0}, V_{\mathrm{S}0})$ and the anisotropic perturbed medium by $(\rho, V_{\mathrm{P}}, V_{\mathrm{S}}, \delta^{(1)}, \delta^{(2)}, \delta^{(3)}, \varepsilon^{(1)}, \varepsilon^{(2)}, \gamma^{(1)}, \gamma^{(2)})$. The perturbations in isotropic parameters that cause scattering are, then, fractional changes in density $\Delta\rho/\rho = (\rho - \rho)/\rho$, P-wave velocity $\Delta V_P/V_P = (V_{\mathrm{P}} - V_{\mathrm{P}0})/V_{\mathrm{P}}$ and S-wave velocity $\Delta V_S/V_S = (V_{\mathrm{S}} - V_{\mathrm{S}0})/V_{\mathrm{S}}$. Because the reference medium is isotropic, the anisotropic parameters themselves act as perturbations. The angle between the incident and scattered wavefield, referred to as the opening angle, is denoted $2\theta_{\mathrm{P}}$. From the results that we obtained in previous section, it follows that the scattering potential for PP-wave is given by

$$\mathrm{S}^{\mathrm{E}}_{\mathrm{PP}} = \rho_0^{-1}\mathbb{S} = \mathrm{S}^{\mathrm{IE}}_{\mathrm{PP}} + \mathrm{S}^{\mathrm{AE}}_{\mathrm{PP}}, \tag{7.8}$$

where the isotropic-elastic (IE) and anisotropic-elastic (AE) parts are

$$\mathrm{S}^{\mathrm{IE}}_{\mathrm{PP}} = -(1 + \cos 2\theta_{\mathrm{P}} - 2V^2_{\mathrm{SP}} \sin^2 2\theta_{\mathrm{P}})A_\rho - 2A_{V_{\mathrm{P}}} + 4V^2_{\mathrm{SP}} \sin^2 2\theta_{\mathrm{P}} A_{V_{\mathrm{S}}}, \tag{7.9}$$

$$\begin{aligned}\mathrm{S}^{\mathrm{AE}}_{\mathrm{PP}} = &\left[4V_{\mathrm{SP}}^2\cos^2\varphi(\gamma^{(1)}-\gamma^{(2)}) - 2^{-1}(\sin^2\varphi\delta^{(1)}+\cos^2\varphi\delta^{(2)})\right]\sin^2 2\theta_{\mathrm{P}} \\ &- 2\left[\cos^2\varphi\sin^2\varphi\delta^{(3)} + \sin^4\varphi\varepsilon^{(1)} + \left(\cos^2\varphi+\cos^2\varphi\sin^2\varphi\right)\varepsilon^{(2)}\right]\sin^4\theta_{\mathrm{P}}.\end{aligned} \tag{7.10}$$

Here A_ρ is the fractional perturbation in density, $A_{V_{\mathrm{P}}}$ is the fractional perturbation in the P-wave velocity, and $A_{V_{\mathrm{S}}}$ is the fractional perturbation in the S-wave velocity. It is apparent that: (1) the anisotropic parameters do not influence the scattered wave for a vertically-incident wave, and (2) to recover the isotropic scattering potential, one may set the anisotropic parameters to zero.

By inspection of (7.10), the scattered wave is observed to be sensitive to the difference $\gamma^{(S)} = \gamma^{(1)} - \gamma^{(2)}$ rather than $\gamma^{(1)}$ and $\gamma^{(2)}$ individually. For VTI media, $\varepsilon^{(1)} = \varepsilon^{(2)} = \varepsilon$, $\delta^{(1)} = \delta^{(2)} = \delta$ and $\gamma^{(S)} = \delta^{(3)} = 0$, and as a result the anisotropic part of the scattering potential reduces to

$$\mathrm{S}^{\mathrm{AE}}_{\mathrm{PP,VTI}} = -2\sin^2\theta_{\mathrm{P}}\delta - 2\sin^4\theta_{\mathrm{P}}(\varepsilon-\delta). \tag{7.11}$$

In fact, for small angles of incidence, the second term is negligible compared to the first term, that is, the effect of δ dominates over that of ε. For HTI media, $\varepsilon^{(1)} = 0$, $\varepsilon^{(2)} = \varepsilon^{(V)}$, $\delta^{(1)} = \delta^{(2)} = \delta^{(V)}$ and $\gamma^{(S)} = \gamma$, $\delta^{(1)} = 0$, $\delta^{(2)} = \delta^{(V)}$ and $\delta^{(3)} = \delta^{(V)} - 2\varepsilon^{(V)}$ so the anisotropic part of the scattering potential reduces to

$$\begin{aligned}\mathrm{S}^{\mathrm{AE}}_{\mathrm{PP,HTI}} =& 2\sin^2\theta_{\mathrm{P}}\cos^2\theta_{\mathrm{P}}\cos^2\varphi\left[8V_{\mathrm{SP}}^2\gamma - \delta^{(V)}\right] \\ &- 2\cos^2\varphi\left[\sin^2\varphi\delta^{(V)} + \cos^2\varphi\varepsilon^{(V)}\right]\sin^4\theta_{\mathrm{P}}.\end{aligned} \tag{7.12}$$

More details regarding the anisotropic parameters in HTI and VTI media and their connection to the parameters in orthorhombic media can be found in (Tsvankin, 1997, 1996).

In figures 7.4 and 7.3 the sensitivities of the scattered P-wave to perturbations in anisotropic parameters versus incident phase angle are plotted.

Specular scattering or reflection (involving two homogeneous half-spaces separated by a plane boundary) and volume scattering from a point perturbation from a homogeneous background, are asymptotically equivalent with diminishing contrast and opening angle. In our case the corresponding system of isotropic/anisotropic half-spaces involves a low contrast medium with boundary separating an isotropic elastic half-space from an anisotropic elastic medium with weak anisotropic properties. In Figure 7.2b such a low contrast, two layer medium is illustrated. The upper layer is an isotropic-elastic medium defined by

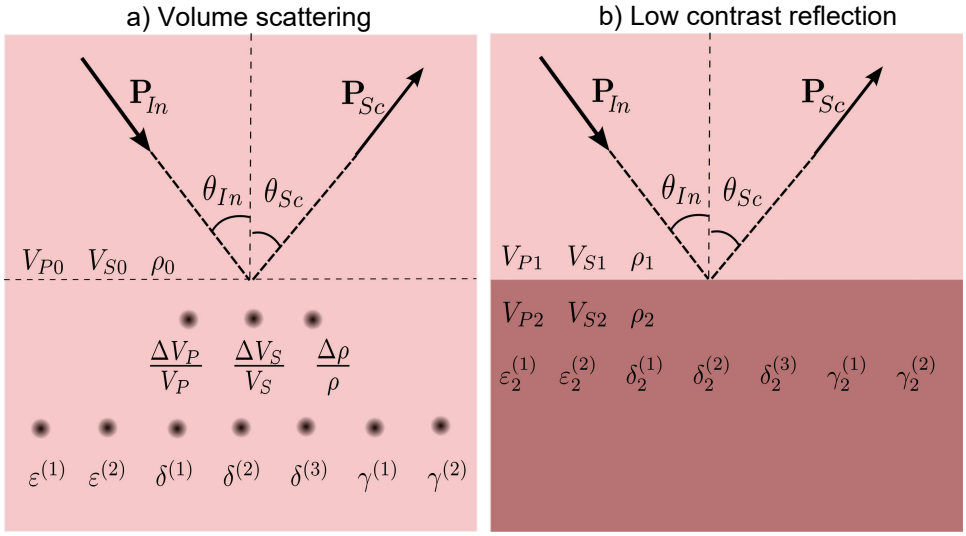

Figure 7.2: The low contrast model vs volume scattering model. (a) The boundary is assumed to involved welded contact between two media whose properties differ only slightly. Upper layer is isotropic elastic media defined by its P-wave velocity V_{P1}, S-wave velocity V_{S1}, and its density ρ_1. Lower layer is elastic orthorhombic media, by $V_{\mathrm{P2}}, V_{\mathrm{S2}}, \rho_2$ and seven Thompson parameters $\varepsilon_2^{(1)}, \varepsilon_2^{(2)}, \delta_2^{(1)}, \delta_2^{(2)}, \delta_2^{(3)}, \gamma_2^{(1)}, \gamma_2^{(2)}$. Incident and reflected propagation vectors are denoted by $\mathbf{P}_{\mathrm{i}}$ and $\mathbf{P}_{\mathrm{r}}$ respectively and θ_{P} is the incident phase angle. (b) Reference medium is perturbed by volume scattering perturbations; Back ground medium is isotropic elastic characterized by $V_{\mathrm{P0}}, V_{\mathrm{S0}}, \rho_0$ and perturbations are $\Delta V_{\mathrm{P}}, \Delta V_{\mathrm{S}}, \Delta\rho$ and in anisotropic parameters $\varepsilon^{(1)}$,$\varepsilon^{(2)}$, $\delta^{(1)}$,$\delta^{(2)}$,$\delta^{(3)}$,$\gamma^{(1)}$,$\gamma^{(2)}$

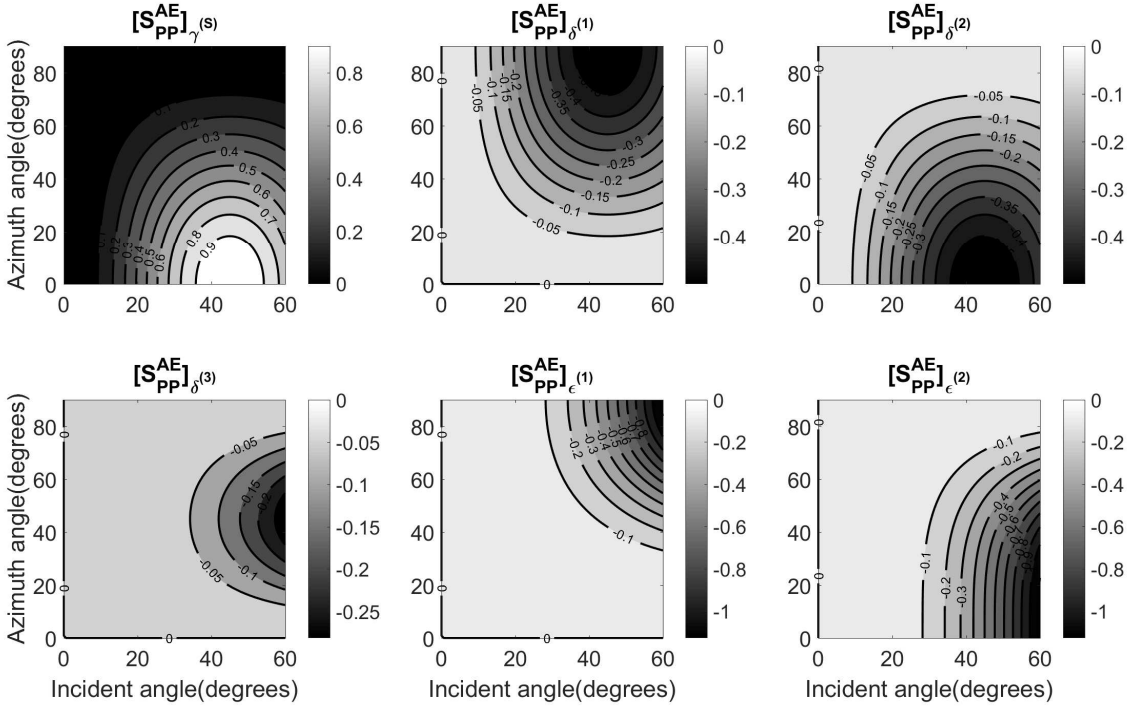

Figure 7.3: The maps of sensitivity of PP-scatter wave to the Thomsen parameters. Vertical axis is azimuth angle and horizontal axis is incident phase angle.

$(\rho_1, \mathrm{V_{P1}}, \mathrm{V_{S1}})$ in contact with a plane interface separating the top layer from the anisotropic elastic lower layer defined by $\left(\rho_2, , \mathrm{V_{P2}}, \mathrm{V_{S2}}, \delta_2^{(1)}, \delta_2^{(2)}, \delta_2^{(3)}, \varepsilon_2^{(1)}, \varepsilon_2^{(2)}, \gamma_2^{(1)}, \gamma_2^{(2)}\right)$. Fractional changes in isotropic properties are given by the fractional change in P-wave velocity, $\mathrm{A_{V_P}} = \Delta \mathrm{V_P}/\bar{\mathrm{V}}_\mathrm{P}$ where $\Delta \mathrm{V_P} = \mathrm{V_{P1}} - \mathrm{V_{P2}}$ and $\bar{\mathrm{V}}_\mathrm{P} = (\mathrm{V_{P1}} + \mathrm{V_{P2}})/2$ are respectively the difference and average of the the P-wave velocity in the lower and upper media; fractional changes in S-wave velocity, $\mathrm{A_{V_S}} = \Delta \mathrm{V_S}/\bar{\mathrm{V}}_\mathrm{S}$ where $\Delta \mathrm{V_S} = \mathrm{V_{S1}} - \mathrm{V_{S2}}$ and $\bar{\mathrm{V}}_\mathrm{S} = (\mathrm{V_{S1}} + \mathrm{V_{S2}})/2$, and fractional changes in density, $\mathrm{A}_\rho = \Delta\rho/\rho$ where $\Delta\rho = \rho_2 - \rho_1$ and $\rho = (\rho_2 + \rho_1)/2$. Linearizations are performed based on the anisotropic parameters in the lower layer rather than the differences in anisotropic parameters.

The scattering potentials that we obtained in the previous section can be used to obtain the amplitude variation with offset equations previously derived using the linearization of the Zoeppritz equations (Rüger, 1997). This can be seen intuitively from the fact that reflection coefficient is related to the scattering potential by

$$\mathrm{R_{PP}^E} = -\rho_0^{-1}(2\cos\theta_P)^{-2}\mathrm{S_{PP}^E} = \mathrm{R_{PP}^{IE}} + \mathrm{R_{PP}^{AE}},$$

	Volume scattering			Low-contrast reflection		
	Reference medium	Actual medium	Fractional perturbation	Upper layer	Lower layer	Fractional perturbation
Isotropic-Elastic	ρ_0 V_{P0} V_{S0}	ρ V_P V_S	$\frac{\rho-\rho_0}{\rho}$ $\frac{V_S-V_{S0}}{V_S}$ $\frac{V_P-V_{P0}}{V_P}$	ρ_1 V_{P1} V_{S1}	ρ_2 V_{P2} V_{S2}	$\frac{\rho_2-\rho_1}{2(\rho_2+\rho_1)}$ $\frac{V_{P2}-V_{P1}}{2(V_{P2}+V_{P1})}$ $\frac{V_{S2}-V_{S1}}{2(V_{S2}+V_{S1})}$
Isotropic-Viscoelastic	Q_{P0} Q_{S0}	Q_P Q_S	$\frac{Q_P-Q_{P0}}{Q_P}$ $\frac{Q_S-Q_{S0}}{Q_S}$	Q_{P1} Q_{S1}	Q_{P2} Q_{S2}	$\frac{Q_{P2}-Q_{P1}}{2(Q_{P2}+Q_{P1})}$ $\frac{Q_{S2}-Q_{S1}}{2(Q_{S2}+Q_{S1})}$
Anisotropic-Elastic	0	$\varepsilon^{(1)}$ $\delta^{(3)}$ $\varepsilon^{(2)}$ $\gamma^{(1)}$ $\delta^{(1)}$ $\gamma^{(2)}$ $\delta^{(2)}$	$\varepsilon^{(1)}$ $\delta^{(3)}$ $\varepsilon^{(2)}$ $\gamma^{(1)}$ $\delta^{(1)}$ $\gamma^{(2)}$ $\delta^{(2)}$	0	$\varepsilon_2^{(2)}$ $\delta_2^{(3)}$ $\varepsilon_2^{(1)}$ $\gamma_2^{(1)}$ $\delta_2^{(1)}$ $\gamma_2^{(2)}$ $\delta_2^{(2)}$	$\varepsilon_2^{(2)}$ $\delta_2^{(3)}$ $\varepsilon_2^{(1)}$ $\gamma_2^{(1)}$ $\delta_2^{(1)}$ $\gamma_2^{(2)}$ $\delta_2^{(2)}$
Anisotropic-Viscoelastic	0	$\varepsilon_Q^{(1)}$ $\delta_Q^{(3)}$ $\varepsilon_Q^{(2)}$ $\gamma_Q^{(1)}$ $\delta_Q^{(1)}$ $\gamma_Q^{(2)}$ $\delta_Q^{(2)}$	$\varepsilon_Q^{(1)}$ $\delta_Q^{(3)}$ $\varepsilon_Q^{(2)}$ $\gamma_Q^{(1)}$ $\delta_Q^{(1)}$ $\gamma_Q^{(2)}$ $\delta_Q^{(2)}$	0	$\varepsilon_{Q2}^{(1)}$ $\delta_{Q2}^{(3)}$ $\varepsilon_{Q2}^{(2)}$ $\gamma_{Q2}^{(1)}$ $\delta_{Q2}^{(1)}$ $\gamma_{Q2}^{(2)}$ $\delta_{Q2}^{(2)}$	$\varepsilon_{Q2}^{(1)}$ $\delta_{Q2}^{(3)}$ $\varepsilon_{Q2}^{(2)}$ $\gamma_{Q2}^{(1)}$ $\delta_{Q2}^{(1)}$ $\gamma_{Q2}^{(2)}$ $\delta_{Q2}^{(2)}$

Table 7.3: A table illustrating the perturbation terms used in volume scattering and low-contrast reflectivity. Medium properties are classified into isotropic-elastic, isotropic-viscoelastic, anisotropic-elastic and anisotropic-viscoelastic. In volume scattering scheme, the actual medium which is anisotropic-viscoelastic splits into the isotropic reference medium filled by the perturbations in medium properties. Since the reference medium is isotropic, anisotropic parameters in actual medium act as perturbations.

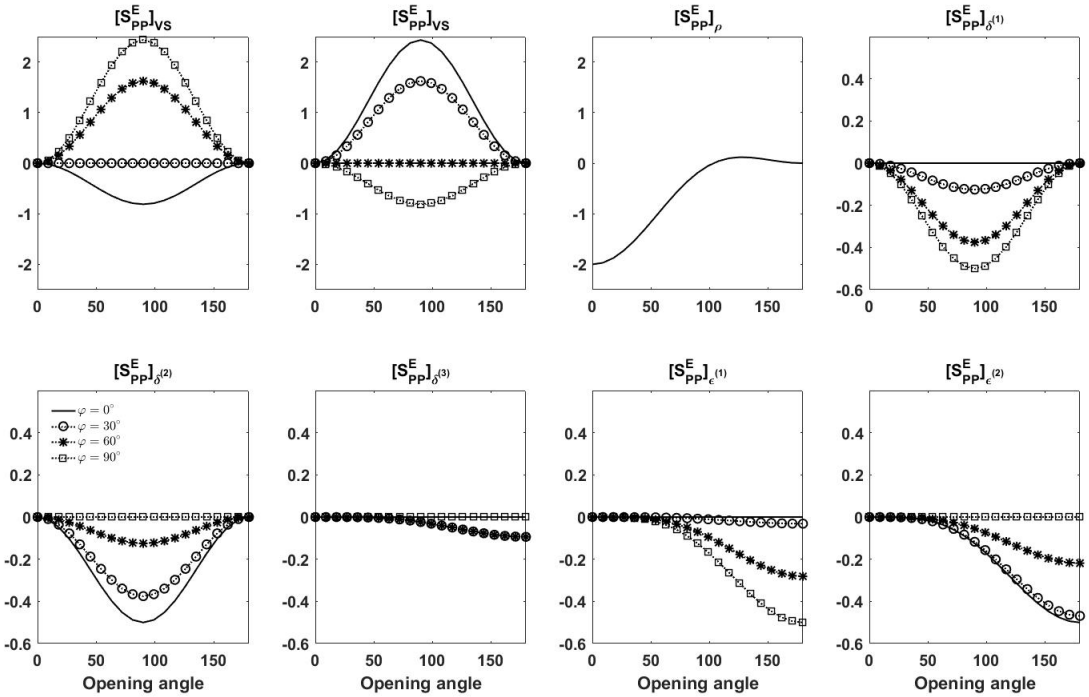

Figure 7.4: Sensitivity of the PP-scatter wave to the Thomsen parameters for azimuth angles 0°, 45°, 60°, 90°. Horizontal axis is opening angle $2\theta_P$.

where the isotropic-elastic reflection coefficient is

$$\mathrm{R}^{\mathrm{IE}}_{\mathrm{PP}} = 2^{-1}\mathrm{A}_{\mathrm{Z_P}} + \left(2^{-1}\mathrm{A}_{\mathrm{V_P}} - 2\mathrm{V}^2_{\mathrm{SP}}\mathrm{A}_{\mu}\right)\sin^2\theta_P + 2^{-1}\mathrm{A}_{\mathrm{V_P}}\tan^2\theta_P\sin^2\theta_P$$

and anisotropic elastic reflection coefficient is

$$\begin{aligned}\mathrm{R}^{\mathrm{AE}}_{\mathrm{PP}} =& 2^{-1}\left\{\delta^{(2)}_2 + \sin^2\varphi\left[\delta^{(1)}_2 - \delta^{(2)}_2 - 8\mathrm{V}^2_{\mathrm{SP}}\gamma^{(S)}_2\right]\right\}\sin^2\theta_P \\ &+ 2^{-1}\left\{\cos^2\varphi\sin^2\varphi\left[\delta^{(3)}_2 + \varepsilon^{(2)}_2 - \varepsilon^{(1)}_2\right] + \sin^2\varphi\left[\varepsilon^{(1)}_2 - \varepsilon^{(2)}_2\right] + \varepsilon^{(2)}_2\right\}\tan^2\theta_P\sin^2\theta_P,,\end{aligned} \tag{7.13}$$

and where $\mathrm{Z_P} = \rho\mathrm{V_P}$ is the P-wave impedance, $\mu = \rho V_S^2$ is the shear modulus, with the corresponding fractional changes $\mathrm{A_{Z_P}}$ and A_{μ}. Equation (7.13) is the linearized reflection coefficient as commonly expressed in the literature (Rüger, 1997; Cervený and Psencík, 1998; Rüger, 2002) for weak contrast interfaces separating two weakly orthorhombic media. As the incident half-space (i.e., the upper layer) is anisotropic, these authors used the complicated form of the polarization and slowness vectors for incident and reflected waves. After solving of the Zoeppritz equations, the amplitude of the reflected wave is linearized, obtaining equation

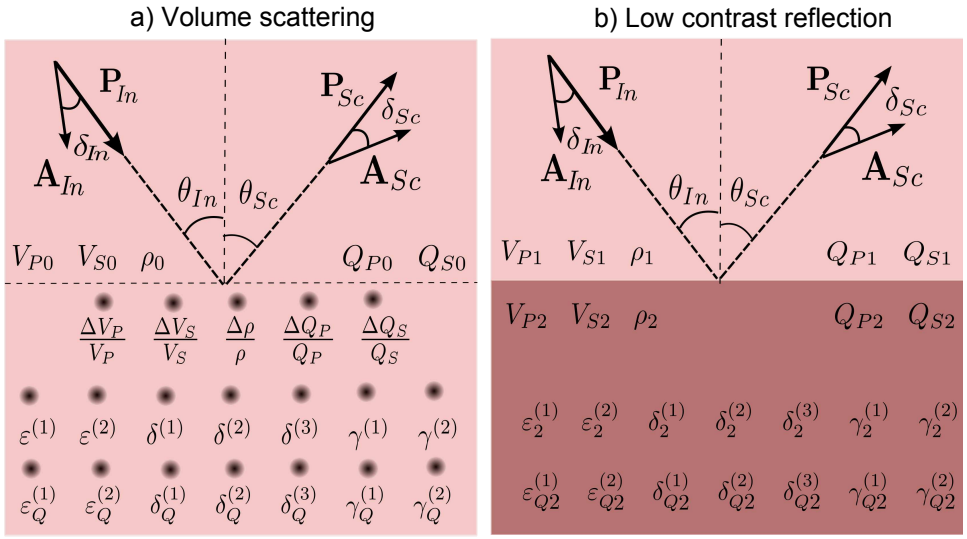

Figure 7.5: The low contrast model vs volume scattering model. (a) The boundary is assumed to involved welded contact between two media whose properties differ only slightly. Upper layer is isotropic viscoelastic media defined by its P-wave velocity V_{P1}, S-wave velocity V_{S1}, P-wave quality factor Q_{P1}, S-wave quality factor Q_{S1} and its density ρ_1; Lower layer is viscoelastic orthorhombic media, by by $V_{\mathrm{P2}}, V_{\mathrm{S2}}, Q_{\mathrm{P2}}, Q_{\mathrm{S2}}$ and ρ_2, seven anisotropic Thompson parameters $\varepsilon_2^{(1)}, \varepsilon_2^{(2)}, \delta_2^{(1)}, \delta_2^{(2)}, \delta_2^{(3)}, \gamma^{(1)}, \gamma^{(2)}$ and seven anisotropic-viscoelastic Thompson parameters $\varepsilon_{\mathrm{Q2}}^{(1)}, \varepsilon_{\mathrm{Q2}}^{(2)}, \delta_{\mathrm{Q2}}^{(1)}, \delta_{\mathrm{Q2}}^{(2)}, \delta_{\mathrm{Q2}}^{(3)}, \gamma_{\mathrm{Q2}}^{(1)}, \gamma_{\mathrm{Q2}}^{(2)}$. Incident and reflected attenuation angles are the equal by applying the Snell's law denoted by δ_{i}.(b) Reference medium is perturbed by volume scattering perturbations; Back ground medium is isotropic viscoelastic characterized by $V_{\mathrm{P0}}, V_{\mathrm{S0}}, Q_{\mathrm{P0}}, Q_{\mathrm{S0}}, \rho_0$ and perturbations are ΔV_{P},ΔV_{S},$\Delta\rho$ and in anisotropic parameters $\varepsilon^{(1)}$,$\varepsilon^{(2)}$,$\delta^{(1)}$,$\delta^{(2)}$,$\delta^{(3)}$,
$\gamma^{(1)}$,$\gamma^{(2)}$ and anisotropic viscoelastic parameters $\varepsilon_{\mathrm{Q}}^{(1)}$,$\varepsilon_{\mathrm{Q}}^{(2)}$,$\delta_{\mathrm{Q}}^{(1)}$,$\delta_{\mathrm{Q}}^{(2)}$,$\delta_{\mathrm{Q}}^{(3)}$,$\gamma_{\mathrm{Q}}^{(1)}$,$\gamma_{\mathrm{Q}}^{(2)}$. $\mathbf{P}_{\mathrm{Pi}}$ is the incident propagation vector; $\mathbf{P}_{\mathrm{Pr}}$ is the reflected(scattered) propagation vector; $\mathbf{A}_{\mathrm{Pi}}$ is the incident attenuation vector; $\mathbf{A}_{\mathrm{Pr}}$ is the reflected(scattered) attenuation vector and δ_{P} is the attenuation angle which is the same for incident and reflected wave.

(7.13). In our derivation, we used the incident half-space as an isotropic reference medium and used the polarizations and velocities for an isotropic media and obtained the same results. We conclude that for a low-contrast medium with two weakly-anisotropic half-spaces the linearized reflection coefficients are the same as those for which the incident half-space is isotropic.

For an isotropic upper half-space over a VTI medium, the anisotropic part of the reflectivity reduces to $2^{-1}(\sin^2\theta_P \tan^2\theta_P \varepsilon_2 + \sin^2\theta_P \delta_2)$ (Rüger, 1997). For HTI media, the anisotropic part of the reflectivity reduces to (Rüger, 2002)

$$\begin{aligned} \mathrm{R}^{\mathrm{AE}}_{\mathrm{PP,HTI}} =& 2^{-1}\left(\delta_2^{(V)}\cos^2\varphi - 8\mathrm{V}^2_{\mathrm{SP}}\sin^2\varphi\gamma_2\right)\sin^2\theta_P \\ &+ 2^{-1}\cos^2\varphi\left(\sin^2\varphi\delta_2^{(V)} + \cos^2\varphi\varepsilon_2^{(V)}\right)\tan^2\theta_P\sin^2\theta_P. \end{aligned} \tag{7.14}$$

The result in equation (7.10), which embodies our formulation of the anisotropic scattering potential, is therefore consistent with the previously-derived reflection coefficients for a boundary separating an isotropic medium from an anisotropic medium. In our derivation we have assumed that the actual medium is anisotropic-elastic and decomposable into an isotropic background with perturbations in both elastic and anisotropic parameters for actual medium. This is (within the linearized Zoeppritz solution framework) equivalent to the case of a low contrast planar boundary between an isotropic medium over an anisotropic medium. However, we saw that the linearized reflection coefficients are the same as those for which an anisotropic medium overlies an anisotropic medium, i.e., the case that background medium is also anisotropic. If we replace the anisotropic parameters in the lower medium with fractional differences in properties, the linearized reflection coefficient for an orthorhombic medium is obtained. To obtain the first order reflection coefficients in anisotropic media, in other words, we do not need to consider the anisotropic form of the polarizations and slowness vectors.

We have thus far considered only an elastic background. Let us now explicitly include the viscoelastic component of the stiffness tensor components. In figure 7.5a, a viscoelastic-orthorhombic medium, broken up into an isotropic-viscoelastic reference medium with perturbations in both viscoelastic and anisotropic parameters, is illustrated. Perturbations in isotropic parameters are, as in the non-attenuating cases, are expressed in terms of fractional changes in density, and P- and S-wave velocities, but now additionally with P- and

S-wave quality factors; perturbations in anisotropic parameters are the values of anisotropic and viscoelastic-anisotropic parameters. A key aspect of the viscoelastic extension of the scattering potential is the inclusion of the attenuation angle, which is the angle between the propagation and attenuation angle (Borcherdt, 2009).

The anelasticity of the medium supports two classes of waves: those with parallel propagation and attenuation vectors, called homogeneous waves, and those with a non-zero angle between the attenuation and propagation vectors, called inhomogeneous waves. For an isotropic viscoelastic background, we have $\mathrm{Q}_{440} = \mathrm{Q}_{550} = \mathrm{Q}_{\mathrm{S}0}$ and $\mathrm{Q}_{330} = \mathrm{Q}_{110} = \mathrm{Q}_{\mathrm{P}0}$. For a homogeneous incident wave we furthermore have $\mathrm{S}_{\mathrm{PP}} = \mathrm{S}^{\mathrm{E}}_{\mathrm{PP}} + i\mathrm{S}^{\mathrm{H}}_{\mathrm{PP}}$, where $\mathrm{S}^{\mathrm{H}}_{\mathrm{PP}}$ is the contribution of the anelasticity to the scattering potential (superscript H refers to the homogeneity of the incident wave). This contribution is, in detail,

$$\begin{aligned}\mathrm{S}^{\mathrm{H}}_{\mathrm{PP}} =& 2(\mathrm{Q}^{-1}_{\mathrm{S}0} - \mathrm{Q}^{-1}_{\mathrm{P}0})V^2_{\mathrm{SP}} \sin^2 2\theta_{\mathrm{P}} A_{\mu} + \mathrm{Q}^{-1}_{\mathrm{P}0} A_{Q_{\mathrm{P}}} - 2\mathrm{Q}^{-1}_{\mathrm{S}0} V^2_{\mathrm{SP}} \sin^2 2\theta_{\mathrm{P}} A_{Q_{\mathrm{S}}} \\ &+ 2\mathrm{Q}^{-1}_{\mathrm{S}0} V^2_{\mathrm{SP}} \sin^2 2\theta_{\mathrm{P}} \cos^2\varphi(\gamma^{(1)}_{\mathrm{Q}} - \gamma^{(2)}_{\mathrm{Q}}) - \mathrm{Q}^{-1}_{\mathrm{P}0} \sin^2\theta_{\mathrm{P}} \cos^2\theta_{\mathrm{P}} (\sin^2\varphi \delta^{(1)}_{\mathrm{Q}} + \cos^2\varphi \delta^{(2)}_{\mathrm{Q}}) \\ &- \mathrm{Q}^{-1}_{\mathrm{P}0} \sin^4\theta_{\mathrm{P}} \left[\cos^2\varphi \sin^2\varphi \delta^{(3)}_{\mathrm{Q}} + \sin^4\varphi \varepsilon^{(1)}_{\mathrm{Q}} + \left(\cos^2\varphi + \cos^2\varphi \sin^2\varphi\right) \varepsilon^{(2)}_{\mathrm{Q}}\right].\end{aligned} \tag{7.15}$$

To examine how attenuation influences the scattered, or AVO, response, we consider the two layer model in which the upper layer is isotropic-viscoelastic and lower layer is anisotropic-viscoelastic (Figure 7.5b). The linearized PP reflection coefficient is $\mathrm{R}_{\mathrm{P}} = \mathrm{R}^{\mathrm{E}}_{\mathrm{P}} + i\mathrm{R}^{\mathrm{H}}_{\mathrm{P}}$, where the contribution due to attenuation is

$$\mathrm{R}^{\mathrm{H}}_{\mathrm{PP}} = -\rho_0^{-1}(2\cos\theta_P)^{-2}\mathrm{S}^{\mathrm{H}}_{\mathrm{PP}} = \mathrm{A}^{\mathrm{H}}_{\mathrm{PP}} + \mathrm{B}^{\mathrm{H}}_{\mathrm{PP}} \sin^2\theta_{\mathrm{P}} + \mathrm{C}^{\mathrm{H}}_{\mathrm{PP}} \sin^2\theta_P \tan^2\theta_P \tag{7.16}$$

where

$$\begin{aligned}\mathrm{A}^{\mathrm{H}}_{\mathrm{PP}} =& -(4\mathrm{Q}_{\mathrm{P}0})^{-1} A_{Q_{\mathrm{P}}} \\ \mathrm{B}^{\mathrm{H}}_{\mathrm{PP}} =& -2(\mathrm{Q}^{-1}_{\mathrm{S}0} - \mathrm{Q}^{-1}_{\mathrm{P}0}) V^2_{\mathrm{SP}} A_{\mu} - (4\mathrm{Q}_{\mathrm{P}0})^{-1} A_{Q_{\mathrm{P}}} + 2\mathrm{Q}^{-1}_{\mathrm{S}0} V^2_{\mathrm{SP}} A_{Q_{\mathrm{S}}} \\ &- 2\mathrm{Q}^{-1}_{\mathrm{S}0} V^2_{\mathrm{SP}} \cos^2\varphi(\gamma^{(1)}_{\mathrm{Q}} - \gamma^{(2)}_{\mathrm{Q}}) + 4^{-1}\mathrm{Q}^{-1}_{\mathrm{P}0}(\sin^2\varphi \delta^{(1)}_{\mathrm{Q}} + \cos^2\varphi \delta^{(2)}_{\mathrm{Q}}) \\ \mathrm{C}^{\mathrm{H}}_{\mathrm{PP}} =& -(4\mathrm{Q}_{\mathrm{P}0})^{-1} \left\{A_{Q_{\mathrm{P}}} - \left[\cos^2\varphi \sin^2\varphi \delta^{(3)}_{\mathrm{Q}} + \sin^4\varphi \varepsilon^{(1)}_{\mathrm{Q}} + \left(\cos^2\varphi + \cos^2\varphi \sin^2\varphi\right) \varepsilon^{(2)}_{\mathrm{Q}}\right]\right\},\end{aligned} \tag{7.17}$$

It has been shown that attenuation affects both the intercept and gradient of the linearized PP reflection coefficients in viscoelastic-isotropic media (Moradi and Innanen, 2016;

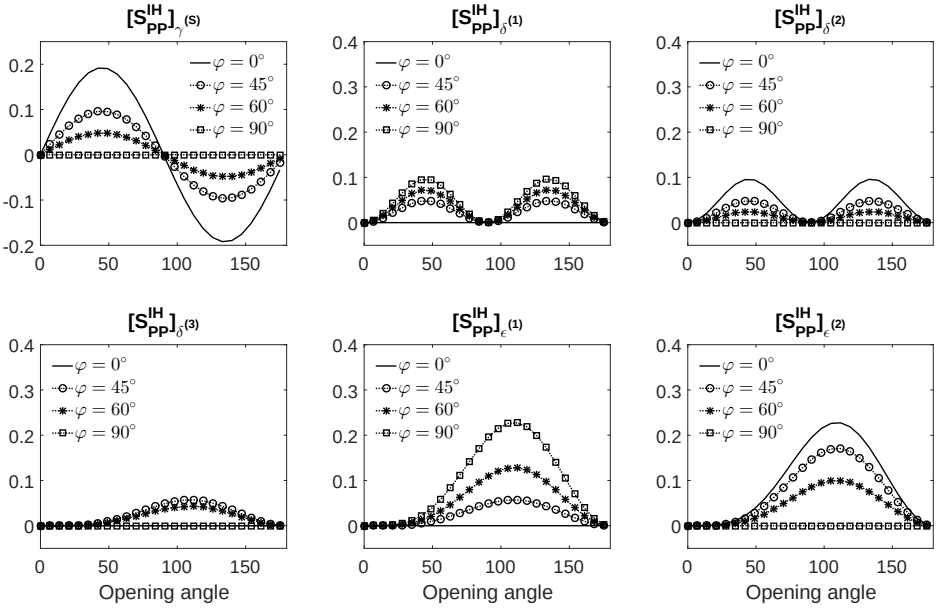

Figure 7.6: Sensitivity of the PP-scatter wave to the anisotropic-viscoelastic parameters for azimuth angles 0°, 45°, 60°, 90°. Horizontal axis is opening angle $2\theta_P$.

Samec and Blangy, 1992). Analysis of the exact PP reflection coefficient near the critical angle indicates that the attenuation and anisotropy do not affect the normal incident reflectivity (Carcione et al., 1998). Our linearized reflection coefficient forms predict that only the P-wave quality factor influences vertically-incident waves— there is no influence of anisotropic and anisotropic-viscoelastic parameters on the reflection coefficient at normal incidence. The parameter $\delta_Q^{(2)}$ only contributes in the small angle reflection coefficient, whereas $\varepsilon_Q^{(2)}$ dicates the large incident angle behaviour. There is no influence of the anisotropic Thompson parameters $\delta^{(2)}$ and $\varepsilon^{(2)}$ on the imaginary parts of reflection coefficients. In the case that anisotropy goes to zero, our results reduce to the AVO equations PP-waves in low-loss viscoelastic media, for homogeneous incident wave (Moradi and Innanen, 2016).

In Figure 7.6 the sensitivity of the scattered wave into the anisotropic parameters for inhomogeneous wave is plotted versus incident wave for different values of azimuth angles. For azimuth angle $\varphi = 90°$, the inhomogeneous part of the scattering potential is sensitive only to $\delta^{(1)}$ and $\varepsilon^{(1)}$. However the later two parameters have no effect on $\mathrm{S}_{\mathrm{PP}}^{\mathrm{VIH}}$ for azimuth angle $\varphi = 0°$.

For incident inhomogeneous waves, the reflectivity formula is $\mathrm{R_{PP}} = \mathrm{R}_{\mathrm{PP}}^{\mathrm{E}} + i\mathrm{R}_{\mathrm{PP}}^{\mathrm{H}} + i\mathrm{R}_{\mathrm{PP}}^{\mathrm{IH}}$,

where the contribution of the inhomogeneity of the wave is

$$\begin{aligned}\mathrm{R}_{\mathrm{PP}}^{\mathrm{IH}} =& -\mathrm{Q}_{\mathrm{P0}}^{-1}\tan\delta_{\mathrm{P}}\mathrm{V}_{\mathrm{SP}}^{2}\sin 2\theta_{P}\mathrm{A}_{\mu}+2^{-1}\mathrm{Q}_{\mathrm{P0}}^{-1}\tan\delta_{\mathrm{P}}\tan\theta_{P}(1+\tan^{2}\theta_{P})\mathrm{A}_{\mathrm{Vp}}\\ &+4^{-1}\mathrm{Q}_{\mathrm{P0}}^{-1}\tan\delta_{\mathrm{P}}\left(\delta_{2}^{(2)}+\sin^{2}\varphi\left[\delta_{2}^{(1)}-\delta_{2}^{(2)}-8\mathrm{V}_{\mathrm{SP}}^{2}\gamma_{2}^{(S)}\right]\right)\sin 2\theta_{P}\\ &+2^{-1}\mathrm{Q}_{\mathrm{P0}}^{-1}\tan\delta_{\mathrm{P}}\left(\cos^{2}\varphi\sin^{2}\varphi(\delta_{2}^{(3)}+\varepsilon_{2}^{(2)}-\varepsilon_{2}^{(1)})+\sin^{2}\varphi(\varepsilon_{2}^{(1)}-\varepsilon_{2}^{(2)})+\varepsilon_{2}^{(2)}\right)\tan^{3}\theta_{P}.\end{aligned}$$

At normal incidence, the inhomogeneity of the wave has no effect on the reflectivity. This term is controlled by changes in density, P- and S-wave velocity and anisotropic parameters $\delta^{(2)}$, $\varepsilon^{(2)}$ and $\gamma^{(S)}$. It is not sensitive into the changes in P- and S-wave quality factors, nor is it sensitive to changes in anisotropic-viscoelastic parameters.

7.6 Conclusion and summary

The Born approximation can be used to describe the various process in FWI and also helps to visualize and understand qualitatively the coda waves. In some circumstances, volume scattering behaves like low contrast reflection in a good approximation.

Scattering potentials for attenuative anisotropic media provides a simple tool to evaluate the Fréchet kernels, and this is relevant to FWI applications where Fréchet kernels are regarded as a sensitivity kernels. Moreover, the study of scattering potentials highlights the dependency of linearized reflection coefficients to anisotropy and attenuation. Attenuation and anisotropy are essential in amplitude variation with offset (AVO) trends as they change the amplitude and phase of the scattered wave field from geological interfaces. In this research, we derived the analytic forms of the components of the scattering potentials for scattering of the homogeneous waves in attenuative orthorhombic media. These expressions for scattering potentials which are the sensitivity kernels are involved in building the framework for FWI. Furthermore we showed that how these scattering potentials reduce to the linearized reflection coefficients. It can be seen that for normal incident or zero offset only attenuation in medium affect the P-wave reflection coefficient. Anisotropic-viscoelastic parameters affect the nonnormal incidence part of the reflectivity. Only gradient term is sensitive to the changes in S-wave quality factor, however the changes in P-wave quality factor affects the both intercept and curvature terms.

We believe the results presented in this paper might be a very fruitful approach to development of the theory of seismic modeling and inversion, especially in the new applications of FWI, such as in identifying quality factors and anisotropic-viscoelastic parameters and improving the imaging of subsurface materials.

There are also other avenues to pursue, including any inversion scenario where attenuation presence in anisotropic media. It is useful to inspect the results of scattering potentials to determine whether we can construct a framework for full waveform inversion for a medium with both attenuation and anisotropy.

In our analysis we make use of volume scattering based on the first order perturbation called Born approximation. The principle, which has made the formulations possible, is the division of the actual medium to an isotropic reference medium filled by perturbations in anisotropic properties.

One of the purpose of the this research is to provide a framework for the AVO/AVAZ and Full waveform Inversion (FWI) in medium with both anisotropy and attenuation. One would like to have some idea of the importance of the effects of attenuation and anisotropy of the scattering potentials that technically are the sensitivity kernels for the FWI. Although some works have been done on the linearized reflection coefficients in attenuative anisotropic media, in the context of volume scattering is largely unexplained area. We will be concerned here with orthorhombic media with weak anisotropic and attenuation properties. We derive the scattering framework to describe the interaction of the seismic waves in a viscoelastic orthorhombic media. We study two cases: first we assume that the wave propagates in the isotropic elastic reference medium and scattered by the perturbations in anisotropic orthorhombic media. This is equivalent to the two layer media model whose the upper layer is isotropic elastic media and the lower layer is anisotropic orthorhombic media. In second case it is assumed that the reference medium is isotopic viscoelastic media scattered by the perturbations in attenuative anisotropic orthorhombic media. We shall examine analytically the relationship between the results obtained from the linearization of the exact solutions. We show that the derived scattering potentials reduced to the reflection coefficients from the boundary separating an isotropic layer from anisotropic layer.

There is one important conclusion in the analysis of the converted P-wave in this paper.

We show that there is no analytical distinction between the behaviour of the linearized reflection coefficients for incident isotropic layer and anisotropic incident layer. In the volume scattering point of view, the scattering potentials and radiation patterings for either isotropic or anisotropic reference media are the same. Whenever we deal with the first order perturbation for weak anisotropy, we can use the isotropic polarization and slowness vectors for reference medium. This greatly simplifies the analytical expressions, which is complicated by using the analytical form of the polarization and slowness vectors in anisotropic media. There are two important results of this development: The recognition of the significance of the effects of both anisotropy and attenuation on linearized reselection coefficients and sensitivity kernels in FWI. The development accomplished here is primarily a guide to sensitivity analysis and model parametrization for FWI.

Chapter 8

Summary and Future Work

In this thesis a comprehensive development of FWI sensitivity analysis and AVO/AVAz in context of volume scattering theory for media with both anisotropy and attenuation is presented. There are three types of waves in a viscoelastic media: Primary (P) waves, Type-I Secondary (or SI) waves and Type II Secondary (or SII) waves. Within our framework we developed a new set of canonical results set alongside those of layered media: for viscoelastic-isotropic media, we showed that P- and SI-waves can be scattered into each other, but SII-waves can only be scattered into other SII-waves. Five properties cause scattering of waves: density, P- and S-velocities and attenuation quantities related to the P- and S-waves. We showed in detail that, and how, small changes in each of these properties scatter waves with specific radiation patterns in phase angle. We also for the first time showed how to include the attenuation angle in a specific set of scattering equations referred to as the AVO (Amplitude Variation with Offset) equations. The attenuation angle characterizes the direction of maximum attenuation in the earth. To derive the AVO equations for viscoelastic media we employed two approaches: the first is called the Born approximation. The second approach is a traditional technique based on the linearization of exact solutions of the wave equation, which is called the Aki-Richards approach. We proved that both approaches are equivalent. We further carried out a detailed analysis of how in detail the scattering radiation patterns depend on fractional and absolute changes in anisotropic and attenuative properties of the medium. In particular we showed how to decompose the P-to-P, P-to-SI, SI-to-SI and SII-to-SII scattering potentials into elastic, anisotropic, viscoelastic and anisotropic-viscoelastic components. Elastic components included fractional changes in density, vertical P-wave velocity and vertical S-wave velocity; anisotropic components included changes in the anisotropic Thomsen parameters; viscoelastic components included fractional changes in vertical P- and S-wave quality factors and fractional changes in density, vertical P-wave velocity and vertical S-wave velocity; anisotropic components included changes in Q-dependent Thomsen parameters. The elastic and anisotropic components are the real part

of the scattering potential and viscoelastic and anisotropic-viscoelastic components are the imaginary parts of the scattering potential.

With the volume scattering framework we have developed for the anisotropic-viscoelastic media, we carry out the detailed sensitivity analysis for scattered waves to suggest optimal model parametrization for FWI. This analysis is the first step in developing the FWI in anisotropic-viscoelastic media.

We also modified the 2D finite difference code developed by Martin and Komatitsch (2009a) to simulate wave propagation in a low contrast viscoelastic media. We examined and confirmed the validity of the radiation patterns previously obtained from Born approximations using the numerical modeling of the scattering from variations in viscoelastic parameters.

As a further step we can generalize the viscoelastic finite difference modeling to include anisotropy. In this case, we have the attenuative slow and fast P- and S-waves. The same approach for memory variables is applicable here, but more complicated forms are required. After simulating viscoelastic waves in anisotropic media we also can carry out adjusted sensitivity analysis as obtained using the Born approximation by generating the radiation patterns generated by the perturbations in medium properties in a synthetic model.

Solution of the forward problem allows us to generate synthetic or simulated seismograms as measured above an anisotropic-viscoelastic medium. A summation of the squares of the differences between the generated waveforms and observed seismograms, called the misfit function, characterizes the inverse problem treated by FWI. The objective of FWI is to find the global minimum of the misfit function, i.e., find model parameters that minimize the difference between observed and simulated data. A commonly used minimization technique in FWI is based on the gradient or local slope of the misfit function. To calculate the derivatives of the model parameters which make up this slope, we have to correlate forward-modelled wave with the backward propagating (adjoint wave). Backpropagation of waves in an attenuative medium itself is an open problem with tentative solutions found in the literature, and proper inclusion of these in elastic/anisotropic FWI will form a significant contribution in exploration geophysics.

References

Aki, K. and Richards, P. G. (2002). *Quantitative Seismology*. University Science Books, 2nd edition.

Alkhalifah, T. and Plessix, R.-É. (2014). A recipe for practical full-waveform inversion in anisotropic media: An analytical parameter resolution study. *Geophysics*, 79(3):R91–R101.

Bai, T. and Tsvankin, I. (2016). Time-domain finite-difference modeling for attenuative anisotropic media. *Geophysics*, 81(2):C69–C77.

Bai, T., Tsvankin, I., and Wu, X. (2017). Waveform inversion for attenuation estimation in anisotropic media. *Geophysics*, 82(4):1–79.

Bakulin, A., Grechka, V., and Tsvankin, I. (2000a). Estimation of fracture parameters from reflection seismic data-part I: HTI model due to a single fracture set. *Geophysics*, 65(6):1788–1802.

Bakulin, A., Grechka, V., and Tsvankin, I. (2000b). Estimation of fracture parameters from reflection seismic data-part III: Fractured models with monoclinic symmetry. *Geophysics*, 65(6):1818–1830.

Bakulin, A., Grechka, V., and Tsvankin, I. (2000c). Estimation of fracture parameters from reflection seismic datapart II: Fractured models with orthorhombic symmetry. *Geophysics*, 65(6):1803–1817.

Bansal, R. and Sen, M. K. (2010). Ray-Born inversion for fracture parameters. *Geophysical Journal International*, 180(3):1274–1288.

Barton, N. (2007). *Rock quality, seismic velocity, attenuation and anisotropy*. CRC press.

Behura, J. and Tsvankin, I. (2009a). Reflection coefficients in attenuative anisotropic media. *Geophysics*, 74(5):WB193–WB202.

Behura, J. and Tsvankin, I. (2009b). Role of the inhomogeneity angle in anisotropic attenuation analysis. *Geophysics*, 74(5):WB177–WB191.

Beretta, M. M., Bernasconi, G., and Drufuca, G. (2002). AVO and AVA inversion for fractured reservoir characterization. *Geophysics*, 67(1):300–306.

Beylkin, G. (1985). Imaging of discontinuities in the inverse scattering problem by inversion of a causal generalized radon transform. *J. Math. Phys.*, 26:99–108.

Beylkin, G. and Burridge, R. (1990). Linearized inverse scattering problems in acoustics and elasticity. *Wave motion*, 12:15–52.

Bickel, S. H. and Natarajan, R. R. (1985). Plane-wave Q deconvolution. *Geophysics*, 50:1426–1439.

Bickle, M. J. (2009). Geological carbon storage. *Nature Geoscience*, 2(12):815–818.

Blanch, J. O., Robertsson, J. O. A., and Symes, W. W. (1995). Modeling of a constant Q: methodology and algorithm for an efficient and optimally inexpensive viscoelastic technique. *Geophysics*, 60(1):176–184.

Bleistein, N. (1979). Velocity inversion procedure for acoustic waves. *Geophysics*, 44(6):1077–1087.

Borcherdt, R. D. (1971). Inhomogeneous body and surface plane waves in a generalized viscoelastic half space. *Ph.D. thesis*.

Borcherdt, R. D. (1973a). Energy and plane waves in linear viscoelastic media. *J. Geophys. Res.*, 78:24422453.

Borcherdt, R. D. (1973b). Rayleigh-type surface wave on a linear viscoelastic half-space. *J. Acoust. Soc. Am.*, 54:16511653.

Borcherdt, R. D. (1977). Reflection and refraction of Type-II S waves in elastic and anelastic media. *Bull. Seismol. Soc. Am.*, 67:43–67.

Borcherdt, R. D. (1982). Reflection-refraction of general P- and Type-IS waves in elastic and anelastic solids. *Geophys. J. R. Astron. Soc.*, 70:621–638.

Borcherdt, R. D. (1988). Volumetric strain and particle displacements for body and surface waves in a general viscoelastic half-space. *Geophys. J. R. Astron. Soc.*, 93:215–228.

Borcherdt, R. D. (2009). *Viscoelastic waves in layered media*. Cambridge University Press.

Borcherdt, R. D., Glassmoyer, G., and Wennerberg, L. (1986). Influence of welded boundaries in anelastic media on energy flow and characteristics of general P, SI and SII body waves: Observational evidence for inhomogeneous body waves in low-loss solids. *J. Geophys. Res.*, 91:503–518.

Borcherdt, R. D. and Wennerberg, L. (1985). General p, type-I S, and type-II S waves in anelastic solids: Inhomogeneous wave fields in low-loss solids. *Bull. Seismol. Soc. Am.*, 75:1729–1763.

Burridge, R., Maarten, V., Miller, D., and Spencer, C. (1998). Multiparameter inversion in anisotropic elastic media. *Geophysical Journal International*, 134(3):757–777.

Carcione, J. M. (1993). Seismic modeling in viscoelastic media. *Geophysics*, 58:110–120.

Carcione, J. M. (1997). Reflection and transmission of qP-qS plane waves at a plane boundary between viscoelastic transversely isotropic media. *Geophysical Journal International*, 129(3):669–680.

Carcione, J. M. (2007). *Wave fields in real media: Wave propagation in anisotropic, anelastic, porous and electromagnetic media*, volume 38. Elsevier.

Carcione, J. M., Helle, H. B., and Zhao, T. (1998). Effects of attenuation and anisotropy on reflection amplitude versus offset. *Geophysics*, 63(5):1652–1658.

Carcione, J. M., Kosloff, D., and Kosloff, R. (1988a). Viscoacoustic wave propagation simulation in the earth. *Geophysics*, 53:769–777.

Carcione, J. M., Kosloff, D., and Kosloff, R. (1988b). Wave propagation simulation in a linear viscoelastic medium. *Geophysical Journal*, 95:597–611.

Castagna, J. P. and Backus, M. M. (1993). *Offset-dependent reflectivity: Theory and practice of AVO analysis*. Soc. Expl. Geophys.

Causse, E., Mittet, R., and Ursin, B. (1999). Preconditioning of full-waveform inversion in viscoacoustic media. *Geophysics*, 64:130–145.

Cervený, V. and Psencík, I. (1998). PP-wave reflection coefficients in weakly anisotropic elastic media. *Geophysics*, 63(6):2129–2141.

Cervený, V. and Psencík, I. (2005a). Plane waves in viscoelastic anisotropic media I. theory. *Geophys. J. Int.*, 161:197–212.

Cervený, V. and Psencík, I. (2005b). Plane waves in viscoelastic anisotropic media II. numerical examples. *Geophys. J. Int.*, 161:213–229.

Červenỳ, V. and Pšenčík, I. (2008). Quality factor Q in dissipative anisotropic media. *Geophysics*, 73(4):T63–T75.

Cervený, V. and Psencík, I. (2008). Weakly inhomogeneous plane waves in anisotropic, weakly dissipative media. *Geophys. J. Int.*, 172:663–673.

Chapman, M., Liu, E., and Li, X.-Y. (2006). The influence of fluid sensitive dispersion and attenuation on AVO analysis. *Geophysical Journal International*, 167(1):89–105.

Charara, M., Barnes, C., and Tarantola, A. (2000). Full waveform inversion of seismic data for a viscoelastic medium. In *Methods and Applications of Inversion*, pages 68–81. Springer.

Chopra, S. and Marfurt, K. J. (2007). *Seismic attributes for prospect identification and reservoir characterization*. Society of Exploration Geophysicists and European Association of Geoscientists and Engineers.

Clayton, R. W. and Stolt, R. H. (1981). A Born-WKBJ inversion method for acoustic reflection data. *Geophysics*, 46(11):1559–1567.

da Silva, N. V., Ratcliffe, A., Vinje, V., and Conroy, G. (2016). A new parameter set for anisotropic multiparameter full-waveform inversion and application to a north sea data set. *Geophysics*, 81(4):U25–U38.

Dahl, T., , and Ursin, B. (1992). Non-linear AVO inversion for a stack of anelastic layers. *Geophysical Prospecting*, 40:243–265.

Deschamps, M. and Assouline, F. (2000). Attenuation along the poynting vector direction of inhomogeneous plane waves in absorbing and anisotropic solids. *Acustica*, 86:295–302.

Far, M. E. (2011). *Seismic characterization of naturally fractured reservoirs*. PhD thesis, University of Houston.

Far, M. E. and Hardage, B. (2016). Fracture characterization using converted waves. *Geophysical Prospecting*, 64(2):287–298.

Far, M. E., Sayers, C. M., Thomsen, L., Han, D.-h., and Castagna, J. P. (2013a). Seismic characterization of naturally fractured reservoirs using amplitude versus offset and azimuth analysis. *Geophysical Prospecting*, 61(2):427–447.

Far, M. E., Thomsen, L., and Sayers, C. M. (2013b). Seismic characterization of reservoirs with asymmetric fractures. *Geophysics*, 78(2):N1–N10.

Fatti, J. L., Smith, G. C., Vail, P. J., Strauss, P. J., and Levitt, P. R. (1994). Detection of gas in sandstone reservoirs using AVO analysis: A 3-D seismic case history using the geostack technique. *Geophysics*, 59(9):1362–1376.

Fichtner, A. (2010). *Full Seismic Waveform Modelling and Inversion*. Springer, Heidelberg.

Fichtner, A. and van Driel, M. (2014). Models and Frechet kernels for frequency-(in)dependent Q. *Geophys. J. Int.*, 198:1878–1889.

Flugge, W. (1967). *Viscoelasticity*. Waltham.

Foster, D., Keys, R., and Lane, F. (2010). Interpretation of AVO anomalies. *Geophysics*, 75:75A3–75A13.

Futterman, W. I. (1962). Dispersive body waves. *Journal of Geophysical research*, 67(13):5279–5291.

Gholami, Y., Brossier, R., Operto, S., Ribodetti, A., and Virieux, J. (2013). Which parameterization is suitable for acoustic vertical transverse isotropic full waveform inversion? part 1: Sensitivity and trade-off analysis. *Geophysics*, 78(2):R81–R105.

Grasso, J. and Wittlinger, G. (1990). Ten years of seismic monitoring over a gas field. *Bulletin of the Seismological Society of America*, 80(2):450–473.

Hak, B. and Mulder, W. A. (2011). Seismic attenuation imaging with causality. *Geophysical Journal International*, 184(1):439–451.

Hargreaves, N. D. and Calvert, A. J. (1991). Inverse Q-filtering by Fourier transform. *Geophysics*, 56:519–527.

He, W. and Plessix, R.-É. (2016). Analysis of different parameterisations of waveform inversion of compressional body waves in an elastic transverse isotropic earth with a vertical axis of symmetry. *Geophysical Prospecting*.

Hearn, D. J. and Krebes, E. S. (1990). Complex rays applied to wave propagation in a viscoelastic medium. *Pure and Applied Geophysics*, 132:401–415.

Hicks, G. and Pratt, R. G. (2001). Reflection waveform inversion using local descent methods: estimating attenuation and velocity over a gas-sand deposit. *Geophysics*, 66:598–612.

Huang, W., Briers, R., Rokhlin, S. I., and Leroy, O. (1994). Experimental study of inhomogeneous wave reflection from a solid-air periodically rough boundary using leaky rayleigh waves. *J. Acoust. Soc. Am.*, 96:363–369.

Ikelle, L. T. and Amundsen, L. (2005). *Introduction to Petroleum Seismology*. Society of Exploration Geophysicists.

Ikelle, L. T., Amundsen, L., Gangi, A., and Wyatt, S. B. (2003). Kirchhoff scattering series: Insight into the multiple attenuation method. *Geophysics*, 68(1):16–28.

Innanen, K. A. (2009). Born series forward modelling of seismic primary and multiple reflections: an inverse scattering shortcut. *Geophys. J. Int.*, 177:1197–1204.

Innanen, K. A. (2011). Inversion of the seismic AVF/AVA signatures of highly attenuative target. *Geophysics*, 76(2):R1–R14.

Innanen, K. A. (2012). Anelastic P-wave, S-wave and converted-wave AVO approximations. *74th EAGE Conference and Exhibition, Extended Abstracts*, page P197.

Innanen, K. A. (2014). Seismic AVO and the inverse hessian in precritical reflection full waveform inversion. *Geophysical Journal International*, 199(2):717–734.

Innanen, K. A. and Lira, J. E. (2010). Direct nonlinear Q compensation of seismic primaries reflecting from a stratified, two-parameter absorptive medium. *Geophysics*, 75(2):V13–V23.

Innanen, K. A. and Weglein, A. B. (2007). On the construction of an absorptive-dispersive medium model via direct linear inversion of reflected seismic primaries. *Inverse Problems*, 23:2289–2310.

Jílek, P. (2001). *Modeling and inversion of converted-wave reflection coefficients in anisotropic media: A tool for quantitative AVO analysis*. PhD thesis, Colorado School of Mines.

Jílek, P. (2002). Converted ps-wave reflection coefficients in weakly anisotropic media. *Pure and Applied Geophysics*, 159(7-8):1527–1562.

Kamei, R. and Pratt, R. (2013). Inversion strategies for visco-acoustic waveform inversion. *Geophysical Journal International*, 194(2):859–884.

Keating, S. and Innanen, K. A. (2017). Characterizing and mitigating uncertainty in the physics of attenuation in an-acoustic full wave- form inversion. In *SEG Technical Program Expanded Abstracts 2017 (submitted)*. Society of Exploration Geophysicists.

Krebes, E. (1983). The viscoelastic reflection/transmission problem: two special cases. *Bulletin of the Seismological Society of America*, 73(6A):1673–1683.

Krebes, E. S. (1984). On the reflection and transmission of viscoelastic waves-some numerical results. *Geophysics*, 49:1374–1380.

Lehocki, I., Avseth*, P., and Veggeland, T. (2014). Nonlinear inversion of PP-and PS-reflection data using Aki-Richards approximation. In *SEG Technical Program Expanded Abstracts 2014*, pages 548–552. Society of Exploration Geophysicists.

Lumley, D. (2010). 4D seismic monitoring of CO 2 sequestration. *The Leading Edge*, 29(2):150–155.

Margrave, G. F., Stewart, R. R., and Larsen, J. A. (2001). Joint PP and PS seismic inversion. *The Leading Edge*, 20(9):1048–1052.

Martin, R. and Komatitsch, D. (2009a). seismic-ADEPML-2D-viscoelastic-RK4-eighth-order.f90: 2D ADE-PML program for an isotropic viscoelastic medium using an eighth-order finite-difference spatial operator and fourth-order Runge-kutta implicit, semi implicit or explicit time scheme. *http://komatitsch.free.fr/README-seismic-cpml.html*, 179(1):333–344.

Martin, R. and Komatitsch, D. (2009b). An unsplit convolutional perfectly matched layer technique improved at grazing incidence for the viscoelastic wave equation. *Geophysical Journal International*, 179(1):333–344.

Masmoudi, N. and Alkhalifah, T. (2016). A new parameterization for waveform inversion in acoustic orthorhombic media. *Geophysics*, 81(4):R157–R171.

Matson, K. H. (1997). *An inverse scattering series method for attenuating elastic multiples from multicomponent land and ocean bottom seismic data*. PhD thesis, University of British Columbia.

Métivier, L., Brossier, R., Operto, S., and Virieux, J. (2015). Acoustic multi-parameter FWI for the reconstruction of P-wave velocity, density and attenuation: preconditioned truncated newton approach. In *SEG Technical Program Expanded Abstracts 2015*, pages 1198–1203. Society of Exploration Geophysicists.

Moradi, S. and Innanen, K. A. (2013). Viscoelastic scattering potentials and inversion sensitivities. *CREWES Research Report*, 25.

Moradi, S. and Innanen, K. A. (2015a). Linearized AVO in viscoelastic media. In *SEG Technical Program Expanded Abstracts 2015*, pages 600–606. Society of Exploration Geophysicists.

Moradi, S. and Innanen, K. A. (2015b). Scattering of homogeneous and inhomogeneous seismic waves in low-loss viscoelastic media. *Geophys. J. Int.*, 202:1722–1732.

Moradi, S. and Innanen, K. A. (2016). Viscoelastic amplitude variation with offset equations with account taken of jumps in attenuation angle. *Geophysics*, 81(3):N17–N29.

Odebeatu, E., Zhang, J., Chapman, M., Liu, E., and Li, X. Y. (2006). Application of spectral decomposition to detection of dispersion anomalies associated with gas saturation. *The Leading Edge*, 25:206–210.

Oh, J.-W. and Alkhalifah, T. (2016). Elastic orthorhombic anisotropic parameter inversion: An analysis of parameterization. *Geophysics*, 81(6):C279–C293.

Operto, S., Gholami, Y., Prieux, V., Ribodetti, A., Brossier, R., Metivier, L., and Virieux, J. (2013). A guided tour of multiparameter full-waveform inversion with multicomponent data: From theory to practice. *The Leading Edge*, 32(9):1040–1054.

Operto, S., Miniussi, A., Brossier, R., Combe, L., Haller, N., Kjos, E., Métivier, L., Milne, R., Ribodetti, A., Song, Z., et al. (2015). Efficient 3D frequency-domain full-waveform inversion of ocean-bottom cable data-application to valhall in the visco-ac. In *77th EAGE Conference and Exhibition 2015*.

Ostrander, W. (1984). Plane-wave reflection coefficients for gas sands at nonnormal angles of incidence. *Geophysics*, 49(10):1637–1648.

Pan, W., Innanen, K. A., Margrave, G. F., Fehler, M. C., Fang, X., and Li, J. (2016). Estimation of elastic constants for HTI media using gauss-newton and full-newton multiparameter full-waveform inversion. *Geophysics*, 81(5):R275–R291.

Plessix, R., Milcik, P., Rynja, H., Stopin, A., Matson, K., and Abri, S. (2013). Multiparameter full-waveform inversion: Marine and land examples. *The Leading Edge*, 32(9):1030–1038.

Plessix, R.-E. and Cao, Q. (2011). A parametrization study for surface seismic full waveform inversion in an acoustic vertical transversely isotropic medium. *Geophysical Journal International*, 185(1):539–556.

Prieux, V., Brossier, R., Operto, S., and Virieux, J. (2013). Multiparameter full waveform inversion of multicomponent ocean-bottom-cable data from the valhall field. part 1: Imaging compressional wave speed, density and attenuation. *Geophysical Journal International*, page ggt177.

Ren, H., Goloshubin, G., and Hilterman, F. J. (2009). Poroelastic analysis of amplitude-versus-frequency variations. *Geophysics*, 74:N41–N48.

Ribodetti, A. and Virieux, J. (1998). Asymptotic theory for imaging the attenuation factor Q. *Geophysics*, 63:1767–1778.

Robertsson, J. O. A., Blanch, J., and Symes, W. (1994). Viscoelastic finite difference modelling. *Geophysics*, 59:1444–1456.

Rüger, A. (1997). P-wave reflection coefficients for transversely isotropic models with vertical and horizontal axis of symmetry. *Geophysics*, 62(3):713–722.

Rüger, A. (1998). Variation of P-wave reflectivity with offset and azimuth in anisotropic media. *Geophysics*, 63(3):935–947.

Rüger, A. (2002). *Reflection coefficients and azimuthal AVO analysis in anisotropic media*. Society of Exploration Geophysicists.

Rutherford, S. R. and Williams, R. H. (1989). Amplitude-versus-offset variations in gas sands. *Geophysics*, 54(6):680–688.

Samec, P. and Blangy, J. (1992). Viscoelastic attenuation, anisotropy, and AVO. *Geophysics*, 57(3):441–450.

Sato, H., Fehler, M. C., and Maeda, T. (2012). Seismic wave propagation and scattering in the heterogeneous earth.

Sava, P. and Biondi, B. (2004a). Wave-equation migration velocity analysis. II. subsalt imaging examples. *Geophysical Prospecting*, 52(6):607–623.

Sava, P. and Biondi, B. (2004b). Wave-equation migration velocity analysis.I. theory. *Geophysical Prospecting*, 52(6):593–606.

Sayers, C. M. (2009). Seismic characterization of reservoirs containing multiple fracture sets. *Geophysical Prospecting*, 57(2):187–192.

Sayers, C. M. and Dean, S. (2001). Azimuth-dependent AVO in reservoirs containing non-orthogonal fracture sets. *Geophysical Prospecting*, 49(1):100–106.

Sayers, C. M. and Rickett, J. E. (1997). Azimuthal variation in AVO response for fractured gas sands. *Geophysical Prospecting*, 45(1):165–182.

Schmalholz, B. Q. S. M. and Podladchikov, X. Y. (2009). Low-frequency reflections from a thin layer with high attenuation caused by interlayer flow. *Geophysics*, 74:N15–N23.

Schwaiger, H. F., Aldridge, D. F., and Haney, M. M. (2007). Full waveform 3D synthetic seismic algorithm for 1D layered anelastic models. *American Geophysical Union, Fall Meeting 2007, abstract*, S41A:0238.

Shuey, R. (1985). A simplification of the zoeppritz equations. *Geophysics*, 50(4):609–614.

Stewart, R. R., Gaiser, J. E., Brown, R. J., and Lawton, D. C. (2002). Converted-wave seismic exploration: Methods. *Geophysics*, 67(5):1348–1363.

Stewart, R. R., Gaiser, J. E., Brown, R. J., and Lawton, D. C. (2003). Converted-wave seismic exploration: Applications. *Geophysics*, 68(1):40–57.

Stolt, R. H. and Weglein, A. B. (2012). *Seismic imaging and inversion: application of linear inverse theory*. Cambridge Univ. Press, Cambridge.

Stovas, A. and Ursin, B. (2003). Reflection and transmission responses of layered transversely isotropic viscoelastic media. *Geophysical Prospecting*, 51(5):447–477.

Tarantola, A. (1986). A strategy for nonlinear elastic inversion of seismic reflection data. *Geophysics*, 51(10):1893–1903.

Thomsen, L. (1986). Weak elastic anisotropy. *Geophysics*, 51(10):1954–1966.

Thomsen, L. (1993). Weak anisotropic reflections. *Offset-dependent reflectivityTheory and practice of AVO analysis: Soc. Expl. Geophys*, pages 103–111.

Tonn, R. (1990). The determination of the seismic quality factor Q from VSP data: a comparison of different computational methods. *Geophysical Prospecting*, 39:1–27.

Tsvankin, I. (1996). P-wave signatures and notation for transversely isotropic media: An overview. *Geophysics*, 61(2):467–483.

Tsvankin, I. (1997). Anisotropic parameters and P-wave velocity for orthorhombic media. *Geophysics*, 62(4):1292–1309.

Tsvankin, I., Gaiser, J., Grechka, V., Van Der Baan, M., and Thomsen, L. (2010). Seismic anisotropy in exploration and reservoir characterization: An overview. *Geophysics*, 75(5):75A15–75A29.

Ursin, B. and Stovas, A. (2002). Reflection and transmission responses of a layered isotropic viscoelastic medium. *Geophysics*, 67:307–323.

Virieux, J. and Operto, S. (2009). An overview of full-waveform inversion in exploration geophysics. *Geophysics*, 74:WCC1–WCC26.

Wang, Y. (2006). Inverse Q-filter for seismic resolution enhancement. *Geophysics*, 71:V51–V60.

Warner, M., Ratcliffe, A., Nangoo, T., Morgan, J., Umpleby, A., Shah, N., Vinje, V., Štekl, I., Guasch, L., Win, C., et al. (2013). Anisotropic 3d full-waveform inversion. *Geophysics*, 78(2):R59–R80.

Weglein, A. B. (2013). A timely and necessary antidote to indirect methods and so-called P-wave FWI. *The Leading Edge*, 32(10):1192–1204.

Weglein, A. B., Araújo, F. V., Carvalho, P. M., Stolt, R. H., Matson, K. H., Coates, R. T., Corrigan, D., Foster, D. J., Shaw, S. A., and Zhang, H. (2003). Inverse scattering series and seismic exploration. *Inverse Problems*, pages R27–R83.

Weglein, A. B. and Dragoset, W. H. (2005). *Multiple Attenuation*. Society of Exploration Geophysicists.

Weglein, A. B., Gasparotto, F. A., Carvalho, P. M., and Stolt, R. H. (1997). An inverse-scattering series method for attenuating multiples in seismic reflection data. *Geophysics*, 62(6):1975–1989.

Weglein, A. B., Zhang, H., Ramirez, A. C., Liu, F., and Lira, J. (2009). Clarifying the underlying and fundamental meaning of the approximate linear inversion of seismic data. *Geophysics*, 74:WCD1–WCD13.

Wennerberg, L. (1985). Snell's law for viscoelastic materials. *Geophys. J. R. astr. Soc.*, 81:13–18.

White, J. E. (1965). Reflections from lossy media. *Journal of the Acoustical Society of America*, 38:604–607.

Wu, R. and Aki, K. (1985). Scattering characteristics of elastic waves by an elastic heterogeneity. *Geophysics*, 50:582–595.

Wu, X., Chapman, M., Li, X.-Y., and Boston, P. (2014). Quantitative gas saturation estimation by frequency-dependent amplitude-versus-offset analysis. *Geophysical Prospecting*, 62(6):1224–1237.

Yang, P., Brossier, R., Métivier, L., and Virieux, J. (2016). A review on the systematic formulation of 3-D multiparameter full waveform inversion in viscoelastic medium. *Geophysical Journal International*, 207(1):129–149.

Zhang, C. and Ulrych, T. J. (2007). Seismic absorption compensation: a least squares inverse scheme. *Geophysics*, 72:R109–R114.

Zhao, H., Gao, J., and Liu, F. (2014). Frequency-dependent reflection coefficients in diffusive-viscous media. *Geophysics*, 79:T143–T155.

Zhu, Y. and Tsvankin, I. (2006a). Plane-wave attenuation anisotropy in orthorhombic media. *Geophysics*, 72(1):D9–D19.

Zhu, Y. and Tsvankin, I. (2006b). Plane-wave propagation in attenuative transversely isotropic media. *Geophysics*, 71(2):T17–T30.

Copyright and Permissions

Dear Shahpoor Moradi,

RE. Shahpoor Moradi and Kristopher A. Innanen. Scattering of homogeneous and inhomogeneous seismic waves in low-loss viscoelastic media. Geophysical Journal International (2015) 202 (3): 1722-1732

My apologies for the delay in responding to you and thank you for your email requesting permission to reuse all or part of your article in a thesis/dissertation. As part of your copyright agreement with Oxford University Press you have retained the right, after publication, to use all or part of the article and abstract, in the preparation of derivative works, extension of the article into a booklength work, in a thesis/dissertation, or in another works collection, provided that a full acknowledgement is made to the original publication in the journal. As a result, you should not require direct permission from Oxford University Press to reuse you article. Authors may upload a PDF of the accepted manuscript to institutional and/or centrally organized repositories and/or in free public servers, upon acceptance for publication in the journal. Authors may upload the version of record to institutional and/or centrally organized repositories and/or in free public servers, upon publication in the journal.

Please Note: Inclusion under a Creative Commons License or any other Open-Access License allowing onward reuse is prohibited. If you have any other queries, please feel free to contact us.

Kind regards,

Permissions Assistant, Rights Department Academic and Journals Divisions—Global Business Development Oxford University Press — Great Clarendon Street — Oxford — OX2 6DP

Dear Shahpoor,

You are permitted to use the paper you reference in your PhD thesis. Such use is covered under SEGs green open-access policy, available here:

http://seg.org/Publications/Policies-and-Permissions/Open-Access-Policy

Thank you for publishing in Geophysics.

Sincerely,

Associate Executive Director, Knowledge Management Society of Exploration Geophysicists (SEG) 8801 South Yale Avenue, Suite 500 Tulsa, OK 74137-3575 USA